# The developmental heterogeneity of NK cells and its alteration in mice with conditional Raptor- or Rictor-deficiency and a patient with GATA2$^{T354M}$ mutation

A Dissertation

Presented to the Faculty of the Graduate School of Biomedical Sciences

At the Medical College of Wisconsin

In Partial Fulfillment of the Requirements for the

Degree of Doctor of Philosophy

By

**Chao Yang**

Department of Microbiology and Immunology

March 2019

**Dissertation Committee**

Subramanian Malarkannan, PhD (Chairman)

Joseph T. Barbieri, PhD

John A. Corbett, PhD

Scott S. Terhune, PhD

Calvin B. Williams, MD, PhD

Barbara L. Kee, PhD (The University of Chicago)

# Abstract

Natural killer (NK) cells are innate lymphocytes capable of mediating both cytotoxicity and cytokine production in response to transformed or virally infected cells. NK cells go through several developmental stages to achieve functional maturity. The developmental heterogeneity is conventionally defined by the expression of cell surface markers. Through utilizing single-cell RNA-sequencing (scRNA-seq) technology, we defined the developmental heterogeneity of both murine and human NK cells based on transcriptome of individual cell. We found five distinct NK populations in the murine bone marrow (BM) named as immature NK, transitional NK1, transitional NK2, transitional NK3, and terminally mature NK. In the BM of six healthy donors, we found seven distinct NK clusters named as $CD56^{bright}$ NK, transitional NK, active NK, adaptive NK, mature NK, terminally mature NK, and inflamed NK. We found similar NK populations in the blood of two healthy donors except for the adaptive NK and inflamed NK. These data not only expanded our current knowledge on the developmental heterogeneity of NK cells but also revealed unique transcriptome profile associated with each NK subset.

The developmental progression of NK cells is governed by both extrinsic and intrinsic factors. Previous study has revealed the indispensable role of mechanistic target of rapamycin (mTOR) in regulating the development of murine NK cells. However, the unique roles of mTOR complex 1 (mTORC1) or mTOR complex 2 (mTORC2) in regulating this process remain unknown. Through disrupting the formation of mTORC1 or mTORC2 specifically in NK cells, based on the expression of cell surface markers, we

found that mTORC1 was critical for the early developmental progression, while mTORC2 regulated the terminal maturation. Mechanistically, mTORC2 regulated the expression of T-bet, master transcription factor critical for terminal maturation of NK cells, through $Akt^{S473}$-FoxO1 axis. Surprisingly, we found more immature NK subset within the mTORC2-deficient NK cells than the mTORC1-deficient NK cells based on transcriptome-defined maturity, contradictory to the cell surface markers-indicated maturity. Further exploration of T-bet-deficient NK cells revealed even more pronounced immature phenotype compared to mTORC2-deficient NK cells. The expression of immature NK cell signature genes was up-regulated in T-bet-deficient NK cells. These data uncovered the previously unappreciated role of T-bet in suppressing the immature NK transcriptional signature during the development of NK cells.

Specific to the development of human NK cells, $CD56^{bright}$ NK cells are believed to be the precursors of $CD56^{dim}$ NK cells. Based on the transcriptome and pseudotime analyses, we found a transitional population between $CD56^{bright}$ and $CD56^{dim}$ NK cells supporting this ontogenetic relationship. However, there are a few evidences challenging this dogma. One of them is that patients with *GATA2* mutation only possess $CD56^{dim}$ but not $CD56^{bright}$ NK cells. The reason behind this observation remains unknown. We identified a unique donor with $GATA2^{T354M}$ mutation who was at the early stage of the disease (clinically asymptomatic). We found reduced but not diminished $CD56^{bright}$ NK cells in this donor. scRNA-seq analysis of NK cells from this donor revealed a larger transcriptomic alteration in the $CD56^{bright}$ compared to $CD56^{dim}$ NK population. Coinciding with this observation, we found increased cell death in the $CD56^{bright}$

compared to $CD56^{dim}$ NK compartment in the $GATA2^{T354M}$ donor. These observations revealed the potential reason for diminished $CD56^{bright}$ NK cells in patients with *GATA2* mutations and shed light on the potential mechanisms behind the defects.

# Table of Contents

Abstract ..... 2
List of Figures ..... 8
List of Tables ..... 10
Abbreviations ..... 11
Acknowledgments ..... 13
Chapter 1 – General Introduction ..... 16
1.1 The natural killer cells ..... 17
1.1.1 NK cells in health and disease ..... 17
1.1.2 Development of murine NK cells ..... 24
1.1.3 Development of human NK cells ..... 27
1.1.4 Transcriptional regulation of NK cell development ..... 30
1.1.5 IL-15 in the development of NK cells ..... 34
1.2 mTOR and mTOR complexes ..... 38
1.2.1 Mechanistic target of rapamycin and mTOR complexes ..... 38
1.2.2 mTOR complex 1 signaling ..... 43
1.2.3 mTOR complex 2 signaling ..... 47
1.2.4 mTOR in the immune system ..... 49
1.2.5 mTOR in NK cells ..... 52
1.3 GATA2 and *GATA2* mutations ..... 54
1.3.1 GATA2 ..... 54
1.3.2 GATA2 deficiency syndrome ..... 58
1.3.3 NK cells in GATA2 deficiency syndrome ..... 61
Chapter 2 – Experimental Procedures ..... 63
2.1 Mice ..... 64
2.2 Cell preparation from different organs in mice ..... 64
2.3 Human sample collection and preparation ..... 65
2.4 Flow cytometry and cell sorting ..... 66
2.5 Western Blotting ..... 67
2.6 RT-qPCR ..... 67
2.7 Bulk RNA-seq and analysis ..... 68
2.8 ScRNA-seq and analysis ..... 69

2.9 ChIP-seq analysis ..... 71
2.10 B16F10 lung metastasis model ..... 71
2.11 *In vivo* splenocytes rejection assay ..... 72
Chapter 3 – mTORC1 and mTORC2 differentially regulate the development of NK cells ..... 73
3.1 Introduction ..... 74
3.2 Results ..... 76
3.2.1 mTORC1 is critical for homeostasis and differentiation of NK cells ..... 76
3.2.2 mTORC2 is required for terminal maturation of NK cells ..... 81
3.2.3 mTORC1 and mTORC2 differentially regulate the expression of T-box transcription factors ..... 85
3.2.4 mTORC1 and mTORC2 differentially regulate the expression of CD122 and STAT5 activation ..... 88
3.2.5 Altered transcriptome in NK cells lack of mTORC1 or mTORC2 correlates with impaired NK cell development ..... 90
3.2.6 mTORC2 regulates the terminal maturation of NK cells through $Akt^{S473}$-FoxO1-T-bet axis ..... 94
3.2.7 Disruption of mTORC2 does not affect mTORC1 activation ..... 101
3.2.8 Defective anti-tumor response in *Rptor* or *Rictor* cKO mice ..... 103
3.3 Conclusions ..... 106
3.4 Discussion ..... 107
Chapter 4 – mTORC2-$Akt^{S473}$-FoxO1-T-bet axis suppresses the transcriptional signature of immature NK cells during the development of NK cells ..... 111
4.1 Introduction ..... 112
4.2 Results ..... 114
4.2.1 The heterogeneity of murine BM $CD3\varepsilon^{-}CD122^{+}$ cells ..... 114
4.2.2 Five distinct BM NK subsets defined by transcriptome ..... 118
4.2.3 The relative maturity of the three transitional NK subsets ..... 121
4.2.4 Raptor- or Rictor-deficient cells cluster separate from WT cells ..... 125
4.2.5 Transcriptome similarity between Raptor- or Rictor-deficient NK cells with their corresponding WT cells ..... 128
4.2.6 Transcriptome-defined maturity of Raptor- or Rictor-deficient NK cells ..... 131
4.2.7 T-bet-deficient NK cells have a transcriptional profile similar to the iNK cluster ..... 135
4.2.8. T-bet indirectly suppresses the expression of immature NK signature genes ..... 139
4.2.9 Deletion of FoxO1 rescue the altered transcriptome of Rictor-deficient NK cells ..... 143
4.3 Conclusions ..... 147

4.4 Discussion ..... 148
Chapter 5 – The developmental heterogeneity of human NK cells in healthy donors and a patient with GATA2$^{T354M}$ mutation ..... 151
5.1 Introduction ..... 152
5.2 Results ..... 154
5.2.1 scRNA-seq analysis of Lin$^{-}$CD7$^{+}$ cells from human BM and blood ..... 154
5.2.2 The developmental heterogeneity of human NK cells from BM and blood ..... 158
5.2.3 The existence of a transitional population between CD56$^{brignt}$ and CD56$^{dim}$ NK cells 161
5.2.4 Active NK subset at steady-state ..... 166
5.2.5 Unique transcriptomic profile of adaptive NK cells ..... 171
5.2.6 Terminally-mature NK cells exhibit unique transcriptional profile ..... 176
5.2.7 BM and blood contain similar developmental NK clusters ..... 181
5.2.8 Pseudotime reveals CD56$^{bright}$ is the precursor of CD56$^{dim}$ NK cells ..... 183
5.2.9 Altered NK cell transcriptome in GATA2$^{T354M}$ donor ..... 187
5.3 Conclusions ..... 194
5.4 Discussion ..... 195
Chapter 6 – General Conclusions ..... 198
Chapter 7 – General Discussion ..... 201
7.1 The linear development model of NK cells – true or not ..... 202
7.2 mTORC1 and the development of NK cells – questions remain to be answered ..... 204
7.3 More to be learned from FoxO1 and T-bet in the development of NK cells ..... 208
7.4 The 'active NK' cluster identified in both human and mice ..... 210
7.5 Metadata-determined cellular identity ..... 211
References ..... 214

# List of Figures

**Figure 1.1 NK cells in health and disease** ..... 18
**Figure 1.2. Mechanisms of target cell recognition by NK cells** ..... 22
**Figure 1.3. The lineage commitment and differentiation of murine NK cells in the BM** ..... 25
**Figure 1.4. The commitment and differentiation of human NK cells** ..... 28
**Figure 1.5. Transcription factors involved in the development of murine NK cells** ..... 31
**Figure 1.6. Transcription factors involved in the commitment and differentiation of human NK cells** ..... 33
**Figure 1.7. Trans-presentation of IL-15 and IL-15 signaling** ..... 35
**Figure 1.8. mTOR and mTOR complex** ..... 40
**Figure 1.9. Protein domain structure of mTOR, Raptor, Rictor, and mSin1** ..... 41
**Figure 1.10. The upstream and downstream of mTORC1 and mTORC2** ..... 45
**Figure 1.11. Domain structure of the GATA family transcription factors** ..... 55
**Figure 3.1. mTORC1 is required to maintain the homeostatic NK cellularity** ..... 77
**Figure 3.2. Raptor is required for the maturation of NK cells** ..... 80
**Figure 3.3. Homeostatic NK cellularity is impaired in Rictor cKO mice** ..... 82
**Figure 3.4. mTORC2 is pivotal for the terminal maturation of NK cells** ..... 84
**Figure 3.5. mTORC1 and mTORC2 differentially regulate the expression of Eomes and T-bet** ..... 87
**Figure 3.6. mTORC1 and mTORC2 differentially regulate the expression of CD122 and STAT5 activation** ..... 89
**Figure 3.7. Transcriptome analyses of Raptor- or Rictor-deficient NK cells** ..... 91
**Figure 3.8. mTORC2 is required for T-bet expression through regulation of FoxO1 during NK cell development** ..... 96
**Figure 3.9. Deletion of Foxo1 rescues the NK cellularity and terminal maturation defects in Rictor cKO mice** ..... 100
**Figure 3.10. Disruption of mTORC2 does not affect mTORC1 activation** ..... 102
**Figure 3.11. Impaired anti-tumor activity in Rptor or Rictor cKO mice** ..... 104
**Figure 4.1. scRNA-seq analysis of CD3ε$^{-}$CD122$^{+}$ murine BM cells from three mutant mice and their corresponding WT mice.** ..... 116
**Figure 4.2. Transcriptome-based classification of conventional murine NK cells** ..... 119
**Figure 4.3. The relative maturity of the five distinct NK clusters** ..... 124
**Figure 4.4. Unbiased clustering analysis of Raptor- or Rictor-deficient cells** ..... 127
**Figure 4.5. Transcriptome similarity between Raptor- or Rictor-deficient NK cells with their corresponding WT cells** ..... 129
**Figure 4.6. The identity of the Raptor- or Rictor-deficient NK cells defined by machining learning classifiers** ..... 133
**Figure 4.7. Unbiased clustering analysis of CD3ε$^{-}$CD122$^{+}$ cells from BM of the Tbx21 KO mouse** ..... 136
**Figure 4.8. scRNA-seq analysis of T-bet-deficient NK cells.** ..... 138
**Figure 4.9. T-bet is unlikely to directly bind and suppress the expression of large amount of immature NK genes** ..... 140

**Figure 4.10. T-bet- or Rictor-deficiency does not result in large alteration in the expression of known transcription factors critical for the development of NK cells.** ..... 143
**Figure 4.11. Deletion of Foxo1 in Rictor-deficient NK cells correct the abnormal induction of the immature NK transcriptional signature** ..... 145
**Figure 5.1. Phenotypical analyses of $Lin^{-}CD7^{+}$ cells from BM and blood** ..... 155
**Figure 5.2. Quality control of the scRNA-seq datasets** ..... 156
**Figure 5.3. Unbiased clustering of human NK cells from BM** ..... 159
**Figure 5.4. Unbiased clustering of human NK cells from blood** ..... 160
**Figure 5.5. The identification of $CD56^{bright}$ NK population** ..... 163
**Figure 5.6. Identification of 'CD56$^{bright}$ NK' cluster and a potential transitional population between $CD56^{bright}$ and $CD56^{dim}$ NK cells** ..... 165
**Figure 5.7. Active NK cells with unique transcriptome profile** ..... 167
**Figure 5.8. Identification of the 'Active NK' cluster with cell surface markers** ..... 169
**Figure 5.9.. Identification of adaptive NK cells from 24-year old female donor** ..... 172
**Figure 5.10. Features associated with the 'Adaptive NK' cluster** ..... 174
**Figure 5.11. Functional mature NK clusters** ..... 177
**Figure 5.12. Unique transcriptional profile associated with the 'Terminal NK' cell cluster** ..... 179
**Figure 5.13. Unbiased clustering of human NK cells from BM and blood of same donor** ..... 182
**Figure 5.14. Single cell trajectory analysis reveals a linear NK cell developmental pathway, maturing from $CD56^{bright}$ to $CD56^{dim}$ NK cells** ..... 185
**Figure 5.15. Exploration of the branches in the single cell trajectory analysis** ..... 186
**Figure 5.16. GATA2 mutation results in larger transcriptome alteration in $CD56^{bright}$ NK cells compared to $CD56^{dim}$ NK cells** ..... 188
**Figure 5.17. Features associated with the $GATA2^{T354M}$ donor NK cells** ..... 191

# List of Tables

**Table 4.1. The accuracy and error rates of the five distinct machining learning classifiers** ..... 131

# Abbreviations

4EBP ..... Eukaryotic translation initiation factor 4E-binding protein
AML ..... Acute myeloid leukemia
AMPK ..... AMP-activated protein kinase
APC ..... Antigen presenting cell
ATF ..... Activating transcription factor
BM ..... Bone marrow
C/EBP ..... CCAAT-enhancer-binding protein
CAR ..... Chimeric antigen receptor
CD11b SP ..... CD11b single positive
CD27 SP ..... CD27 single positive
cDKO ..... Conditional double knockout
ChIP ..... Chromatin immunoprecipitation
ChIP-seq ..... Chromatin immunoprecipitation sequencing
cKO ..... Conditional knockout
CLP ..... Common lymphoid progenitor
CMV ..... Cytomegalovirus
CREB ..... cAMP response element binding protein
CTLA-4 ..... Cytotoxic T-lymphocyte-associated protein 4
CTR ..... Cell trace red
CTV ..... Cell trace violet
CyTOF ..... Mass cytometry
DC ..... Dendritic cell
DCML ..... Dendritic cell, monocyte, B and NK lymphoid
DEG ..... Differential expressed gene
DEPTOR ..... DEP domain containing mTOR interacting protein
DL ..... Deep learning
DP ..... CD27/CD11b double positive
EBV ..... Epstein–Barr virus
eEFs ..... Eukaryotic elongation factors
eIF4F ..... Eukaryotic initiation factor 4F
eIFs ..... Eukaryotic initiation factors
EILPs ..... Early innate lymphoid progenitor
FACS ..... Fluorescence-activated cell sorting
FVB ..... Friend leukemia virus B
GAP ..... GTPase activating protein
GB ..... Gradient boosting
GC ..... Germinal center
GIMAP ..... GTPase of the immunity-associated protein
GL ..... Generalized linear
GSEA ..... Gene set enrichment analysis
GvHD ..... Graft versus host disease
GvT ..... Graft versus tumor
HLA ..... Human leukocyte antigen
HOMER ..... Hypergeometric optimization of motif enrichment
HPV ..... Human papillomavirus
ICOS ..... Inducible T-cell costimulator

IEG ..... Immediate early gene
ILCs ..... Innate lymphoid cells
iNK ..... Immature natural killer
KIR ..... Killer-cell immunoglobulin-like receptor
Lin ..... Lineage
LMPP ..... Lymphoid-primed multipotent progenitor
MACS ..... Model-based analysis of ChIP-Seq
MAPK ..... Mitogen-activated protein kinase
MAST ..... Model-based analysis of single-cell transcriptomics
MCMV ..... Murine cytomegalovirus
MDS ..... Myelodysplastic syndrome
MEP ..... Megakaryocyte–erythroid progenitor
MHC ..... Major histocompatibility complex
mLST8 ..... Mammalian lethal with Sec13 protein 8
mNK ..... Mature NK
MonoMAC ..... Monocytopenia with *Mycobacterium avium* complex
mSin1 ..... Mammalian stress-activated protein kinase interacting protein 1
mTOR ..... Mechanistic target of rapamycin
mTORC1 ..... Mechanistic target of rapamycin complex 1
mTORC2 ..... Mechanistic target of rapamycin complex 2
NK ..... Natural killer
NKP ..... Natural killer progenitor
NKR ..... Natural killer receptor
PAP ..... Pulmonary alveolar proteinosis
PBMC ..... Peripheral blood mononuclear cell
PC ..... Principle component
PH ..... Pleckstrin homology
PRAS40 ..... Proline-rich Akt substrate of 40 kDa
Protor1/2 ..... Protein observed with Rictor-1/2
PRR ..... Pattern recognition receptor
Raptor ..... Regulatory protein associated with mTOR
RBC ..... Red blood cell
RF ..... Random forest
Rictor ..... Rapamycin-insensitive companion of mTOR
S6K1 ..... Ribosomal protein S6 kinase beta-1
scRNA-seq ..... Single-cell RNA-sequencing
*SNORD3* ..... *Small nucleolar RNA, C/D box 3*
SRA ..... Sequence read archive
SREBP ..... Sterol regulatory element-binding protein
SRF ..... Serum response factor
termNK ..... Terminally mature NK
Th ..... T helper
TLR ..... Toll-like receptor
TOP ..... Terminal oligopyrimidine
transNK ..... Transitional NK
TSC ..... Tuberous sclerosis complex
t-SNE ..... t-distributed stochastic neighbor embedding
XGB ..... Extreme gradient Boosting

# Acknowledgments

First of all, I want to express my sincere gratitude to my Ph.D. mentor, Dr. Subramaniam Malarkannan who has been a great mentor and friend to me. Without your 100% support and encouragement, I would not be able to achieve much in the graduate school. I learned from you to be a scientist starting with respecting everyone. I admire your devotion of mentoring and helping everyone around you to achieve the best of them. I will always keep that in mind. I would also like to thank our clinical PI, Dr. Monica Thakar. Thank you for sharing all the clinical insights with us. The stories from the clinics always give us the deepest satisfaction and motivation. Personally, I also want to thank you for the efforts of providing all the clinical samples for my project. Without your contribution, none of that would ever happen. For the past members of the Malar/Thakar lab, Kamal, Kristina, and Linda, although we have only been working together for a short period time, much has been learned from all of you. I really cherish the time we spent together. As a graduate student, I want to say thank you to our big brother Alex, Abel who has graduated last year. As a senior student, you basically answering questions to everyone in the lab. Your kindness and sincerity will always be in my mind. Besides Malar, the person I learned most from the lab will be Zachary, Gerbec. Starting from my 1$^{st}$-year rotation, you have been helping me through my entire graduate school time. It is a privilege to be your colleague and friend. I believe you will be a great mentor someday and best wishes to the family. I also want to thank you Jason Siebert, MSTP student in the lab. I admire your intelligence in computer science and appreciate all the help and support you have given me for the project we worked together. I look forward to our next collaboration. I want to say thank you to Kate Dixon for making the lab more like a

family to me. It is so nice to witness you and Alex starting a family. Best wishes to you. I also want to thank our post-doc Arash Nanbakhsh. One important thing I learned from you is how to keep pursuing a project and make it better. In addition, thank you to our lab manager, Shunhua Lao, for taking care of the lab and facilitating our projects. I also want to thank Sandy in Dr. Riese's lab for her support and collaboration.

I want to express my special gratitude to my thesis committee members, Drs. Joe Barbieri, John Corbett, Scott Terhune, and Cal Williams from MCW and Dr. Barbara Kee from the University of Chicago as the external committee member. Thank you for all the valuable inputs you gave for my projects in our committee meetings; Thank you for supporting me when I need references for grand or job applications; Thank you for encouraging me to keep working hard in the scientific career.

Being at the Blood Research Institute for the past four years, I could not ask for a better work environment. I want to thank you Dr. Gil White for making that happen. I would not be able to finish my projects without help from all the amazing people at BRI. I want to say thank you to the BRI principal investigators, Drs. Mat Riese, Sid Rao, Weiguo Cui, Deming Wang, Qizhen Shi, Nan Zhu and Karen Carlson for your help and support. Special thanks to Bill Cashdollar, Benedetta Bonacci, Yongwei, Zheng, Mark Zogg, Michael Reimer, Cynthia Opansky, Brad Best, Robert Burns, David Schauder, and Kirthi Pulakanti for all the help you have gave me for my projects. Being the first awardee, special thanks from me to Dr. Sadler's family in supporting the establishment of the J.

Evan Sadler Graduate Scholar Award in the Blood Research Institute and deep condolence for the family's loss.

I would like to thank you all the staff, especially Kathy Thompson, in the Department of Microbiology and Immunology for the organization and assistance of scientific and non-scientific events. Thank you for the interdisciplinary program in biomedical science for admitting me as a graduate student at MCW. I also want to thank you the graduate school of biomedical science for helping me fulfill all the requirements for the degree of Doctor of Philosophy. Special thank you to Nai-Fen Su for her patient and prompt help with my post-doctoral position application.

I want to thank you my parents in supporting me pursuing my dream. Thank you for all the comfort and encouragement from my mother. You have always been my role model and I will continue be brave and optimistic like you. I also want to thank you all my dear friends. Being able to share joys and pains with all of you is what supports me going through the past five years. I want to give special gratitude to Juan Chen, my roommate, who has been an amazing friend to me. At last, I want to thank myself in continuously working hard and doing good job.

# Chapter 1 – General Introduction

## 1.1 The natural killer cells

### 1.1.1 NK cells in health and disease

#### The discovery of NK cells

NK cells are a group of innate lymphoid cells (ILCs) that have naturally occurring anti-tumor functions [1]. The initial observation of NK cells was made in experiments designed for the study of cytotoxicity T lymphocytes [2, 3]. Until 10 years later, researchers started to realize the existence of a real non-T lymphocytes population that has anti-tumor properties [4-7]. In contrast to T cells, NK cells are naturally cytotoxic without the need of prior exposure to antigens [4, 7]. With the initial detection of NK cell activity in the human PBMC and rodent splenocytes [5, 6, 8, 9], we now know NK cells are widely spread across both lymphoid and non-lymphoid organs [10].

#### NK cells in health and disease

The importance of the NK cells in the immune system were demonstrated in both human NK cell deficiency and genetically-modified mouse models [11, 12]. Individuals with absent or loss of functions of NK cells suffer from reoccurring herpesviral infections [11]. The two critical effector functions of NK cells are production of inflammatory cytokines and cytotoxicity, both of which have a profound impact in immune responses against both infections and malignancies (**Figure 1.1**) [13, 14]. In addition, recent discoveries have also started to reveal the critical role of NK cells in anti-inflammatory responses, tissue repair, and autoimmunity (**Figure 1.1**) [15-17].

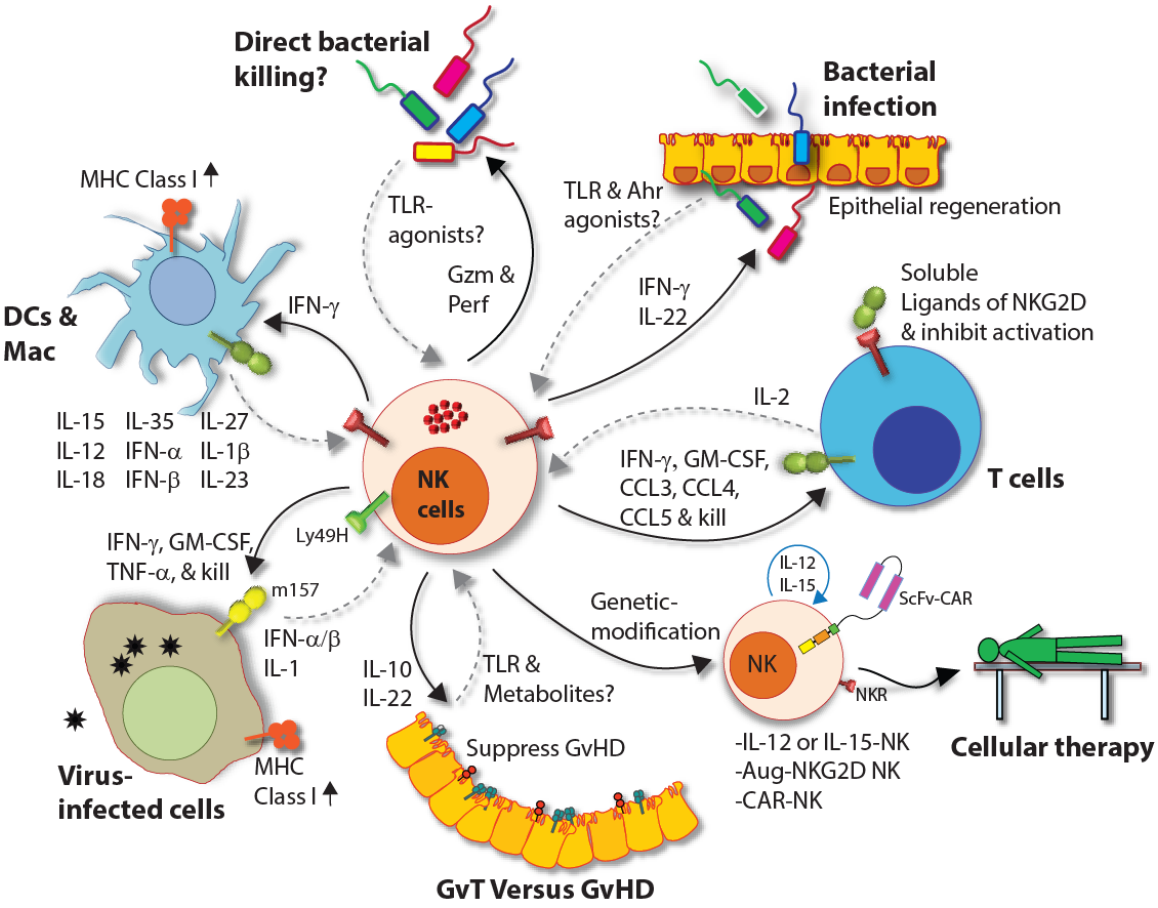


**Figure 1.1 NK cells in health and disease**

As a critical type of lymphocytes, NK cells play critical role in both innate and adaptive immunity. During infections, the activated DCs and Macrophages (Mac) produced large amounts of pro-inflammatory cytokines including IFN-α/β, IL-12, IL-18, etc. Those cytokines stimulate NK cells and promote the production of IFN-γ, TNF-α and GM-CSF which not only promote the maturation of DCs and Mac but also shape the T cell differentiation. Besides cytokines-mediated contain of the virus-infected cells and bacteria dissemination, NK cells also directly lyse pathogens or pathogen-infected cells. Clinically, following hematopoietic stem cell transplantation, the grafted NK cells exhibit strong anti-tumor effects (GvT) and also produce immune-suppressive cytokine IL-10 to dampen the graft versus host disease (GvHD. Therapeutically, allogenic NK cell transplantation has been effective in treating hematologic malignancies. In vitro cytokine priming, chimera antigen receptor (CAR), and inhibitory receptor blockade have been

used to augment the function of human NK cells for clinical utilization. Adopted from Abel et al., *Front. Immunol.*, 2018 [14].

**NK cells in infections**

As a critical branch of innate immunity, NK cells contribute to the protection of hosts from various pathogen. One of the well-established features of NK cells is the anti-viral function, especially against the herpesvirus family [11]. The Cytomegalovirus (CMV) represents the mostly-studied viral infection model for NK cells. Both NK cell depletion and adoptive transfer experiments have established the antiviral function of NK cells against CMV in mice [12]. Mechanistically, NK cells distinguish healthy cells versus the virus-infected cells through several mechanisms. The healthy cells are defined as immunological "self" through the recognition of MHC class I molecules on the cell surface which interact with inhibitory Ly49 receptors in mice or KIRs in human to initiate negative signaling that increases the activation threshold of NK cells (**Figure 1.2.A**) [18]. Virus-infected cells often down-regulate MHC class I molecules to avoid the attack from $CD8^+$ T cells [19]. Nevertheless, those cells are particularly vulnerable to NK cell-mediated clearance and treated as the immunological "non-self" (**Figure 1.2.B**) [20]. In addition, viral infections often induce the expression of ligands that are normally absent on the healthy cells [21]. These stress-induced ligands serve as the "danger signals" and interact with activating receptors on NK cells to overrule the negative signaling initiated by MHC class I molecules, the immunological "induced-self" model (**Figure 1.2.C**) [21]. For example, murine CMV (MCMV) infection leads to the expression of m157, a MCMV-encoded glycoprotein specifically recognized by the

activating Ly49H receptor on murine NK cells [22]. This interaction activates NK cells and initiates the production of large amounts of pro-inflammatory cytokines and direct cytolytic clearance of the virus-infected cells [23, 24]. The murine stains which do not contain Ly49H-expressing NK cells are susceptible to the MCMV infection [25]. NKG2C recognizing the HLA-E loaded with human CMV viral peptide is presumably the human counterpart of the m157-Ly49H axis [26-29]. The similar immunosurveillance mechanism has been found in influenza infection where the virus-encoded hemagglutinin is recognized by another activating receptor, Ncr1, expressed on NK cells [30]. Besides direct control of viral infections, NK cells also shapes the adaptive immune response [31]. The pro-inflammatory cytokines, especially IFN-γ, produced by NK cells regulate the differentiation of Th1 cells, a critical T cell subset that controls viral infections [32].

NK cells also respond to bacterial infections either direct recognition through pattern recognition receptors (PRRs) or indirect activation by cytokines produced by infected cells or antigen presenting cells (APCs) [33, 34]. NK-mediated direct killing of bacteria-infected cells relies on delivery of granzymes and initiation of cell death program in the target cells [35-37]. IFN-γ production from NK cells have been shown to be critical for the early control of *Listeria monocytogenes* infection [38, 39]. Moreover, NK cells have been reported to be involved in several other microbial infections including *Staphylococcus aureus*, *Lactobacillus johnsonii*, *Mycobacterium tuberculosis*, and *Mycobacterium bovis* bacille Calmette-Guérin [35, 40-42]. In addition to bacterial infections, NK cells also contribute to the anti-fungi immune response through various

mechanisms including perforin-mediated destruction of fungal membranes, direct phagocytosis, and production of pro-inflammatory cytokines [43-46].

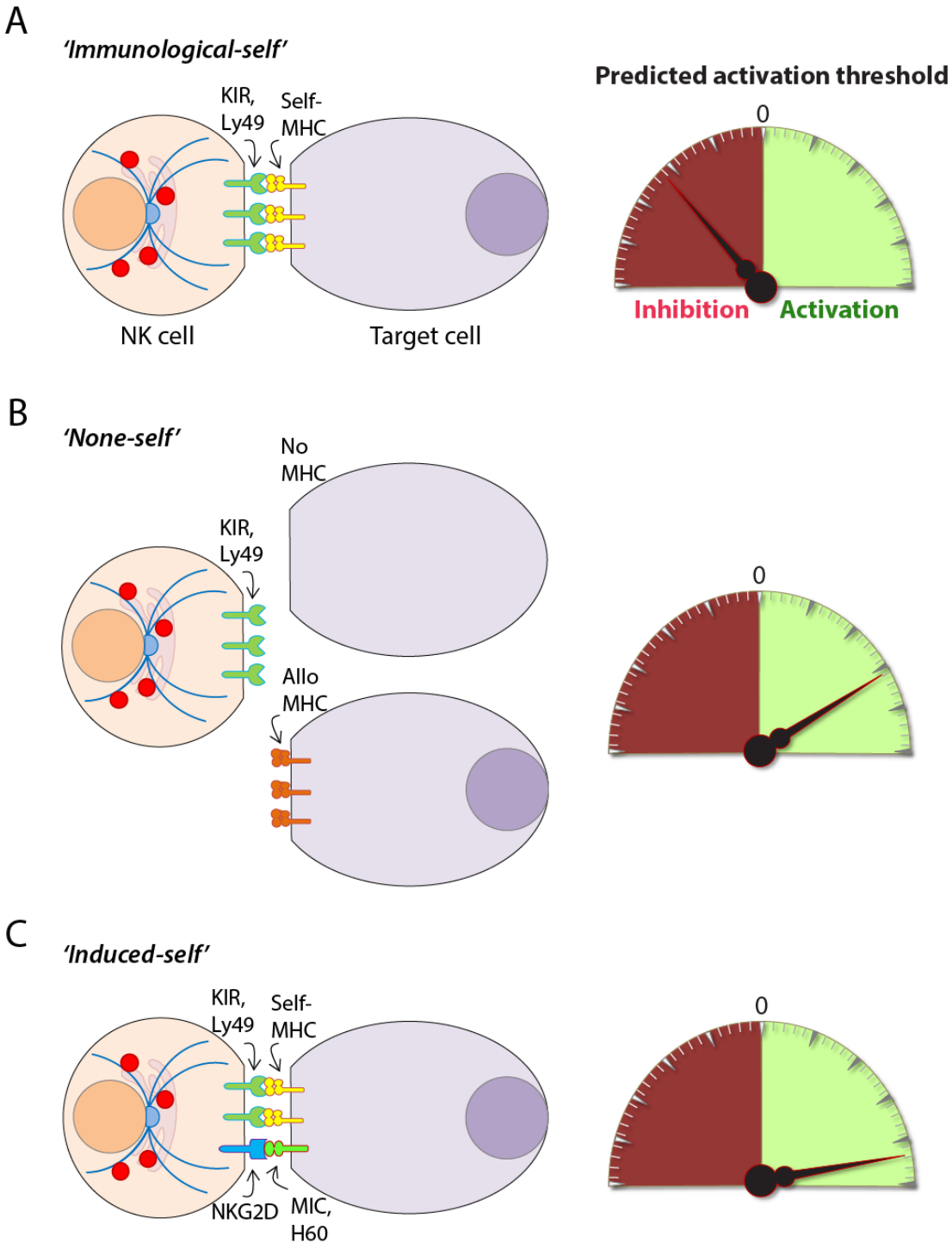

**Figure 1.2. Mechanisms of target cell recognition by NK cells**

(**A**) The healthy cells are considered as the immunologic "self" which will not be attacked by NK cells due to the negative signaling initiated by the MHC class I molecules which are expressed on the surface of nearly all somatic cells. (**B**) Pathogen-infected cells and tumor cells often down-regulate the MHC class I molecules to escape from the T cell-mediated immunosurveillance. However, the loss of the negative signaling to NK cells results in activation of NK cells and destruction of these immunological "non-self" cells. In addition, in the transplant setting, although cells in the recipients still obtain surface expression of MHC class I molecule, these allogenic or haploidentical MHC class I molecules cannot be recognized by the donor-derived NK cells and will be treated as immunological "non-self". (**C**) Pathogens invasion or cellular transformation often induces expression of ligands that are absent in healthy cells. These stress-induced ligands are "danger signals" recognized by activating receptors that leads to the activation of NK cells, the "induced-self" model. Adopted from Abel et al., *Front. Immunol.*, 2018 [14].

## NK cells in cancer and clinical utilization

Since the discovery of NK cells, the exploration of NK-mediated anti-tumor response have been extensively studied in both mice and human [47, 48]. Studies in human have demonstrated a correlation between NK cell activity to the cancer incidence [49]. The presence of tumor-infiltrating NK cells also serves a biomarker of clinical outcomes in several solid tumors [50-52]. The anti-tumor effect of NK cells has been well-characterized in the setting of hematopoietic stem cell transplantation [53]. As the first repopulated lymphoid cell type, NK cells exhibit robust anti-tumor effect known as the graft-versus-tumor (GvT) effect [53]. The seminal work in 2002 demonstrated the increased efficacy of NK cell-mediated GVT and reduced graft-versus-host disease (GvHD) in allotransplants [54]. Since then, both allogeneic and haploidentical NK cell

adoptive transfer strategies have been widely tested and used in treating various hematological malignancies and they seems to be well-tolerated by the recipients [55, 56]. Recent studies also started to explore the efficacy of haploidentical NK cell transplantation in treating solid tumors [53, 57].

Similar to anti-viral immunity, the recognition of transformed cells by NK cells is achieved by the continuous scanning of cell surface MHC class I molecules and stress-induced ligands (**Figure 1.2**) [20, 58]. The balanced signaling outcome from the activating and inhibitory receptors dictate the function of NK cells. The utilization of allogeneic NK cells is a great example of reducing the inhibitory signaling to achieve augmented anti-tumor effects. Recent studies have also explored the possibility of increasing the activating signaling of NK cells in malignancies. One example is the stabilization of stress-induced ligands MICA and MICB on tumor cells to enhance NK cells-mediated tumor suppression through activating receptor NKG2D [59]. In addition, immune checkpoint inhibitors and chimeric antigen receptor (CAR) have also been applied to NK cell-based immunotherapy against cancer with promising clinical results (**Figure 1.1**) [60-64].

1.1.2 Development of murine NK cells

In mice, NK cells are commonly defined by the cell surface expression of NK1.1 (NKR-P1C), Ncr1 or CD49b within the lineage-negative population (Lineage (Lin) includes CD3ε, CD19, Ly6C/G, Ter119). NK1.1 (NKR-P1C) is frequently used in the C57BL/6 mice [65, 66], while Ncr1 or CD49b are useful NK markers in other mouse strains [67, 68]. Percentage of NK cells among the lymphocyte population ranges from 2–5% in inbred mice, which is doubled in the wild mice [69, 70].

BM is the *bona fide* anatomic location for NK cell commitment and development in mice. Three major lymphoid lineage cell types, T, B, and NK cells, all differentiated from the common lymphoid progenitor (CLP) cells [71]. The expression of IL-15/IL-2 receptor β chain (CD122) is the hallmark of commitment to the NK cell lineage from the common lymphoid progenitor (CLP) cells [72]. Thus, the original definition of NK progenitor (NKP) is a $Lin^{-}CD122^{+}$ cell without cell surface expression of NK-lineage marker NK1.1. However, the $Lin^{-}CD122^{+}NK1.1^{-}$ cells are still a heterogeneous population as approximately only one in ten cells can give rise to NK cells *in vitro* [73]. Recently, with the identification and establishment of innate lymphoid cells (ILCs), the lineage commitment of NK cells has been refined. Now we know the CLPs give rise to the early innate lymphoid progenitors (EILPs) which has the capacity to differentiate into all three ILC lineages and conventional NK cells (**Figure 1.3**) [74]. In addition, the definition of NKPs has now been refined to $Lin^{-}Flt3^{-}CD27^{+}2B4^{+}CD127^{+}CD122^{+}NK1.1^{-}$ cells which have a 50% chance to develop into NK cells *in vitro* [75, 76].

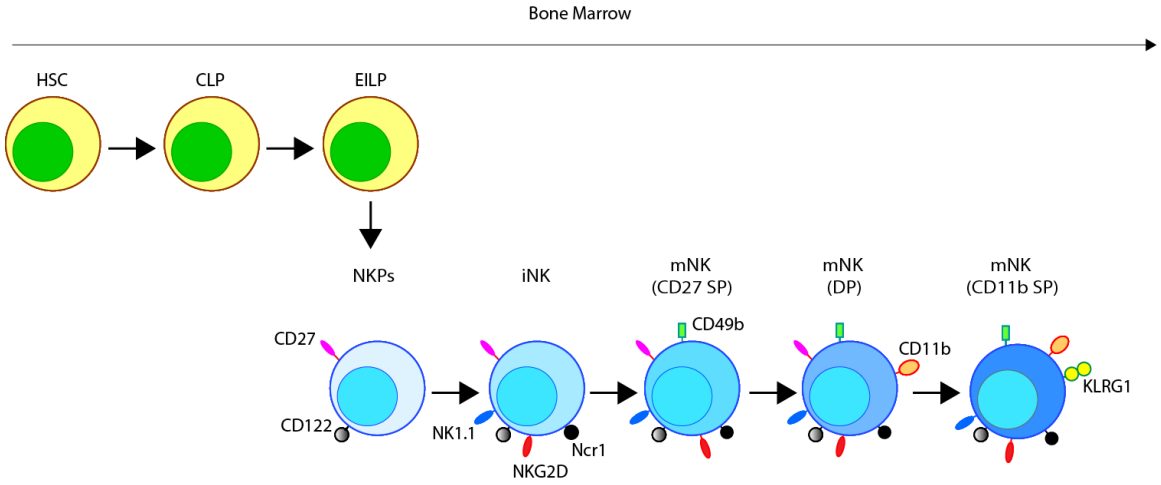


**Figure 1.3. The lineage commitment and differentiation of murine NK cells in the BM**

Downstream of the common lymphoid progenitors (CLPs), a fraction of the early innate lymphoid progenitors (EILP) give rise to the NK progenitors (NKPs) marked by the expression of CD122. After NK-lineage commitment, the activating receptors including NK1.1, NKG2D, and Ncr1 start to express. The absence or presence of CD49b on the cell surface marks the immature NK (iNK) and mature NK (mNK) stage, respectively. The differential expression of CD27 and CD11b further divides the mNK into three developmental stages. The CD27 single positive (SP) NK cells up-regulate CD11b and become CD27/CD11b double positive (DP). The DP stage cells further mature and down-regulate CD27 to be the CD11b SP stage cells, the terminal differentiation stages also marked by the expression of KLRG1. Adopted from Abel et al., *Front. Immunol.*, 2018 [14].

Following commitment, NK lineage cells go through step-wise developmental process to become functionally mature NK cells. The $Lin^{-}CD122^{+}NK1.1^{+}CD27^{+}CD49b^{-}$ population represents the immature NK (iNK) cells (**Figure 1.3**) [67, 77-79]. The activating receptors NK1.1, NKG2D and Ncr1 start to express at this iNK stage [14, 80]. Following the expression of CD49b, the developmental stages of murine NK cells further classified into three stages based on two cell surface markers CD27 and CD11b [78, 81]. The

relatively immature $CD27^{+}CD11b^{-}$ (CD27 single positive, SP) NK cells develop into $CD27^{-}CD11b^{+}$ (CD11b single positive, SP) terminally mature with a transitional stage of $CD27^{+}CD11b^{+}$ (double positive, DP) cells [82]. The terminal CD11b SP NK cells are also marked with expression of KLRG1 (**Figure 1.3**) [83]. The expression of Ly49 receptor family members also happens after the CD49b expression, a group of markers important for functional maturation of NK cells. Although it is generally thought that NK cells have increased functional capacity as they mature, *ex vivo* functional assay has indicated reduced functional activity of the terminal CD11b SP cells compared to the DP cells [81] indicating additional regulatory mechanisms acquired during maturation [14]. As the NK cells proceed to the DP stage, they up-regulates the expression of S1pr5 which facilitates the migration of NK cells to the periphery where they continue the developmental program [84]. The distinct peripheral environment at different anatomic location is likely to further shape the development of NK cells.

1.1.3 Development of human NK cells

Human NK cells are conventionally identified as $Lin^{-}CD56^{+}$ cells (Lin includes CD3ε, CD19, CD14, CD20, and CD34) which account for 5–15% of the peripheral blood lymphocytes in healthy individuals [85, 86]. Unlike murine NK cells which primarily develop in the BM, most of human NK precursors and immature cells are found in the secondary lymphoid organs [86, 87]. Along the human hematopoietic pathway, the lymphoid-primed multipotent progenitors (LMPPs) ($Lin^{-}CD34^{+}CD38^{-}CD90^{-}CD45RA^{+}$) give rise to CLPs ($Lin^{-}CD34^{+}CD38^{+}CD10^{+}$) [88]. A small fraction of the CLPs further differentiates into committed NKPs with no other lineage potential defined recently as $Lin^{-}CD34^{+}CD38^{+}CD123^{-}CD45RA^{+}CD7^{+}CD10^{+}CD127^{-}$ cells (**Figure 1.4**) [89]. Based on the 6-stage NK cell developmental model proposed by Caligiuri, MA and colleagues [86, 90], additional developmental stages potentially exist between the newly defined NKP and $CD56^{+}$ NK cells which warrants further investigation.

Majority of the $Lin^{-}CD56^{+}$ cells are NK-lineage cells with a small fraction mixed with ILC progenitors or ILC-lineage cells [86, 90]. The recently identified cell surface marker NKp80 is useful to tease those cells apart from conventional NK cells which can be defined as $Lin^{-}CD56^{+}NKp80^{+}$ cells (**Figure 1.4**) [91]. Based on the level of CD56 expression, the $Lin^{-}CD56^{+}NKp80^{+}$ cells are further divided into $CD56^{bright}$ and $CD56^{dim}$ NK cells [92, 93]. The $CD56^{bright}$ NK cells express higher level of NKG2A/CD94 and

CD62L and mostly locate in the secondary lymphoid organs [94]. The killer-cell immunoglobulin-like receptors (KIRs) important for the NK cell education in humans is

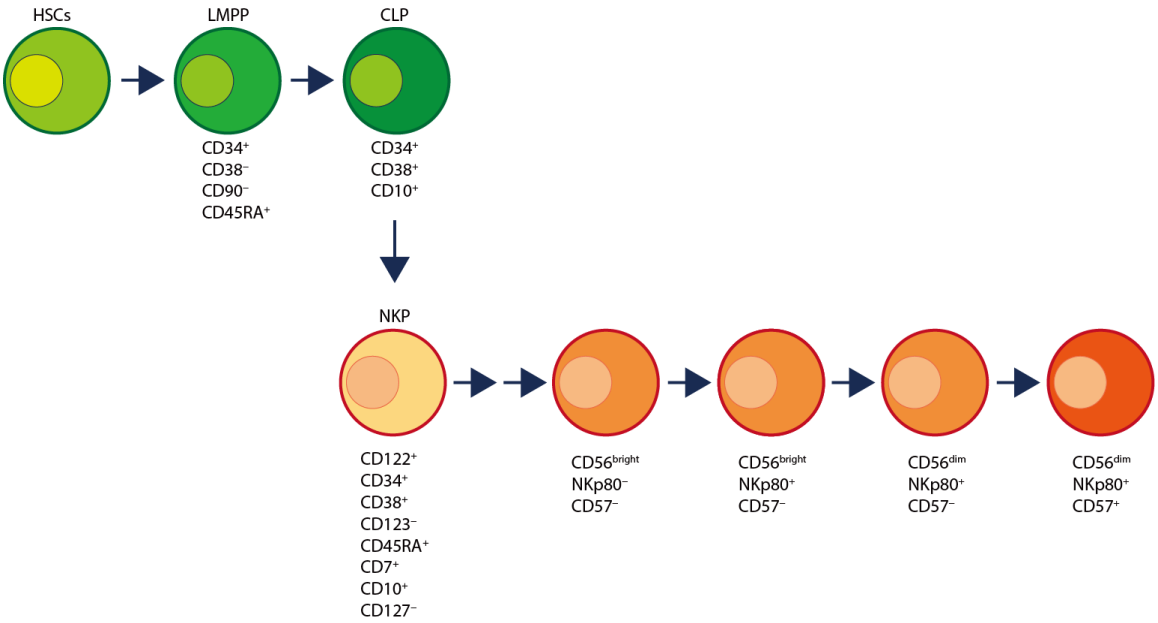


**Figure 1.4. The commitment and differentiation of human NK cells**

Compared to murine NK cells, the commitment and maturation stages of human NK cells are not well-defined. The current human NK progenitors (NKPs) are defined as $Lin^{-}CD34^{+}CD38^{+}CD123^{-}CD45RA^{+}CD7^{+}CD10^{+}CD127^{-}$ cells, arising from a fraction of common lymphoid progenitors (CLPs). The intermediate developmental stages between NKPs and $CD56^{+}$ NK cells remain to be further characterized. The $Lin^{-}CD56^{+}NKp80^{+}$ cells represent the pool of conventional NK cells with no features associated with other ILC-lineages. Based on the expression level of CD56 and CD57, this pool of NK cells can be further divided into three subsets: $CD56^{bright}$, $CD56^{dim}CD57^{-}$, and $CD56^{dim}CD57^{+}$ cells. Substantial evidence indicates the relative immature $CD56^{bright}$ NK cells are precursors of $CD56^{dim}$ NK cells. The $CD56^{dim}CD57^{+}$ population represents the terminally-mature human NK cells. Adopted from Abel et al., *Front. Immunol.*, 2018 [14].

first detectable in this stage [90]. Functionally, $CD56^{bright}$ NK cells have an increased capacity of cytokine production compared to $CD56^{dim}$ NK cells which are potently cytotoxic [86, 93]. The $CD56^{dim}$ NK population is further divided into two groups based on the expression of CD57, where $CD57^{+}$ cells form a terminally mature subset with a greater killing capacity (**Figure 1.4**) [95, 96].

$CD56^{bright}$ NK cells are believed to be the precursors of $CD56^{dim}$ NK cells with a preponderance of evidence supporting this linear progression model [87]. Nevertheless, contradictory reports challenge this dogma [97-99]. Fate mapping experiment using DNA barcode technique in rhesus macaque demonstrates that $CD56^{bright}$ and $CD56^{dim}$ NK cells derive from different precursor populations [98]. Further, individuals with *GATA2* heterozygous mutations have been reported to possess only $CD56^{dim}$ NK cells, apparently bypassing the $CD56^{bright}$ stage [97]. $CD56^{bright}$ NK cells has also been proposed to be an independent ILC1 population based on the function and transcriptome similarity between these two populations [99].

In contrast to the NK subsets defined by the current developmental paradigm, mass cytometry (CyTOF)-based immune profiling has revealed thousands of phenotypically distinct NK cells on the combinatorial expression of 28 cell surface receptors [100]. This contrast emphasizes the importance of further defining the heterogeneity of NK population using other modalities.

1.1.4 Transcriptional regulation of NK cell development

The developmental process of NK cells is precisely regulated by temporal activation of stage-specific transcription factors (**Figure 1.5**). In the early developmental stages, transcription factors Ets-1 and PU.1 has been shown to regulate the transition from CLPs to NKPs, while E4BP4 is critical in the induction of CD122 and NKP commitment [101-104]. E4BP4 also induces the expression of Id2 and Eomes, both of which are critical in immature NK cells development and the transition to the later stages [105-109]. However, E4BP4 seems to be dispensable after the NK-lineage commitment as *Ncr1*$^{iCre}$-mediated deletion of *Nfil3* (gene encoding E4BP4) does not alter the development of NK cells [110].

Although the recently refined NKPs can be detected through *Id2*-reporter mice [75], Id2 itself is dispensable for the commitment of NKPs [107]. However, the Id2-deficient NK cells failed to transit from the immature NK to the mature NK cells [106, 107]. Although Id2 does not contain DNA-binding domain, it can form heterodimer with members from E protein transcription factor family and suppress the transcriptional program controlled by the E proteins [111]. This feature is critical for the maintenance of the NK versus the T cell lineage [107, 112]. In addition, recent study also found that Id2 also tunes the IL-15 signaling during the development of NK cells [108]. Downstream of E4BP4, another transcription factor that is critical for the development of immature NK to the mature NK cells is Eomes [109]. Majority of the Eomes-deficient NK cells are in the relatively immature CD27 SP stage [109]. Moreover, Eomes is also critical for the expression of

CD122, IL-2/15 receptor β chain [109, 113]. Irf2 is also intrinsically required for the differentiation from the iNK to the mNK stage [114, 115]. Specific to the Runx transcription factors, Runx3 is abundantly expressed in the iNK cells [116]. The expression of dominant-negative Runx3 impaired the maturation of iNK cells [116], a phenotype further validated in the Runx3-deficient mice [117]. In addition, transcription factor Tox1 also intrinsically regulates the development of NK cells from the immature to the mature stage [118]. A recent study reported accumulated CD27 SP stage NK cells in *Ncr1*-mediated Gata3-deficient mice [119], although Gata3 is conventionally believed to be the master transcription factor for the development of thymic NK cells [120].

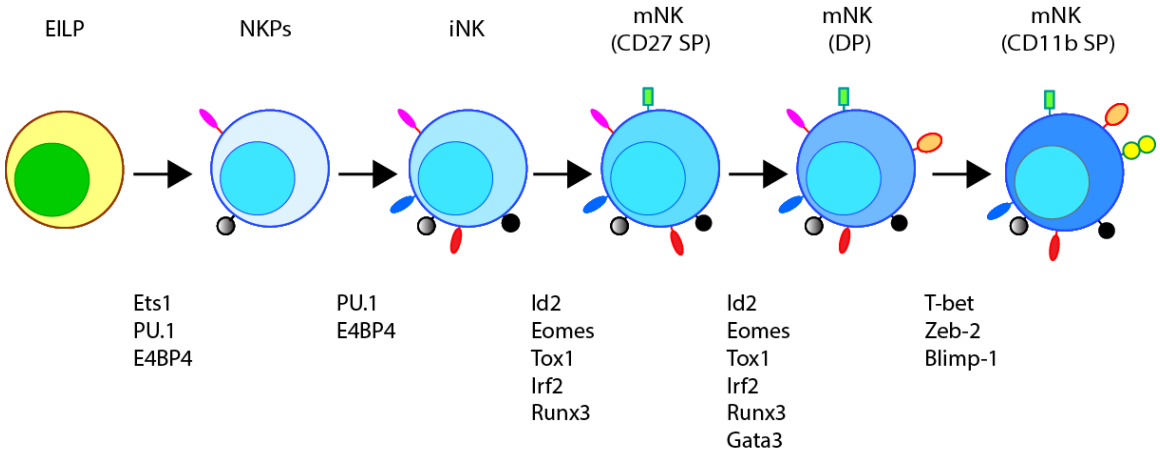


**Figure 1.5. Transcription factors involved in the development of murine NK cells**

The commitment and differentiation of NK cells are tightly controlled by distinct transcription factors. Ets1, PU.1, and E4BP4 are critical for the early commitment of NK cells. E4BP4 directly regulates the expression of CD122. Downstream of E4BP4, Id2 and Eomes are critical in promoting the maturation of iNK along with Runx3, Tox1, and Gata3, although the precise function and regulation of these transcription factors requires further dissection. T-bet is the master regulator of the terminal maturation. Downstream of

T-bet, Zeb-2 and Blimp1 also regulate the terminal differentiation program. Adopted from Abel et al., *Front. Immunol.*, 2018 [14].

T-bet seems to be the master transcription factor governing the terminally mature NK cells indicated by the complete loss of CD11b SP NK cells in T-bet-deficient mice [121]. Although belongs to the same T-box transcription factor family as Eomes, T-bet seems to be dispensable for the expression of CD122 [121]. Both Zeb2 and Blimp1 has been indicated as the downstream targets of T-bet and facilitate the terminal maturation program [122, 123]. In addition, the expression of T-bet is suppressed by another transcription factor FoxO1 in NK cells [124].

The knowledge regarding the transcriptional regulation of NK cell development is mostly obtained from genetical knockout mice. The information regarding transcriptional regulation of human NK cell development is limited mostly due to insufficient *in vitro* or *in vivo* systems to study the differentiation of human NK cells (**Figure 1.6**). The expression of T-box transcription factors EOMES and T-BET in humans seems to follow the similar pattern in mice. The relative immature $CD56^{bright}$ NK cells express higher level of EOMES but lower level of T-BET compared to relatively mature $CD56^{dim}$ NK cells [125]. Individuals with GATA2 mutations selectively lose the $CD56^{bright}$ NK cells which is discussed in detail later [97]. The expression of GATA3 is higher in the $CD56^{bright}$ compared to the $CD56^{dim}$ NK cells [120]. Whether GATA3 is also important for the maintenance of $CD56^{bright}$ NK cells remains to be determined. Both TOX-1 and TOX-2 have been shown to regulate the development of human NK cells [126, 127].

TOX-2 directly binds to the promoter region of *TBX21* (T-BET) and promote the expression of T-BET in human NK cells [127]. Constitutive expression of either ID2 or ID3 in the thymic bipotential T/NK progenitors results in preferential differentiation into NK cells using *in vitro* culture systems, which indicates potential role of Id proteins in the development of human NK cells [128, 129].

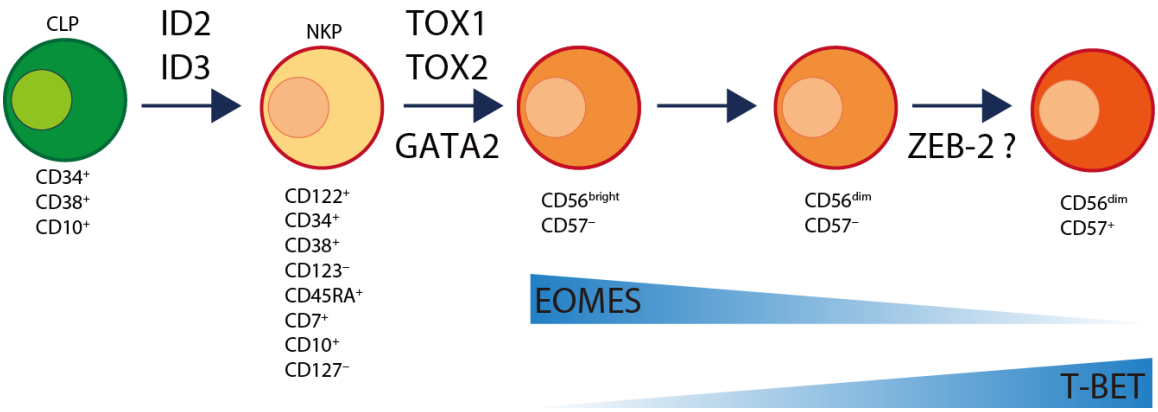


**Figure 1.6. Transcription factors involved in the commitment and differentiation of human NK cells**

Compared to the murine system, less is known about the transcriptional control of human NK cell development. *In vitro* studies have indicated that ID2 and ID3 prefer the NK-lineage differentiation. Both TOX1 and TOX2 are important for the differentiation of NKPs to the $CD56^{+}$ cells. $CD56^{bright}$ NK cells are selectively absent from individuals with *GATA2* mutations. The expression of Eomes and T-bet gradually decreases or increases as the human NK cell mature, respectively. Whether ZEB-2 is also important for the terminal maturation of human NK cells remains to be determined.

1.1.5 IL-15 in the development of NK cells

**Common gamma chain cytokines**

Cytokines are essential mediators for the maintenance and function of the immune system. Specific to the development of NK cells, the common gamma (γc) chain cytokine family is essential as individuals with common gamma chain (CD132) mutations develop severe immunodeficiency with nearly complete loss of NK cells [130]. CD132 deficiency in mice also eradicates the NK compartment [131]. There are five members in the γc family (IL-2, IL-4, IL-7, IL-15, and IL-21), all of which use the γc chain for signaling [132]. Although sharing the γc chain and initiating the JAK-STAT pathway, the distinction among the γc chain cytokine family comes from the unique receptor complexes and the differential activation of distinct STAT molecules.

**IL-15 and trans-presentation**

Through the genetic ablation of individual cytokine members or receptors, the importance of IL-15 in the development of NK cells is now well-established. Both IL-15 and IL-2 can bind to the receptor complex formed by IL-2/15R (CD122) and γc chain (CD132) [133-135]. The difference between these two comes from the distinct a chain of the receptor complex. IL-2 binds to the heterotrimeric receptors composed of CD122, CD132 and IL-2Rα (CD25) with high affinity [136, 137]. In contrast, IL-15 has the similar high-affinity binding with IL-15Rα (CD215) alone [138]. As the expression of IL-15 and IL-15Rα occur in the same cells, this high affinity interaction results in membrane bound IL-

15/IL-15Rα complex [138]. Therefore, the IL-15 signaling initiates through trans-presentation of IL-15 anchored by IL-15Rα in the neighboring cells to the IL-2/15Rβ/γc complex-baring cells (**Figure 1.7.A**) [139, 140]. Genetic deletion of *Il15* or *Il15ra* but not *Il2* results in similar loss of mature NK cells seen in the γc chain-deficient mice, firmly establishing the central role of IL-15 in the development of NK cells [141-143]. Notably, IL-15 seems to be dispensable for the differentiation of NKPs as normal number of NKPs were found in the γc chain-deficient mice [143].

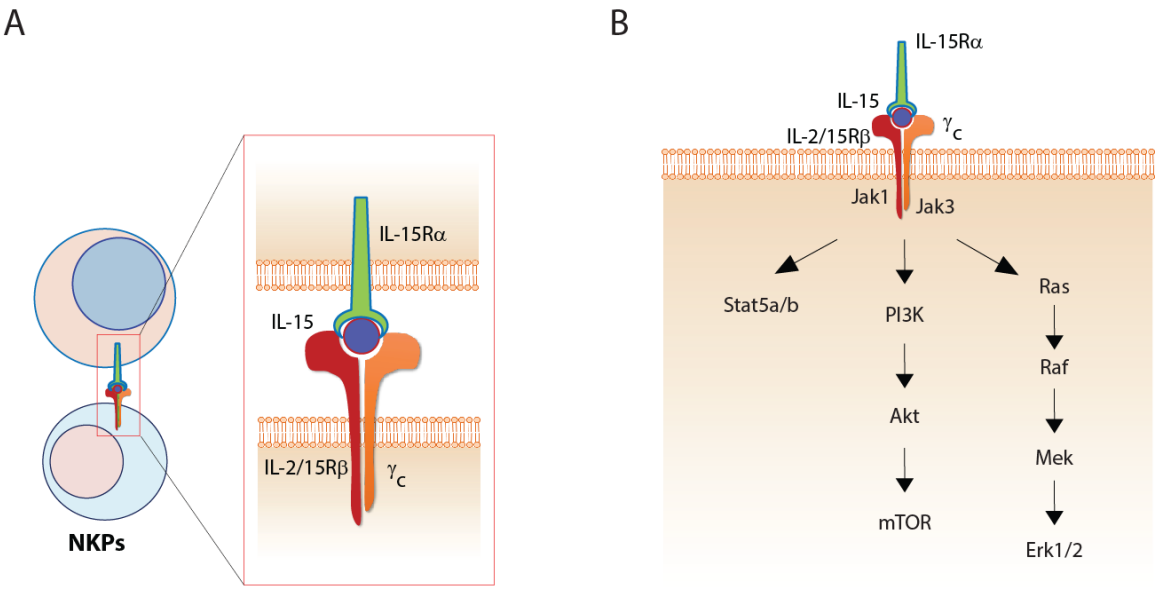


**Figure 1.7. Trans-presentation of IL-15 and IL-15 signaling**

(**A**) Due to the high-affinity interaction between IL-15 and IL-15Rα and their co-expression in the same cells, majority of IL-15 is bound by IL-15Rα on the cell surface and trans-presented to the IL-15/2Rβ/γc receptor complex in the nearby cells, for example NKPs. (**B**) Upon IL-15 binding, three major pathways are initiated: the Jak-Stat5 pathway, the PI3K-Akt-mTOR pathway, and the Ras-Raf-Mek-Erk1/2 MAPK pathway.

**IL-15 signaling**

Sharing the same IL-2/15Rβ/γc receptor complex, much of the signaling events downstream of IL-15 is learned from the IL-2 signaling. Downstream of IL-15 receptors, three major pathways are initiated including the Jak1/3-Stat5a/b pathway, the PI3K-mTOR pathway, and the MAPK pathway (**Figure 1.7.B**) [144]. As IL-15 is critical to the NK-lineage, recent works have revealed the unique role of each signaling component in the development of NK cells. Upon IL-2 or IL-15 binding, Jak1 and Jak3 are associated with the IL-2/15Rb and γc [145-148]. As kinases, Jak1 and Jak3 phosphorylates Tyr392 and Tyr510 at the H-region which serve as critical docking sites for downstream functional proteins including transcription factors Stat5a and Stat5b [149, 150]. Serving as the first signaling module, it is not surprising that loss of Jak3 completely eradicate NK cells in mice [151]. Downstream of Jak1/3, both Stat5a and Stat5b are important to maintain the NK pool in mice with Stat5b deficiency resulting in a more severe loss of NK cells compared to Stat5a deficiency [152, 153]. Recent work has also demonstrated a correlation between the number of splenic NK cells and the copy number of Stat5a/b [154]. One critical function of Stat5 is to maintain the expression of anti-apoptotic protein Bcl2 to sustain the survival of NK cells [154-156].

Another critical pathway initiated downstream of IL-15 receptors is the PI3K-mTOR pathway. Class IA PI3Ks include p100a, p100b, and p100d and they are recruited to the membrane-proximal via a regulatory subunit [157]. Both p100b and p100d have been shown to be critical for the development of NK cells, although the detailed mechanisms

require further investigation [158-160]. The function of p100a in the development of NK cells has not been tested. Downstream of PI3K, the metabolic sensor mTOR is also critical for the development of NK cells which is discussed in detail later [161]. Although MAPK pathway has been implicated in the proliferation and effector functions of NK cells [162, 163], its precise role in the development of NK cells remains elusive.

## 1.2 mTOR and mTOR complexes

### 1.2.1 Mechanistic target of rapamycin and mTOR complexes

**Mechanistic target of rapamycin**

As the name illustrated, the protein mechanistic target of rapamycin (previously known as mammalian target of rapamycin, mTOR) is tightly associated with the chemical compound rapamycin (clinically knowns sirolimus) (**Figure 1.8.A**). In fact, the discovery of mTOR comes after rapamycin. In 1964, soil samples from the South Pacific island of Rapa Nui (also known as Easter Island) were collected by a Canadian expedition for the purpose of discovering anti-microbial agents. Rapamycin were found in one of these samples with high anti-fungi, anti-tumor and immunosuppressive effects [164-166]. It was named based after the island's name Rapa. In 1992, Chung and colleagues found that it is important for Rapamycin to form complexes with peptidyl-prolyl isomerase FKBP1A (also known as FKBP12) to exhibit its anti-proliferation function [167, 168]. Later on, the genetic screening of rapamycin resistance identified TOR/DRR gene. In 1994, three independent groups identified the target of rapamycin-FKBP12 complex in mammalian cells and named it as mammalian target of rapamycin which was changed to mechanistic target of rapamycin later [169-171]. For the past twenty-five years, myriad researchers have worked on this particular protein and revealed its essential role in regulating the growth of organisms [172].

**mTOR complexes**

The mechanistic target of rapamycin (mTOR) is a 289 kDa evolutionarily conserved serine/threonine kinase that belongs to the phosphoinositide 3-kinase-related protein kinases (PIKK) family [173]. Along with its associated proteins, mTOR forms two structurally distinct complexes, mTOR complex 1 (mTORC1) and mTOR complex 2 (mTORC2) with unique substrate specificities and functions (**Figure 1.8.B**) [173]. mTORC1 consist of mTOR, Raptor (regulatory protein associated with mTOR), mLST8 (mammalian lethal with Sec13 protein 8), PRAS40 (proline-rich Akt substrate of 40 kDa), and DEPTOR (DEP domain containing mTOR interacting protein) [173]. Genetic studies have demonstrated that Raptor is the critical protein in the formation of mTORC1 [174, 175]. On the other hand, mTORC2 comprises mTOR, Rictor (rapamycin-insensitive companion of mTOR), mSin1 (mammalian stress-activated protein kinase interacting protein 1), Protor1/2 (protein observed with Rictor-1/2), mLST8, and DEPTOR [173]. Both Rictor and mSin1 are essential for the formation of mTORC2 [176-180].

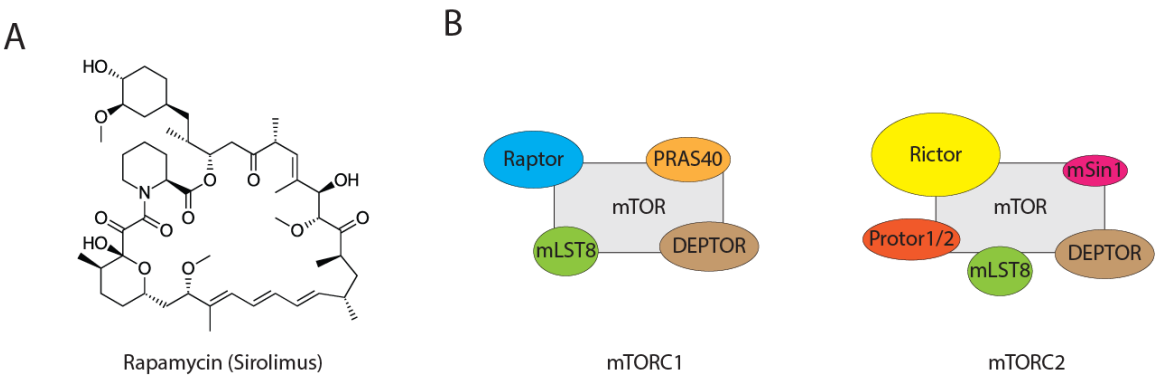

**Figure 1.8. mTOR and mTOR complex**

The discovery of anti-fungi chemical compound rapamycin reveals the mechanistic target of Rapamycin (mTOR), a critical metabolic protein and its associated complexes. (A) The chemical structure of rapamycin. (B) The composition of mTOR complex 1 (mTORC1) and mTOR complex 2 (mTORC2). DEPTOR and mLST8 are the shared components of the two complexes. Raptor and PRAS40 are unique to mTORC1, while Rictor, mSin1, and Protor1/2 are unique to mTORC2.

There are five major structural domains of mTOR: the tandem HEAT domain, the FAT (FRAP, ATM, and TRRAP, all PIKK family members) domain, the FRB (FKBP12/rapamycin binding) domain, and the FATC (FAT C-terminus) domain (from N-terminus to C-terminus) (**Figure 1.9**) [181]. The tandem HEAT domain mediates the protein-protein interaction between mTOR and Raptor as well as the dimerization of two copy of mTORC1 [182-184]. In addition to tandem HEAT domain, Raptor contains a N-terminus conserved domain and seven WD40 repeats which might also interact with mTOR or other mTORC1-associated proteins (**Figure 1.9**). The domain structure is less clear for the Rictor. Through protein sequence and domain database, it predicted that Rictor also contains HEAT repeats and WD40 domains, presumably for interaction with mTOR [185]. Pleckstrin homology domains may also present in Rictor and mediate the signal transduction and subcellular localization [185]. Another *bona fide* mTORC2 component, mSin1, has a central conserved domain, a Ras-binding domain and a C-terminal pleckstrin homology domain [186, 187]. The PH domain of mSin1 has been shown to interact with the kinase domain of mTOR (**Figure 1.9**) [188].

The different composition of the accessory proteins determines that only the FRB domain in mTORC1, but not mTORC2, is accessible to the FKBP12/rapamycin complex. This results in potent inhibition of mTORC1, but not mTORC2, by rapamycin. However, prolonged incubation with rapamycin also inhibits mTORC2 signaling due to compromised formation of mTORC2 as rapamycin-bound mTOR is unable to be incorporated into mTORC2 [189].

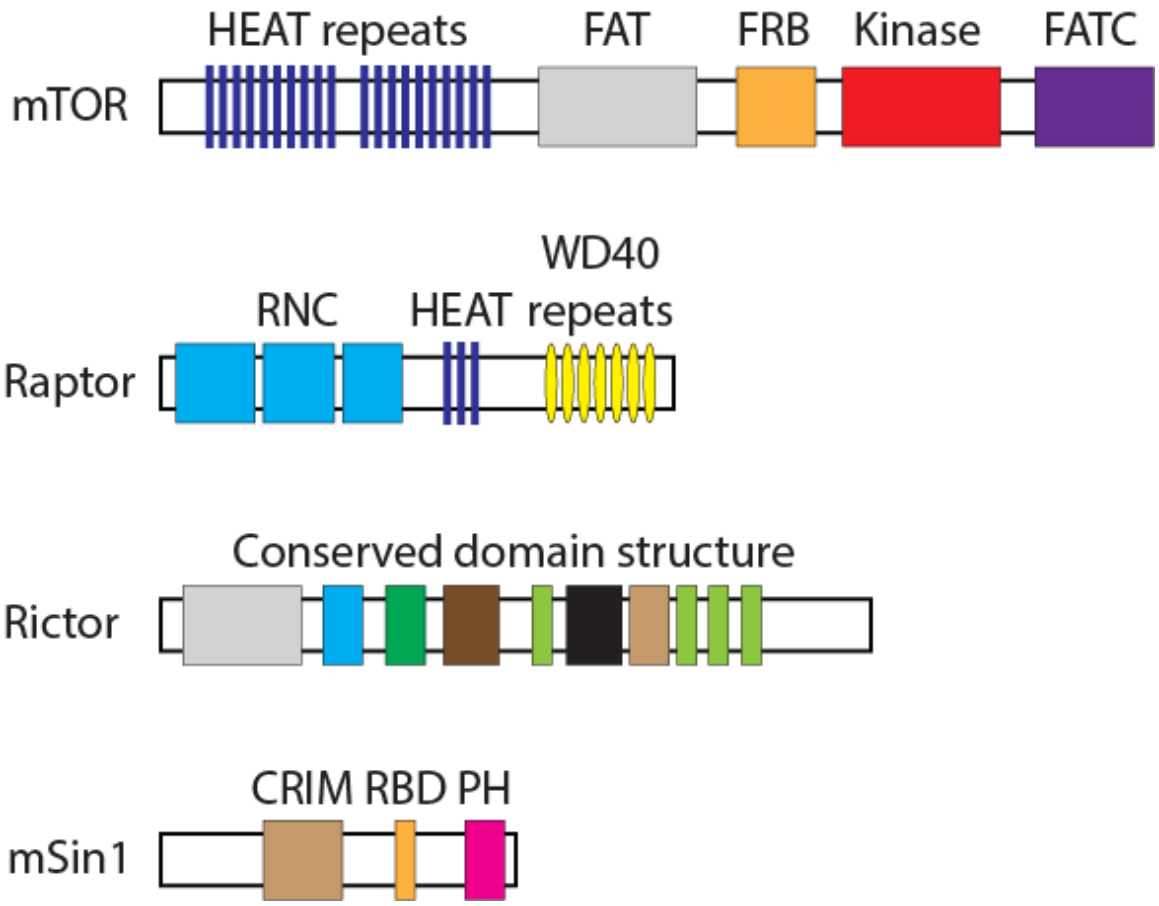


**Figure 1.9. Protein domain structure of mTOR, Raptor, Rictor, and mSin1**

HEAT repeats: tandem repeats of the anti-parallel α-helices important for protein-protein interaction; FAT: a domain found common in PIK-related kinases subfamilies **F**RAP, **A**TM and **T**RRAP subfamilies; FRB: FKBP12-rapamycin-binding (FRB) domain; FATC: FAT C-terminus; RNC: Raptor N-terminal conserved

domain; WD40 repeats: tandem repeats of a structural domain composed about 40 amino acids terminating with tryptophan and aspartic acid (WD). CRIM: conserved region in the middle; RBD: Ras-binding domain. PH: pleckstrin homology domain. The functional domains of Rictor are unknown with some structure domains that are conserved among species.

1.2.2 mTOR complex 1 signaling

**Upstream of mTORC1**

The activation of mTORC1 is tightly controlled by the availability of nutrients as mTORC1-mediated anabolism requires sufficient energy and metabolites for synthesis of macromolecules. Growth factor and mitogen-defendant pathways are potent stimuli for the activation of mTORC1 (**Figure 1.10**). A central molecule that govern the activation of mTORC1 through pro-growth signaling is the heterotrimeric Tuberous Sclerosis Complex (TSC) comprising TSC1, TSC2, and TBC1D7 [190]. TSC functions as a GTPase activating protein (GAP) that inhibit the activity of small GTPase Rhab which binds and activates mTORC1 [191-193]. Both PI3K-PDK1-Akt and MAPK pathways promotes the phosphorylation of TSC2 and inhibits the function of TSC [194-197]. Inhibition of TSC further allows the GTP-bound Rhab to activate mTORC1 (**Figure 1.10**).

Besides the growth factor-like stimuli, the sensing of sufficient amino acids is also required for the activation of mTORC1. The presence of amino acids anchored mTORC1 in the lysosomal membrane through the heterodimeric Rag GTPase [198, 199]. This enable activation of mTORC1 by Rheb which is also present in the lysosomal membrane [200]. Under cellular stress conditions, the activation of mTORC1 is suppressed mainly through AMPK-mediated phosphorylation and activation of TSC2 or direct phosphorylation of Raptor [201, 202]. Inhibition of Rag GTPases has also been shown to contribute to the inhibition of mTORC1 [203].

**Downstream of mTORC1**

As activation of mTORC1 promotes cellular growth and proliferation, the downsteam targets of mTORC1 are often involved in synthesis of protein, lipid, and nuclear acids. The best characterized downstream targets of mTORC1 are 4EBPs and S6K1, both of which are highly involved in protein synthesis pathway (**Figure 1.10**). The major mRNA translation pathway in the cell, 5′-cap-dependent mRNA translation, requires the formation of eIF4F complex [204]. One critical component in the eIF4F complex is eIF4E which recognizes the 5′-cap of mRNA [204]. 4EBPs bind eIF4E and inhibit the assembly of the eIF4F complex which in turn inhibit the 5′-cap-dependent mRNA translation [205]. mTORC1 sequentially phosphorylates multi-sites on 4EBPs and dissociate 4EBPs from eIF4E to promote 5′-cap-dependent mRNA translation [206, 207]. Studies have also demonstrated that mTORC1-4EBPs axis mostly affect a group of mRNAs named 5′-TOP mRNA which contains 5′-terminal oligopyrimidine motif [208, 209]. Majority of protein products translated from the 5'-TOP mRNA are involved in protein synthesis [209].

Another well-established mTORC1 target, S6K1 also regulates protein translation. mTORC1 phosphorylates S6K1 at Thr389 in the hydrophobic motif which result in conformational changes that leads to further phosphorylation by PDK1 [210-212]. The phosphorylated and activated S6K1 promotes 5′-cap-dependent mRNA translation by phosphorylating eIF4B, a critical component of eIF4F complex [213]. S6K1 can also phosphorylate and promote degradation of PDCD4, a negative regulator of mRNA translation [214]. Besides promoting protein synthesis, S6K1 also phosphorylates and

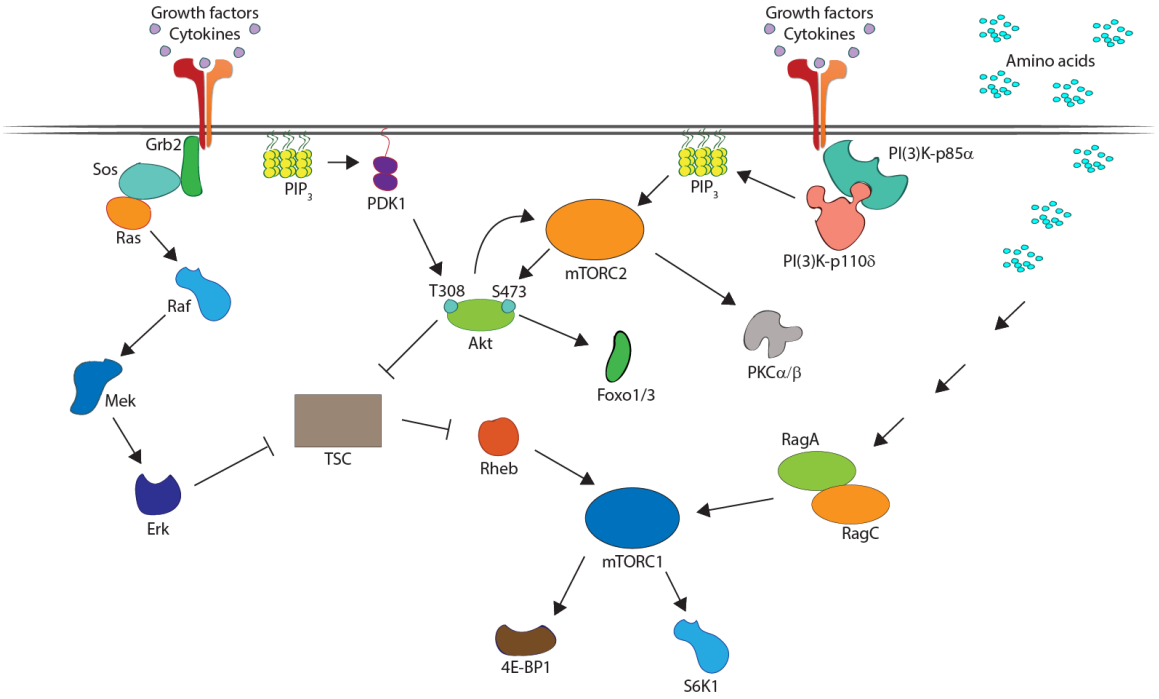


**Figure 1.10. The upstream and downstream of mTORC1 and mTORC2**

Growth factors and cytokines are potent stimulators of the PI3K-Akt-mTOR pathway. Specific to the mTORC1 pathway, the tuberous sclerosis complex (TSC) functions as a GTPase-activating protein (GAP) which inhibits the activity of Rheb, a small GTPase absolutely required for the activation of mTORC1. Thus, TSC is a central negative regulator of mTORC1 signaling. The activated Akt or Erk, downstream of PI3K-Akt or MAPK pathway, respectively, phosphorylates TSC and inhibits its GAP activity resulting in activation of mTORC1. In addition, amino acids are required for anchoring mTORC1 on the lysosomal membrane where Rheb locates. This is achieved through the Rag complex. Downstream of mTORC1, 4E-BPs and S6Ks are the major targets. As for the mTORC2 pathway, $PI(3,4,5)P_3$ induces conformational changes of mSin1 and releases the block of the kinase domain of mTOR. Akt can also phosphorylates mSin1 and in turn activates mTORC2. Downstream of mTORC2, the major target in the phosphorylation of Akt at Serine473 site. This phosphorylation enables Akt to phosphorylates and inhibits FoxO1. PKC kinase family is also the target of mTORC2.

activates sterol regulatory element-binding protein 1 and 2 (SREBP1 and SREBP2) which promotes *de novo* lipid synthesis that are critical for cell growth and proliferation [215]. In addition to S6K1, mTORC1 also has been shown to promote SREBP pathway through regulation of lipin 1 [216]. In addition to lipid metabolism, recent studies have established the mTORC1-S6K1 axis in regulating the *de novo* purine and pyrimidine synthesis [217-219].

1.2.3 mTOR complex 2 signaling

**Upstream of mTORC2**

Unlike the specific inhibition of mTORC1 by rapamycin, currently there is no mTORC2-specific inhibitor, which at least partially delays the study of mTORC2. For a long time, the upstream activator of mTORC2 is unknown. The inhibition of mTORC2 activity by wortmannin, a specific PI3K inhibitor, has led to the speculation that mTORC2 is downstream of the PI3K pathway [220]. Indeed, Liu et al., has found that the pleckstrin homology (PH) domain of mSin1 interacts with the kinase domain of mTOR and inhibits the kinase activity of mTORC2. The PtdIns(3,4,5)$P_3$ generated by PI3K interacts with the PH domain and releases the inhibition of the kinase domain of mTOR (**Figure 1.10**) [188]. Besides this allosteric activation of mTORC2, Akt, downstream of PI3K, phosphorylates mSin1 at Thr86 site and promotes the activation of mTORC2 (**Figure 1.10**) [221]. Whether this phosphorylation also promotes the release of inhibition mediated by the PH domain remains unknown. In addition, Zinzalla et al., has reported that PI3K signaling promotes the association of mTORC2 with ribosome and this spatial regulation also induces the activation of mTORC2, although the mechanism behind this observation is unknown [222]. Interestingly, mTORC1 can indirectly influence the activation of mTORC2 through a negative feedback loop going through S6K1-Grb2 or S6K1-IRS1 axis to inhibit insulin-mediated PI3K activation [223-226].

**Downstream of mTORC2**

The most well-characterized downstream targets of mTORC2 is Akt (**Figure 1.10**). Phosphorylation of Akt at Ser473 site is exclusively mediated by mTORC2 and therefore is standard measurement of mTORC2 activity [180, 227]. Although Akt is upstream of mTORC1, phosphorylation of Ser473 on Akt does not seem to affect the activation of mTORC1 [227]. Mechanistically, phosphorylation of Thr308 mediated by PDK1, instead of Ser473, is critical for the kinase activity of Akt [228, 229], while the Ser473 phosphorylation seems to dictate the substrate specificity of Akt [179]. Akt-mediated phosphorylation of FoxO1/FoxO3a requires mTORC2 and this axis is important in regulating apoptosis and proliferation (**Figure 1.10**) [179, 227].

Before the identification of Akt downstream of mTORC2, two independent groups have found another protein within the same AGC kinase family, PKCα that is phosphorylated by mTORC2 and regulates cytoskeleton remodeling [176, 177]. Subsequently, more members from the PKC family were found to be the targets of mTORC2 and involved in the regulation of cytoskeleton (**Figure 1.10**) [230, 231]. Moreover, AGC family kinase SGK1 which regulates the ion transport is also identified to be the target of mTORC2 [232].

1.2.4 mTOR in the immune system

**mTOR in the adaptive immunity**

Being the metabolic sensor that governs fundamental cellular events, mTOR plays a critical role in almost all immune cells. More knowledge has been gained on the role of mTOR in adaptive immune branches, especially T cells [233]. mTORC1 has been shown to be essential for T cell aviation and clonal expansion. Naïve $CD4^+$ T cells lack mTOR fail to differentiation of into Th1, Th2 or Th17 under different skewing conditions *in vitro* and *in vivo* [234, 235]. Specifically, mTORC1 is more important for the differentiation of Th1 and Th17 cells [234, 235], while mTORC2 regulates the differentiation of Th2 cells [236]. Surprisingly, inhibition or conditional deletion of mTOR in T cells promotes regulatory T cells differentiation and this skewing phenotype depends on inhibition of both mTORC1 and mTORC2 [235]. However, it is important to point out that although excessive mTORC1 activity impairs the differentiation and function of regulatory T cells, the expression of effector functional molecules including ICOS and CTLA-4 in regulatory T cells requires basal activity of mTORC1 [237]. In addition, recently, two independent groups reported the critical role of both mTORC1 and mTORC2 in regulating the differentiation of Tfh cells critical to the humoral response [238, 239].

As for $CD8^+$ T cells, inhibition of mTOR can promote effector to memory differentiation with more potent recall responses[240, 241]. Inhibition or disrupting the formation of either mTORC1 or mTORC2 promotes the memory phenotype though through distinct

mechanisms [233, 240-242]. The phenomenon that mTOR activation is critical for the generation of effector T cells while mTOR inhibition promotes the regulatory and memory population formation is consistent with the unique metabolic profiles associated with these cell types [243]. Both effector $CD4^+$ and $CD8^+$ T cells switch from catabolism to anabolism which requires the activation of mTOR [244-247]. In contrast, the regulatory and memory T cells mainly rely on AMPK-mediated fatty acid oxidation for their maintenance [248, 249].

mTOR also plays an indispensable in the development and functions of B cells [250]. mTORC1 has been shown to be critical in regulating the development of early B cell development downstream of IL-7R signaling. Deletion of *Rptor* or rapamycin treatment block the B cell development in the pre-B cell stage [251, 252]. In contrast, mTORC2 regulates the development of mature B cells [253, 254]. In terms of the germinal center (GC) response and antibody production, specific disruption of mTORC1 results in reduced GC size, antibody production, somatic hypermutation and immunoglobin class switching [255-257]. Genetic deletion of *Rictor* also resulted in reduced antibody response [258]. However, studies with low-dose mTOR kinase inhibitors revealed increased immunoglobin class switching and high-affinity antibody generation implying the level of mTORC2 activation matters [259].

**mTOR in the innate immunity**

Interestingly, opposite to the pro-inflammatory role of mTOR in adaptive immune response, mTOR rather plays an anti-inflammatory role in innate immune system [260]. Both pharmacological inhibition of mTOR and genetic ablation have induced increased production of IL-12 from monocytes or primary myeloid DC [261, 262]. mTORC1 and mTORC2 inhibit the induction of IL-12 through different mechanisms [263, 264]. On the contrary, both complexes positive regulates the expression of immunosuppressive cytokine, IL-10. mTOR is also involved in macrophage polarization [261-263, 265]. Consistent with the anti-inflammatory role, both mTOR complexes seems to promote M2 macrophage differentiation while inhibit the inflammatory M1 macrophage formation [266-268]. In addition, mTOR also negatively influences the antigen-presenting process. Inhibition of mTOR increases the expression of co-stimulatory molecule CD86 and decreases the expression of inhibitory molecule PD-L1 [262, 269-271]. In contrast, constitutive activation of mTORC1 results in reduced expression of MHC II molecules [272]. This rather contradictory regulation of inflammation through mTOR in innate and adaptive immune response is proposed be a regulatory mechanism that tightly controls the amount of inflammation during infection [260].

1.2.5 mTOR in NK cells

Compare to other immune cell types, the role of mTOR in NK cells biology has only been revealed recently. The most studied role of mTOR in NK cells is IL-15-mediated NK cell priming [161, 273, 274]. Cytokines can rapidly and continuously activate NK cells especially during early phase of infection [275]. Among those cytokines, IL-15 has been shown to be critical for NK cell development and effector functions [275, 276]. Low dose of IL-15 is sufficient to sustain survival signaling in NK cells, while high dose of IL-15 promotes NK cell proliferation and effector molecules expression [161, 275]. Marcais A. et al., demonstrated the critical role of mTOR in proliferation and granzyme B expression-mediated by IL-15 during viral infection using a NK cell-specific *Mtor* knockout mouse [161]. They also demonstrated that NK cell development is impaired in these mice [161]. Most of the functional defects have been attributed to mTORC1 due to similar alterations induced by rapamycin [273, 277]. mTORC1-mediated glycolysis has been related to the function of NK cells [274, 277]. Immunosuppressive cytokine TGF-β suppresses the function of NK cells through inhibition of mTORC1 [278]. Besides cytokines-mediated signaling, mTOR is also activated downstream of NK activating receptors and its activity is associated with the responsiveness of the cells [279]. The role of mTORC2 in NK cells, however, is completely lacking. Despite the important role of mTOR in NK cell development and effector functions, there are still important questions regarding each mTOR complex in the biology of NK cells. Some of them are: 1) What is the differential role of each mTOR complex in different stages of NK cell development? 2) Is there a role of mTORC2 in IL-15-mediated NK cell activation? 3) What is the role of each mTOR complex in activating receptor-mediated activation of NK cells? 4) What

are the underlying mechanisms that each mTOR complex utilizes in regulating development and effector functions of NK cells? Given the central role of mTOR in fundamental cellular functions, it is necessary and essential to further study the role of each mTOR complex in the biology of NK cells.

## 1.3 GATA2 and *GATA2* mutations

### 1.3.1 GATA2

#### GATA transcription factor family

The GATA transcription factor family is mostly known for its critical role in the development of organisms ranging from early embryonic development to later specific cell lineage determination in various tissues [280, 281]. In vertebrates, the family contains six members (GATA1/2/3/4/5/6) with similar domain structures (**Figure 1.11**). As transcription factors, all GATA members contain two highly conserved zinc-figure DNA binding domains [282]. These domains recognize consensus DNA sequencing (A/T) GATA (A/G) which the family is named after [282]. The N-terminus contain the transcriptional activation domains which are involved in binding other transcription factors or chromatin modulators [280, 283]. The N- and C-terminals have less similarity among the six members, which are responsible are the functional diversity [280].

Based on the expression and function pattern, originally, GATA1/2/3 were considered as one subgroup that is critical for the hematopoietic system, while GATA4/5/6 are grouped together as the cardiac GATA subgroup [280]. As we now know that the expression and function of the GATA family range to almost every tissue in the body, this classification is no longer precise. Unlike most of transcription factors which require open chromatin for binding, GATA family members function as pioneer transcription factors that bind DNA and promote the loosen of chromatin by recruiting other co-factors [284-287]. In

addition, the expression of one GATA family member can be tightly regulated by another member of the family known as the “GATA switch” [288]. This regulation enables precise temporal expression of specific family members that serve unique and pivotal functions [288].

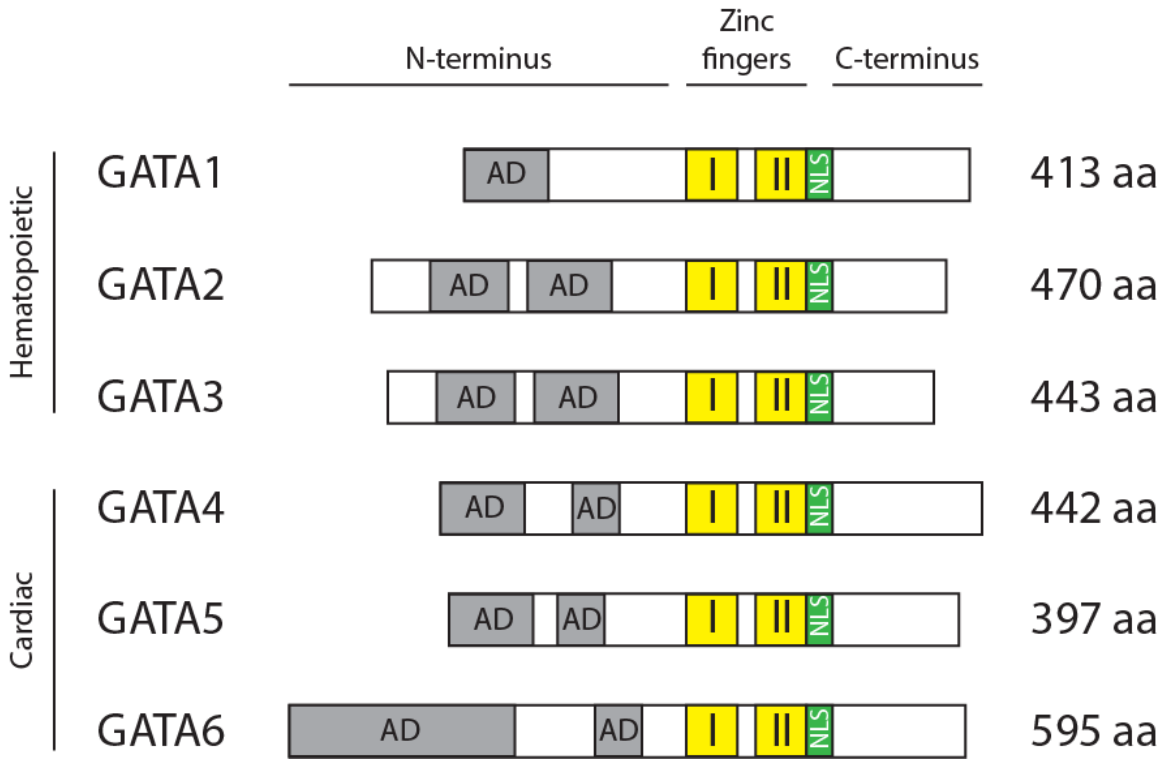


**Figure 1.11. Domain structure of the GATA family transcription factors**

Based on the expression and functional importance, GATA1/2/3 are grouped together as the hematopoietic GATA, while GATA4/5/6 are named as the cardiac GATA. The domain structure among the GATA family is mostly conserved in the zinger finger DNA-binding domains. The activation domain (AD) in the N-terminus and the C-terminus are less conserved and dictate the functional diversity of distinct GATA factors.

**GATA2 in hematopoiesis**

Being the member of the hematopoietic GATA2 subgroup, GATA2 plays an essential role in the hematopoiesis. Mice with homozygous deletion of GATA2 die around E10.5 due to severe anemia [289]. Although the mice were live with heterozygous deletion of GATA2, the adult hematopoietic stem cells were significantly impaired with increased cell death and reduced self-renew capacity [290]. The vital role of GATA2 in maintain the hematopoietic stem cells and progenitor cells are well-established in both mice and human [291-294]. GATA2 also play important roles in lineage specification during the hierarchical hematopoietic cell differentiation. GATA2 has been shown to be critical in mast cell development [291]. Moreover, GATA2 favors the differentiation of megakaryocytes over erythroid cells from the megakaryocyte-erythroid progenitor cell (MEP) [295]. In addition, GATA2 is also critical for the development of DCs and antagonize the expression of GATA3 in DC progenitor cells to suppress the differentiation of lymphoid lineage cells [296].

**GATA2 in the development of other tissues**

Besides the pivotal role of GATA2 in the development of hematopoietic system, recent studies have uncovered the important function of GATA2 in the development of other tissues. Rescue experiments using GATA2 artificial chromosome in *Gata2*$^{-/-}$ mice revealed critical role of GATA2 in the urogenital development [297]. GATA2 has also shown to be important in regulating lymphatic vasculature in both mice and human [298, 299]. Moreover, GATA2 regulates the self-renew of mesenchymal stem cell and

differentiation of adipocytes and osteoblasts [300-302]. In addition, GATA2 is also important for the development of sympathetic neurons and midbrain GABAergic neurons [303, 304].

1.3.2 GATA2 deficiency syndrome

**Heterozygous *GATA2* mutations in human**

Much of the knowledge related to the functions of GATA2 came from the patients with naturally occurring *GATA2* heterozygous mutations. The human GATA2 gene locates in the long arm of chromosome at position 21.3 [305, 306]. In 2009, a group from France reported a large interstitial 3q21.1-q21.3 deletion in a pediatric patient, the first likely reported GATA2 mutation case [307]. So far there are more than 200 heterozygous *GATA2* mutations cases reported [308, 309]. Almost around the same time, GATA2 mutations have been linked to several clinical diseases including AML, MDS, MonoMAC syndrome, Emberger syndrome, and DCML deficiency [310-313]. Now we termed these *GATA2* mutation-mediated clinical symptoms as the "GATA2 deficiency syndrome" [314, 315].

Within the germline *GATA2* mutation cases, one-third of them are inherited with the rest happened *de novo* [305]. The single nucleotide polymorphism resulting in single amino acid substitution represents the most prevalent mutation type with the T354M mutation represents nearly half of all reported *GATA2* mutations [305]. The clinical symptoms resulted from these mutations are mostly due to GATA2 haploinsufficiency as the frame-shift or gene deletion mutation has the similar clinical manifestation compared to the amino acid substitution [305, 314]. T354M mutation has also been shown to have a dominant negative effect, while one gain of function mutation L359V has been reported [310, 316].

**Clinical symptoms**

The disease onset, penetration, and clinical manifestation vary significantly among patients with *GATA2* mutations. Recently, two large cohort studies revealed that the disease onset ranges from 5 to 55 years old [308, 309]. The most consistent symptoms in these patients are the loss of B cells, NK cells, and mononuclear cells which happen gradually as the disease progresses [308, 309]. The clinical asymptomatic GATA2 mutation carriers have about 90% chance of developing MDS eventually [305, 308]. The critical role of GATA2 in maintaining the hematopoietic stem cells is likely contributes to part of the symptoms. In contrast with the requirement of continuous replenishment, T cells can persist in the adult without the stem-cells derived precursor cells. Therefore, the number of T cells is largely unaltered in these patients. However, an inversion of CD4 versus CD8 T cell ratio has been observed in some of the patients which has been linked to the chronic infection status in these patients [305, 308, 312].

A direct consequence of the immunological deficiency caused by *GATA2* mutations is the pathogenic infections. The most frequent infections seen in these patients are human papillomavirus (HPV) infection and mycobacteria infection [305, 314]. In addition to infections, the incidence of solid tumor malignancy is also higher in patients with GATA2 mutations, notably the HPV and EBV-related neoplasia [308, 309]. Due to the loss of alveolar macrophages, patients are likely to have pulmonary misfunction and prone to develop pulmonary alveolar proteinosis (PAP) [317]. Moreover, consistent with

GATA2 in regulating the development of lymphatic vasculature [298, 299], lymphedema has also happened in some of the patients especially with whole gene deletion of GATA2 [318].

**Treatment**

Hematopoietic stem cell transplantation is the still the most efficient way to treat patients with GATA2 deficiency [319, 320]. With diverse onset and disease progression, there is currently no precise guidelines regarding the time of transplantation. However, transplantation prior to the onset of leukemia and severe complications is encouraged [315]. Besides bone marrow transplantation, the antibiotics could help to prevent the bacterial infection especially the mycobacteria [305, 315]. As the immune system is less impaired in the early stage of the disease, it is prudent to vaccinate children carrying GATA2 mutation against HPV [315]. As the clinical symptoms progress over the years, it is important to monitor patients' status regularly especially the blood count, bone marrow biopsy and pulmonary function [305, 315].

1.3.3 NK cells in GATA2 deficiency syndrome

Mace et al. conducted the first detailed analysis of NK cells in patients with *GATA2* heterozygous mutation [97]. The most important conclusion from the study is that $CD56^{bright}$, but not $CD56^{dim}$, NK cells are missing in these patients, which was validated later by a larger cohort study [97, 308]. $CD56^{bright}$ NK cells are believed to be the precursors of $CD56^{dim}$ NK cells [321]. The selective absent of $CD56^{bright}$ NK cells seems to contradict to the well-established ontogenetic relationship between these two human NK subsets. A reduced number and impaired function of the $CD56^{dim}$ compartment is also observed [97, 308]. *In vitro* differentiation study indicated that GATA2 is intrinsically required for the differentiation of NK cells from $CD34^{+}$ precursors [97]. The compromised renew and differentiation of hematopoietic stem cells partially contribute to the reduced number of NK cells. There is more GATA2 protein present in the $CD56^{bright}$ compared to the $CD56^{dim}$ NK cells consistent with a more pronounced defect in the $CD56^{bright}$ compartment [97]. Besides the possibility of independent precursor of $CD56^{dim}$ NK cells, there are other potential mechanisms could explain this phenomenon. GATA2 could be more important for the homeostatic maintenance of $CD56^{bright}$ NK cells proposed by the authors from the first report [97]. The expression of CD56 itself requires GATA2 which potentially masks the true $CD56^{bright}$ cell identity in those patients [321]. More detailed work is required to address these hypotheses, though it is extremely rare to find patients with *GATA2* mutation that still have some $CD56^{bright}$ NK cells in the blood. As more $CD56^{bright}$ NK cells are found in the secondary lymphoid organs, it is also valuable, if possible, to evaluate NK cells in these organs in patients with *GATA2* mutation. A recent study also found that patients with GATA2 mutation still contain

adaptive NK cells which potentially relates to the frequent viral infections in these patients [322]. In addition, the expression of the chemokine receptor, CXCR4 is reduced on NK cells from these patients resulting in impaired migratory response to the ligand, CXCL12 *in vitro* [323]. The physiological significance of this observation is unknown.

# Chapter 2 – Experimental Procedures

## 2.1 Mice

*Rptor*$^{fl/fl}$, *Rictor*$^{fl/fl}$, *Foxo1*$^{fl/fl}$ and *Tbx21*$^{-/-}$ mice were purchased from the Jackson Laboratory (Bar Harbor, ME). *Ncr1*$^{iCre}$ mice were a generous gift from Dr. Eric Vivier. *Rptor*$^{fl/fl}$, *Rictor*$^{fl/fl}$, *Tbx21*$^{-/-}$, and *Ncr1*$^{iCre}$ mice are in C57BL/6 background. The *Foxo1*$^{fl/fl}$ mice were in FVB background. The *Rptor*$^{fl/fl}$ or *Rictor*$^{fl/fl}$ mice were bred with *Ncr1*$^{iCre}$ mice to generate *Rptor*$^{fl/fl}$ *Ncr1*$^{iCre/WT}$ or *Rictor*$^{fl/fl}$ *Ncr1*$^{iCre/WT}$ mice. The *Rictor*$^{fl/fl}$ *Ncr1*$^{iCre/WT}$ mice were further bred with *Foxo1*$^{fl/fl}$ mice to generate mice with the following genotypes: *Rictor*$^{fl/+}$ *Foxo1*$^{fl/+}$ *Ncr1*$^{iCre/WT}$, *Rictor*$^{fl/fl}$ *Foxo1*$^{fl/+}$ *Ncr1*$^{iCre/WT}$, *Rictor*$^{fl/fl}$ *Foxo1*$^{fl/fl}$ *Ncr1*$^{iCre/WT}$, *Rictor*$^{fl/+}$ *Foxo1*$^{fl/fl}$ *Ncr1*$^{iCre/WT}$. All mice were maintained in pathogen-free conditions at the Biological Resource Center at the Medical College of Wisconsin. Female and male littermate mice between the ages of 8 to 12 weeks were used. All animal protocols were approved by Institutional Animal Care and Use Committee.

## 2.2 Cell preparation from different organs in mice

Bone marrow cells were flushed, and a single cell suspension was made by passing through the syringe/needles. Cells from spleen and lymph nodes were prepared by gently grinding the dissected organs with micro slides (VWR, Radnor, PA). Blood was drawn from the cheeks and mixed with 3.8% sodium citrate (Ricca Chemical Company, Batesville, IN). Red blood cells were lysed by RBC lysis buffer (Thermo-Fisher Scientific, Waltham, MA). For liver lymphocytes acquisition, 10 mL PBS was injected into a hepatic artery to perfuse the blood from the liver. After dissecting and grinding the

liver, lymphocytes were separate through Percoll (Sigma, St. Louis, MO) gradient centrifugation (40% and 60%).

### 2.3 Human sample collection and preparation

All healthy human bone marrow and blood were de-identified samples. All fresh BM and blood samples from healthy donors for the scRNA-seq and flow cytometry experiments were obtained from the Stem Cell and Xenograft Core of the University of Pennsylvania, PA. All samples were provided anonymously after informed consent. The samples were shipped overnight and processed immediately upon receipt. Buffy coat from healthy donors used for flow cytometry experiments were ordered from Blood Center of Wisconsin, WI. The blood samples from the $GATA2^{T354M}$ donor and the corresponding healthy control were obtained from the Children's Hospital of Wisconsin under an approved IRB by the Medical College of Wisconsin. These two samples were obtained at the same time and processed immediately after collection.

BM and blood sample were diluted with ice-cold PBS containing 2 mM EDTA and carefully layered over lymphoprep (STEMCELL Technologies, Vancouver, Canada), and then centrifuged at 440 × g for 35 min at 20 °C without brake. After aspirating the upper layer, mononuclear cells at the interphase were carefully transferred and washed once with PBS containing 2 mM EDTA before downstream process.

**2.4 Flow cytometry and cell sorting**

Flow cytometry analyses were conducted in LSR-II (BD Biosciences, San Jose, CA) or MACSQuant Analyzer 10 (Miltenyi Biotec, Bergisch Gladbach, Germany) and analyzed with FlowJo software (FlowJo LLC, Ashland, OR). IFN-γ and Granzyme B intracellular staining were conducted using BD Cytofix/Cytoperm buffer (BD Biosciences, San Jose, CA). Ki-67, Eomes, and T-bet intracellular staining were conducted using Foxp3/Transcription Factor Staining Buffer Set (Thermo-Fisher Scientific, Waltham, MA). For FoxO1 intracellular staining and phosphor-flow analysis, BD Phosflow Lyse/Fix Buffer and Perm Buffer III were used (BD Biosciences, San Jose, CA). All procedures were performed following instructions from manufactures. For murine cell sorting, NK cells were first enriched using negative selection kit (STEMCELL Technologies, Vancouver, Canada). All human cell sorting was conducted without prior enrichment. The specific cells were further sorted by FACSAria or FACSMelody (BD Biosciences, San Jose, CA), and the purity was generally above 95%. The following antibodies were used: CD3 (17A2), NK1.1 (PK136), CD49b (DX5), CD27 (LG.7F9), CD11b (M1/70), KLRG1 (2F1), NCR1 (29A1.4), NKG2D (CX5), Ly49H (3D10), NKG2A/C/E (20d5), CD122 (5H4 or TM-b1), Ki-67 (SolA15), Eomes (Dan11mag), T-bet (4B10), CD127 (A7R34), CD244.2 (eBio244F4), CD107a (eBio1D4B), IFN-γ (XMG1.2), Streptavidin-PE, Donkey anti-Rabbit 2$^{nd}$ antibodies are from Thermo-Fisher Scientific (Waltham, MA); Ly49D (4E5), CD45.2 (104), CD132 (TUGm2), CD135 (A2F10), Biotin-Ccr7 (4B12) are from Biolegend (San Diego, CA); Ly49A (A1), Ly49G2 (4D11), Ly49C/I (5E6), p-STAT5$^{Y694}$ (47) are from BD Pharmingen (San Jose,

CA); p-Akt$^{S473}$ (D9E), p-rpS6$^{S240/244}$ (D68F8), p-4E-BP1$^{T37/46}$ (236B4), p-FoxO1$^{T24}$/FoxO3a$^{T32}$ are from Cell Signaling Technology (Danvers, MA).

**2.5 Western Blotting**

Fresh FACS-sorted or IL-2-cultured NK cells were lysed in ice-cold 0.3% CHAPS lysis buffer (25 mM HEPES, pH 7.4; 150 mM NaCl; 1 mM EDTA and 0.3% CHAPS) with phosphatase inhibitor cocktail, PhosSTOP (Roche Diagnostics GmbH, Mannheim, Germany) and proteinase inhibitor cocktail (Sigma, St Louis, MO). Lysates were incubated for 30 mins on ice, centrifuged at 15,000 *g* for 10 min at 4°C. For Western blotting, cell lysates were separated by SDS-PAGE; transferred to PVDF membrane and probed with primary and the secondary Abs conjugated with horseradish peroxidase. The signal was detected by autoradiography films (LabScientific Inc., Livingston, NJ). The following antibodies were used: Raptor (24C12), Rictor (53A2) are from Cell Signaling Technology (Danvers, MA); β-Actin (ACTBD11B7) is from Santa Cruz Biotechnology (Dallas, TX).

**2.6 RT-qPCR**

Total RNA was extracted from sorted cells using RNeasy Micro Kit (Qiagen, Hilden, Germany). Reverse transcription was conducted using iScript cDNA synthesis kit (Bio-Rad, Hercules, CA). qPCR were performed in Applied Biosystem 7500 (Thermo-Fisher Scientific, Waltham, MA) with SYBR Green-based detection. The transcript levels of □-Actin were used as a control. Primers used for the qPCR reactions in this study were as

follows: *Tbx21*-F: 5′-GCCAGGGAACCGCTTATATG-3′, *Tbx21*-R: 5′-GACGATCATCTGGGTCACATTGT-3′; *S1pr5*-F: 5′-GCCTGGTGCCTACTGCTACAG-3′, *S1pr5*-R: 5′-CCTCCGTCGCTGGCTATTTCC-3′; *Bcl2*-F: 5′-CTCGTCGCTACCGTCGTGACTTCG-3′, *Bcl2*-R:5′-CAGATGCCGGTTCAGGTACTCAGTC-3′; *Klf2*-F: 5′-CTCAGCGAGCCTATCTTG-3′, *Klf2*-R: 5′-AGAGGATGAAGTCCAACAC-3′; *Il7r*-F: 5′-GACTACAGAGATGGTGACAG-3′, *Il7r*-R: 5′-GGTGACATACGCTTCTTCT-3′; *Ccr7*-F: 5′-CCAGCAAGCAGCTCAACATT-3′; *Ccr7*-R: 5′-GCCGATGAAGGCATACAAGA-3′; *ctb*-F: 5′-GGCTGTATTCCCCTCCATCG-3′, *ctb*-R: 5′-CCAGTTGGTAACAATGCCATGT-3′.

**2.7 Bulk RNA-seq and analysis**

Total RNA was extracted from Trizol followed by poly-A-purification, transcription, and chemically fragmentation using Illumina's TruSeq RNA library kit using the manufacturer's protocol (Illumina, Inc., San Diego, CA, USA). Individual libraries were prepared for each sample, indexed for multiplexing, and then sequenced on either Illumina HiSeq2500 or Illumina NextSeq500.

After sequencing, fastq files were pre-generated by Illumina's Basespace. We downloaded the fastq files, and used the transcriptional aligner Salmon v0.12 [324], with an index built on the mm10 reference transcriptome [325, 326] downloaded from the UCSC genome browser. Following pseudo-alignment, we used tximport [327] and

DESeq2 [328] to analyze differential gene expression between wild type and knock out NK cells. Finally, we used gene set enrichment analysis, to identify potential downstream transcription factor targets and enrichment of T-bet targets from the T-bet ChIP-Seq analysis.

**2.8 ScRNA-seq and analysis**

After sorting, cells were washed once with ice-cold PBS containing 10% FBS post-sorting and counted using hemocytometer. After that, the cells were loaded to 10X chromium machine (10X Genomics, San Francisco, CA) and run through the library preparation procedures following guidance from the Chromium Single Cell 3' Reagent Kits v2. The libraries were quantified using NEBNext Library Quant Kit (NEW ENGLAND Biolabs, Ipswich, MA) and sequenced via Illumina NextSeq 500 (Illumina, San Diego, CA).

After the sequencing, the raw data from each sample was demultiplexed, aligned to mm10 reference genome, and UMI counts were quantified using the 10X Genomics Cell Ranger pipeline (v2.1.1, 10X Genomics). Then, we continued the data analysis with the filtered barcode matrix files using the Seurat package (v2.3.1) [329] in R (v3.4.3 or above). For initial quality control step, we filtered out the cells that expressed less than 200 genes or more than 2,500 genes. We also removed cells with more than 5% mitochondrial transcripts content. Gene expression values for each cell were log-normalized and scaled by a factor of 10,000. To prevent clusters from being biased by

cellular library size or mitochondrial transcript content, gene expression values were scaled based on the number of UMIs in each cell and the cell mitochondrial transcript content. We combined cells from all three WT mice or same anatomic locations from healthy donors to increase the power of unsupervised clustering analysis [330]. Based on the PCElbowPlot, we picked certain number of principal components (PCs) for the clustering analysis when that number reached to the baseline of the standard deviation of PC. Specific to the choice of cluster resolution, we used the "Clustree" function to visualize the clustering progression and picked the highest resolution that still gave stable clusters. Cell clusters were visualized using t-distributed Stochastic Neighbor Embedding plots (t-SNE). For differential gene expression, we used Model-based Analysis of Single-cell Transcriptomics (MAST) test [331] (logfc $\geq$ 0.25, min.pct = 0.1) and only select the genes with adjust p-value smaller than 0.05. For gene set enrichment analysis (GSEA), we used fgsea function with gene sets from the Broad Institute's molecular signatures database [332, 333]. All the p-value shown in the figures were adjusted for multiple gene sets enrichment comparison. In order to predict cellular differentiation, cells were ordered in pseudotime using Monocle2 (v2.6.4) [334]. All significant DEGs across five NK clusters with ave_logFC > 0.25 were used to order the cells. Finally, to predict the developmental cluster of the cells from the knock out mice we utilized one of several classifiers including: a generalized linear model, a gradient boost model, a deep learning neural network model, and a xgboost model, from the h2o package [335]. Further we used the Seurat wrapper for the Random Forest classifier from the ranger package [336]. These classifiers were trained on a random sample made up of 80 percent of the wild type NK cell non-scaled transcription data, using cross-validation and accuracy as a target

end-point for the classifier to avoid overfitting. The accuracy and error of the machine learning classifiers was measured by using the classifier to predict the developmental cluster of the remaining 20 percent of the wild type NK cells which had a known cluster identity and had not been used in the initial training.

**2.9 ChIP-seq analysis**

The T-bet ChIP-seq dataset was published previously [337]. After downloading the fastq files from Sequence Read Archive (SRA), the raw fastq sequence data from the T-bet ChIP sample and the input sample were aligned to the mouse genome mm10 individually using bowtie2 [338]. Significant T-bet binding peaks were identified using MACS2 with a peak q-value cutoff of 1x10^-5 [339]. These significant peaks were then annotated using the 'annotate peaks' tool from the HOMER package [340]. A gene set of potential T-bet target genes was produced by selecting protein-coding genes with significant T-bet peaks within the gene-body or promoter.

**2.10 B16F10 lung metastasis model**

B16F10 melanoma cells growing in log phase were harvested and resuspended in PBS. $2\times10^5$ cells were injected into mice through the tail vein. 14 days post-injection, the recipient mice were sacrificed. The lungs were perfused with 20 mL PBS and dissected for image acquisition.

### 2.11 *In vivo* splenocytes rejection assay

Splenocytes from WT C57BL/6 mice and *β2m*$^{-/-}$ C57BL/6 mice were harvested and labeled with Cell Trace Violet (CTV) or CTV plus Cell Trace Red (CTR), respectively. Then, the WT and *β2m*$^{-/-}$ splenocytes were mixed at 1:1 ratio. The exact percentage of WT and *β2m*$^{-/-}$ cells (within lymphocytes gate) in the mixture was analyzed by flow cytometry before injection. The ratio of *β2m*$^{-/-}$/WT before the injection is marked as $R_{pre}$. Total $5\times10^6$ cells mixed cells were then retro-orbitally injected into recipient mice. 18 hours post-injection, the splenocytes from recipient mice were analyzed by flow cytometry. The percentages of WT and β2m$^{-/-}$ cells within the lymphocytes gate were acquired. The ratio of *β2m*$^{-/-}$/WT after injection was marked as $R_{post}$. Percentage cytotoxicity was calculated as: % Clearance = $[1-(R_{post}/R_{pre})]\times100$.

# Chapter 3 – mTORC1 and mTORC2 differentially regulate the development of NK cells

## 3.1 Introduction

mTOR is an evolutionarily conserved serine/threonine kinase that forms two functionally distinct complexes, mTOR complex 1 (mTORC1) and mTOR complex 2 (mTORC2) [173, 341]. Raptor and Rictor are the defining components of mTORC1 and mTORC2, respectively [174-177]. These complexes regulate cell growth, proliferation, and metabolism, and play an indispensable role in immune cells [173, 233, 341, 342]. The activation of mTORC1 involves the canonical PI3K-PDK1-Akt-TSC1/2-mTORC1 pathway [173, 181]. Although less is known about the upstream activator of mTORC2, PtdIns(3,4,5)$P_3$, which is generated by PI3K [343], has been shown to be critical [188].

Signaling through IL-15 receptors is obligatory for NK cell development [131, 141, 344], and activation of PI3K is one component of IL-15 receptors signaling [345, 346]. These imply that both mTORC1 and mTORC2 are essential for NK cell development. Indeed, *Ncr1*$^{iCre}$-mediated NK cell-specific ablation of mTOR results in impaired development and effector functions [161]. While this study reveals the requirement of mTOR itself, the independent contributions of each mTOR complex in NK cell development remain elusive. Previous studies have demonstrated that PDK1, an upstream activator of mTORC1, regulates early NK cell development by inducing Nfil3 which drives the transcription of *Eomes* [347]. FoxO1, a downstream effector of mTORC2, negatively regulates the terminal maturation of NK cells through direct inhibition of the transcription of *Tbx21* (the gene encoding T-bet) [124]. Based on these, we hypothesized that

mTORC1 and mTORC2 regulate NK cell development through differentially driving the expression of T-box transcription factors.

## 3.2 Results

### 3.2.1 mTORC1 is critical for homeostasis and differentiation of NK cells

To define the role of mTORC1 in NK cell homeostasis, we generated NK cell-specific conditional knockout (cKO) mice by breeding *Rptor*$^{fl/fl}$ mice (*loxp* sites targeting exon 6) with *Ncr1*$^{iCre}$ knockin mice. Expression of Cre driven by *Ncr1* promoter resulted in the deletion of *Rptor* and functional loss of mTORC1 during the immature NK cell stage. Loss of Raptor protein in NK cells was verified by western blot (**Figure 3.1.A**). Phenotypic analyses revealed that the frequency of NK cells was increased in the BM of *Rptor* cKO compare to WT mice, while percentages of NK cells in the periphery were significantly reduced (**Figure 3.1.B**). The lymphocytes counts were comparable between WT and *Rptor* cKO mice in both BM and spleen (**Figure 3.1.C**).

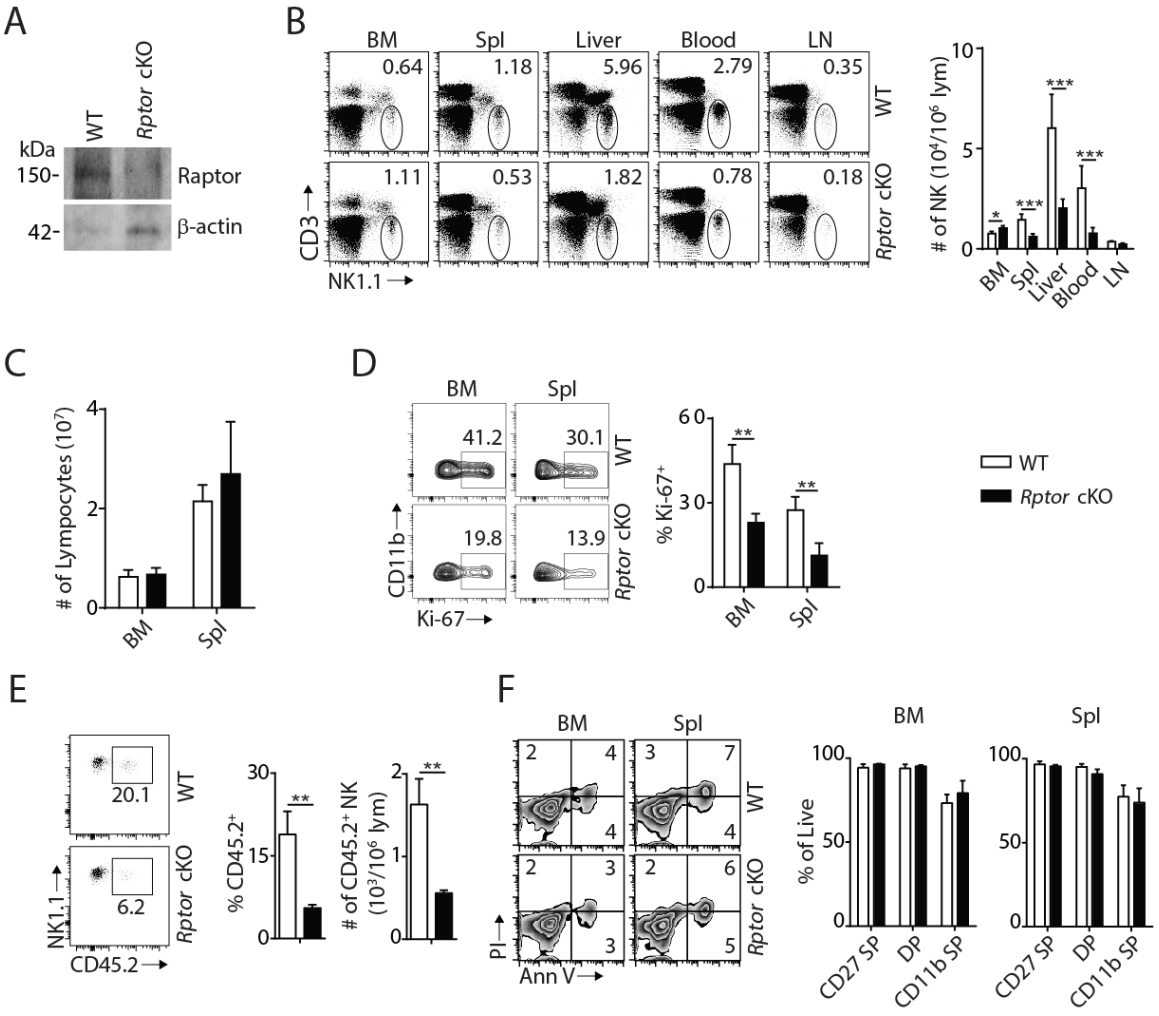


**Figure 3.1. mTORC1 is required to maintain the homeostatic NK cellularity**

(**A**) Raptor expression in freshly-isolated NK cells from WT and *Rptor* cKO mice was evaluated via western blot. (**B**) CD3, NK1.1 staining of cells from various organs (left) and quantification of NK cells in each organ of WT and *Rptor* cKO mice (right). n=4-8 pooled from two to four independent experiments. (**C**) BM and spleen lymphocytes count in WT and *Rptor* cKO mice. n=4 pooled from two independent experiments. (**D**) Ki-67 staining was used to assess steady-state proliferation of NK cells gated on $CD27^+$ population (left), and percentage of Ki-$67^+$ cells (right). n=3 pooled from three independent experiments. (**E**) Percentage of NK cells that are in the sinusoidal compartment of BM was demonstrated by CD45.2 staining (left) and quantified as both percentage and number of $CD45.2^+$ NK cells per million lymphocytes

(right). n=3 pooled from three independent experiments. (**F**) The viability of freshly-isolated NK cells from BM and spleen of WT and *Rptor* cKO mice was evaluated by Annexin V (Ann V) and Propidium iodide (PI) staining (top). Percentage of live cells (Ann $V^{-}PI^{-}$) in each population gated by CD27 and CD11b was quantified (bottom). n=3 pooled from three independent experiments. All bar graphs present the mean ± SD. Statistical significance was calculated using Two-way ANOVA (B, C, D, F) or unpaired Student t-test (E). *p < 005; **p < 0.01; ***p < 0.001.

To explain the reduced NK cell number in the periphery of *Rptor* cKO mice, we investigated cell proliferation, migration, and viability. The percentage of proliferating NK cells was significantly reduced in *Rptor* cKO mice at steady-state, as evidenced by Ki-67 staining (**Figure 3.1.D**). Increased cell number in the BM suggested a potential impairment in the trafficking of NK cells. To test this, WT and *Rptor* cKO mice were intravenously injected with an anti-CD45.2 antibody, sacrificed after two minutes, and their BM cells were analyzed. This allowed us to quantify the number of NK cells in the sinusoidal versus parenchymal regions of the BM, an indicator of NK cell trafficking under steady state [348]. The frequency and number of $CD45.2^{+}$ NK cells were significantly reduced in *Rptor* cKO mice, indicating impairment in the trafficking of NK cells (**Figure 3.1.E**). There were no differences in cell viability between WT and *Rptor* cKO NK cells, as demonstrated by Annexin V and Propidium iodide staining (**Figure 3.1.F**). These data showed that disruption of mTORC1 impairs homeostatic NK cell proliferation and migration, but not viability.

Next, we investigated the role of mTORC1 in NK cell differentiation. Expression of CD122, NK1.1, and DX5 indicated a reduction of the mNK population in the spleen, while the iNK population was similar between WT and *Rptor* cKO mice (**Figure 3.2.A**), which matches with the onset of *Ncr1* expression occurring at the late stage of iNK. No significant changes were observed among NKPs, iNKs, and mNKs in the BM (**Figure 3.2.A**). We then focused our analyses on NK cell maturation using cell surface markers CD27 and CD11b. Raptor deficiency resulted in a significant block in the transition from the CD27 SP to DP stage in both the BM and periphery (**Figure 3.2.B and 3.2.C**). Consistent with this, the frequency of KLRG1-expressing NK cells was also significantly reduced in all organs tested (**Figure 3.2.D**). Analyses of other activating and inhibitory cell surface receptors indicated further developmental defects including reduced expression of Ly49D, Ly49G2, and Ly49H (**Figure 3.2.E**). Collectively, we conclude that mTORC1 is required for maintaining NK cell homeostasis through proliferation, migration, and differentiation.

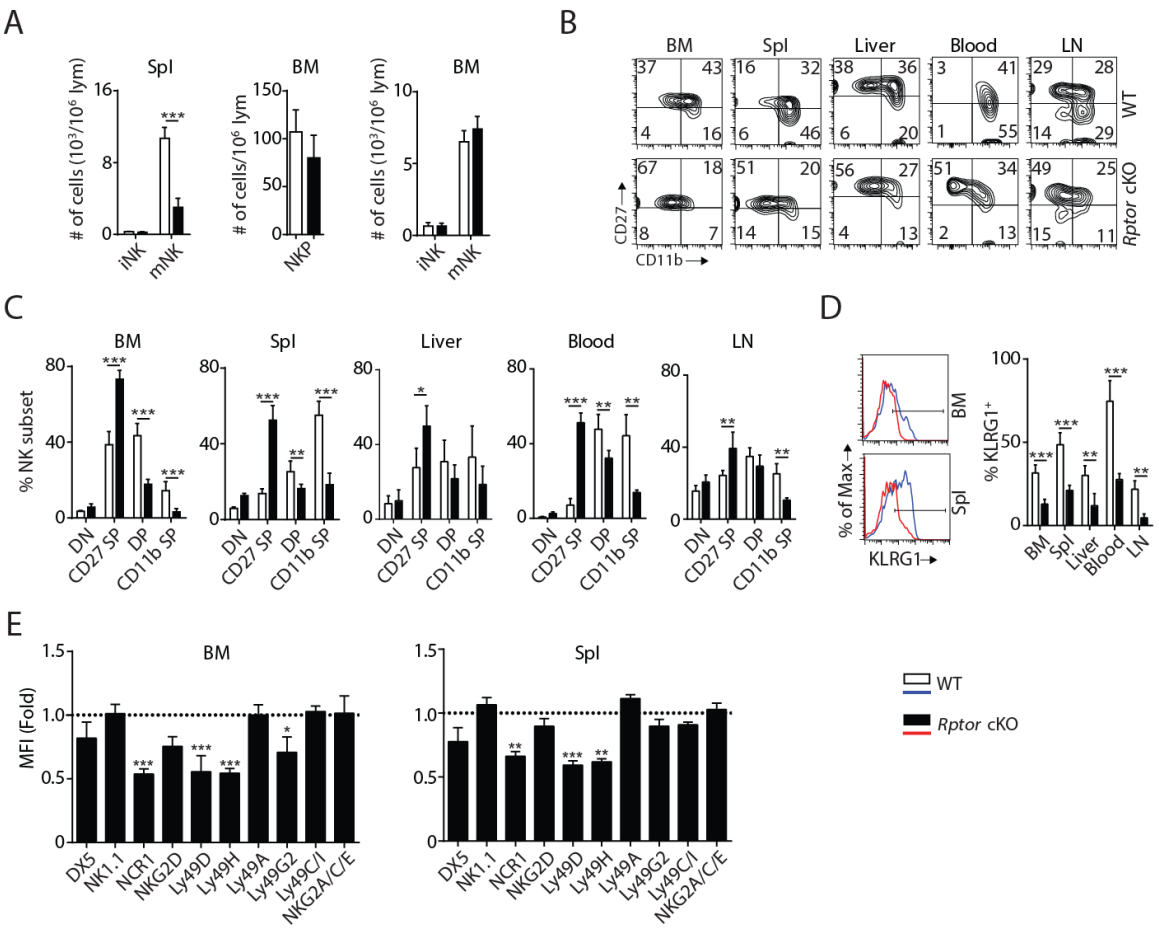


**Figure 3.2. Raptor is required for the maturation of NK cells**

(**A**) Number of iNKs (CD3$^-$CD122$^+$NK1.1$^+$DX5$^-$), mNKs (CD3$^-$CD122$^+$NK1.1$^+$DX5$^+$) in the spleen and NKPs (CD3$^-$Flt3$^-$CD27$^+$2B4$^+$CD127$^+$CD122$^+$ NK1.1$^-$), iNKs, mNKs in the BM from *Rptor* cKO mice were quantified using flow cytometry. n=3-5 pooled from two or three independent experiments. (**B**) CD27 and the CD11b expression on NK cells from BM, spleen, liver, blood and lymph node (LN) were assessed by flow cytometry. (**C**) Percentage of each NK subsets defined by CD27/CD11b in different organs was quantified. n=4 pooled from two to four independent experiments. (**D**) The KLRG1 expression on gated NK cells from BM and spleen of WT and *Rptor* cKO mice (left) and percentage of KLRG1$^+$ cells within NK populations from different organs (right). n=4 pooled from two independent experiments. (**E**) Expression of various maturation markers on NK cells was shown as fold change in MFI normalized to WT. n=4 pooled from two independent experiments. All bar graphs present the mean ± SD. Statistical significance was calculated using Two-way ANOVA. *p < 005; **p < 0.01; ***p < 0.001.

3.2.2 mTORC2 is required for terminal maturation of NK cells

To elucidate the role of mTORC2 in NK cell development, we crossed *Rictor*$^{fl/fl}$ mice (*loxp* sites targeting exon 11) with *Ncr1*$^{iCre}$ mice to generate conditional knockout of *Rictor* in NK cells. The loss of Rictor protein was verified by western blot (**Figure 3.3.A**). Unlike *Rptor* cKO mice, loss of mTORC2 did not change frequency or number of NK cells in the BM (**Figure 3.3.B**); however, the percentages of NK cells were drastically reduced in the periphery with the exception of inguinal lymph nodes (**Figure 3.3.B**). The absolute numbers of lymphocytes were comparable between WT and *Rictor* cKO mice in both BM and spleen (**Figure 3.3.C**). The reasons for the reduction in NK cell numbers in *Rictor* cKO mice could be due to altered proliferation, migration or viability. Ki-67 staining indicated the frequency of proliferating NK cells at steady-state was significantly reduced in *Rictor* cKO compare to WT mice (**Figure 3.3.D**). Although the total numbers of NK cells in the BM were similar (**Figure 3.3.B**), CD45.2 staining revealed a significantly higher number of NK cells in the parenchymal region in *Rictor* cKO compare to WT mice, implying a potential defect in their migration (**Figure 3.3.E**). Rictor deficiency did not affect the viability of NK cells (**Figure 3.3.F**). Together, we conclude that loss of mTORC2 results in defective NK cell proliferation and migration that lead to a reduction of their numbers in the periphery.

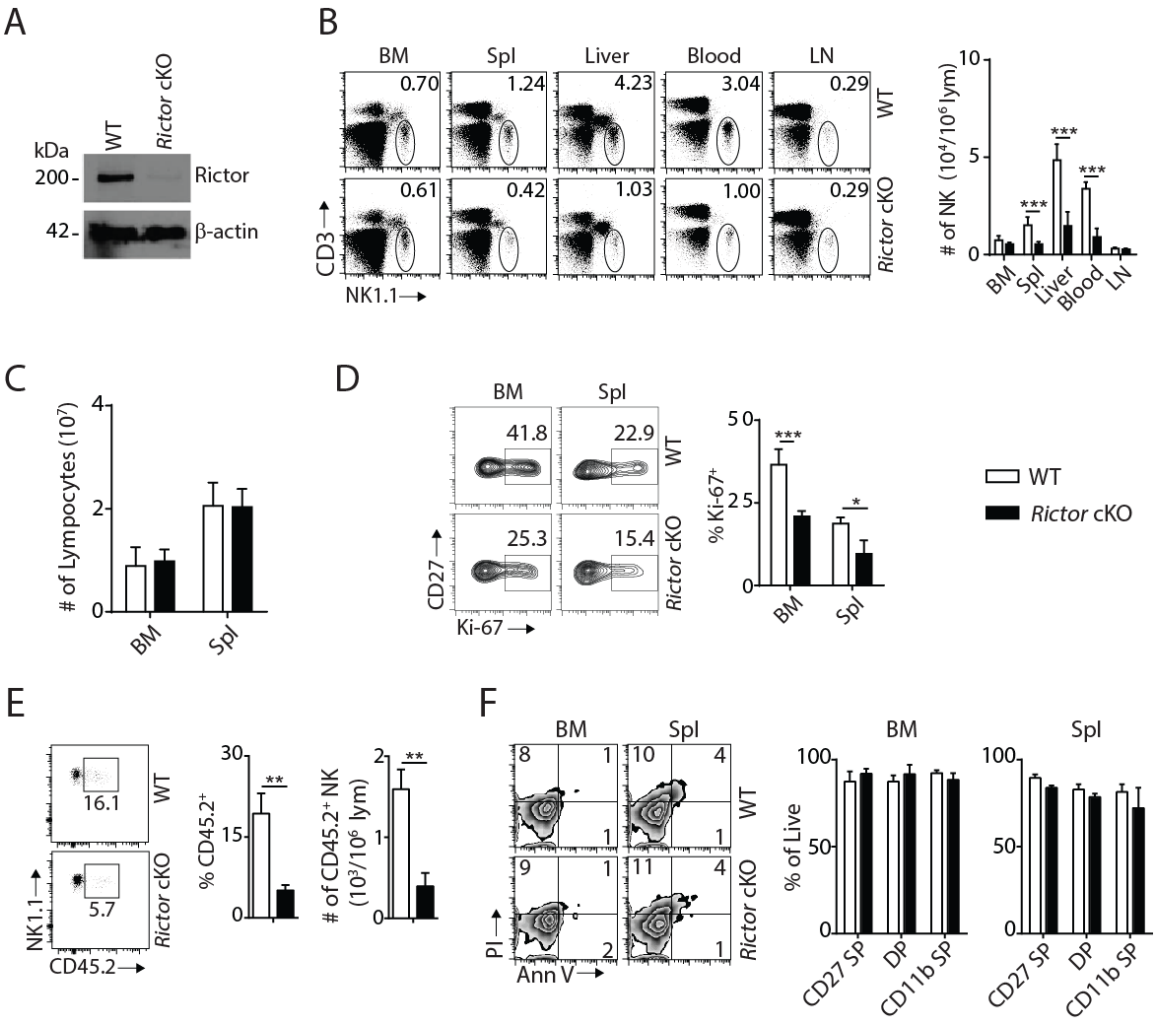


**Figure 3.3. Homeostatic NK cellularity is impaired in *Rictor* cKO mice**

(**A**) Rictor expression in IL-2-cultured NK cells isolated from WT and *Rictor* cKO mice was evaluated via western blot. A representative of three independent experiments. (**B**) CD3, NK1.1 staining of cells from various organs (left) and quantification of NK cells in each organ of WT and *Rictor* cKO mice (right). n=4-7 pooled from two to four independent experiments. (**C**) BM and spleen lymphocytes count in WT and *Rictor* cKO mice. n=4 pooled from two independent experiments. (**D**) Ki-67 staining was used to assess steady-state proliferation of NK cells gated on $CD27^+$ population (left), and percentage of Ki-$67^+$ cells (right). n=3 pooled from three independent experiments. (**E**) Percentage of NK cells that are in the sinusoidal compartment of BM was demonstrated by CD45.2 staining (left) and quantified as both percentage and number of $CD45.2^+$ NK cells per million lymphocytes (right). n=3 pooled from three independent experiments. (**F**) The viability of freshly-isolated NK cells from BM and spleen of WT and

*Rictor* cKO mice was evaluated by Annexin V (Ann V) and Propidium iodide (PI) staining (top). Percentage of live cells (Ann $V^{-}PI^{-}$) in each population gated by CD27 and CD11b was quantified (bottom). n=3 pooled from three independent experiments. All bar graphs present the mean ± SD. Statistical significance was calculated using Two-way ANOVA (B, C, D, F) or unpaired Student t-test (E). *p < 005; **p < 0.01; ***p < 0.001.

The reduced total NK cell number in the spleen of *Rictor* cKO mice was exclusively associated with a reduction in the mNK population (**Figure 3.4.A**). Similarly, there are no significant changes among NKPs, iNKs, and mNKs in the BM (**Figure 3.4.A**). Distinct from *Rptor* cKO mice where NK cell maturation was blocked at the CD27 SP stage, loss of Rictor impaired NK cell maturation from the DP stage to CD11b SP stage in both the BM and peripheral organs (**Figure 3.4.B and 3.4.C**). This defect in terminal maturation was further validated by a significant reduction in KLRG1-expressing NK cells in all organs tested (**Figure 3.4.D**). Loss of Rictor also resulted in an altered expression profile of cell surface receptors in NK cells. Expression of activating or inhibitory Ly49 receptors was reduced, while NK1.1 and DX5 expression were increased on *Rictor* cKO NK cells (**Figure 3.4.E**). We conclude that mTORC2 is required for the terminal maturation of NK cells, and therefore regulates NK cell development at a different stage than that of mTORC1.

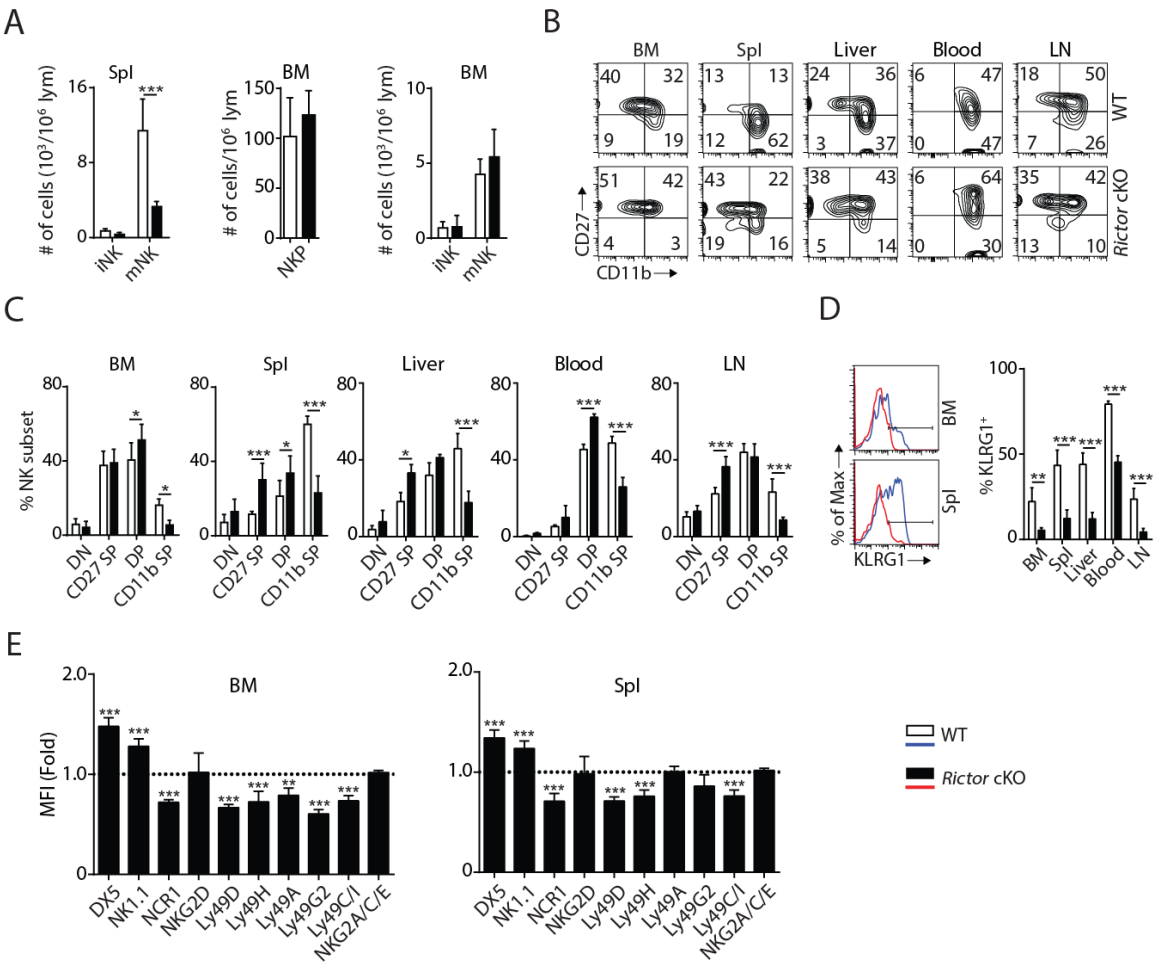


**Figure 3.4. mTORC2 is pivotal for the terminal maturation of NK cells**

(**A**) Number of iNKs ($CD3^{-}CD122^{+}NK1.1^{+}DX5^{-}$), mNKs ($CD3^{-}CD122^{+}NK1.1^{+}DX5^{+}$) in the spleen and NKPs ($CD3^{-}Flt3^{-}CD27^{+}2B4^{+}CD127^{+}CD122^{+}NK1.1^{-}$), iNKs, mNKs in the BM from *Rictor* cKO mice were quantified using flow cytometry. n=3-4 pooled from two or four independent experiments. (**B**) CD27 and the CD11b expression on gated NK cells from BM, spleen, liver, blood, and lymph nodes of WT and *Rictor* cKO mice were assessed by flow cytometry. (**C**) The KLRG1 expression on gated NK cells from BM and spleen of WT and *Rictor* cKO mice (left) and percentage of $KLRG1^{+}$ cells within NK populations from different organs (right). (**D**) Percentage of each NK subsets defined by CD27/CD11b in each organ was quantified (right). n=3-6 pooled from two, three or six independent experiments. (**F**) Expression of various maturation markers on NK cells was shown as fold change in MFI normalized to WT. n=4 pooled from two independent experiments. All bar graphs present the mean ± SD. Statistical significance was calculated using Two-way ANOVA. *p < 005; **p < 0.01; ***p < 0.001.

### 3.2.3 mTORC1 and mTORC2 differentially regulate the expression of T-box transcription factors

T-box transcription factors Eomes and T-bet are critical for NK cell maturation [109, 121, 349]. Accumulation of CD27 SP NK cells in *Rptor* cKO mice (**Figure 3.2.B and 3.2.C)** was similar to earlier findings in *Eomes*$^{fl/fl}$ *Vav*$^{Cre}$ mice or Eomes-negative NK cells that naturally occur in the liver of WT mice [109]. This prompted us to evaluate the expression of Eomes in Raptor-deficient NK cells. Intracellular staining revealed a significant reduction in the protein levels of Eomes in CD27 SP, DP and CD11b SP NK cells from *Rptor* cKO mice (**Figure 3.5.A**). Compare to Eomes, the expression of T-bet was minimal in NK cells within the BM (**Figure 3.5.B**) that was consistent with earlier reports [349]. Loss of Raptor resulted in a moderate reduction in T-bet protein level in NK cells from the spleen (**Figure 3.5.B**). On the other hand, the normal developmental progression from the CD27 SP to DP stage (**Figure 3.4.B and 3.4.C**) correlated with unaltered expression of Eomes in Rictor-deficient NK cells (**Figure 3.5.C**). The defect in the terminal maturation of NK cells in *Rictor* cKO mice mimicked the maturation defects seen in *Tbx21* KO mice [109, 121]. We found the expression of T-bet indeed is significantly reduced in NK cells from the spleen of *Rictor* cKO mice (**Figure 3.5.D**).

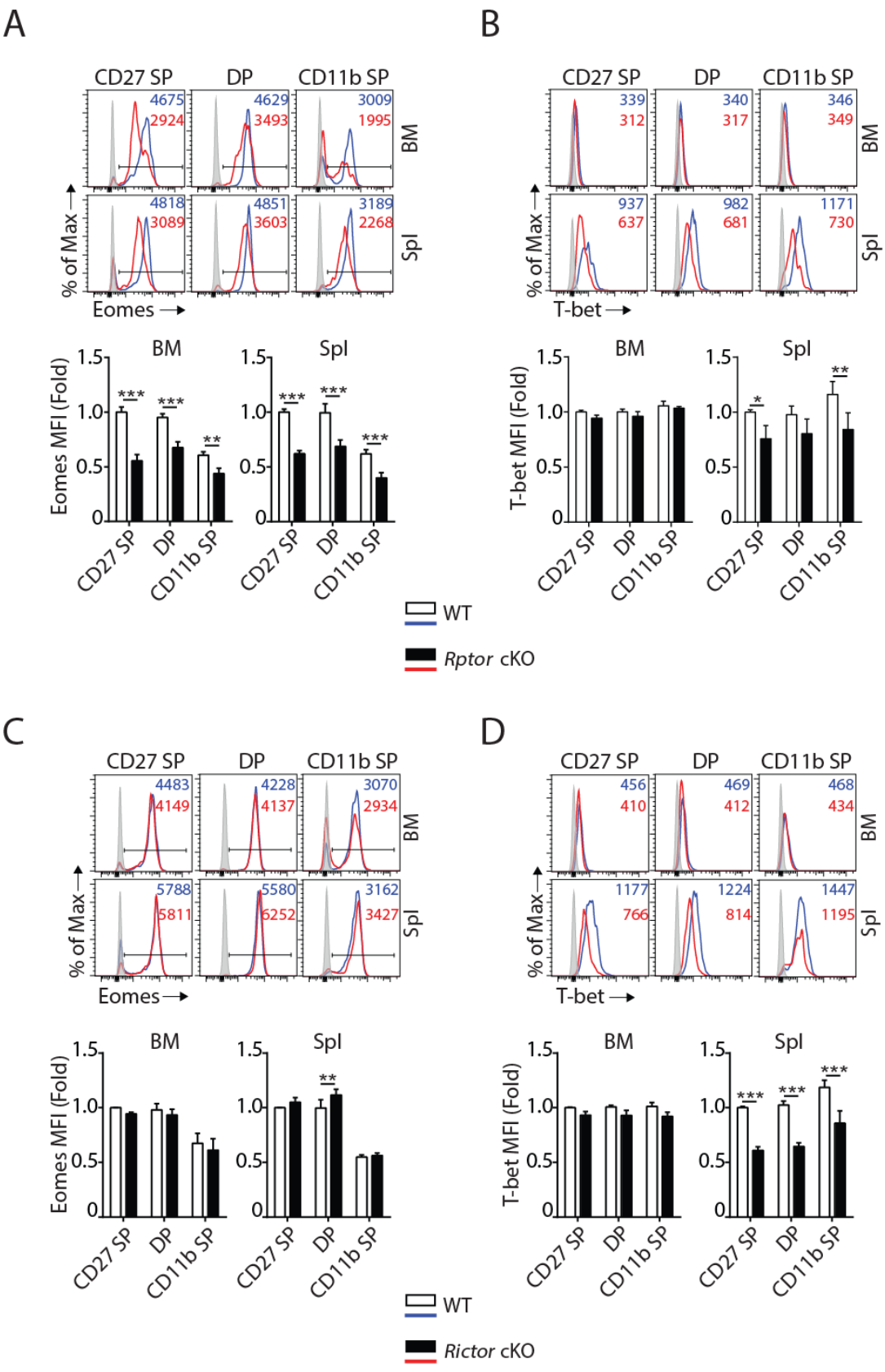
A
B
C
D
CD27 SP
DP
CD11b SP
BM
Spl
% of Max
Eomes
T-bet
Eomes MFI (Fold)
T-bet MFI (Fold)
WT
Rptor cKO
Rictor cKO

**Figure 3.5. mTORC1 and mTORC2 differentially regulate the expression of Eomes and T-bet**

(**A to D**) Histogram of Eomes (**A, C**) and T-bet (**B, D**) expression on each NK cell population gated by CD27 and CD11b of *Rptor* (**A, B**) or *Rictor* (**C, D**) cKO mice and their corresponding WT control. The histogram in grey presents the unstained control (top). Mean fluorescent intensity (MFI) is shown as fold change normalized to WT CD27 SP population (bottom). n=4 pooled from three independent experiments. All bar graphs present the mean ± SD. Statistical significance was calculated using Two-way ANOVA. *p < 005; **p < 0.01; ***p < 0.001.

3.2.4 mTORC1 and mTORC2 differentially regulate the expression of CD122 and STAT5 activation

Eomes binds to the promoter of *Il2rβ* (gene encoding IL-15/IL-2 receptor β chain, CD122) and activates its expression [113]. Given that Eomes expression is down-regulated (**Figure 3.5.A**), we asked whether or not CD122 expression is impaired in *Rptor* cKO mice. Flow analyses revealed that the expression of CD122 was significantly reduced on per cell basis in *Rptor* cKO compared to WT mice in all three subsets of NK cells from BM and spleen (**Figure 3.6.A**) The reduction of CD122 expression in *Rptor* cKO NK cells also led to reduced STAT5 phosphorylation following *ex vivo* IL-15 stimulation **(Figure 3.6.B**). These results indicate that besides mTORC1-mediated signaling, other pathways downstream of IL-15 receptors were sub-optimal in *Rptor* cKO NK cells, which may also have potentially contributed to the developmental defects.

Similar to Eomes, T-bet has also been shown to regulate CD122 expression in T cells [113]. Therefore, we evaluated the CD122 expression and IL-15 receptor signaling in *Rictor* cKO NK cells. Unlike *Rptor* cKO NK cells that had significant reduction in CD122 expression (**Figure 3.6.A**), *Rictor* cKO NK cells exhibited only a moderate reduction (**Figure 3.6.C**), which was consistent with the notion that Eomes, but not T-bet, plays a critical role in maintaining CD122 expression in NK cells [113, 121]. In addition, IL-15-mediated STAT5 phosphorylation was intact in *Rictor* cKO NK cells (**Figure 3.6.D**).

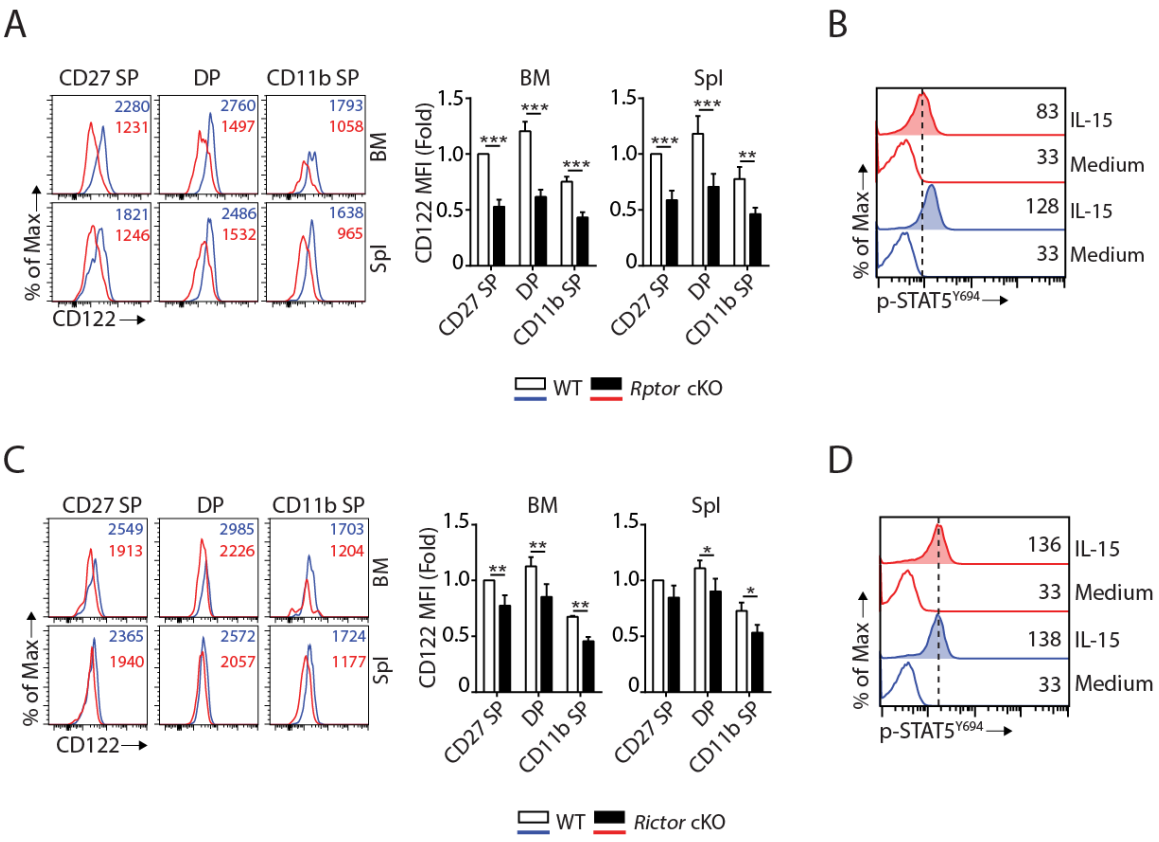


**Figure 3.6. mTORC1 and mTORC2 differentially regulate the expression of CD122 and STAT5 activation**

(**A**) Histogram of CD122 expression on each NK population gated by CD27 and CD11b of WT and *Rptor* cKO mice (left). MFI of CD122 was normalized to WT CD27 SP population (right). n=3 pooled from three independent experiments. (**B**) Splenocytes from WT or *Rptor* cKO mice were stimulated with either medium or 100 ng/mL IL-15 for 1 hour. Phosphorylation of $STAT5^{Y694}$ was detected by phosphor-flow and shown as the representative histogram of three independent experiments. (**C, D**) CD122 expression (**C**) and IL-15-mediated STAT5 activation (**D**) in WT or Rictor-deficient NK cells. Same experimental procedures as (A) and (B). All bar graphs present the mean ± SD. Statistical significance was calculated using Two-way ANOVA. *p < 005; **p < 0.01; ***p < 0.001.

3.2.5 Altered transcriptome in NK cells lack of mTORC1 or mTORC2 correlates with impaired NK cell development

To further explore the mechanism on how mTORC1 and mTORC2 differentially regulate the development of NK cells, we performed RNAseq analyses using FACS-sorted BM NK cells from *Rptor* cKO, *Rictor* cKO and their respective WT mice (n = 3 per group). To reduce the developmental bias, we sorted $CD11b^{-}$ BM NK cells from littermate WT and *Rptor* cKO mice or $CD27^{+}$ BM NK cells from littermate WT and *Rictor* cKO mice. Compared to their corresponding WT, 2,963 genes in *Rptor* cKO NK cells and 829 genes in *Rictor* cKO NK cells were differentially expressed (DE; FDR < 0.05). Of which 406 DE genes were overlapped between *Rptor* and *Rictor* cKO NK cells, indicating a more profound transcriptomic alteration in *Rptor* cKO NK cells compared to *Rictor* cKO NK cells (**Figure 3.7.A**). After normalizing the level of each transcript in the *Rptor* or *Rictor* cKO NK cells to its corresponding WT, we plotted all the genes using the volcano plots, demonstrating the overall change in the transcriptomic profile (**Figure 3.7.B and 3.7.C**). The orange/red dots represent genes that are significantly increased, while the aqua/dark blue dots represent genes that are significantly decreased in Raptor- and Rictor-deficient NK cells compared to the corresponding WT counterparts. Several key transcripts are highlighted in **Figure 3.7.B and 3.7.C**.

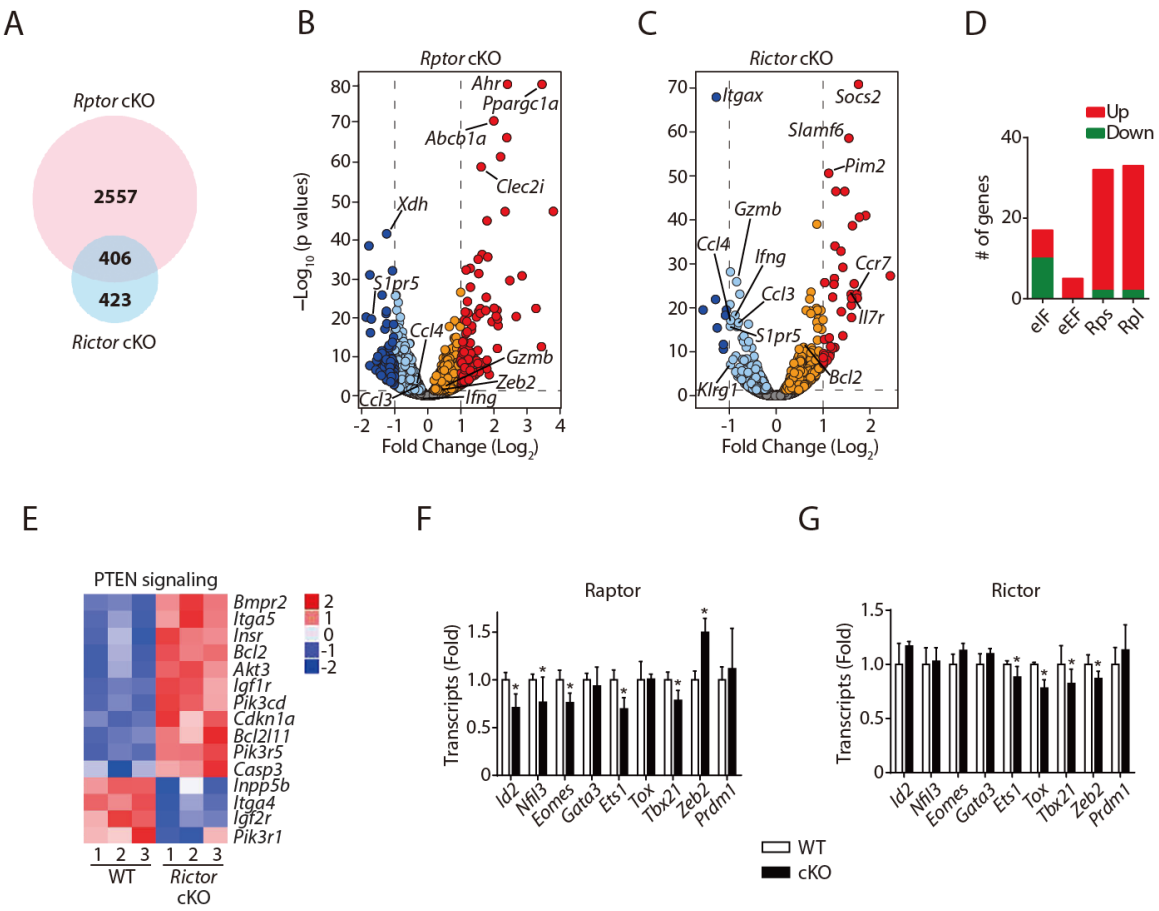


**Figure 3.7. Transcriptome analyses of Raptor- or Rictor-deficient NK cells**

RNAseq was conducted using CD11b$^{-}$ BM NK cells from littermate WT and *Rptor* cKO mice or CD27$^{+}$ BM NK cells from littermate WT and *Rictor* cKO mice. (n = 3 per group). (**A**) Venn diagram demonstrating the number of genes that are differentially expressed (FDR < 0.05) in Raptor- or Rictor-deficient NK cells compared to their corresponding littermate WT control cells and the overlapping between those two genes list. (**B, C**) Volcano plot demonstrating the overall transcriptome alterations in Raptor- (**B**) or Rictor-deficient (**C**) NK cells compared to their corresponding littermate WT control cells. The orange/red dots represent genes that are significantly increased, while the aqua/dark blue dots represent genes that are significantly decreased in Raptor- and Rictor-deficient NK cells compared to the corresponding WT counterparts. We plotted all the genes with –Log$_{10}$(p values) greater than 80 at the y-axis equal to 80. (**D**) A number of significantly up-regulated or down-regulated genes encoding proteins belonging to eIFs, eEFs, ribosome small (Rps) or large (Rpl) subunits family in *Rptor* cKO NK cells are quantified and presented in the bar graph. (**E**) Enrichment of PTEN signaling in *Rictor* cKO NK cells were

demonstrated via the heatmap. (**F**, **G**) mRNA level of key transcription factors governing NK cell development in Raptor- (**F**) or Rictor- (**G**) deficient NK cells normalized to corresponding WT control.

Ingenuity Pathway Analysis (IPA) revealed distinct gene ontology enrichment in *Rptor* and *Rictor* cKO NK cells. As downstream targets of mTORC1, the top three significantly enriched signaling pathways in *Rptor* cKO NK cells are eIF2, eIF4/P70S6K, and mTOR signaling ($p = 5.53 \times 10^{-23}$, $2.15 \times 10^{-14}$, and $4 \times 10^{-14}$, respectively), consistent with mTORC1 being the bona fide regulator of protein synthesis [208]. Unexpectedly, the Z-scores of those three pathways are positive (Z-score = 3.833, 0.894, and 0.73, respectively), which indicates higher translational activity in *Rptor* cKO NK cells. After a thorough examination of the molecular signature of those three enriched pathways, we found that Raptor deficiency results in increased transcription of genes encoding proteins that comprise the translation machinery such as eIFs, eEFs and ribosome proteins (**Figure 3.7.D**). This not only explains the positive Z-scores of those three pathways but reveals that compensatory pathways are initiated in *Rptor* cKO NK cells to overcome the impaired protein translation. As for *Rictor* cKO NK cells, the PTEN signaling pathway is impaired ($p = 1.73 \times 10^{-5}$, Z-score = –1.069) as demonstrated by increased expression of receptors (*Insr, Igf1r*) involving growth factors signaling or proteins (*Pik3cd, Pik3r5*) comprising PI(3)K and decreased expression of phosphatase (*Inpp5b*) that dampen the inositol phosphates signaling (**Figure 3.7.E**). This indicates that there is a potential positive regulation of PTEN by mTORC2 to balance the $PI(3,4,5)P_3$-mediated activation of mTORC2 [188].

Using RNA sequencing data, we examined the expression levels of key transcription factors governing different developmental stages of NK cells. The expression of transcription factors such as Nfil3, Id2, and Eomes that are critical for NK cell commitment and early development are reduced in *Rptor* but not in *Rictor* cKO NK cells (**Figure 3.7.F and 3.7.G**). The expression of T-bet and Zeb2 which promote terminal mature NK cell development were significantly reduced in *Rictor* cKO mice (**Figure 3.7.G**). This expression pattern correlates with early NK cell development impairment in *Rptor* cKO mice versus terminal maturation defect seen in *Rictor* cKO mice.

3.2.6 mTORC2 regulates the terminal maturation of NK cells through Akt$^{S473}$-FoxO1-T-bet axis

Consistent with reduced T-bet expression in mRNA (**Figure 3.7.G**) and protein level (**Figure 3.5.D**), we found a significant enrichment of T-bet target genes ($p = 4.59 \times 10^{-14}$, Z-score = –1.429) in *Rictor* cKO NK cells (**Figure 3.8.A**). The well-established T-bet-induced genes (*Klrg1, Ifng, Gzmb, S1pr5, Zeb2*) [350] were reduced in *Rictor* cKO NK cells (**Figure 3.8.A and 3.7.C**). Next, we seek to uncover the mechanism through which mTORC2 regulates the expression of T-bet. Earlier work showed that mTORC2 phosphorylates Serine$^{473}$ on Akt, which is critical for Akt to phosphorylate FoxO transcription factors [227, 351]. After Akt-mediated phosphorylation, modulator protein 14-3-3 binds to FoxO transcription factors and reduces their transcriptional activity by blocking DNA binding and accelerating nuclear exportation [351, 352]. Among the FoxO families, FoxO1 is the most abundant one expressed in NK cells and has been shown to negatively regulate the terminal maturation of NK cells by suppressing the transcription of *Tbx21* [124, 353]. Thus, we hypothesized that mTORC2 regulates T-bet expression through the Akt$^{S473}$-FoxO1 axis.

To test this hypothesis, we first evaluated the phosphorylation of Akt and FoxO1. Lack of Rictor resulted in a reduced level of Akt$^{S473}$ phosphorylation in the NK cells from BM (**Figure 3.8.B, top**). Consistent with this, we also detected reduced phosphorylation of FoxO1$^{T24}$ in these *Rictor* cKO NK cells (**Figure 3.8.B, bottom**). These data suggested

that the transcriptional activity of FoxO1 is higher in *Rictor* cKO compared to WT NK cells.

Indeed, we found a significant enrichment of FoxO1 target genes ($p = 4.46 \times 10{-}9$, Z-score = 1.719) in *Rictor* cKO NK cells compared with WT in the IPA analyses (**Figure 3.8.C**). Ouyang W et al. established a FoxO1-dependent transcriptional program in regulatory T cells (Tregs) through comparing transcriptome among WT, FoxO1 KO and FoxO1 constitutively active Tregs [354]. Utilizing FoxO1 target genes described by these authors, we performed gene enrichment analyses of the *Rictor* cKO RNAseq data. Consistent with the IPA analyses, our Fisher's exact test showed enrichment of the FoxO1-target genes with p-value equal to $1.32 \times 10^{-10}$, emphasizing a hyperactive FoxO1 in the *Rictor* cKO NK cells. We further validated several well-established FoxO1 target genes by RT-qPCR using NK cells from both BM and spleen. Consistent with the RNA sequencing data, we found reduced mRNA level of *Tbx21* in $CD27^+$ NK cell subset from both BM and spleen of *Rictor* cKO mice (**Figure 3.8.D**). We also found significantly elevated mRNA level of known FoxO1 activated genes including *Bcl2, Klf2, Il7r* and *Ccr7* in the $CD27^+$ *Rictor* cKO NK cells compared to the WT (**Figure 3.8.D**) [354, 355]. This is also consistent with higher cell surface expression of IL-7Rα and Ccr7 (**Figure 3.8.E and 3.8.F**).

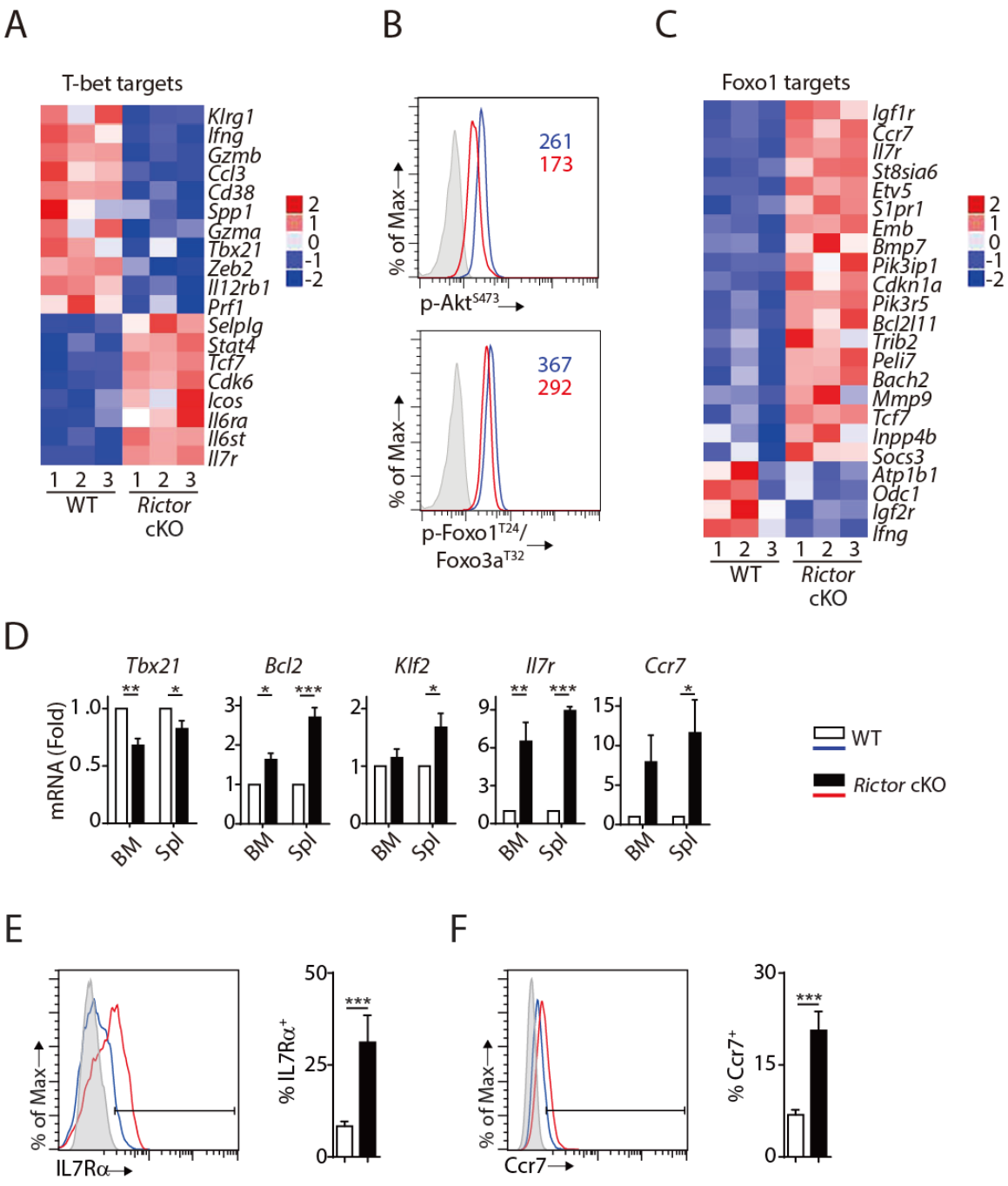


**Figure 3.8. mTORC2 is required for T-bet expression through regulation of FoxO1 during NK cell development**

(**A**) Enrichment of T-bet target genes in *Rictor* cKO NK cells as shown via the heatmap. (**B**) Histogram demonstrating phosphorylation of Akt$^{S473}$ (top) and FoxO1$^{T24}$/FoxO3a$^{T32}$ (bottom) in NK cells from BM of WT or *Rictor* cKO mice. The histogram in grey presents the isotype control. A representative of two or three independent experiments. (**C**) Enrichment of FoxO1 target genes in *Rictor* cKO NK cells as shown

via the heatmap. (**D**) The mRNA level of *Tbx21*, *Bcl2*, *Klf2*, *IL7r,* and *Ccr7* were evaluated by RT-qPCR with sorted fresh $CD27^+$ NK cells from BM and spleen of WT or *Rictor* cKO mice. The data were shown as fold change normalized to WT. n=3-5 pooled from three to five independent experiments. (**E**, **F**) Cell surface expression of IL7Rα (**E**) and Ccr7 (**F**) in $CD27^+$ NK cells from the spleen of WT and *Rictor* cKO mice were detected by flow cytometry as shown in the histogram on the left. Percentage positive cells were quantified on the right. The grey histogram was the unstained control. A representative of two independent experiments with three mice in each. All bar graphs present the mean ± SD expect (D) which is shown as the mean ± SEM. Statistical significance was calculated using Two-way ANOVA (D) or unpaired Student t-test (E, F). *p < 005; **p < 0.01; ***p < 0.001.

To further prove the hypothesis that hyperactive FoxO1 suppress the expression of T-bet and results in terminal maturation defect in Rictor-deficient NK cells, we deleted *Foxo1* in Rictor-deficient NK cells to rescue the impaired expression of T-bet and the terminal maturation defect. We bred the $Rictor^{fl/fl}Ncr1^{Cre/WT}$ mice with $Foxo1^{fl/fl}Ncr1^{WT/WT}$ mice obtained from the Jackson Laboratory. To ensure efficient generation of experimental mice with littermate control, we used $Rictor^{fl/+}Foxo1^{fl/+}Ncr1^{Cre/WT}$ mice as the WT control mice since both Rictor and FoxO1 are haplo-sufficient to the development of NK cells [124, 356]. Due to the mixed background of these mice, we had large variation among each genotype most pronounced in terms of the number of NK cells in these mice (**Figure 3.9.A and 3.9.B**). Nevertheless, consistent with previous observation (**Figure 3.3.B**), we found a decrease in both percentage and absolute number of NK cells in the spleen of *Rictor* cKO mice compared to the WT control (**Figure 3.9.A and 3.9.B**). Importantly, deletion of *Foxo1* in *Rictor* cKO mice rescued the number of NK cells in the spleen to the level compatible to the WT control (**Figure 3.9.A and 3.9.B**). Specific to

the maturation of NK cells, *Rictor* cKO mice had less terminally-mature population compared to the WT control indicated by either the percentage of CD11b SP subset or the KLRG1$^{+}$ NK cells (**Figure 3.9.C - F**), although the difference is less pronounced compared to the previous observation in B6 background mice likely due to the fact that these mixed background mice were generally more mature than the pure B6 background mice at the age of eight weeks. Notably, deletion of *Foxo1* in Rictor-deficient NK cells completely rescued the percentage of CD11b SP subset or the KLRG1$^{-}$ NK cells to the level compatible to the WT control (**Figure 3.9.C - F**). These data indicated that FoxO1 is the transcription factor suppressing the terminal maturation program in Rictor-deficient NK cells. To further explore whether the impaired expression of T-bet is the downstream of hyperactive FoxO1 in Rictor-deficient NK cells, we evaluated the expression of T-bet in the *Rictor*/*Foxo1* cDKO mice. Gated on three subsets of NK cells from the spleen, we found deletion of *Foxo1* in the Rictor-deficient NK cells completely rescued the expression of T-bet in the CD27 SP and DP subsets to the level similar to the corresponding WT control (**Figure 3.9.G**). The rescue was less sufficient in the terminal CD11b SP NK cells (**Figure 3.9.G**). Deletion of *Foxo1* alone resulted in almost a fold induction of the T-bet protein level in all three developmental stages compared to the WT control (**Figure 3.9.G**). These data indicated that, in addition to FoxO1, other factors downstream of mTORC2 are involved in the regulation of T-bet expression.

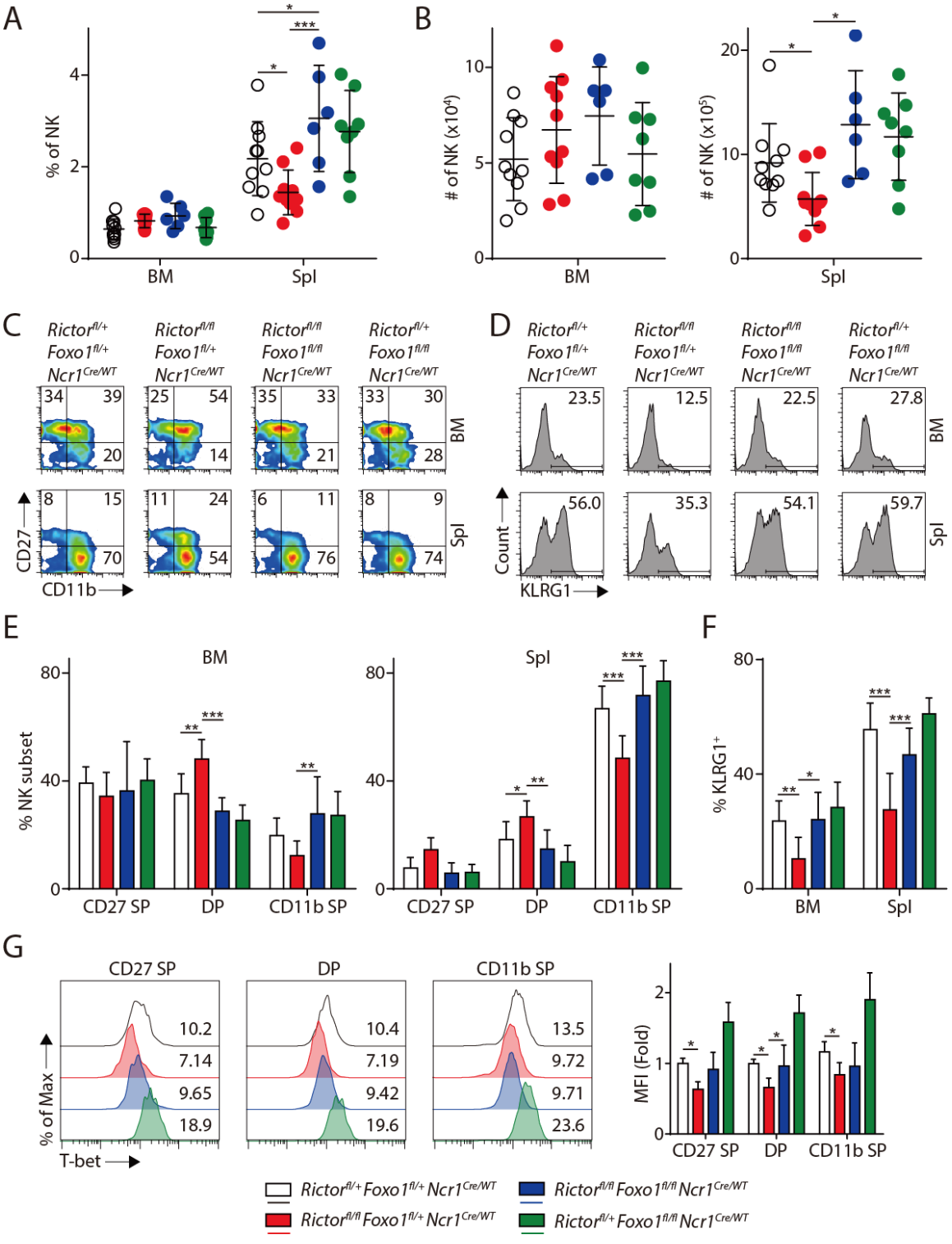
A
% of NK
BM
Spl
B
# of NK (x10⁴)
# of NK (x10⁵)
C
Rictor fl/+ Foxo1 fl/+ Ncr1 Cre/WT
Rictor fl/fl Foxo1 fl/+ Ncr1 Cre/WT
Rictor fl/fl Foxo1 fl/fl Ncr1 Cre/WT
Rictor fl/+ Foxo1 fl/fl Ncr1 Cre/WT
CD27
CD11b
D
Count
KLRG1
E
% NK subset
CD27 SP
DP
CD11b SP
F
% KLRG1+
G
% of Max
T-bet
MFI (Fold)

**Figure 3.9. Deletion of *Foxo1* rescues the NK cellularity and terminal maturation defects in *Rictor* cKO mice**

(**A**) Quantification of the percentage of NK cells in the BM and spleen of the four group mice (gated on $CD3\varepsilon^{-}NCR1^{+}$). Pooled from eight independent experiments. (**B**) Quantification of the absolute number of NK cells in the BM and spleen of the four group mice (gated on $CD3\varepsilon^{-}NCR1^{+}$). Pooled from eight independent experiments. (**C, D**) Reprehensive flow plots demonstrating the expression of CD27/CD11b (**C**) and KLRG1 (**D**) in the NK cells from BM and spleen of the four group mice (gated on $CD3\varepsilon^{-}NCR1^{+}$). (**E, F**) Quantification of each NK subsets defined by the expression of CD27/CD11b (**E**) or KLRG1 (**F**) in BM and spleen of the four group mice (gated on $CD3\varepsilon^{-}NCR1^{+}$). $n \geq 6$, pooled from six independent experiments. (**G**) The protein level of T-bet in three NK subsets defined by the expression of CD27 and CD11b were evaluated by intracellular staining and gated on $CD3\varepsilon^{-}NCR1^{+}$ cells from spleen of the four group mice. The mean fluorescent intensity (MFI) of T-bet was quantified and shown as fold change normalized to the CD27 SP population from WT control. $n \geq 3$, pooled from three independent experiments. All bar graphs present the mean ±. Statistical significance was calculated using Two-way ANOVA. *p < 005; **p < 0.01; ***p < 0.001.

3.2.7 Disruption of mTORC2 does not affect mTORC1 activation

mTORC2 phosphorylates Akt at Serine$^{473}$ and induces maximal kinase activity of Akt [227]. Given that Akt is an upstream activator of mTORC1, we investigated whether a reduction in Akt kinase activity resulting from mTORC2 disruption affects mTORC1 activation. Being downstream of mTORC1, phosphorylation of rpS6 is nearly abolished in Raptor-deficient NK cells, as expected (**Figure 3.10.A, left**). Important, deficiency of mTORC2 does not perturb mTORC1 signaling as phosphorylation of rpS6 is moderately increased in *Rictor* cKO compared to WT NK cells (**Figure 3.10.A, right**). The moderate augmentation in mTORC1 activity could potentially result from reduced PTEN signaling as indicated by the RNA sequencing data (**Figure 3.7.E**). On the other hand, we did observe a moderate decrease in mTORC2 activity indicated by phosphorylation of Akt$^{S473}$ in *Rptor* cKO NK cells stimulated with IL-15 (**Figure 3.10.B, left**). This is potentially due to reduced expression of IL-15/IL-2 receptor β chain (CD122) as the phosphorylation of STAT5 is also moderately reduced in *Rptor* cKO NK cells (**Figure 3.6.A and 3.6.B**). As expected, Akt$^{S473}$ phosphorylation was abolished in *Rictor* cKO NK cells (**Figure 3.10.B, right**). Based on these, we conclude that disruption of mTORC2 does not affect IL-15-mediated mTORC1 activation in NK cells.

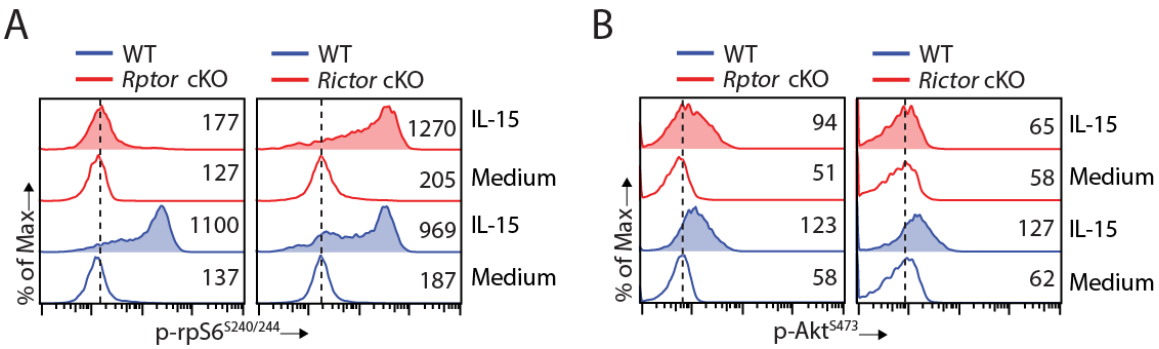

**Figure 3.10. Disruption of mTORC2 does not affect mTORC1 activation**

(**A, B**) Splenocytes from WT, *Rptor* cKO (left) or *Rictor* cKO mice (right) were stimulated with either medium or 100 ng/mL IL-15 for 1 hour. Phosphorylation of $rpS6^{S240/244}$ (**A**) and $Akt^{S473}$ (**B**) were detected by phosphor-flow and shown as the representative histogram of three independent experiments.

3.2.8 Defective anti-tumor response in *Rptor* or *Rictor* cKO mice

To this end, our detailed analyses revealed that both mTORC1 and mTORC2 are critical to the development of NK cells. Next, we asked whether the developmental defects resulting from Raptor or Rictor deficiency might affect physiological response. To address this question, we challenged *Rptor* or *Rictor* cKO mice with B16F10 melanoma cells via tail vein injection, which establishes the lung metastasis tumor model. The critical role of NK cells in anti-tumor immunity has been well established in this model [152, 357, 358]. Compared to corresponding WT control mice, the tumor metastases were much more severe in the lungs of *Rptor* or *Rictor* cKO mice (**Figure 3.11.A - D**). The significant reduction of NK cell number and the terminal mature NK cells in both of the cKO mice might contribute to this defective anti-tumor response. To further investigate the functional defects in these mice, we conducted *in vivo* splenocytes rejection assay using $\beta 2m^{-/-}$ cells, 'missing-self' targets sensitive to NK cells. Similar to the B16F10 tumor challenge, the clearance efficiency of the transferred b2-microglobulin-deficient targets cells was significantly impaired in *Rptor* or *Rictor* cKO mice (**Figure 3.11.E and 3.11.F**). Taken together, these data demonstrated that the NK cell-mediated anti-tumor response is defective in *Rptor* or *Rictor* cKO mice.

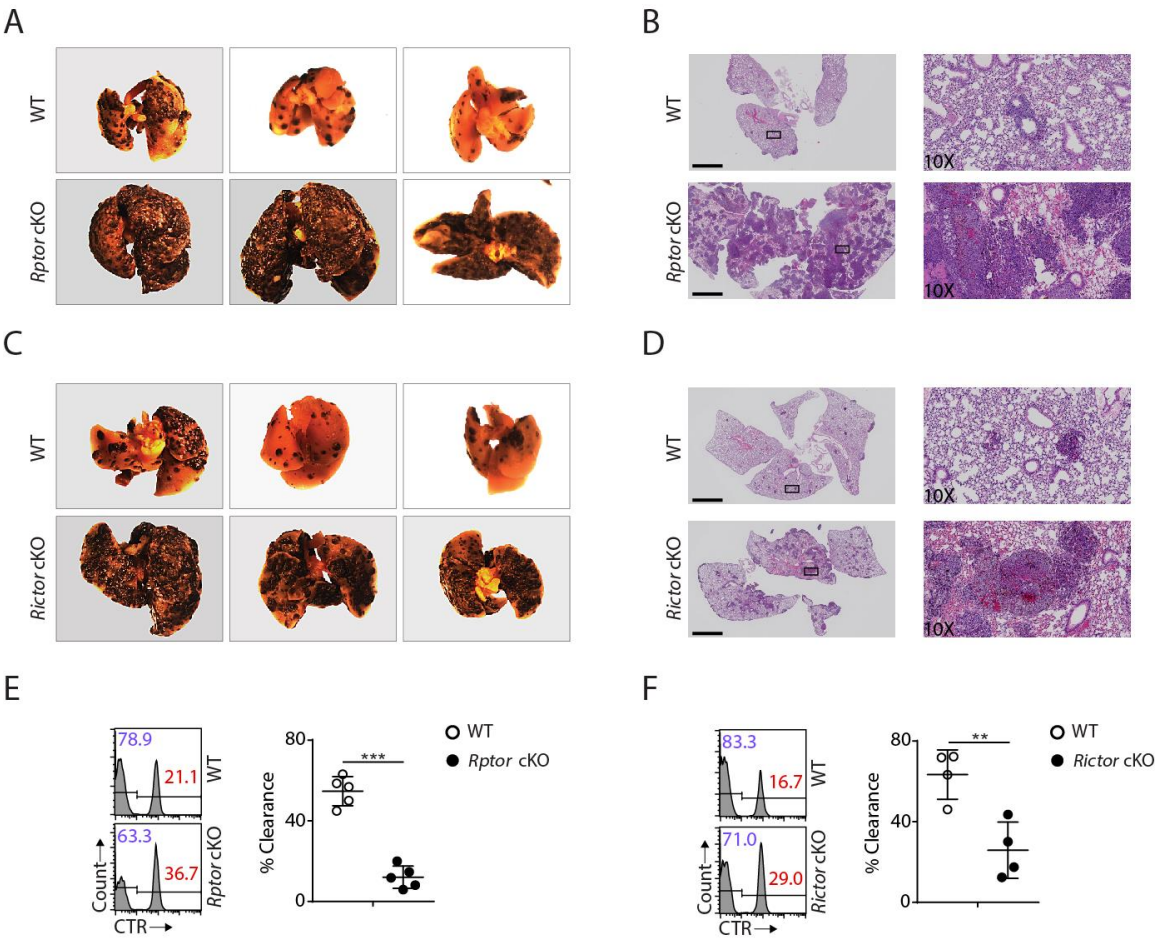


**Figure 3.11. Impaired anti-tumor activity in *Rptor* or *Rictor* cKO mice**

(**A - D**) 200,000 B16F10 tumor cells were intravenously injected into *Rptor* (**A, B**) or *Rictor* (**C, D**) cKO mice and their corresponding WT control mice. 14 days post-injection, the lungs were perfused with PBS and harvested for image acquisition (**A, C**) and HE staining (**B, D**); Scale bars represent 2.5 mm, and the right side are the 10X exploded view of select regions). The representative images were shown. n=3-6 for each genotype from two independent experiments. (**E, F**) CTV-labeled splenocytes from WT C57BL/6 mice were mixed with CTV/CTR-double-labeled splenocytes from $\beta 2m^{-/-}$ C57BL/6 mice at 1:1 ratio. Total $5\times10^6$ cells mixed cells were i.v. injected to *Rptor* (E) or *Rictor* (F) cKO mice and their corresponding WT control mice. 18 hours post-injection, the splenocytes from recipient mice were analyzed by flow cytometry. The percentages of WT and $\beta 2m^{-/-}$ lymphocytes were analyzed as the representative histogram (left, gated on $CTV^+$ lymphocytes). The percentage cytotoxicity was also calculated (right). n=4-5, pooled

from two independent experiments. All bar graphs present the mean ± SD. Statistical significance was calculated using unpaired Student t-test. *p < 005; **p < 0.01; ***p < 0.001.

### 3.3 Conclusions

mTOR plays a critical role in the development and functions of various immune cells [233, 342]. In NK cells, the earlier study revealed the essential role of mTOR in controlling development following Ncr1 expression [161]. Despite these findings, the unique role of each mTOR complex in the development of NK cells remains unknown. In this study, through *Ncr1*$^{iCre}$-mediated conditional deletion of *Rptor* or *Rictor*, we disrupted mTORC1 or mTORC2 specifically in NK cells. Phenotypic analyses revealed that both mTOR complexes are critical for homeostasis of NK cells and that disruption of mTORC1 or mTORC2 results in defective NK cell maturation at distinct developmental stages. The altered expression of Eomes provides a potential mechanistic explanation for the maturation defects of Raptor-deficient NK cells. The hyperactive FoxO1 resulted from loss of mTORC2 suppresses the expression of T-bet and cause the terminal maturation defects of Rictor-deficient NK cells. Deletion of *Foxo1* in *Rictor* cKO mice restored the expression of T-bet and rescued the developmental defects. In the physiological context, neither *Rptor* nor *Rictor* cKO mice demonstrated sufficient NK cell-mediated anti-tumor responses, highlighting the biological consequences of lacking either mTORC1 or mTORC2.

### 3.4 Discussion

In *Rptor* cKO mice, the homeostatic NK cellularity is disrupted as evidenced by reduced NK cell number in the periphery, reduced steady-state proliferation and impaired migration *in vitro*. Moreover, loss of mTORC1 significantly impairs NK cell maturation, as demonstrated by accumulation of CD27 SP population and reduced DP and CD11b SP populations. This defect may directly contribute to the accumulated NK cells in the BM, as they gradually obtain migratory capacity following CD11b expression [359]. Despite these findings from *Rptor* cKO mice, $Ncr1^{Cre}$-mediated deletion of *Pdpk1* or *Tsc1* did not have any impact on NK cell development [347, 360]. This indicates that following Ncr1 expression, mTORC1 is potentially activated through an alternative mechanism instead of the canonical PI3K-PDK1-Akt-TSC1/2-mTORC1 pathway. Further work is required to elucidate these upstream mechanisms that regulate mTORC1 signaling.

mTORC1 regulates protein translation through various mechanisms. One of which directly affects the translation of proteins comprising the translational machinery such as eIFs, eEFs, and ribosomal proteins [208, 209]. However, less is known about the regulation of these proteins at the transcriptional level, especially related to alteration of mTORC1. Our RNAseq analyses revealed that disruption of mTORC1 leads to increased transcripts level of these proteins, implying an alternative pathway that compensates the protein translation defects.

Compared to mTORC1, less is known about mTORC2, mainly due to the lack of mTORC2-specific inhibitors; however, through using the *Ncr1*$^{iCre}$ mice model, we are able to study the role of mTORC2 specifically in NK cells. Our data reveal that mTORC2 is essential for the development of NK cells. NK cell number is significantly reduced in the periphery of *Rictor* cKO mice, and this impairment potentially results from reduced steady-state proliferation. Unlike the maturation impairment at CD27 SP to DP transition in *Rptor* cKO mice, deletion of *Rictor* causes a defect during the transition from the DP to CD11b SP stage. Importantly, when we assess the expression of T-box transcription factors, Eomes expression is comparable between WT and *Rictor* cKO NK cells, which is consistent with an unaltered transition from CD27 SP to DP stages. Normal expression of Eomes is also consistent with unaltered mTORC1 signaling in *Rictor*-deficient NK cells. In contrast, the expression of T-bet is significantly reduced in *Rictor* cKO NK cells, which correlates with the impairment in terminal maturation. Mechanistically, Rictor deficiency results in hyperactive FoxO1 due to abolished mTORC2-Akt$^{S473}$-FoxO1 signaling regulation. The impaired expression of T-bet resulted from hyperactive FoxO1 leads to the terminal maturation defects. Hyperactive FoxO1 also promotes the expression of *Socs2* and *Socs3*, both of which are potent suppressors of IL-15 signaling and potentially results in the impaired homeostatic proliferation of Rictor-deficient NK cells. Thus, deletion of Foxo1 not only rescued the terminal differentiation defects but also the NK cellularity in *Rictor* cKO mice. Although these experimental evidences indicates that the impaired expression of T-bet is responsible for the terminal maturation defects of mTORC2-defiicent NK cells, to definitively approve this, we need to ectopically express T-bet in Rictor-deficient NK cells to rescue the terminal maturation.

The RNAseq analyses also revealed that PTEN signaling is impaired in *Rictor* cKO NK cells, which indicates a balanced activation loop consists of PI(3)K-PI(3,4,5)P3-mTORC2-PTEN. This may contribute to the moderately increased mTORC1 activity in *Rictor* cKO NK cells. Compared to our study, Wang et al., reported similar but more pronounced hyperactive mTORC1 phenotype in Rictor-deficient NK cells at steady-state [356]. Whether the different choice of WT control mice is the reason behind this discrepancy remains to be determined. Nevertheless, their discovery of increased expression of SLC7A5, component of amino acids transporter, and amino acids influx could be another reason for the increased mTORC1 activity in Rictor-deficient NK cells.

Much of this work presented above focus on the role of mTORC1 and mTORC2 in the development of NK cells. The critical role of each mTOR complex in the effector functions of NK cells remains elusive. The defective tumor clearance in *Rptor* or *Rictor* cKO mice is not sufficient to make conclusion regarding the role of each mTOR complex in the effector functions of NK cells as both mice have severe developmental defects. An inducible cKO model using $Ncr1^{ER\text{-}Cre}$ or *in vitro* deletion mediated through TAT-Cre will be instrumental in addressing this issue without affecting the normal maturation of these cells.

In summary, our study reveals the critical and differential role of mTORC1 and mTORC2 in the development of NK cells. Our study implies that clinical manipulation of mTOR

complexes can potentially compromise NK cell development and repopulation following hematopoietic stem cell transplantation.

# Chapter 4 – mTORC2-Akt$^{S473}$-FoxO1-T-bet axis suppresses the transcriptional signature of immature NK cells during the development of NK cells

## 4.1 Introduction

The developmental stages of NK cells have been conventionally defined by the expression of a few cell surface markers. This methodology has been instrumental in delineating the developmental subsets of NK cells. Importantly, it allows detailed study and manipulation of specific NK subsets. However, there are inherent limitations associated with them. Whether the full spectrum of NK cell developmental heterogeneity has been recovered by the cell surface markers-defined stages remains an open question. Based on the CD27/CD11b-defined stages, NK cells deficient with either Id2, Eomes or Gata3 all fail to progress from CD27 SP to DP stages [108, 109, 119]. There is currently no well-accepted model by which to study the developmental differences between these three NK models. In addition, the altered expression of stage-defining cell surface markers in genetically-engineered mice does not necessarily result from developmental changes.

The recent breakthrough in the quantification of transcriptome at a single cell level has offered an unprecedented methodology in determination of cell identity and exploration of cellular heterogeneity. The definition of cell identity based on the expression of thousands of transcripts seems more reliable than the detection of few cell surface markers. Crinier et al., has explored the murine and human NK cells from spleen and blood using single-cell RNA-sequencing (scRNA-seq) technology and identified a novel population in the mouse spleen and revealed the conserved NK subsets in human and mice [361]. However, the developmental heterogeneity of NK cells in the BM, the critical

anatomic location of murine NK cell development, has not been explored. Therefore, we seek to explore the heterogeneity of murine $CD3\varepsilon^{-}CD122^{+}$ cell from BM of WT mice using scRNA-seq technology. We also explored the feasibility of defining NK cell heterogeneity in mutant mice based on transcriptional landscape.

## 4.2 Results

### 4.2.1 The heterogeneity of murine BM CD3ε$^{-}$CD122$^{+}$ cells

The BM is the anatomic location where most conventional murine NK cells develop. Thus, we decided to study the developmental heterogeneity of BM NK cells at single cell level using 10X genomics due to its ability to incorporate a large number of cells. To cover the broad NK cell developmental stages, we sorted CD3ε$^{-}$CD122$^{+}$ population from BM of three mice with either Raptor, Rictor or T-bet deficiency and their corresponding WT mice. The post-sorting purity ranged from 90 to 98% (**Figure 4.1.A**). To validate the NK cell development phenotype specifically in these six mice used, we detected the expression of CD27 and CD11b via flow cytometry using the cells from BM and spleen of these six mice. Consistent with our previous reports [362], in the BM, most of the NK cells from the *Rptor*$^{fl/fl}$ *Ncr1*$^{Cre/WT}$ mouse were CD27 SP. The NK cells from the *Rictor*$^{fl/fl}$ *Ncr1*$^{Cre/WT}$ mouse were unable to fully progress to the CD11b SP stage (**Figure 4.1.B**), and the T-bet-deficient mouse completely lost the CD11b SP NK compartment (**Figure 4.1.B**) [109]. The expression pattern of CD27 and CD11b on NK cells in the spleen also matched with previous reports (**Figure 4.1.B**) [109, 362]. There was no difference in surface expression of CD27/CD11b among the three WT mice (**Figure 4.1.A**).

We started our analyses with focus on exploring the heterogeneity of CD3ε$^{-}$CD122$^{+}$ cells from WT mice using principal component analysis (PCA). To increase the clustering efficiency, we combined all the cells from three WT mice for analysis [330]. After initial

quality control and clustering analysis, we filtered out the contaminating cells from other lineages, particularly those that did not express *Il2rb*. The clustering analysis of the remaining pure CD3ε$^{-}$CD122$^{+}$ cells revealed that the cells from *Tbx21*$^{+/+}$ mouse ordered from the Jackson Laboratory clustered separate from the *Rptor*$^{fl/fl}$ *Ncr1*$^{WT/WT}$ and *Rictor*$^{fl/fl}$ *Ncr1*$^{WT/WT}$ mice housed at the Medical College of Wisconsin animal facility (**Figure 4.1.C**). These data revealed that different housing conditions could result in alteration in the transcriptome profile that leads to individual-specific phenotype in scRNA-seq analysis of NK cells.

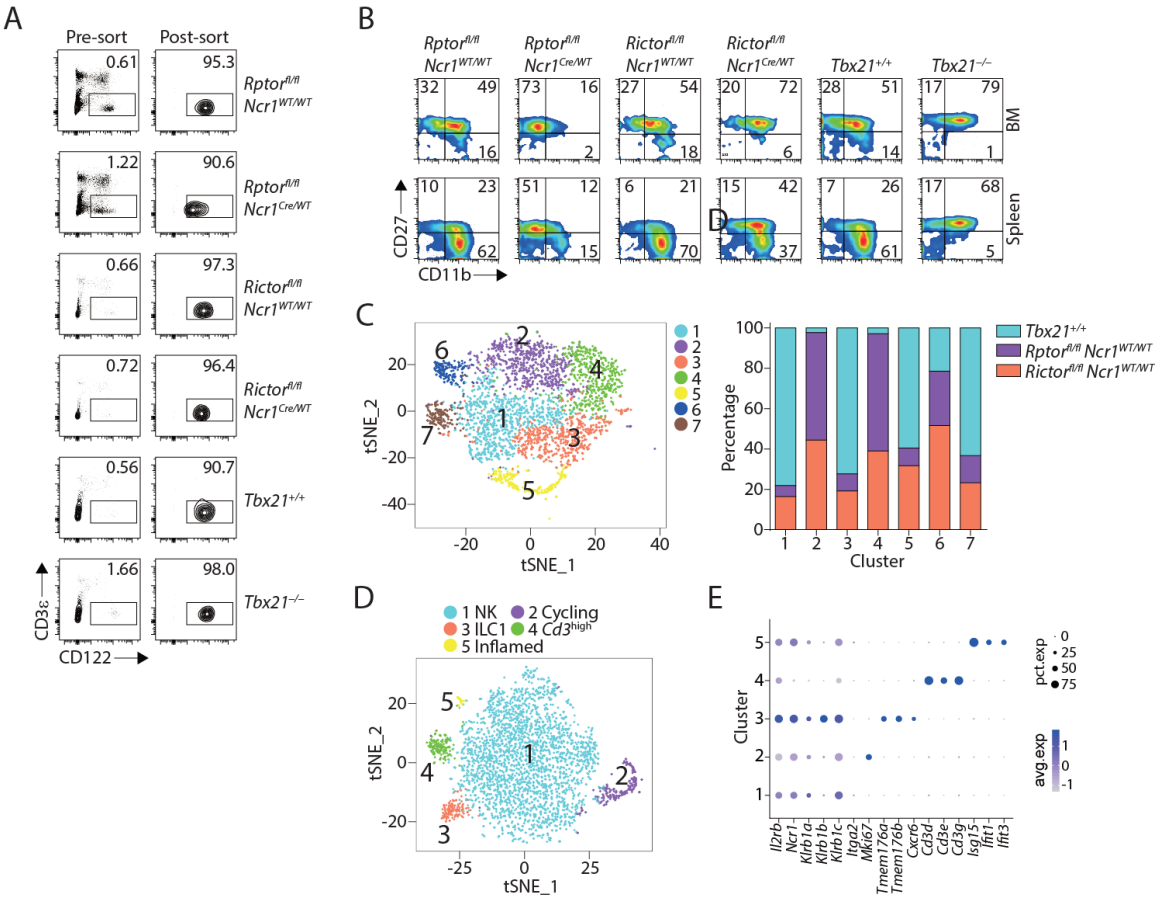

**Figure 4.1. scRNA-seq analysis of CD3ε$^{-}$CD122$^{+}$ murine BM cells from three mutant mice and their corresponding WT mice.**

(**A**) Post-sort purity of the six samples that went through the scRNA-seq experiment. (**B**) The expression of CD27 and CD11b on NK cells (gated on CD3ε$^{-}$NK1.1$^{+}$) from BM and spleen of the six mice used in the scRNA-seq experiment. (**C**) Seven clusters generated from the unbiased clustering analysis of NK cells from three WT mice without scaling the sample origin. (**D**) The composition of the three WT mice within each cluster. The input cell number from each mouse was normalized to be equal. (**E**) With low clustering resolution (0.2), the bulk CD3ε$^{-}$CD122$^{+}$ BM cells from three WT mice were clustered into five distinct populations demonstrated in the tSNE plot. (**F**) The expression of selective genes associated with the identity of each cluster in (E) were shown in dot plot. The size of the dot indicates the percentage of cells expressing the gene within each cluster (pct.exp). The color of the dot indicates the average expression of the gene within each cluster (avg.exp).

Therefore, we scaled the sample variance to ensure the cells from different WT mice cluster together. At low clustering resolution, we found 5 distinct clusters of CD3ε$^{-}$CD122$^{+}$ cells (**Figure 4.1.D**). Through exploring the differential expressed genes (DEGs) of each cluster, we found that cluster #1 were NK cells comprising majority of the CD3ε$^{-}$CD122$^{+}$ cells with high expression of *Ncr1* and three subunits (*Klrb1a*, *Klrb1b,* and *Klrb1c*) of NK1.1 (**Figure 4.1.E**). Cluster #3 were ILC1 indicated by high expression of *Tmem176a/b* and *Cxcr6* (**Figure 4.1.E**) [363]. Notably, *Ncr1* and *Klrb1a*/*b*/*c* were even more highly expressed in the ILC1 cluster than the NK cluster (**Figure 4.1.E**). Cluster #4 was marked with high expression of *Cd3d/e/g* and low *Ncr1* and *Klrb1a*/*b*/*c* expression (**Figure 4.1.E**). This population has been reported before in the scRNA-seq dataset of group 1 ILC in the lung and is potentially related to NK-T lineage [59]. We referred to it as *Cd3*$^{high}$ cluster. ILC1, *Cd3*$^{high}$ cells and NKP potentially make up the

$Lin^{-}CD122^{+}NK1.1^{-}$ cells. The expression of *Mki67* indicated that cells in cluster #2 were cycling (**Figure 4.1.E**). And cells in cluster #5 were activated by inflammatory stimuli as made evident by the high expression of interferon-induced genes (**Figure 4.1.E**). Clusters #2 and #5 cells did not express *Tmem176a/b*, *Cxcr6*, *Cd3d/e/g*, or other lineage-defining transcripts, and therefore, were likely to be conventional NK cells.

4.2.2 Five distinct BM NK subsets defined by transcriptome

Next, we removed clusters #2 to #5 from **Figure 4.1.D** to focus on the analysis of the heterogeneity of the canonical NK cells. Unbiased clustering analysis revealed five distinct NK clusters as shown using a tSNE plot (**Figure 4.2.A**). The three WT mice contributed relatively equally to each cluster, and each wild type had relatively similar proportions of each cluster (**Figure 4.2.B**). Clusters #1 to #5 accounting for 25%, 20%, 25%, 10%, 20% of the bulk NK cells, respectively (**Figure 4.2.B**). Based on the expression of several NK cell maturation-defining markers, we found that cluster #1 represented the most immature NK cells with high expression of *Cd27* and low expression of *Itgam* (CD11b) and Ly49s (*Klra1/3/4/7/8/9*) (**Figure 4.2.C**). The immature nature of cluster #1 was further bolstered by the high transcriptional expression of *Ltb*, *Thy1*, *Cd3d/g*, and *Cd7* (**Figure 4.2.D**), all of which have been shown to be highly expressed in the relatively immature CD27 SP NK cells [82]. On the contrary, the low expression of *Cd27* and high expression of *Itgam* (CD11b) and *Klrg1* marked cluster #5 as the terminally mature NK cells (**Figure 4.2.C**). NK cells are known to acquire effector functions as they mature. The high expression of functional molecules including *Gzma* and *Gzmb* further demonstrated the terminal maturity of cells in cluster #5 (**Figure 4.2.D**). Based on this information, we deemed cluster #1 and #5 as immature NK (iNK) cluster and terminally mature NK (termNK) cluster, respectively, and cluster #2, 3, 4 being transitional NK stages (transNK1, 2, 3, respectively).

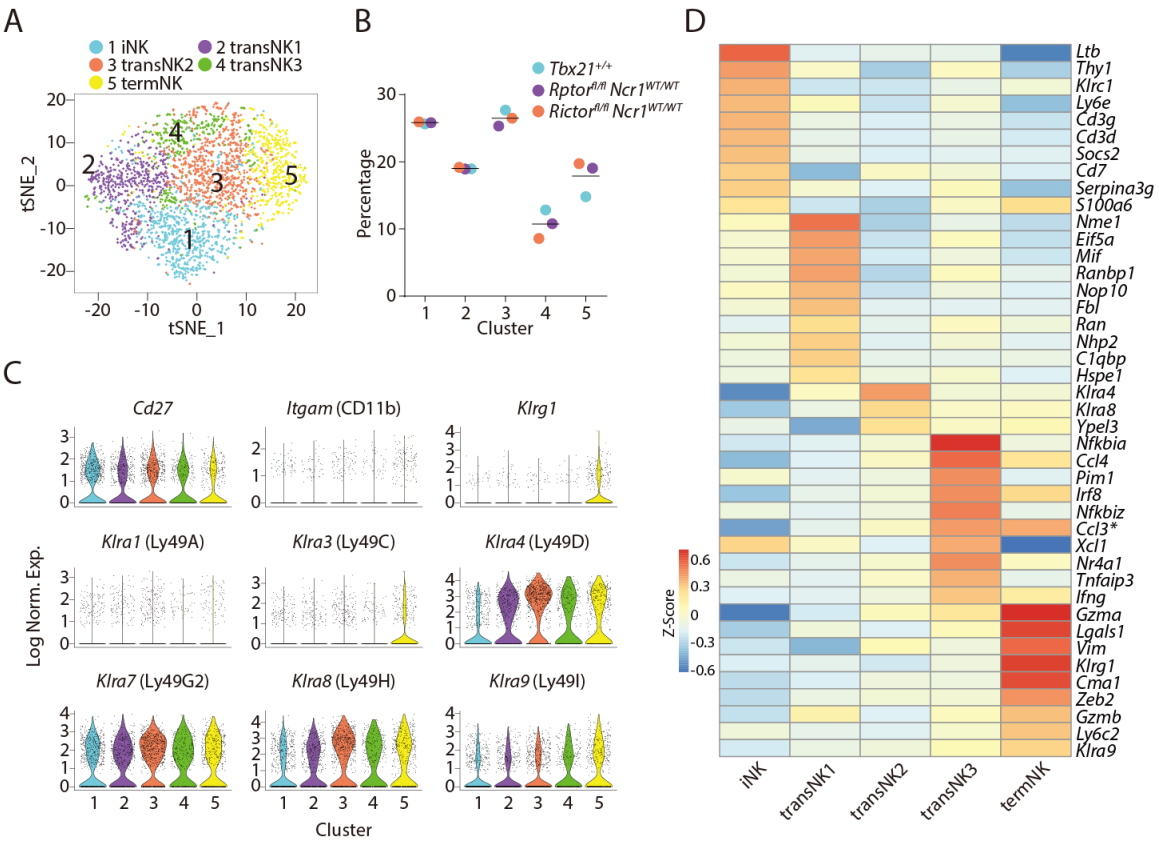


**Figure 4.2. Transcriptome-based classification of conventional murine NK cells**

(**A**) Five distinct clusters identified through unbiased clustering analysis of the NK cluster in Figure 4.2.D. (**B**) The composition of the five NK clusters in each of the WT mouse. (**C**) Violin plots demonstrate the expression of *Cd27*, *Itgam* (CD11b), *Klrg1*, and Ly49 family members in each NK cluster. The y-axis represents log-normalized expression value. (**D**) The average expression of the top 10 up-regulated DEGs (ranked by log fold change) of each NK cluster were plotted using heatmap. The transNK2 cluster only contained three up-regulated DEGs with logfc set at 0.25. * indicates genes that are DEGs of more than one cluster.

Next, we sought to explore the identity of the three transNK clusters. TransNK1 represented a unique NK sub-population with high expression of genes encoding proteins involved in ribosomal biogenesis including ribonucleoproteins (*Nop10*, *Nhp2*, *Gar1*,

*Npm1*, *Npm3*), RNA modification enzymes (*Mettl1*, *Ddx21*, *Fbl*), and GTPase related to nucleocytoplasmic transport (*Ran*, *Ranbp1*). We also found highest expression of genes encoding the ribosomal subunits in this cluster. Gene set enrichment analysis (GSEA) revealed significantly enrichment of transcription factors MYC and E2F in tranNK1 cluster compared to the rest of cells, both of which are involved in cell growth and proliferation [364, 365]. We also found major metabolic pathways were enriched in this cluster including glycolysis, oxidative phosphorylation and fatty acid metabolism. Specific to transNK2, only fewer up-regulated transcripts has been identified (**Figure 4.2.D**). This cluster was featured with high expression of Ly49 family members especially *Klra4* (Ly49D) and *Klra8* (Ly49H) implying unique NK cell educational program of this cluster (**Figure 4.2.C and 4.2.D**). As for the transNK3 cluster, we found many genes in the category of immediate early genes (IEGs) were up-regulated including *Nr4a1*, *Nr4a2*, *Nr4a3*, *Dusp1*, *Junb*, *Nfkbia*, *Nfkbid*, *Nfkbiz*, *Egr1*, etc. This cluster is transcriptionally similar to the novel NK_3 cluster defined previously in the mouse spleen with up-regulation of genes including *Pim1*, *Gadd45b*, *Bhlhe40*, *Irf8*, *Ccl3*, *Ccl4* besides the IEGs.

4.2.3 The relative maturity of the three transitional NK subsets

To further elucidate the relative maturity of the three transitional NK clusters, we explored the transcriptome progression along the maturation process. The Euclidean distance indicated closer transcriptional similarity between transNK1 and transNK2, both of which were transcriptionally closer to the iNK cluster (**Figure 4.3.A**). In comparison, the transNK3 was transcriptionally closer to the termNK cluster (**Figure 4.3.A**). As NK cells progress along the developmental stages, a set of genes will gradually lose their expression versus another set of genes induced over time. Most of these genes are highly expressed at the two developmental extremes: the immature and terminal mature stages. Therefore, we calculated the module score of all five clusters based on the up-regulated or down-regulated DEGs of the iNK and termNK clusters. When we ordered the five clusters as iNK→transNK1→transNK2→transNK3→termNK, the module score based on the up-regulated DEGs of the iNK cluster or the down-regulated DEGs of the termNK cluster gradually declined (**Figure 4.3.B**). In contrast, the module score based on the up-regulated DEGs of the termNK or the down-regulated DEGs of the iNK cluster gradually increased (**Figure 4.3.B**). This indicated a sequential developmental progression of these five clusters in the order list above. To further validate this notion, we analyzed the bulk RNA-seq dataset of CD27 SP, DP and CD11b SP NK subsets published previously and picked the up-regulated DEGs from both CD27 SP and CD11b SP NK subsets as the target gene list (named as "CD27/CD11b gene sets" here) to calculate the module score (**Figure 4.3.C**) [108]. The overall low module score yield indicated the low coverage of the transcriptome in the 10X-based scRNA-seq dataset. Nevertheless, we still found a

trend in increasing expression of terminally mature NK genes and decreasing expression of immature NK genes over the above cluster order (**Figure 4.3.C**).

To further establish the developmental progression of these five clusters, we adopted the Monocle2 pseudotime analysis to simulate the maturation trajectory in an unbiased manner. Based on the transcriptional information, each cell from the five clusters were assigned to the pseudotime trajectory (**Figure 4.3.D**). The pseudotime indicated the maturation order with the least mature cells being identified as the root point of the trajectory. As shown in **Figure 4.3.E**, the far-left side of the trajectory located the least mature NK cell, while the far-right side the trajectory was the most mature population. When we plotted the cells from individual cluster along the trajectory (**Figure 4.3.F**), we found majority of the cells in iNK and tranNK1 clusters dominate the left side of the trajectory indicating an early stage of development. The cells in transNK2 and transNK3 clusters spread across the trajectory, while cell in the termNK cluster dominated the far-right side indicating the terminal differentiation. In combination of the transcriptome signature associated with each cluster and the unbiased analysis of the maturation trajectory, we deemed the relative maturity of this five NK clusters as iNK→transNK→transNK2→transNK3→termNK.

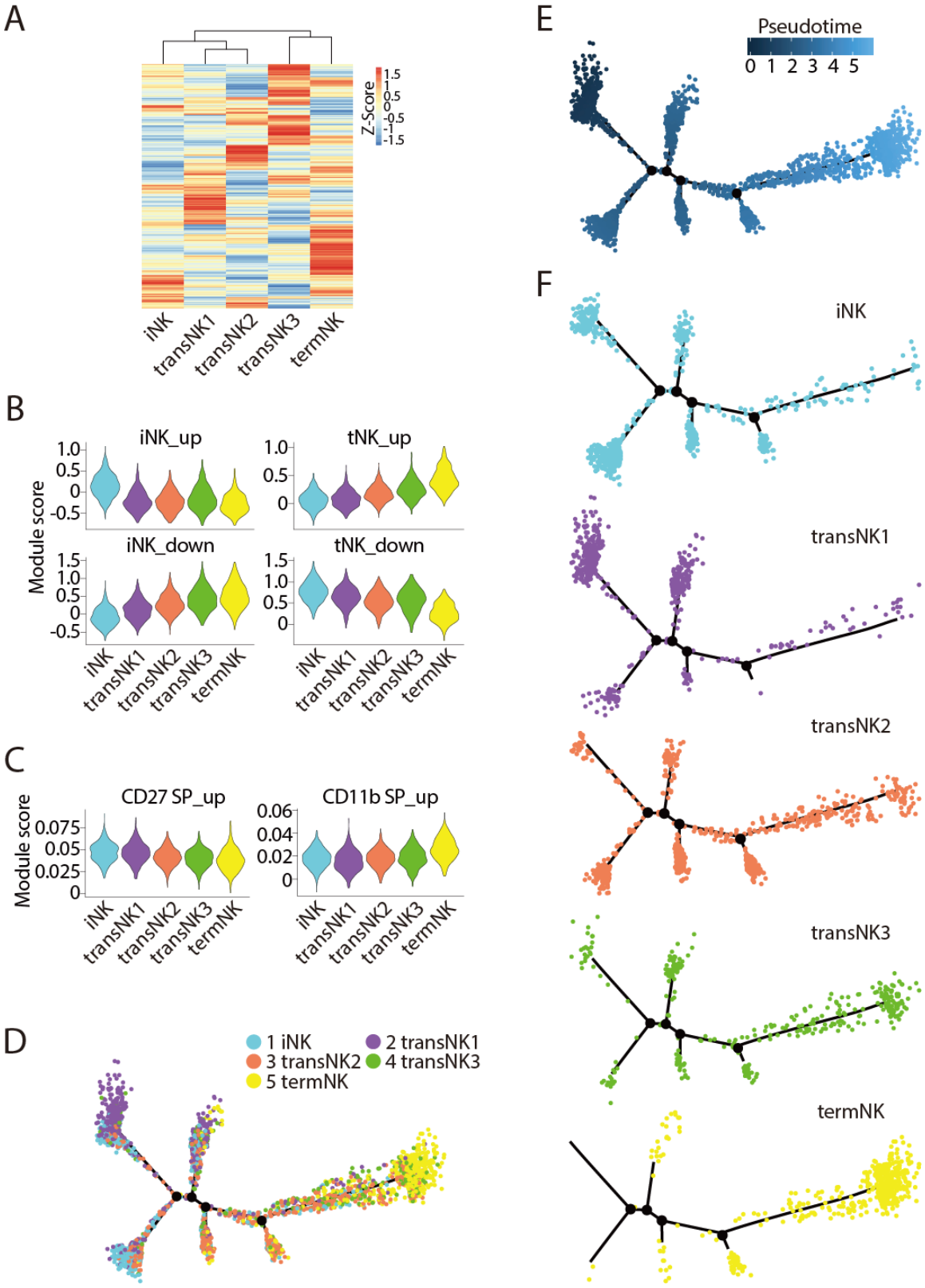
A
Z-Score
1.5
1
0.5
0
-0.5
-1
-1.5
iNK
transNK1
transNK2
transNK3
termNK
B
iNK_up
tNK_up
iNK_down
tNK_down
Module score
C
CD27 SP_up
CD11b SP_up
Module score
D
1 iNK
2 transNK1
3 transNK2
4 transNK3
5 termNK
E
Pseudotime
0 1 2 3 4 5
F
iNK
transNK1
transNK2
transNK3
termNK

**Figure 4.3. The relative maturity of the five distinct NK clusters**

(**A**) The transcriptome similarity among the five NK clusters was evaluated by the hierarchical clustering analysis and visualized via heatmap. Each row represents a variable gene among clusters and each column represents one cluster. (**B**) Module scores were calculated using up-regulated or down-regulated DEGs of iNK and termNK clusters and plotted via violin plots. (**C**) The up-regulated genes in the CD27 SP and CD11b SP subset were extracted from the CD27/CD11b bulk RNA-seq dataset. The expression level of these genes in the five NK clusters were evaluated via calculating module scores and plotted via violin plots. (**D**) Distribution of all five NK clusters along the pseudotime trajectory. (**E**) The relative maturity of the developmental trajectory was indicated as pseudotime. (**F**) Distribution of each NK clusters along the pseudotime trajectory.

4.2.4 Raptor- or Rictor-deficient cells cluster separate from WT cells

The expression of cell surface markers has been conventionally used to define cellular identity. Although it is useful in many cases, there are limitations and potential drawbacks associated with this methodology especially in disordered conditions seen in transgenic mice or patients. Previously, we have characterized the development of Raptor- or Rictor-deficient NK cells that do not possess mTORC1 or mTORC2, respectively [362]. We found differential maturation impairment with Raptor-deficient NK cells accumulating at the CD27 SP stage while Rictor-deficient NK cells being impaired in transition from DP to terminal CD11b SP stage. Using these two transgenic mice lines, we profiled the BM $CD3^{-}CD122^{+}$ cells using scRNA-seq to validate whether transcriptome-based cell stage classification match with previous cell surface markers-defined maturity.

We combined the mutant cells with their corresponding WT cells and conducted PCA-based clustering analysis. Strikingly, nearly all the Raptor-deficient $CD3^{-}CD122^{+}$ cells clustered separately from the WT cells (**Figure 4.4.A**). As illustrated in the t-SNE plot, cluster #1 to #5 were dominated by WT cells, while cluster #6 and #7 were mostly Raptor-deficient cells (**Figure 4.4.A and 4.4.B**). This is consistent with our previous demonstration of a large transcriptome alteration in the absence of Raptor [362]. Cluster #8 is the only cluster that is evenly composite of both Raptor-deficient and WT cells (**Figure 4.4.A and 4.4.B**). The high expression of *Tmem176a/b* and *Cxcr6* revealed cluster #8 were ILC1 while all the rest seven clusters were NK cells (**Figure 4.4.C**).

Comparatively, cluster #1 had higher expression of *Cd3d/e/g*, however, this was not *Cd3*$^{high}$ cluster defined previously based on the high expression of *Ncr1*. Instead, cluster #1 were iNK cells and the higher transcripts level of CD3 chains has been reported before in immature NK cells [366]. We did not find cycling or inflamed cluster in this analysis presumably due to lower cell number from these two samples compared to previous WT NK cell analysis. As the expression of *iCre* driven by *Ncr1* presumably also occurred in the ILC1, this data indicated that mTORC1 is potentially dispensable for the development of ILC1.

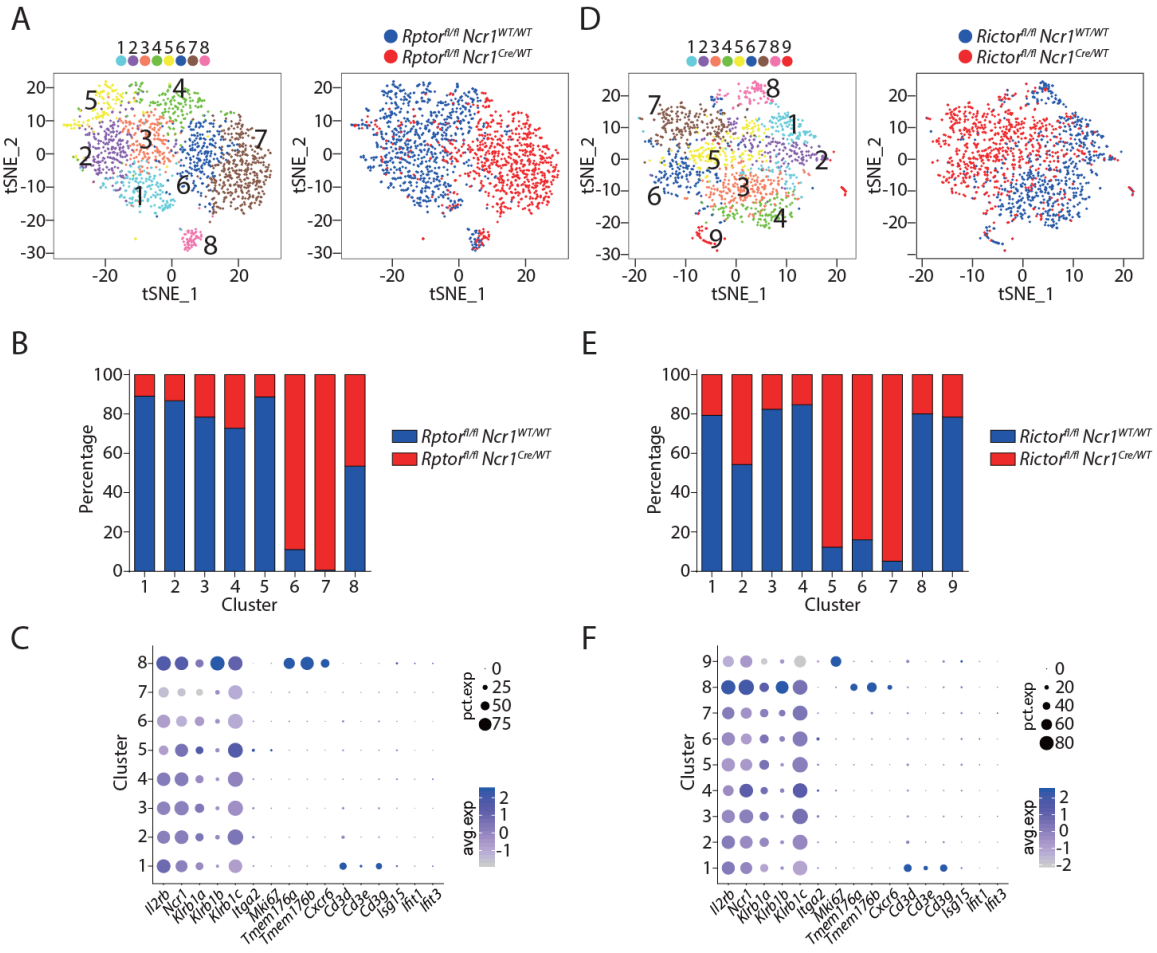

**Figure 4.4. Unbiased clustering analysis of Raptor- or Rictor-deficient cells**

(**A**) Clustering analysis of CD3ε$^{-}$CD122$^{+}$ cells from BM of *Raptor* cKO mouse and the littermate WT mouse. The clusters are displayed as tSNE plots on the left. The cell origin was labeled in the same tSNE plot on the right. (**B**) The composition of the WT and Raptor-deficient cells within each cluster. The input cell number from each mouse was normalized to be equal. (**C**) The same gene list from Figure 4.1.E were used to evaluate the identity of each cluster formed by WT and Raptor-deficient cells. (**D**-**F**) (D), (E) and (F) are same analysis using WT and Rictor-deficient NK cells as (A), (B), and (C), respectively.

Compare to Raptor-deficiency, NK cells absent of Rictor have a more restricted transcriptome alteration [362]. Nevertheless, clustering analysis still largely separated the WT NK cells with the Rictor-deficient NK cells (**Figure 4.4.D and 4.4.E**). Within the nine identified clusters from the CD3ε$^{-}$CD122$^{+}$ cells, cluster#1 to #4 were mostly comprised with WT NK cells, while cluster #5 to #7 were dominated by Rictor-deficient NK cells (**Figure 4.4.D and 4.4.E**). We identified cluster #8 and #9 as ILC1 and cycling cells indicated by the expression of *Tmem176a/b*, *Cxcr6* and Mki67, respectively (**Figure 4.4.F**). The reduced contribution of *Rictor* cKO mice to the ILC1 cluster was potentially due to the impaired expression of T-bet which is critical to the ILC1 lineage (**Figure 4.4.E**) [367]. The reduced cycling cells from the *Rictor* cKO mice was consistent with our previous report [362].

4.2.5 Transcriptome similarity between Raptor- or Rictor-deficient NK cells with their corresponding WT cells

Next, we examined the relationship between the five WT NK clusters and the two Raptor-deficient NK clusters. The DEGs revealed cluster #1 and #5 represents the least and most mature NK clusters in the WT sample, respectively. Module scores based on DEGs of iNK and termNK from above combined WT analysis supported this identity of cluster #1 and #5 (**Figure 4.5.A**). Although majority of the Raptor-deficient NK cells falls into CD27 SP stage, neither cluster #6 or #7 had high expression of the iNK signature genes (**Figure 4.5.A, iNK_up**). Consistent with their immature phenotype, they expressed the termNK signature genes at low level (**Figure 4.5.A, termNK_up**). We also calculated the module score based on the CD27/CD11b gene sets. The iNK and termNK features of cluster #1 and #5 were consistent (**Figure 4.5.B**). The cluster #6 and #7 from the *Rptor* cKO mouse demonstrated similar level of CD27 SP stage signature gene expression as cluster #1 and had lowest CD11b SP stage signature gene expression (**Figure 4.5.B**). The Euclidean distance further emphasized the large transcriptome alteration of Raptor-deficient NK cells as cluster #6 and #7 were distant from the WT clusters (**Figure 4.5.C**).

When we focused on the analysis of NK cells from the *Rictor* WT and cKO mice, the DEGs and module scores based on DEGs of iNK and termNK of combined WT analysis indicated that cluster #1 and #4 represent the iNK and termNK in the *Rictor*$^{fl/fl}$ *Ncr1*$^{WT/WT}$ mouse, respectively, with cluster #2 and #3 being the transitional stages (**Figure 4.5.D**).

Interestingly, all three Rictor-deficient NK cells-dominated clusters (#5, 6, 7) had high expression of up-regulated genes in the iNK cluster to the level similar to the least mature

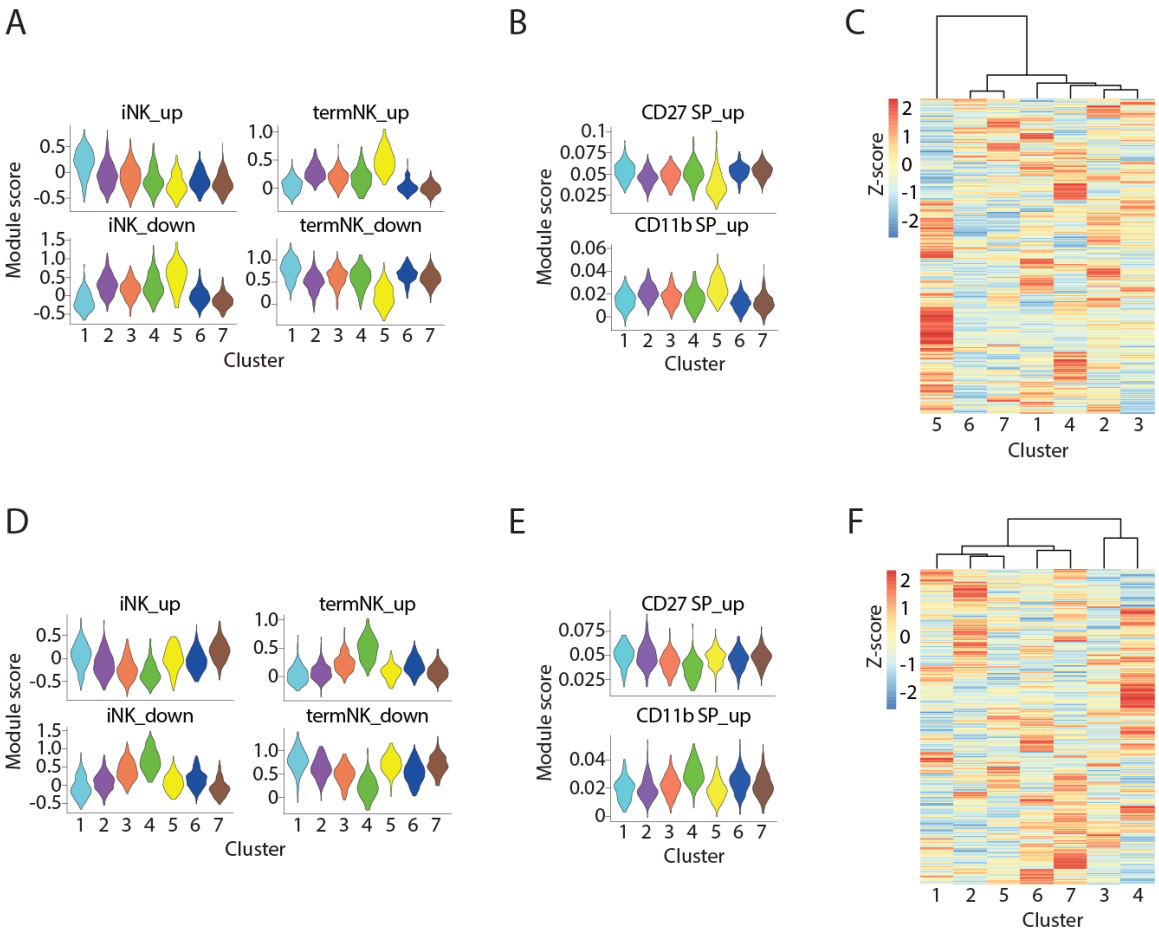


**Figure 4.5. Transcriptome similarity between Raptor- or Rictor-deficient NK cells with their corresponding WT cells**

(**A**) Module scores were calculated using up-regulated or down-regulated DEGs of iNK and termNK clusters and plotted in all the NK clusters formed by WT and Raptor-deficient cells. (**B**) The expression level of CD27 SP and CD11b SP subset signature genes in the NK clusters formed by WT and Raptor-deficient cells were evaluated via calculating module scores and plotted via violin plots. (**C**) The transcriptome similarity among the NK clusters formed by WT and Raptor-deficient cells was evaluated by

the hierarchical clustering analysis and visualized via heatmap. (**D-F**) (D), (E) and (F) are same analysis using WT and Rictor-deficient NK cells as (A), (B), and (C), respectively.

cluster #1 of WT NK cells (**Figure 4.5.D, iNK_up**). Module score based on CD27/CD11b gene sets also demonstrated similar phenomenon, though less striking (**Figure 4.5.E, CD27 SP_up**). The relative expression of signature genes associated with terminally mature NK cells in Rictor-deficient NK clusters (#5, 6, 7) was similar to the transitional NK clusters (#2, 3) from WT mouse (**Figure 4.5.D and 4.5.E**). Strikingly, the hierarchical clustering analysis indicated that nearly all the Rictor-deficient NK cell-dominated clusters (#5, 6, 7) were in closer proximity to the most immature cluster #1 and the less mature transitional cluster #2 of WT mouse (**Figure 4.5.F**). The fact that cluster #1 and #2 only accounted for less than 50% of the WT NK cells emphasized that the Rictor-deficient NK cells were less mature than previously cell surface CD27/CD11b-defined maturity.

4.2.6 Transcriptome-defined maturity of Raptor- or Rictor-deficient NK cells

As both Raptor- and Rictor-deficient NK cells clustered separate from their corresponding WT NK cells, we decided to apply machining learning based algorithm to classify the developmental stages of these genetically-modified NK cells based on the WT controls. In total, we utilized five different machine learning algorithms including generalized linear classifier (GL), gradient boosting classifier (GB), extreme gradient boosting classifier (XGB), random forest classifier (RF), and deep learning classifier (DL, neural networks). To train the classifiers, we took a random sample of 80% of the cells from the combined WT analysis. We tested the prediction accuracy of each classifier using the rest of 20% cells which were not included in the initial training process. As summarized in the **Table 4.1**, the overall accuracy of all classifiers ranged from 60% to 70% with GL and DL being the most accurate. Importantly, all five NK clusters were identified by the classifiers except for the RF classifier which failed to detect the transNK3 subset (**Figure 4.6.A**). The overall composition of the five NK clusters assigned by the machining learning classifiers were similar to the original identity defined in the PCA analysis (**Figure 4.6.A**).

| | Machine learning classifiers | | | | |
|---|---|---|---|---|---|
| Statistic | Generalized Linear (GL) | Gradient Boosted (GB) | XGB Boost (XGB) | Random Forest (RF) | Deep Learning (DL) |
| Test accuracy | 0.700 | 0.660 | 0.610 | 0.600 | 0.690 |
| Cross validation accuracy | 0.630 | 0.630 | 0.590 | 0.550 | 0.660 |
| Mean standard error | 0.320 | 0.310 | 0.340 | 0.440 | 0.310 |
| Mean per class error | 0.400 | 0.410 | 0.440 | 0.520 | 0.370 |

**Table 4.1. The accuracy and error rates of the five distinct machining learning classifiers**

When we applied the classifier algorithms on the *Rptor* cKO samples, we could barely detected transNK3 and termNK clusters (**Figure 4.6.B and 4.6.C**). The most dominant cluster of the *Rptor*$^{fl/fl}$ *Ncr1*$^{Cre/WT}$ mouse was transNK2 accounting for more than 50% of the total Raptor-deficient NK cells (**Figure 4.6.B and 4.6.C**). Based on the cell surface expression of CD27/CD11b, more than 70% of the *Rptor* cKO NK cells in the BM are considered immature CD27 SP NK cells which only accounts for about 30% of WT NK cells [362]. However, based on the transcriptome-defined stages, the least mature iNK cluster only occupied about 20% of the *Rptor* cKO NK cells similar to the WT control (**Figure 4.6.A and 4.6.C**). The fact that half of the Raptor-deficient NK cells were considered as intermediately mature transNK2 cells emphasized that the NK cells from *Rptor*$^{fl/fl}$ *Ncr1*$^{Cre/WT}$ mice might be more mature than previously defined via CD27/CD11b. Notably, one observation that consistent with both cell surface markers- and transcriptome-defined maturity was that *Rptor* cKO mice do not have terminally mature NK cells (**Figure 4.6.C**).

The classification of Rictor-deficient NK cells resulted in a more surprising result with 50% of all *Rictor* cKO NK cells fell into the category of iNK cluster (**Figure 4.6.D and 4.6.E**). This is a drastic contradiction to the cell surface markers-defined maturity which revealed only terminal maturation defects of Rictor-deficient NK cells [362]. This result was consistent with the high expression of iNK signature genes in *Rictor* cKO NK cells and short Euclidean distance between the WT immature NK compartments and all the Rictor-deficient NK cells (**Figure 4.5.D and 4.5.F**). Unlike the

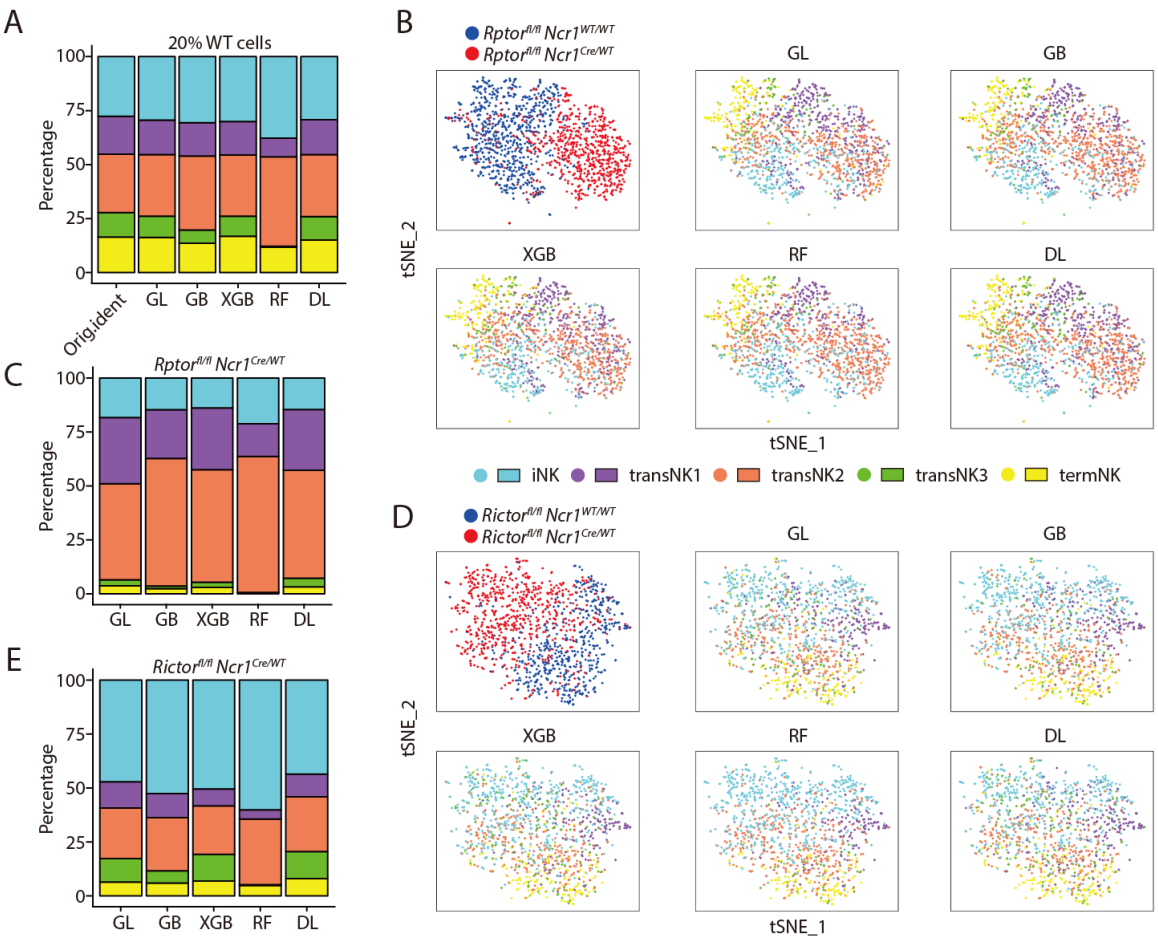


**Figure 4.6. The identity of the Raptor- or Rictor-deficient NK cells defined by machining learning classifiers**

(**A**) The original composition of the five NK clusters in the 20% WT testing cells along with the composition determined by the machining learning classifiers were plotted in the bar graph. (**B**) The identity of each WT and Raptor-deficient NK cells were assigned by five distinct machining learning classifiers as shown in the tSNE plots. (**C**) The composition of the five NK clusters in Raptor-deficient NK cells determined by the machining learning classifiers. (**D, E**) (D) and (E) are same analysis using WT and Rictor-deficient NK cells as (B) and (C), respectively.

*Rptor* cKO sample, we could still detect transNK3 and termNK clusters in *Rictor* cKO NK cells with a reduction in percentage of termNK clusters compared to the littermate

WT mouse consistent with reduced CD11b SP cells in *Rictor* cKO mice (**Figure 4.6.A and 4.6.E**). In summary, through machine learning based classification, we found new insights into the maturity of Raptor- or Rictor-deficient NK cells that were previously masked by the cell surface markers-based definition.

4.2.7 T-bet-deficient NK cells have a transcriptional profile similar to the iNK cluster

In our previous report, we proposed that mTORC2 regulates the terminal maturation of NK cells through Akt$^{S473}$-FoxO1-T-bet axis [362]. As the impaired expression of T-bet in Rictor-deficient NK cells is potentially responsible for the maturation defects, we reasoned whether a large proportion of the T-bet-deficient NK cells are also transcriptionally closer to WT immature NK cells, a phenomenon seen in *Rictor* cKO NK cells. To test this, we conducted the same scRNA-seq experiment using CD3ε$^{-}$CD122$^{+}$ cells from BM of WT and *Tbx21*$^{-/-}$ mice purchased from the Jackson Laboratory. The PCA-based clustering analysis of CD3ε$^{-}$CD122$^{+}$ cells from WT and *Tbx21* KO mice resulted in 12 distinct clusters with nearly complete separation between WT and *Tbx21* KO cells (**Figure 4.7.A and 4.7.B**). Based on the expression of key markers (**Figure 4.7.C**), we found that cluster #1-7 comprised of NK cells. Cluster #8-10 were ILC1, *Cd3*$^{high}$, and inflamed clusters, respectively. Both cluster #11 and #12 were cycling cells with high expression of *Mki67* (Ki-67) (**Figure 4.7.C**). The G2M.Score and S.Score indicated that cells in the cluster #11 were mostly in the S phase while cells in the cluster #12 were mostly in the G2M phase (**Figure 4.7.D**). Illustrated by the distribution, there was almost no ILC1 (#8) and *Cd3*$^{high}$ (#9) cluster cells in the *Tbx21*$^{-/-}$ sample (**Figure 4.7.B**). This was consistent with T-bet being the master transcription factor of ILC1 lineage [367], and the *Cd3*$^{high}$ cluster being a lineage related to NK-T cells which is nearly absent in *Tbx21*$^{-/-}$ mice [121]. The dominance of inflamed cluster (#10) by T-bet-deficient NK cells indicated perturbation of inflammatory response resulted from global deletion of *Tbx21*, which requires further investigation in the future (**Figure 4.7.B**).

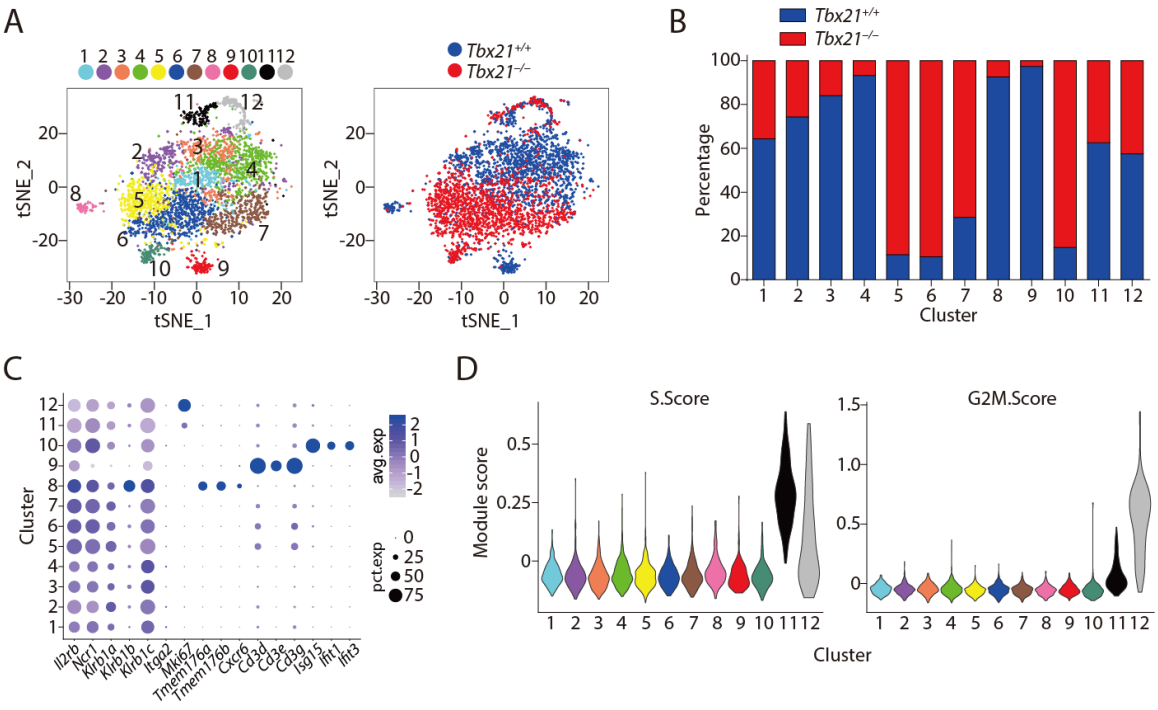


**Figure 4.7. Unbiased clustering analysis of CD3ε⁻CD122⁺ cells from BM of the *Tbx21* KO mouse**

(**A**) Clustering analysis of CD3ε⁻CD122⁺ cells from BM of the *Tbx21* KO mouse and the WT mouse. The clusters are displayed as tSNE plots on the left. The cell origin was labeled in the same tSNE plot on the right. (**B**) The composition of the WT and T-bet-deficient cells within each cluster. The input cell number from each mouse was normalized to be equal. (**C**) The same gene list from Figure 4.1.E were used to evaluate the identity of each cluster formed by WT and T-bet-deficient cells. (**D**) S.Score (left) and G2M.Score (right) were calculated and demonstrated in violin plots.

Next, we focused on the analysis of cluster #1-7 comprised of NK cells. DEGs and module scores indicated that cluster #1 and #4 were the least and most mature NK cluster of WT mouse, respectively (**Figure 4.8.A**). All three T-bet-deficient NK cells-dominated clusters (#5, 6, 7) presented similar module score pattern as the immature cluster #1 in all up- or down-regulated DEGs of iNK or termNK cluster (**Figure 4.8.A**). This pattern was also present in the module scores calculated based on the CD27/CD11b gene set (**Figure**

**4.8.B**). The transcriptional similarity between the least immature WT NK cells (cluster #1) and the bulk T-bet-deficient NK cells (cluster #5, 6, 7) were further manifested by the hierarchical clustering analysis (**Figure 4.8.C**). The short Euclidean distance among these clusters was even more striking compared to the Rictor-deficient NK sample (**Figure 4.5.F**). When we applied the machine learning-based classifiers, more than 60% of the T-bet-deficient NK cells were categorized into the iNK cluster and there were only few cells in the transNK3 and termNK clusters (**Figure 4.8.D and 4.8.E**). Collectively, these data revealed that T-bet-deficient NK cells were less mature than previously defined by cell surface markers. Direct comparison of the bulk WT and *Tbx21*$^{-/-}$ NK cells in the scRNA-seq dataset revealed that T-bet deficiency resulted in up-regulation of immature NK signature genes and down-regulation of terminally mature NK genes (**Figure 4.8.F**). Within the 14 up-regulated genes (logfc $\geq$ 0.25) in the iNK cluster from three WT combined analysis, we found 10 of those genes with significantly increased expression in T-bet deficient NK cells compared to WT NK cells (**Figure 4.8.F**). Within the 56 termNK cluster signature genes (logfc $\geq$ 0.25), we also observed decreased expression of 18 genes in T-bet deficient NK cells compared to WT NK cells (**Figure 4.8.F**). These results imply that the large proportion of T-bet deficient NK cells are halted at the transcriptionally immature NK cell stage.

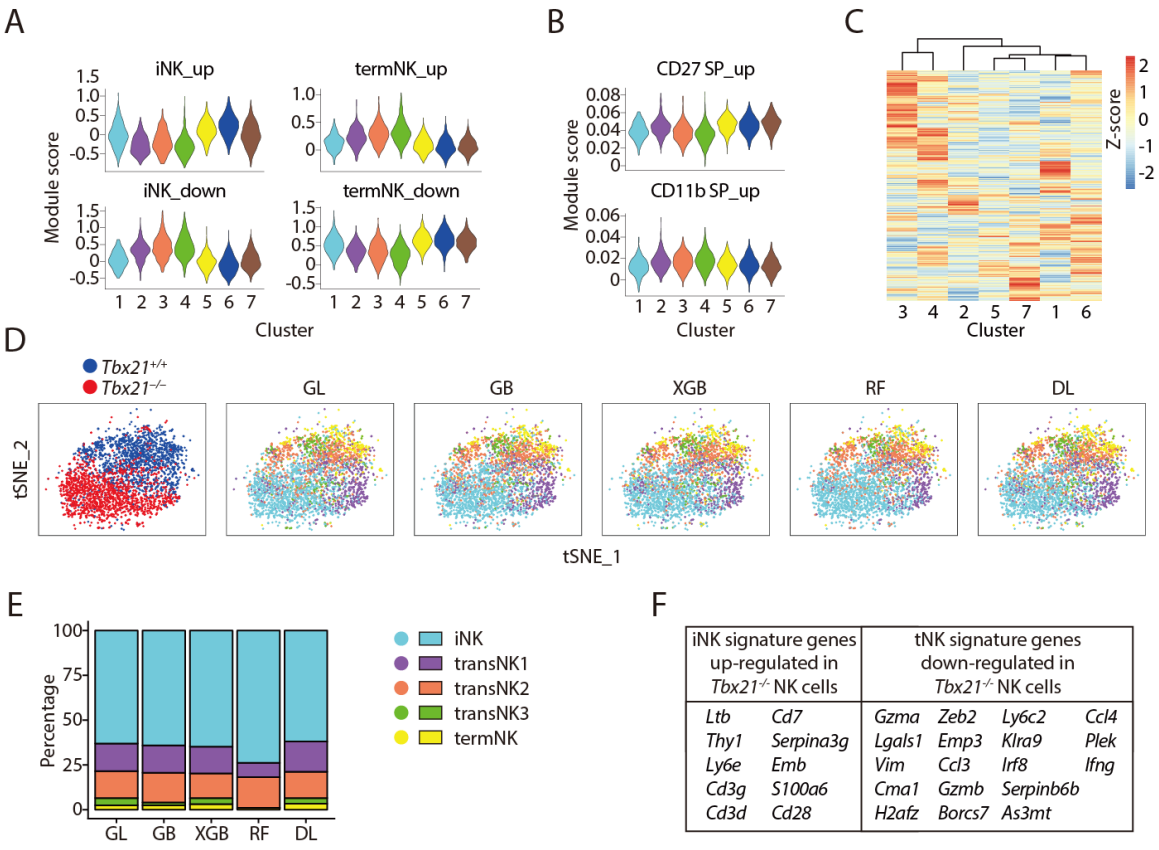


| iNK signature genes up-regulated in *Tbx21*$^{-/-}$ NK cells | | tNK signature genes down-regulated in *Tbx21*$^{-/-}$ NK cells | | | |
|---|---|---|---|---|---|
| *Ltb* | *Cd7* | *Gzma* | *Zeb2* | *Ly6c2* | *Ccl4* |
| *Thy1* | *Serpina3g* | *Lgals1* | *Emp3* | *Klra9* | *Plek* |
| *Ly6e* | *Emb* | *Vim* | *Ccl3* | *Irf8* | *Ifng* |
| *Cd3g* | *S100a6* | *Cma1* | *Gzmb* | *Serpinb6b* | |
| *Cd3d* | *Cd28* | *H2afz* | *Borcs7* | *As3mt* | |

**Figure 4.8. scRNA-seq analysis of T-bet-deficient NK cells.**

(**A**) Module scores were calculated using up-regulated or down-regulated DEGs of iNK and termNK clusters and plotted in all the NK clusters formed by WT and T-bet-deficient cells. (**B**) The expression level of CD27 SP and CD11b SP subset signature genes in the NK clusters formed by WT and T-bet-deficient cells were evaluated via calculating module scores and plotted via violin plots. (**C**) The transcriptome similarity among the NK clusters formed by WT and T-bet-deficient cells was evaluated by the hierarchical clustering analysis and visualized via heatmap. (**D**) The identity of each WT and T-bet-deficient NK cells were assigned by the five machine learning classifier as shown in the tSNE plot. (**E**) The composition of the five NK clusters in T-bet-deficient NK cells determined by the machining learning classifiers. (**F**) With logfc set at 0.25, the iNK signature genes that were significantly up-regulated and the termNK signature genes that were significantly down-regulated in T-bet-deficient NK cells compared to WT NK cells were listed in the table.

4.2.8. T-bet indirectly suppresses the expression of immature NK signature genes

The technical limitation of 10X-based scRNA-seq with capture of the most abundant transcripts only covered partial iNK signature transcripts. To what extent does T-bet suppress the expression of immature NK signature genes is still unknown. To achieve a fair comparison and in-depth coverage of the transcriptome, we conducted bulk RNA-seq analysis using only the $CD27^+$ NK cells from BM of both *Tbx21* WT and KO mice. We first validated the expression of those 28 genes identified in the scRNA-seq dataset (**Figure 4.8.F**). As demonstrated in the heatmap, indeed nearly all the 10 iNK signature genes were significantly up-regulated and the 18 termNK signature genes were significantly down-regulated in the T-bet-deficient NK cells comparing to the WT cells (**Figure 4.9.A**). Next, to obtain a larger immature NK transcriptional signature, we analyzed the CD27/CD11b bulk RNA-seq dataset and found genes that have highest expression in the CD27 SP NK subset with more than one-fold increased expression comparing to both DP and CD11b SP NK cells. In total, we found 796 genes representing the transcriptional signature of the relatively immature CD27 SP NK subset. GSEA revealed that these 796 immature NK signature genes were significantly enriched in the T-bet-deficient NK cells comparing to the WT counterparts, emphasizing that T-bet is required to suppress the expression of genes associated with immature NK cells to a large extent (**Figure 4.9.B**). In summary, these data revealed previously unappreciated role of T-bet in suppressing the immature NK transcriptional signature during the development of NK cells.

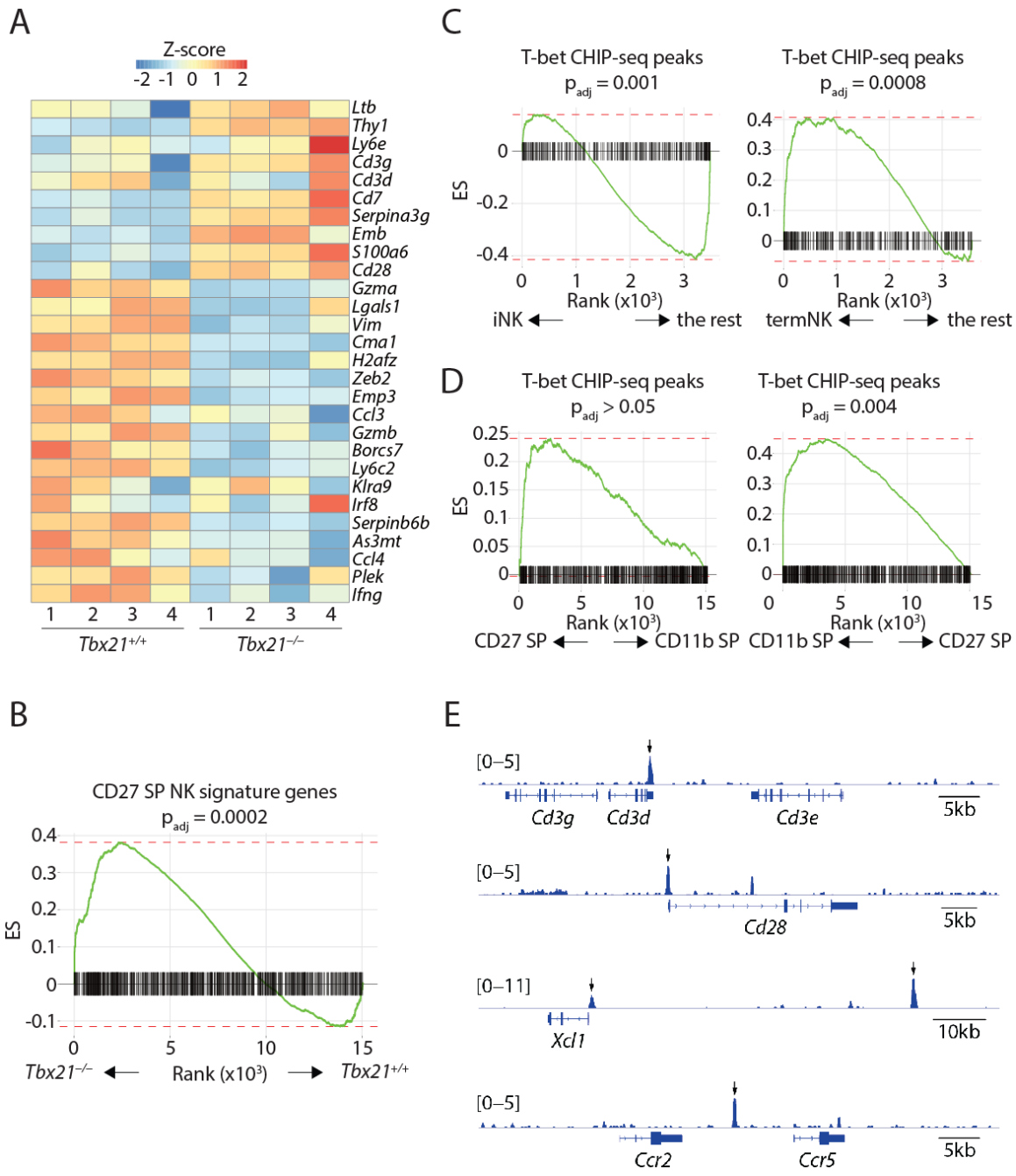


**Figure 4.9. T-bet is unlikely to directly bind and suppress the expression of large amount of immature NK genes**

(**A**) The expression level of the genes listed in Figure 4.8.F in the bulk RNA-seq analysis of the CD27+ WT and T-bet-deficient NK cells were shown in the heatmap. (**B**) The enrichment of CD27 SP NK subset signature genes in the T-bet-deficient NK cells compared to the WT NK cells. (**C**) Depletion of the T-bet CHIP-seq peaks in the iNK cluster compared to the rest of cells (left) and enrichment of the T-bet CHIP-

seq peaks in the termNK cluster compared to the rest of cells (right). (**D**) The T-bet CHIP-seq peaks were significantly enriched in the CD11b SP NK subset compared to the CD27 SP NK subset. (**E**) Examples of immature NK genes up-regulated in T-bet-deficient NK cells with significant binding of T-bet in the regulatory elements. Arrows point the significantly enriched peaks.

With this novel finding that T-bet is required for the suppression of immature NK transcriptional signature, we sought to explore the potential mechanisms for the induction of immature NK genes in T-bet-deficient NK cells. One potential explanation is that T-bet, as a transcription factor, directly binds to the regulatory elements associated with immature NK genes and actively suppresses the expression of these genes. we reanalyzed the recent published T-bet ChIP-seq dataset generated using splenic NK cells *ex vivo* and assessed whether T-bet directly binds around the immature NK genes [337]. With q-value set at $1x10^{-5}$ and focus on the protein-coding genes, we found a list of 654 T-bet binding genes. Next, we used the GSEA to determine whether the T-bet binding genes were enriched in the signature genes associated with either iNK cluster or CD27 SP NK subset. We found a significantly depletion of T-bet binding genes in the iNK cluster comparing to the rest of cells, indicating that T-bet does not directly bind to the majority of these iNK gene (**Figure 4.9.C**). On the contrary, we found the T-bet binding genes were significantly enriched in the termNK cluster comparing to the rest of cells (**Figure 4.9.C**). Similarly, when comparing the CD27 SP with the CD11b SP NK subset in the bulk RNA-seq dataset, we found significantly enrichment of the T-bet ChIP-seq peaks in the CD11b SP NK cells comparing to the CD27 SP compartment (**Figure 4.9.D**). These data were consistent with T-bet being the master transcription factor in driving terminal maturation of NK cells. Nevertheless, we still found several immature NK signature

genes that are up-regulated in T-bet-deficient NK cells with direct T-bet binding of the regulatory regions (**Figure 4.9.E**). The expression of these genes might be subject to direct suppression from T-bet. In conclusion, T-bet is unlikely to directly bind and suppress the large amount of immature NK genes, but there are a few genes could be suppressed by T-bet through this mechanism.

4.2.9 Deletion of FoxO1 rescue the altered transcriptome of Rictor-deficient NK cells

Our second hypothesis was that T-bet regulates the expression and/or activity of other transcription factors which in turn regulate the expression of immature NK genes. We examined the expression of transcription factors that are known to play a role in the development of NK cells and found majority of them had normal expression profile in either T-bet- or Rictor-deficient NK cells (**Figure S6A and S6B**) [368].

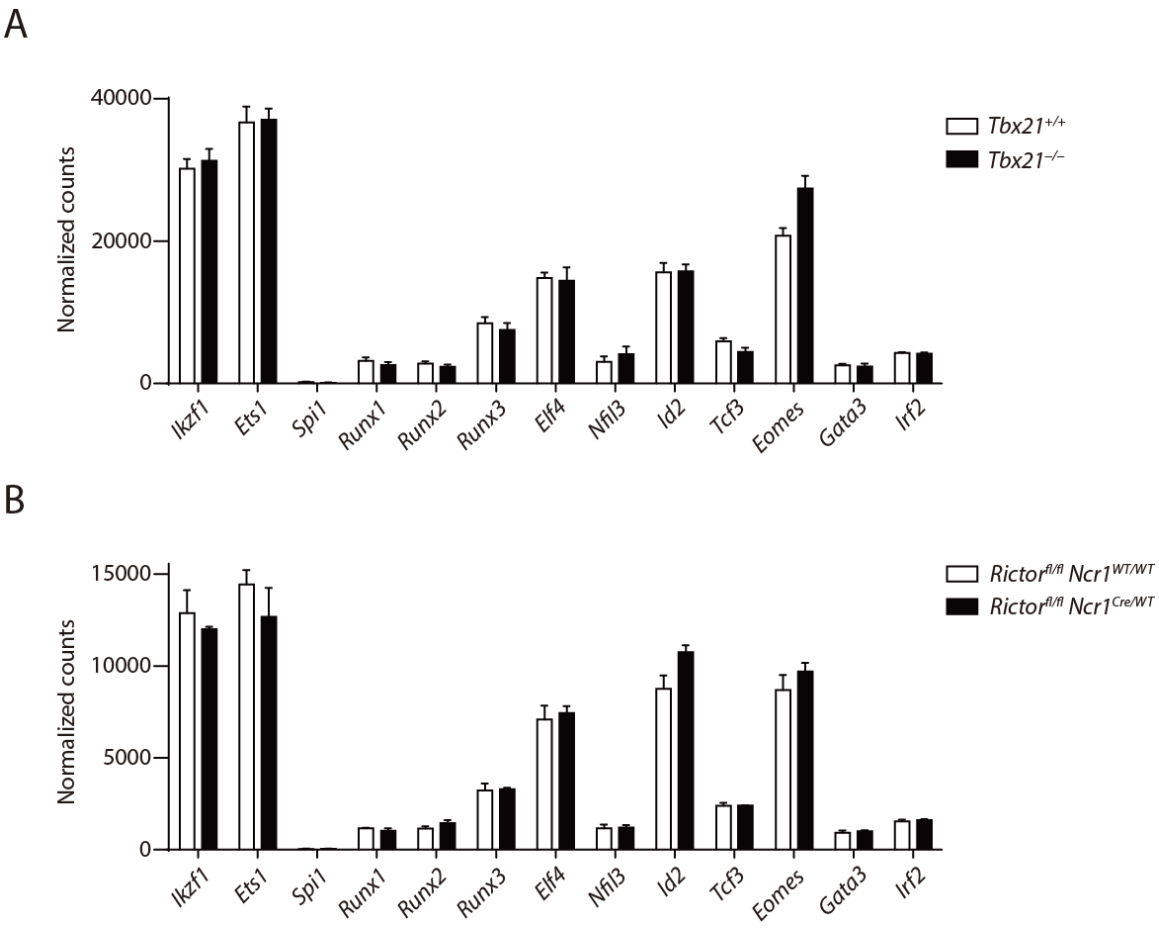


**Figure 4.10. T-bet- or Rictor-deficiency does not result in large alteration in the expression of known transcription factors critical for the development of NK cells.**

(**A, B**) The mRNA level of transcription factors essential for NK cell development in the $CD27^{+}$ T-bet- (A) or Rictor-deficient (B) NK cells and their corresponding WT control.

We next explored the GSEA and looked for enriched or depleted transcription factors in both T-bet- and Rictor-deficient NK cells. Interestingly, we found that transcription factor FoxO1 was enriched in the T-bet-deficient NK cells comparing to WT controls (**Figure 4.11.A**), a phenomenon that we have previously established in the Rictor-deficient NK cells [362]. We also found the transcripts level of *Foxo1* was significantly higher in the T-bet-deficient NK cells indicating that T-bet may suppress the expression of *Foxo1* (**Figure 4.11.B**). The direct binding of T-bet in the intron and upstream regulatory region of *Foxo1* locus further supported this possibility (**Figure 4.11.C**). These data prompted us to hypothesize that Foxo1, which has the highest expression in the CD27 SP subset [124], is essential in driving the expression of immature NK signature genes.

To further explore this hypothesis, we took the previously established *Rictor*/*Foxo1* cDKO mice and asked the question whether deletion of *Foxo1* in Rictor-deficient NK cells could correct the abnormal induction of the immature NK transcriptional signature. We profiled the $CD3\varepsilon^{-}CD122^{+}$ cells from BM of littermate $Rictor^{fl/fl}Foxo1^{fl/+}Ncr1^{Cre/WT}$ and $Rictor^{fl/fl}Foxo1^{fl/fl}Ncr1^{Cre/WT}$ mice using scRNA-seq and classified the NK cells from these mice with machine learning algorithms. Compared to the *Rictor* cKO mouse, the *Rictor*/*Foxo1* cDKO mouse harbored reduced percentage of iNK cluster

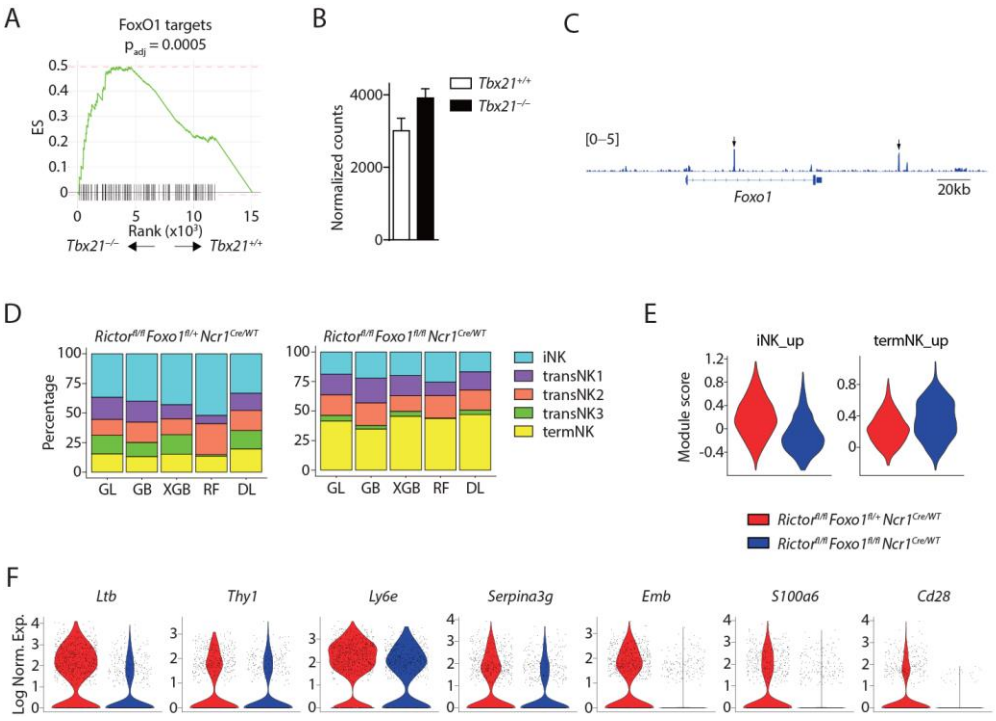


**Figure 4.11. Deletion of *Foxo1* in Rictor-deficient NK cells correct the abnormal induction of the immature NK transcriptional signature**

(**A**) Enrichment of transcription factor FoxO1 in the T-bet-deficient NK cells compared to the WT NK cells. (**B**) The transcripts level of *Foxo1* in the CD27$^{+}$ WT and T-bet-deficient NK cells. (**C**) Significant enrichment of T-bet CHIP-seq peaks at the regulatory elements associated with the *Foxo1* locus. Arrows point the significantly enriched peaks. (**D**) The composition of the five NK clusters in the littermate *Rictor*$^{fl/fl}$*Foxo1*$^{fl/+}$*Ncr*$^{Cre/WT}$ and *Rictor*$^{fl/fl}$*Foxo1*$^{fl/fl}$*Ncr*$^{Cre/WT}$ mice determined by the machining learning classifiers. (**E**) The expression of iNK and termNK signature genes in NK cells from *Rictor*$^{fl/fl}$*Foxo1*$^{fl/+}$*Ncr*$^{Cre/WT}$ and *Rictor*$^{fl/fl}$*Foxo1*$^{fl/fl}$*Ncr*$^{Cre/WT}$ mice were evaluated by module scores and plotted as violin plots. (**F**) The expression of several iNK signature genes in NK cells from *Rictor*$^{fl/fl}$*Foxo1*$^{fl/+}$*Ncr*$^{Cre/WT}$ and *Rictor*$^{fl/fl}$*Foxo1*$^{fl/fl}$*Ncr*$^{Cre/WT}$ mice were demonstrated via violin plots.

and substantially increased percentage of termNK population (**Figure 4.11.D**). We further explored the expression of the immature NK genes in both of the samples and found reduced expression of iNK signature genes in the *Rictor*/*Foxo1* cDKO mouse

compared to the *Rictor* cKO mouse (**Figure 4.11.E**). Consistent with the rescue, we also found increased expression of termNK signature genes in the *Rictor*/*Foxo1* cDKO mouse compared to the *Rictor* cKO mouse (**Figure 4.11.E**). The correction of the abnormal expression of iNK signature genes in the Rictor-deficient NK cells via deletion of *Foxo1* were further manifested with the reduced expression of a few mostly highly expressed iNK genes in the *Rictor*/*Foxo1* cDKO mouse sample (**Figure 4.11.F**). Whether the restored expression of T-bet or complete loss of FoxO1, or potentially both are responsible for the correction of the iNK gene expression requires further dissection in the future.

## 4.3 Conclusions

Through the usage of scRNA-seq technology, we found five distinct NK clusters in the BM of WT mice. Based on the expression of known markers and transcriptional similarity, we delineated the relative maturity of these five NK clusters. Based on the transcriptome information of the WT clusters, we utilized the machining learning classifiers to define the identity of Raptor- or Rictor-deficient NK cells and found maturation profiles of these mutant NK cells distinct from the cell surface markers-based definition that we previously reported [362]. The striking immaturity of the Rictor-deficient NK cells promoted us to evaluate the maturation of the T-bet-deficient NK cells with single-cell transcriptome analysis. We found even more immature NK cells in *Tbx21* KO mice than the *Rictor* cKO mice and significant up-regulation of immature NK transcriptional signature in T-bet-deficient NK cells, a phenomenon that was not appreciated previously. Lastly, through deletion of Foxo1, we corrected the abnormal induction of the immature NK signature genes and fully rescued the Rictor-deficient NK cells at the transcriptional level.

## 4.4 Discussion

With the profiling of CD3ε$^{-}$CD122$^{+}$ cells from the BM of WT mice, we found two distinct cell subsets, the ILC1 and *Cd3*$^{high}$ cells, besides the conventional NK population. These two cell populations presumably contribute to the heterogeneity of CD3ε$^{-}$CD122$^{+}$NK1.1$^{-}$ cells, the original definition of NKPs. We believe the *Cd3*$^{high}$ cells are related to the NK-T cell lineage as this population contains high transcripts level of Cd3d/e/g and is nearly absent in the *Tbx21* KO mice which is known to have fewer NK-T cells [121]. Further investigation of these *Cd3*$^{high}$ cells are warranted. Specific to the five clusters formed by the conventional NK cells, besides the easily identifiable least mature (iNK) and most mature (termNK) clusters, we named the rest three clusters as the transitional NK subsets. TransNK1 are transcriptionally closer to the iNK cluster and demonstrates a proliferative phenotype with high ribosomal contents and active metabolic profile. TransNK3 represents a unique NK subset with high expression of IEGs similar to the novel NK_3 cluster defined previously in the mouse spleen [361]. This group may be upregulating IEG's as a part of the developmental process or they may be a unique NK subset that branches off late in the developmental process.

Although we could not find reliable cell surface markers to faithfully define these five WT NK clusters, it provides an important dataset that we can utilize to profile the NK cells from mutant mice whose transcriptome profile are distinct from WT cells. Previously, we have reported the differential role mTORC1 and mTORC2 in regulating the development of NK cells [362]. Based on the cell surface markers expression, we

found mTORC1 is important for the early NK cell maturation from the CD27 SP to the DP stage, while mTORC2 governs the terminal maturation program, transiting from the DP to the CD11 SP stage. However, through utilizing machining classifiers, we found more immature NK cells in the *Rictor* cKO mice compared to the *Rptor* cKO mice, contradictory to the cell-surface markers-defined maturity. We further profiled the T-bet-deficient NK cells as we previously proposed that the impaired expression of T-bet is responsible for the terminal maturation defect of Rictor-deficient NK cells. Strikingly, we found even more immature NK cells in the *Tbx21* KO mice and a significant up-regulation of immature NK signature genes in the T-bet-deficient NK cells, which reveals a previously unappreciated role of T-bet in suppressing the immature program of NK cells.

The further exploration of the mechanisms underlining the suppressive role of T-bet in regulating the expression of immature NK genes indicated that T-bet binds the regulatory elements of only a few immature NK genes and suppresses their expression in mature NK cells. The increased expression of large number of immature NK genes implied additional transcription factors downstream of T-bet may play a role. We proposed that, in addition to the well-established role of FoxO1 in suppressing the expression of T-bet [124], T-bet can also suppress the expression of FoxO1 as the expression and activity of FoxO1 are increased in T-bet-deficient NK cells, and that this negative feedback loop is part of what defines mature NK cells as a lineage. Based on this information, we hypothesized that hyperactive FoxO1 in both the Rictor- and T-bet-deficient NK cells drive the expression of immature NK genes. One evidence to support this hypothesis is

that deletion of Foxo1 in Rictor-deficient NK cells not only rescues the terminal maturation defects but also corrects the abnormal expression of immature NK genes. More detailed experiments are required to fully establish the reciprocal regulation between FoxO1 and T-bet during the development of NK cells and their precise role in regulating the immature and terminal maturation programs.

In conclusion, through defining the developmental heterogeneity of NK cells from BM using scRNA-seq technology, we revealed previously unappreciated role mTORC2-Akt$^{S473}$-FoxO1-T-bet axis in regulating the expression of immature NK genes during NK cell development. More importantly, through using machining learning algorithms, we presented a new way to define cellular differentiation based on single-cell transcriptome analysis.

# Chapter 5 – The developmental heterogeneity of human NK cells in healthy donors and a patient with $GATA2^{T354M}$ mutation

## 5.1 Introduction

Unlike murine NK cells which primarily develop in the bone marrow (BM), human NK cells are shown to differentiate in the secondary lymphoid organs where most of their precursors and immature cells are located [86, 87]. Recently, the definition of the NK cell-restricted progenitor population has been redefined as $Lin^{-}CD34^{+}CD38^{+}CD123^{-}CD45RA^{+}CD7^{+}CD10^{+}CD127^{-}$ cells as a consistent fraction of putative NK precursors in secondary lymphoid organs turn out to be ILCs or ILC progenitors [89, 369-374]. Majority of the committed NK cells are conventionally identified by cell surface expression of CD56 and are further divided into $CD56^{bright}$ and $CD56^{dim}$ NK cells [92, 93]. $CD56^{bright}$ NK cells are believed to be the precursors of $CD56^{dim}$ NK cells with a preponderance of evidence supporting this linear progression model [87]. Nevertheless, contradictory reports challenge this dogma [97-99]. Fate mapping experiment using DNA barcode technique in rhesus macaque demonstrates that $CD56^{bright}$ and $CD56^{dim}$ NK cells derive from different precursor populations [98]. Further, individuals with *GATA2* heterozygous mutations have been reported to possess only $CD56^{dim}$ NK cells, apparently bypassing the $CD56^{bright}$ stage [97]. $CD56^{bright}$ NK cells has also been proposed to be an independent ILC1 population based on the function and transcriptome similarity between these two populations [99].

Functionally, $CD56^{bright}$ NK cells have an increased capacity of cytokine production compared to $CD56^{dim}$ NK cells which are potently cytotoxic [86, 93]. The $CD56^{dim}$ NK population is further divided into two groups based on the expression of CD57, where

CD57 cells form a terminally mature subset with a greater killing capacity [95, 96]. In contrast to this simple CD56 and CD57-based ($CD56^{bright} \rightarrow CD56^{dim}CD57^{-} \rightarrow CD56^{dim}CD57^{+}$) developmental paradigm, mass cytometry (CyTOF)-based immune profiling has revealed thousands of phenotypically distinct NK cells on the combinatorial expression of 28 cell surface receptors [100]. This contrast emphasizes the importance of further defining the heterogeneity of NK population using other modalities. As we have successfully profiled murine BM NK cells using scRNA-seq technology, we decided to explore the development and heterogeneity of human NK cells based on transcriptome of individual cell.

## 5.2 Results

### 5.2.1 scRNA-seq analysis of Lin$^-$CD7$^+$ cells from human BM and blood

To define the heterogeneity, we performed scRNA-seq experiments using NK cells from BM and the blood of six and two healthy donors, respectively. Among these, two individuals donated both the BM and blood. Since NK progenitors and some immature NK cells do not have detectable CD56 expression on the cell surface, we sorted Lin$^-$CD7$^+$ cells instead of Lin$^-$CD56$^+$ cells to include all the developmental stages of NK cells and ILCs [86]. Within the Lin$^-$CD7$^+$ population of BM or blood,

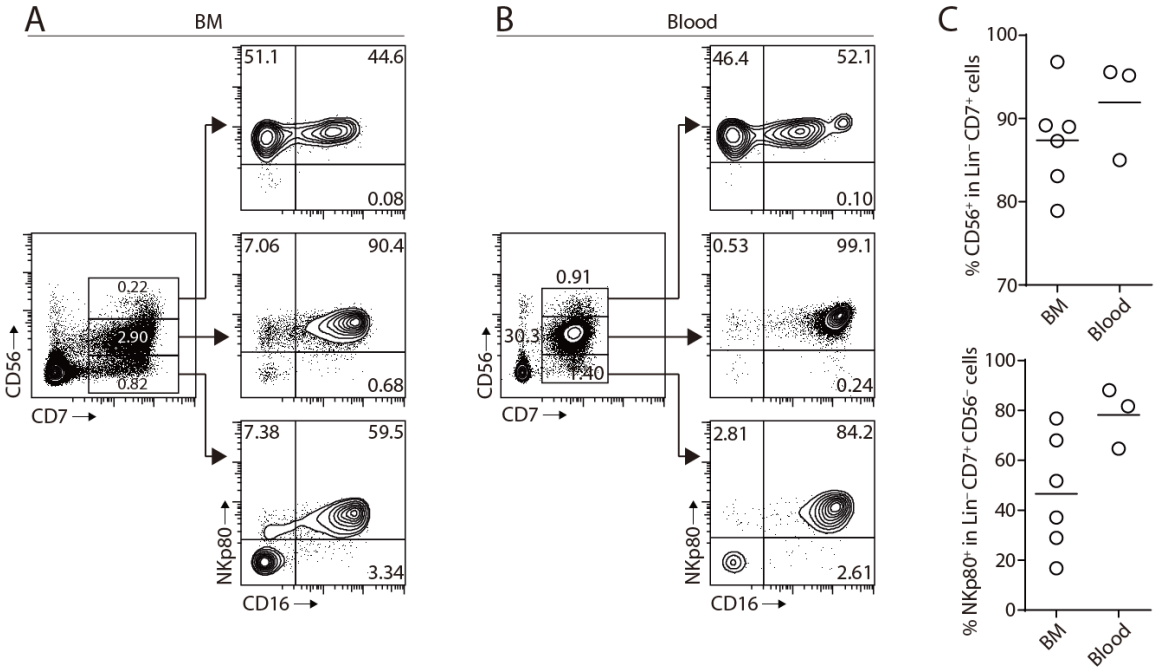

**Figure 5.1. Phenotypical analyses of Lin$^-$CD7$^+$ cells from BM and blood**

(**A**, **B**) Representative flow plots demonstrate the expression of CD56, NKp80, CD16 on Lin$^-$CD7$^+$ cells from BM (**A**) or blood (**B**) of healthy donors. (**C**) Percentage CD56$^+$ cells within Lin$^-$CD7$^+$ population and percentage of NKp80$^+$ cells within Lin$^-$CD7$^+$CD56$^-$ population were quantified.

about 90% are CD56$^+$ (**Figure 5.1**). Importantly, of the remaining CD56$^-$ cells, more than half of them express NKp80 and CD16 indicating that they are mature NK cells that lost CD56 expression on their cell surface (**Figure 5.1**) [91]. The remaining CD7$^+$CD56$^-$CD16$^-$NKp80$^-$ cells could be ILCs/NK progenitors, ILCs, immature NK cells or immature cells with multiple lineages potentials [373]. Finally, as previously reported, we found a population that expresses CD56 but not CD7 that are monocytes/DC-like cells (**Figure 5.1**) [375].

Initial quality control (QC) revealed high NK cell purity, optimal library assembly, and sequencing. Majority of the sequenced cells had more than 3,000 median unique molecular identifiers (UMIs) and a minimum of 1,000 genes associated with the cell barcodes (**Figure 5.2.A**). Most of the cells had less than 7% of the total gene expression transcribed from mitochondrial genes indicating robust cell viability (**Figure 5.2.A**). We combined the cells from six BM donors into one group and the two peripheral blood donors into another for analyses. After the QC filtering, we had a total of 5,847 BM cells and 3,061 blood cells. Initial clustering resulted in nine distinct clusters of Lin$^-$CD7$^+$ cells from BM (**Figure 5.2.B**). As expected, all the clusters have similar level of CD7 expression (**Figure 5.2.C**). Due to relatively low number of genes profiled per cell from

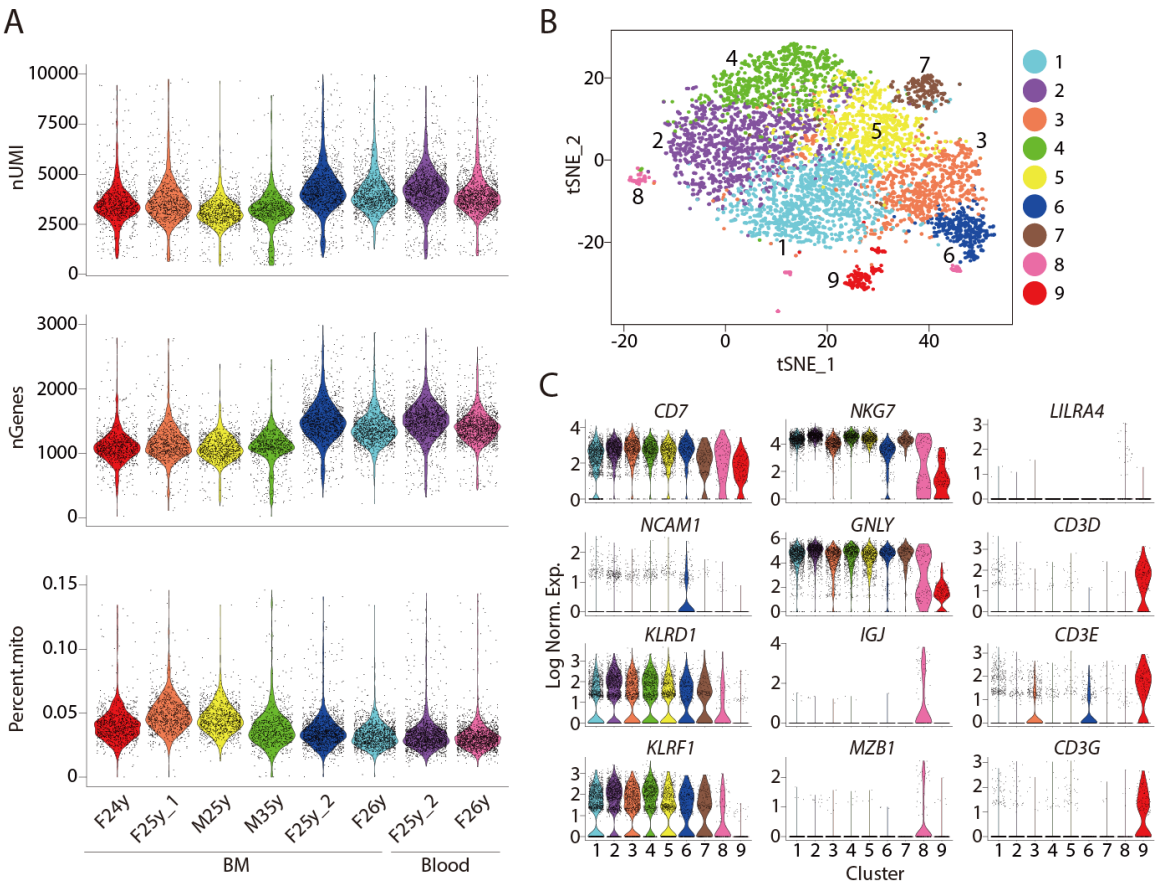


**Figure 5.2. Quality control of the scRNA-seq datasets**

(**A**) Violin plots demonstrate nUMI, nGene and percentage of mitochondria genes in the transcriptome (percent.mito) of every single cell from either BM or blood of 6 healthy donors without prior filtering. (**B**) Clustering analyses of $Lin^{-}CD7^{+}$ BM cells were illustrated via t-SNE plot. (C) The expression of genes defining NK cells, B cells, or T cells in each cluster of $Lin^{-}CD7^{+}$ BM cells were demonstrated via violin plots. The y-axis represents log-normalized expression value.

the 10X platform, CD56 (*NCAM1*) transcripts are not well represented in the dataset (**Figure 5.2.C**). Therefore, we identified another four markers as surrogates of CD56 to define NK-lineage cells. CD94 (*KLRD1*) and NKp80 (*KLRF1*) are well-defined NK cell markers [86]. We also included *NKG7* and *GNLY* as these genes are the most

differentially expressed genes in NK cells compared to other lineage cells in a total peripheral blood mononuclear cell scRNA-seq dataset [376]. Overlaying these four markers with our initial clustering revealed that cluster #8 and #9 are not part of the NK cell lineage (the 10X platform, CD56 (*NCAM1*) transcripts are not well represented in the dataset (**Figure 5.2.C**). We further demonstrated a high expression of B cell or dendritic cell-specific markers (*IGJ/MZB1/LILRA4*) in cluster #8 and T cell-specific markers (*CD3D/E/G*) in cluster #9 (the 10X platform, CD56 (*NCAM1*) transcripts are not well represented in the dataset (**Figure 5.2.C**). Therefore, we excluded cluster #8 and #9 for further analyses to focus on only NK-lineage cells.

5.2.2 The developmental heterogeneity of human NK cells from BM and blood

In the NK-lineage cells, we had 5,567 and 3,046 cells from the BM and blood, respectively. These NK-lineage cells were grouped into seven BM- and five blood-derived clusters visualized using a t-distributed Stochastic Neighbor Embedding (t-SNE) plot where each dot represents a single-cell (**Figure 5.3.A and 5.4.A**). We examined the cluster-defining differentially-expressed genes (DEGs) (**Figure 5.3.B and 5.4.B**) to name each cluster in the BM samples: 'CD56$^{bright}$ NK', 'Transitional NK', 'Active NK', 'Adaptive NK', 'Mature NK', 'Terminal NK', and 'Inflamed NK'. (**Figure 5.3.A**).

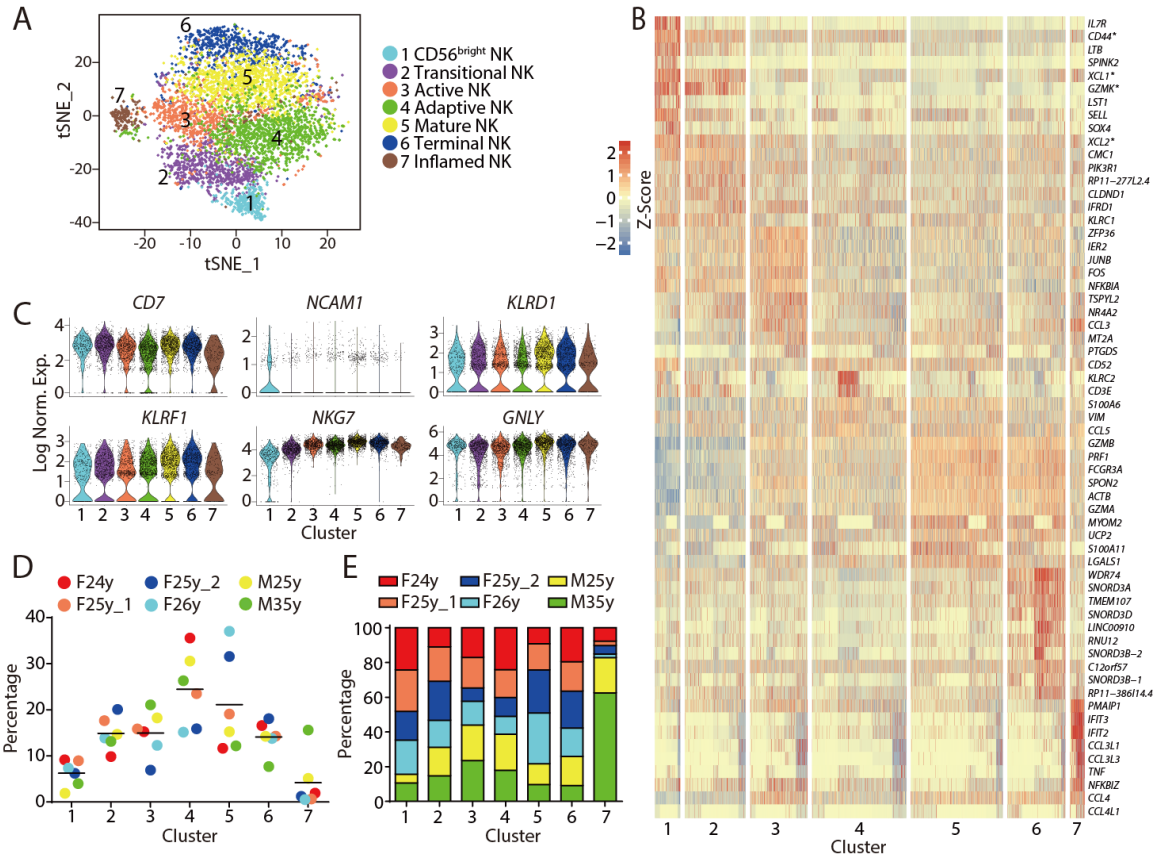

**Figure 5.3. Unbiased clustering of human NK cells from BM**

(**A**) Seven distinct human BM NK clusters were numbered, named and displayed with a t-SNE plot. (**B**) Top 10 up-regulated DEGs (ranked by log fold change) of each cluster were plotted using heatmap. * indicates genes that are DEGs of more than one cluster. (**C**) Violin plots demonstrate the expression of 6 NK-lineage-defining markers of each cluster. The y-axis represents log-normalized expression value. (**D**) Composition of the clusters within each donor. (**E**) Composition of the donors within each cluster. The input cell number from each donor is normalized to be equal.

The blood samples had similar transcriptional clusters with the exception of the 'Adaptive NK' and 'Inflamed NK' for reasons related to specific donors. The basis of these nomenclatures would be discussed in detail later. As expected, all the clusters have high expression of NK cell lineage-defining markers (**Figure 5.3.C and 5.4.C**). We then calculated the relative proportion of each cluster within individual donor (**Figure 5.3.D and 5.4.D**). The standard deviation among healthy individuals in each cluster was generally smaller than 5% with Cluster #4 and #6 in the BM samples reaching up to 10%. To validate whether all these clusters were universal among the donors, we plotted the percentages of individual clusters within each healthy donor (**Figure 5.3.E and 5.4.E**). Most of these clusters were found in all the donor samples apart from the 'Inflamed NK' cluster which was dominated in the 35-year male donor sample (**Figure 5.3.E**).

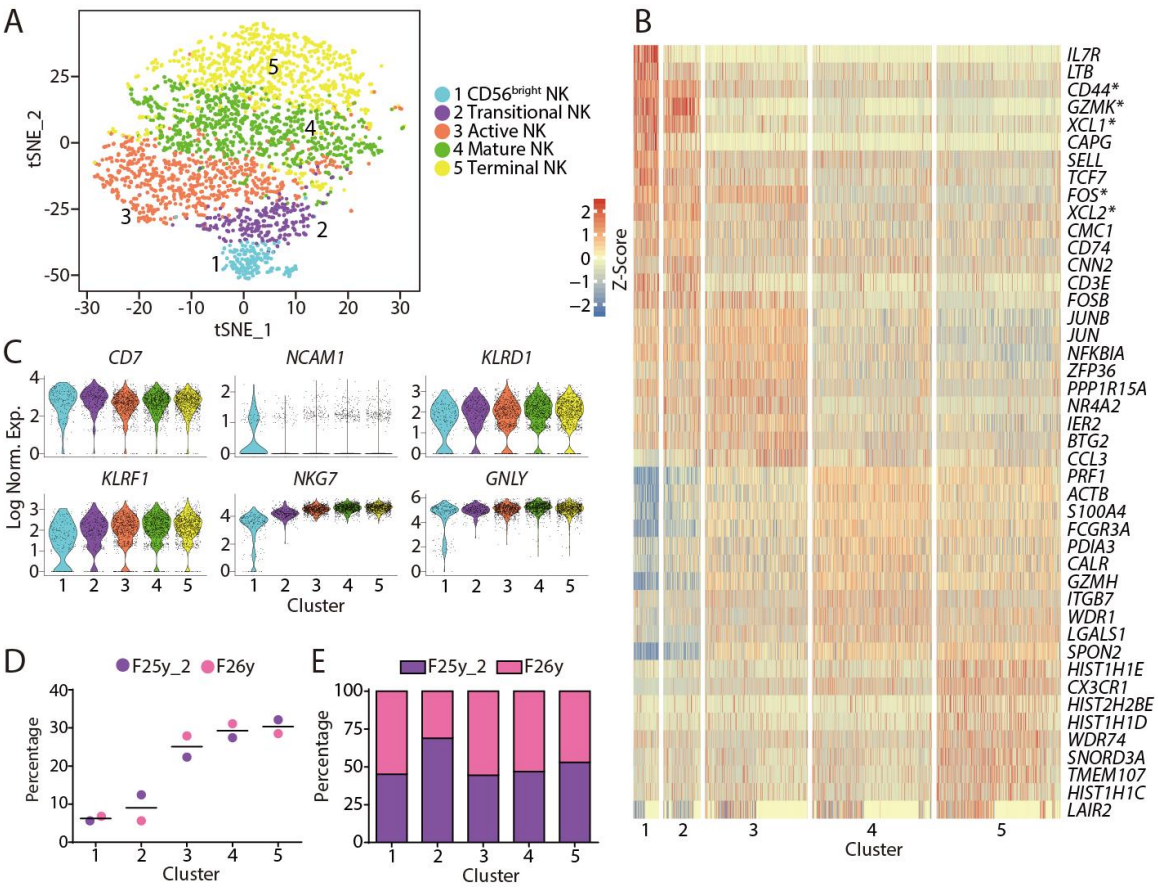


**Figure 5.4. Unbiased clustering of human NK cells from blood**

(**A**) Five distinct human blood NK clusters were numbered, named and displayed with a t-SNE plot. (**B**) Top 10 up-regulated DEGs (ranked by log fold change) of each cluster were plotted using heatmap. * indicates genes that are DEGs of more than one cluster. (**C**) Violin plots demonstrate the expression of 6 NK-lineage defining markers of each cluster. The y-axis represents log-normalized expression value. (**D**) Composition of the clusters within each donor. (**E**) Composition of the donors within each cluster. The input cell number from each donor is normalized to be equal.

5.2.3 The existence of a transitional population between CD56$^{brignt}$ and CD56$^{dim}$ NK cells

Although we hoped to capture more NK progenitors or immature NK cells in the BM and blood via sorting CD7$^{+}$ instead of CD56$^{+}$ NK cells, we were unable to find an early immature cluster using an unbiased approach. This was presumably due to the low abundance of these populations in the BM and blood [87]. When we plotted the NK-lineage markers overlaying the t-SNE cell plot, we did find a small fraction of cells within 'CD56$^{bright}$ NK' cluster that had *CD7* expression, but not *KLRD1* (CD94), *KLRF1* (NKp80), *NKG7*, or *GNLY* as compared to the rest of cells (**Figure 5.5.A**). These cells were unable to form a new cluster in an unbiased manner even when we increased the cluster resolution. The analyses of NK cells from secondary lymphoidal organs will give insights of early NK developmental stages.

Most of the molecular profiling studies related to human NK cells have focused on comparing CD56$^{bright}$ with CD56$^{dim}$ NK cells [100, 377-380]. This information helped us recognize CD56$^{brignt}$ NK cells in the scRNA-seq data. The high expression of IL7RA (*IL7R*), CD62L (*SELL*), NKG2A (*KLRC1*) and granzyme K (*GZMK*) defines the 'CD56$^{bright}$ NK' cluster (**Figure 5.5.B**) [94, 321]. The minimal expression of CD16A (*FCGR3A*) and CD160 (*CD160*) further supports the identity of the 'CD56$^{bright}$ NK' cluster (**Figure 5.5.B**) [381]. Although Killer-cell immunoglobulin-like receptors (KIRs) and CD57 (*B3GAT1*) are not well-represented in the dataset, we still found 'CD56$^{bright}$ NK' cluster has the lowest expression of these mature markers (**Figure 5.5.C**). The 5 to 10% 'CD56$^{bright}$ NK'

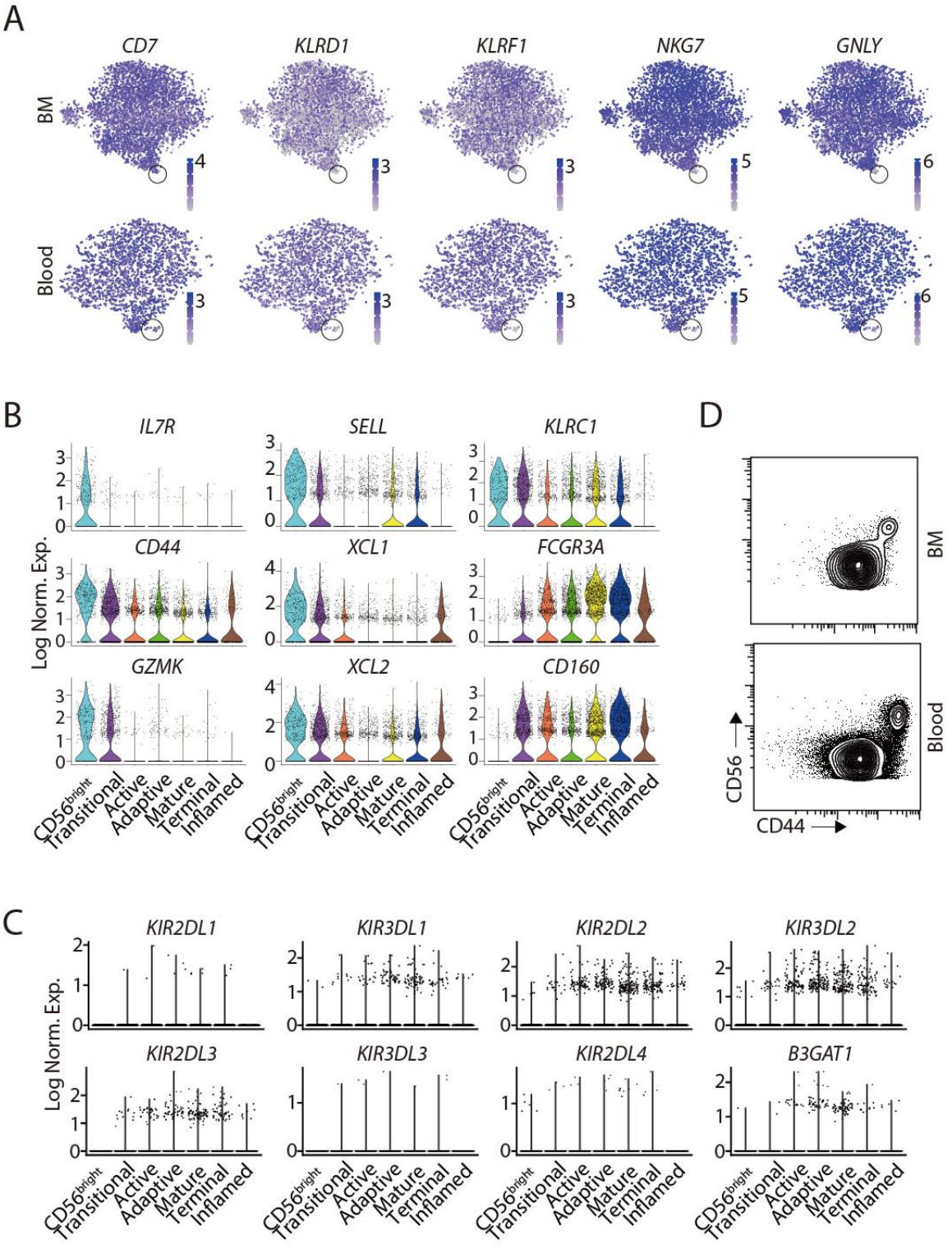
A
CD7
KLRD1
KLRF1
NKG7
GNLY
BM
Blood
B
IL7R
SELL
KLRC1
CD44
XCL1
FCGR3A
GZMK
XCL2
CD160
Log Norm. Exp.
CD56bright
Transitional
Active
Adaptive
Mature
Terminal
Inflamed
D
BM
Blood
CD56
CD44
C
KIR2DL1
KIR3DL1
KIR2DL2
KIR3DL2
KIR2DL3
KIR3DL3
KIR2DL4
B3GAT1

**Figure 5.5. The identification of CD56$^{bright}$ NK population**

(**A**) The expression of markers related to NK-lineage in BM and blood scRNA-seq sample were overlaid to the t-SNE plots. The circle indicated the small fraction of cells that had *CD7*, but not *KLRD1* (CD94), *KLRF1* (NKp80), *NKG7*, or *GNLY* expression compared to the rest of cells. (**B**) The expression of genes known to be highly expressed in CD56$^{bright}$ NK cells were displayed using violin plots of the BM samples. The y-axis represents log-normalized expression value. (**C**) The expression of all detectable KIRs and *B3GAT1* (CD57) in the BM sample was plotted as violin plots. The y-axis represents log-normalized expression value. The proportion of cells expressing these genes was not high enough to draw a violin. (**D**) The expression of CD56 and CD44 on NK cells from BM (top) or blood (bottom) of healthy donors were assessed via flow cytometry. Representative flow plot gated on Lin$^{-}$CD56$^{+}$ cells were shown. n = 5.

cluster in the BM and blood matched the percentage of CD56$^{bright}$ NK cells defined by flow cytometry (**Figure 5.3.D and 5.4.D**). We found that the 'CD56$^{bright}$ NK' cluster had high *CD44* expression (**Figure 5.5.B**), a cell surface marker that has not been reported before on human NK cells. Flow cytometry analyses revealed that all the NK cells from BM and blood are CD44$^{+}$ (**Figure 5.5.D**). Consistent with the higher expression level of CD44 in 'CD56$^{bright}$ NK' cluster, we found all the CD56$^{bright}$ NK cells are also CD44$^{bright}$ (**Figure 5.5.D**). This provides another cell surface maker to differentiate CD56$^{bright}$ NK cells. XCL1 and XCL2 from C chemokine family also demonstrated higher expression level in 'CD56$^{bright}$ NK' cluster consistent with previous data obtained using mass spectrometry (**Figure 5.5.B**) [380]. These two chemokines may also contribute to the pro-inflammatory nature of CD56$^{bright}$ NK cells.

Through the molecular definition of the 'CD56$^{bright}$ NK' cluster, we also found another cluster that is transcriptionally similar to the 'CD56$^{bright}$ NK' cluster as indicated by the small Euclidean distance between these two clusters (**Figure 5.6.A and 5.6.B**). We examined the DEGs and found that this cluster down-regulated several hallmark genes of CD56$^{bright}$ NK cells and up-regulated genes associated with CD56$^{dim}$ NK cells, in particular CD16A (*FCGR3A*) (**Figure 5.5.B**). This strongly implied the existence of a transitional stage between CD56$^{bright}$ and CD56$^{dim}$ NK cells. Therefore, we named this novel subset as the 'Transitional NK' cluster. To further explore this feature, we calculated the module scores based on the up-regulated or down-regulated genes-associated with the 'CD56$^{bright}$ NK' cluster or the 'Mature NK' cluster, transcriptionally representative of CD56$^{bright}$ and functionally-mature CD57$^{+}$ NK cells, respectively. Module score calculates the difference in expression between a gene set of interest and another random selection of genes from the transcriptome and indicates whether gene set of interest is expressed at a higher or lower level than the average [382]. For both up- and down-regulated genes, the 'Transitional NK' cluster had intermediate level of featured gene expression related to CD56$^{bright}$ or CD57$^{+}$ NK cells, especially in the NK cells isolated from the peripheral blood (**Figure 5.6.C and 5.6.D**). The presence of this transitional population supports the notion that immature CD56$^{bright}$ NK cells develop into mature CD56$^{dim}$ NK cells.

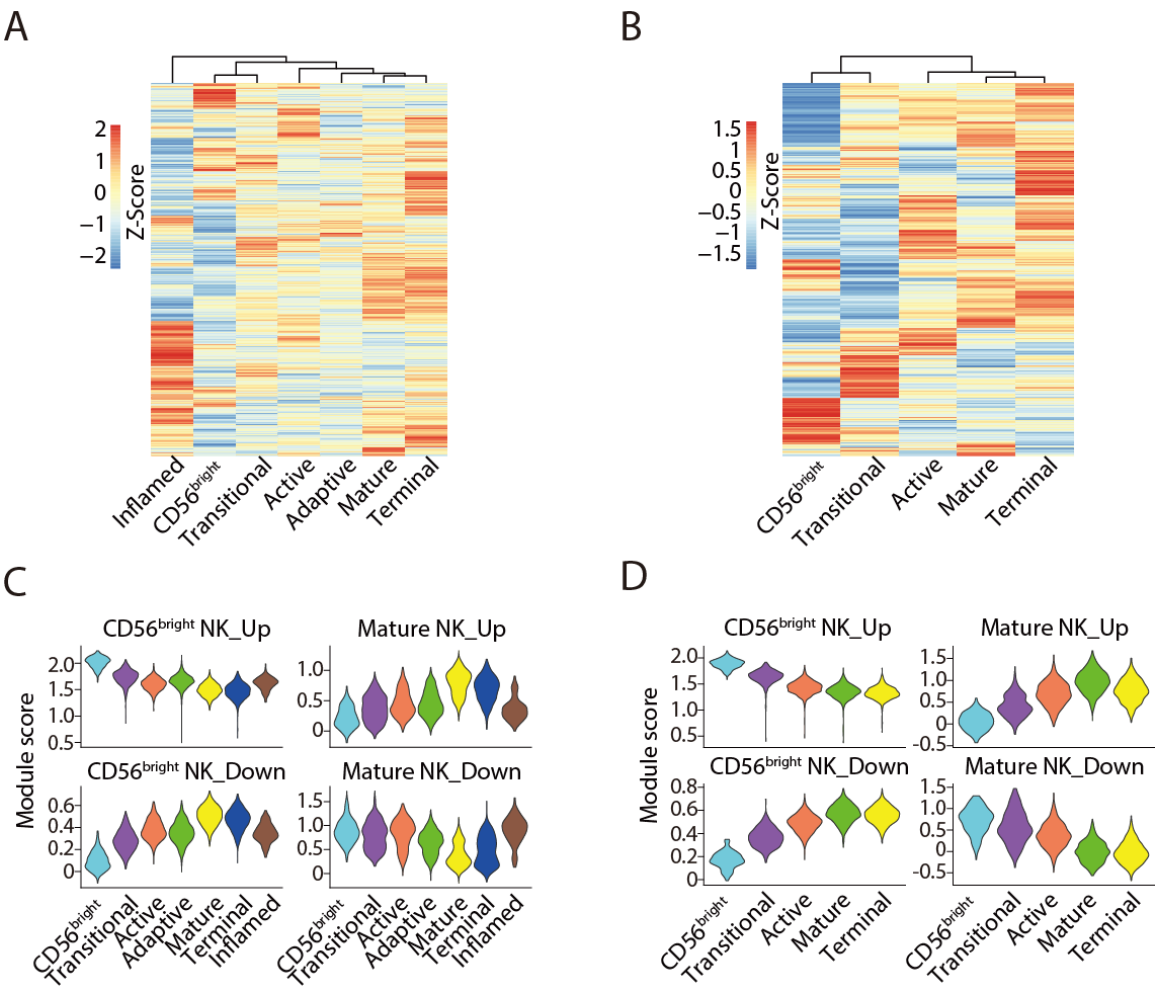


**Figure 5.6. Identification of 'CD56$^{bright}$ NK' cluster and a potential transitional population between CD56$^{bright}$ and CD56$^{dim}$ NK cells**

(**A**, **B**) The transcriptome similarity among clusters of BM (**A**) or blood (**B**) sample was evaluated by the Euclidean distance and visualized via heatmap. Each row represents a variable gene among clusters and each column represents one cluster. (**C**, **D**) Module scores were calculated using up-regulated or down-regulated DEGs of 'CD56$^{bright}$ and Mature NK' clusters from both BM (**C**) and blood (**D**) samples and plotted via violin plots.

5.2.4 Active NK subset at steady-state

One of the clusters that we found in the BM is the ‘Inflamed NK’ cluster. This cluster is mainly composed of cells from the 35-year male donor who only donated the BM sample (**Figure 5.3.E**). The top 10 up-regulated genes associated with this cluster included *IFIT3*, *IFIT2*, *TNF*, and genes encoding chemokines, indicating stimulation of NK cells presumably by interferons (**Figure 5.3.B**). The GSEA results further supported this notion with enrichment of gene sets including IFN-γ signaling, Toll-like receptor (TLR) signaling, and a positive regulation of inflammatory responses in the ‘Inflamed’ NK cluster compared to the rest of the cells. (**Figure 5.7.A**). This cluster also had a high *CD69* expression (**Figure 5.7.B**). All these implied an active inflammation state that was ongoing when the BM was collected from the 35-year male donor. This observation also explained the asymmetric composition of the cluster.

Interestingly, we found a second cluster with cells in activating status that we labeled as the ‘Active NK’ cluster. Unlike the ‘Inflamed NK’ cluster, we found the ‘Active NK’ cluster from all the donors in both the BM and blood (**Figure 5.3.E and 5.4.E**). The active nature of this cluster was demonstrated by the fact that the ‘Inflamed NK’ cluster also highly expressed the up-regulated DEGs associated with the ‘Active NK’ cluster (**Figure 5.7.C, left**). Conversely, the ‘Active NK’ cluster had a relatively higher module score defined by up-regulated DEGs associated with the ‘Inflamed NK’ cluster (**Figure 5.7.C, right**). More than 50% of the DEGs of this cluster were either transcription factors

or involved in transcriptional regulation. Importantly, among these genes, we found several that belong to the immediate early genes (IEGs) category including *NR4A2*,

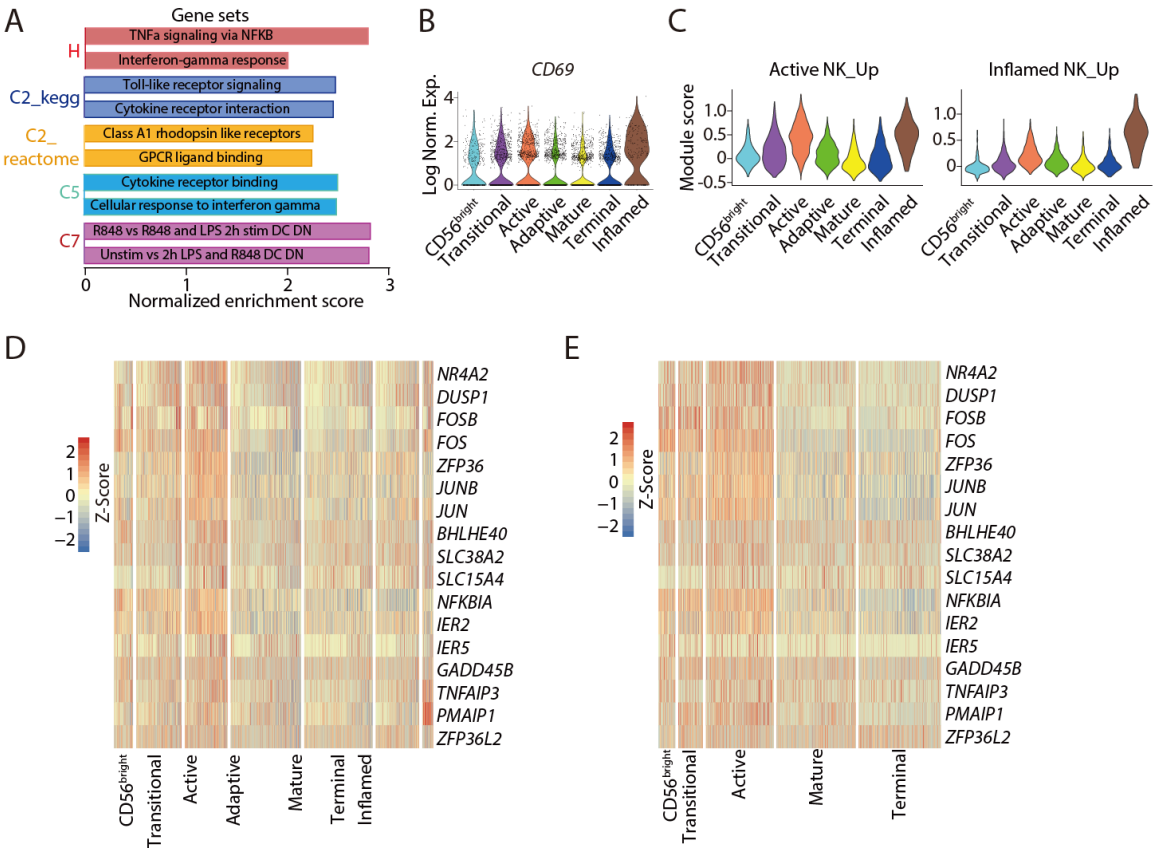


**Figure 5.7. Active NK cells with unique transcriptome profile**

(**A**) Top two enriched gene sets (ranked by normalized enrichment score) of five different datasets from GSEA of the 'Inflamed NK' cluster compared to the rest of the cells were plotted. (**B**) The expression of *CD69* in the BM sample was shown as violin plot. The y-axis represents log-normalized expression value. (**C**) Module score were calculated using up-regulated DEGs of 'Active NK' (left) or 'Inflamed NK' (right) cluster from BM sample and plotted via violin plots. (**D, E**) Up-regulated IEGs from 'Active NK' cluster were plotted using heatmap of the BM (D) and blood (E) sample.

*DUSP1*, *FOSB*, *FOS*, *JUN*, and *JUNB* (**Figure 5.7.D and 5.7.E**) [383]. These IEGs are induced rapidly in response to stimuli without nascent protein synthesis [384]. GSEA revealed three major results on the 'Active NK' cluster comparing to the rest of the NK cells: 1) transcriptionally active; 2) activation of several signaling pathways including KRAS-MAPK, TRAF6-NF-κB; and 3) activation by various stimuli or receptors including TNF-α, IL-2, TLR or GPCR. The top 20 hits from the C3 motif gene sets analyses centered around the activation of ATF/CREB (activating transcription factor/cAMP response element binding protein) and C/EBP (CCAAT-enhancer-binding protein) transcription factor families, both of which are known to be involved in the induction of IEGs [384, 385]. Collectively, these findings implied an active state of the cells in this cluster. We hypothesize that this potentially reflect homeostatic activation of NK cells via certain stimuli, for example stimulation via trans-presentation of IL-15 [386].

Following the identification of this novel cluster, we sought to identify what cell surface markers define this cluster with flow cytometry. The only cell surface proteins encoded in DEG set of this cluster were CD69 and CXCR4 (**Figure 5.7.B and 5.8.A**). CD69 is not the optimal cell surface marker to identify the 'Active NK' cluster via flow cytometry as we could only detect $CD69^+$ NK cells in the BM (**Figure 5.8.B**) [387]. On the contrary, we indeed detected $CXCR4^+$ NK cells in both BM and blood via flow cytometry (**Figure 5.8.C**). Importantly, we found higher percentage of $CXCR4^+$ NK cells in the blood than the BM (**Figure 5.8.C**), consistent with the scRNA-seq dataset. Based on the DEGs (**Figure 5.3.B and 5.4.B**), the Euclidean distance (**Figure 5.6.A and 5.6.B**), and module

score analyses (**Figure 5.6.C and 5.6.D**), the 'Active NK' cluster is potentially within the CD56$^{dim}$ NK population with a decreased expression of the genes-encoding cytolytic proteins compared to the 'Mature NK' cluster.

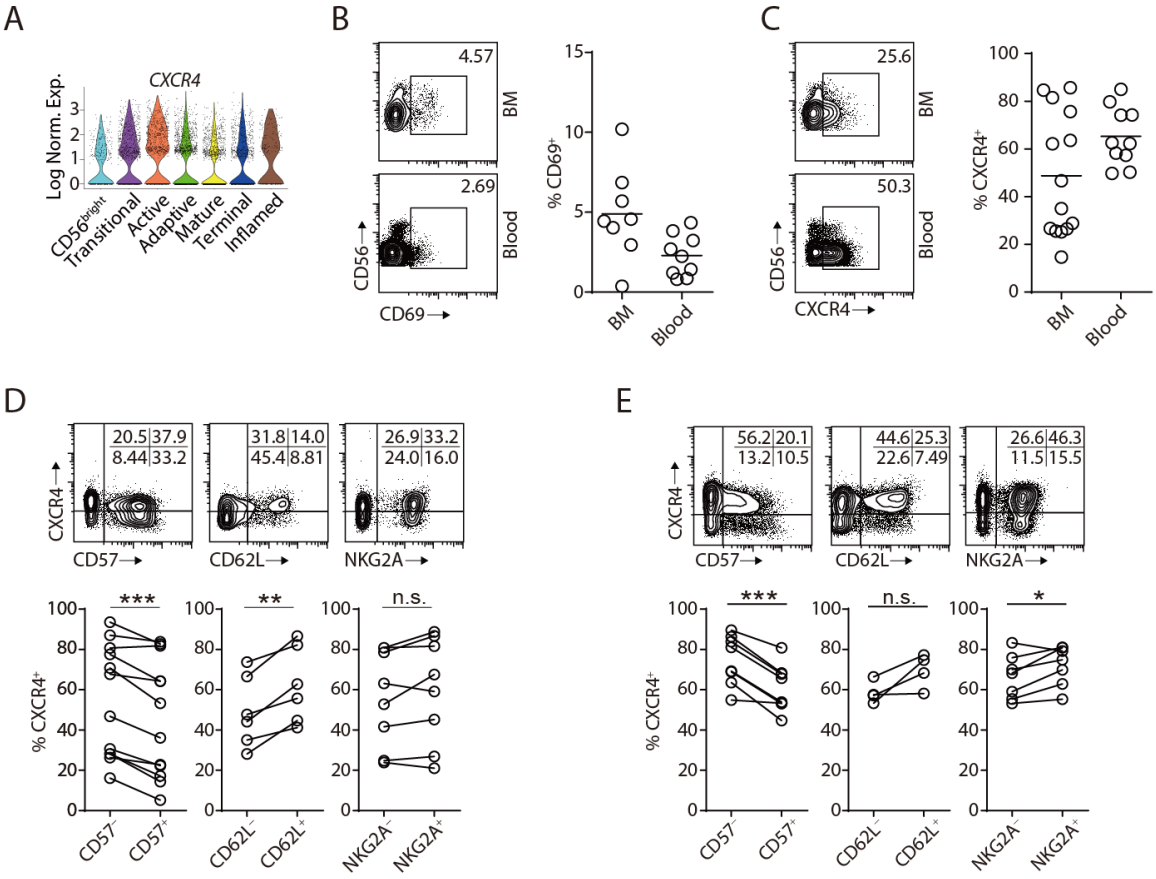


**Figure 5.8. Identification of the 'Active NK' cluster with cell surface markers**

(**A**) The expression of *CXCR4* in the BM sample was shown as violin plot. The y-axis represents log-normalized expression value. (**B, C**) Percentage of CD69$^{+}$ (B) and CXCR4$^{+}$ (C) NK cells (gated on Lin$^{-}$CD56$^{+}$ cells) were evaluated via flow cytometry. (**D, E**) The expression of CXCR4 in CD57$^{+/-}$, CD62L$^{+/-}$, or NKG2A$^{+/-}$ CD56$^{dim}$ NK populations from BM (D) and blood (E) was assessed via flow cytometry (top). Percentage of CXCR4$^{+}$ cells within each population were quantified (bottom).

Therefore, based on the earlier studies [96, 388], we used NKG2A, CD62L and CD57 to assess the maturity of $CD56^{dim}CXCR4^{+}$ NK cells in both BM and blood. The cell surface expression of NKG2A and CD62L are known to decrease as NK cells mature, whereas CD57 is generally considered the marker for terminally-mature NK cells [94]. Flow cytometry analyses revealed that there are $CXCR4^{+}$ NK cells in both negative and positive compartments of all three markers; therefore, CXCR4 is not an ideal marker to define developmental stages of NK cells (**Figure 5.8.D and 5.8.E**). Nevertheless, we did find a higher percentage of CXCR4 cells among the CD57 NK cells compared to the CD57 NK cells in both the BM and blood (**Figure 5.8.D and 5.8.E**). This implied that NK cells down-regulate CXCR4 as they become functionally mature, matching the scRNA-seq dataset (**Figure 5.8.A**). Consistently we also found a higher percentage of CXCR4 cells in NKG2A or CD62L NK cells than the negative compartments (**Figure 5.8.D and 5.8.E**).

Based on our flow cytometry data, we concluded that the 'Active NK' cluster might not represent a unique developmental stage. We reasoned that the 'Active NK' cluster might be a mix of cells from different developmental stages receiving stimuli that result in this unique transcriptome profile. The existence of this novel NK cluster reveals homeostatic activation of NK cells, which may have considerable impacts on NK cell survival, proliferation or differentiation.

5.2.5 Unique transcriptomic profile of adaptive NK cells

Another subset of NK cells that we identified was the 'Adaptive NK' cluster, which was found in the BM. This cluster featured with high expression of *KLRC2* (NKG2C) which has been used as a marker for the adaptive NK cells resulting from human cytomegalovirus (HCMV) infection [389]. Heatmap of DEGs showed that only a fraction of cells in this cluster had high *KLRC2* expression (**Figure 5.3.B**). When we plotted *KLRC2* expression with individual donors within the 'Adaptive NK' cluster, we found that only the 24-year old female donor had high *KLRC2* expression (**Fig. 5.9.A**). Thus, we conducted the cluster analyses using cells only from 24-year old female sample. Due to the low cell number, we only found four clusters including 'CD56$^{bright}$ NK', 'Active NK', 'Mature NK', and 'Adaptive NK' (**Figure 5.9.B and 5.9.C**). Indeed, the 'Adaptive NK' cluster was marked with high *KLRC2* expression comprising 40% of the total NK cells from the 24-year old female sample (**Figure 5.9.D**). Previous work from Schlums et al., has discovered that adaptive NK cells from HCMV$^{+}$ donors express less FcεRγ (*FCER1G*), SYK (*SYK*), EAT-2 (*SH2D1B*), and PLZF (*ZBTB16*) compared to other NK subsets [390]. Consistent with this, we found a large reduction in the expression of *FCER1G* and *ZBTB16* in the 'Adaptive NK' cluster compared to the 'Active/Mature NK' clusters from the 24-year old female sample (**Figure 5.9.E**). The expression of *SYK* and *SH2D1B* was not well-represented in the dataset (**Figure 5.9.E**).

Next, we focused our analyses on the NK cells from the 24-year old female donor. Interestingly, we found high *CD3E/D/G* expression in the 'Adaptive NK' cluster (**Figure 5.10.A**). We were confident that this cluster was not contaminating T cells based on the

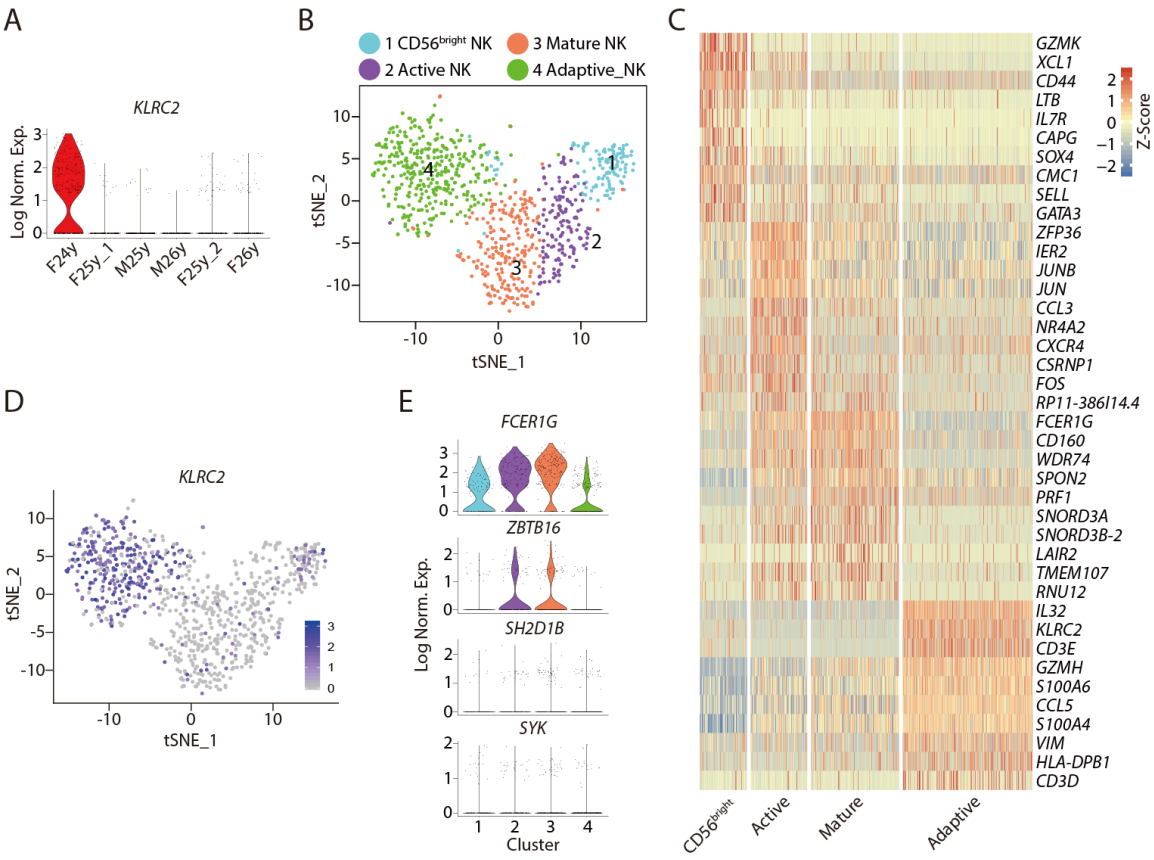


**Figure 5.9. Identification of adaptive NK cells from 24-year old female donor**

(**A**) The expression of *KLRC2* in each donor cells within the 'Adaptive NK' cluster were shown in violin plots. The y-axis represents log-normalized expression value. (**B**) t-SNE plot demonstrates four distinct NK clusters from BM of the 24-year old female donor. (**C**) Top 10 up-regulated DEGs (ranked by log fold change) of each cluster from 24-year female sample were plotted using heatmap. (**D**) The expression of *KLRC2* of 24-year old female sample were overlaid on the t-SNE plot. (**E**) Violin plots demonstrate the

expression of *FCER1G, ZBTB16, SH2D1B, and SYK* in four clusters from the 24-year old female donor sample. The y-axis represents log-normalized expression value.

98.8% post-sorting purity of the 24-year old female sample (**Figure 5.10.B**). To further confirm the existence of the adaptive NK cells in the 24-year old female sample, we stained for NKG2C in the cryo-preserved samples from four of our six donors (not enough sample left to preserve for the other two donors). To ensure the exclusion of T cells, we included CD3ε, TCRα/β, and TCRγ/δ in the staining. Evidently, only the 24-year old female sample had large percentage of cells expressing NKG2C (**Figure 5.10.C**). The percentage of $NKG2C^{+}$ NK cells in that sample was about 46%, matching the scRNA-seq data. The fact that some of the cells from '$CD56^{bright}$ NK' cluster also possessed *KLRC2* expression fit nicely with the flow cytometry analysis, emphasizing the true presentation of the $NKG2C^{+}$ NK cells in the scRNA-seq data (**Figure 5.9.D and 5.10.C**). The increased expression of *CD3E/D/G* mRNA indicated epigenetic alteration in the adaptive NK cells.

An important aspect of the adaptive lymphocytes is their rapid and robust functional capacity compared to naïve cells. Surprisingly, the 'Adaptive NK' cluster has less cytolytic molecules expression compared to the 'Mature NK' cluster (**Figure 5.9.C**). One potential explanation was that the functional molecules were already expressed and stored as proteins in these cells and therefore we no longer detected active transcription of those genes. In line with this idea, GSEA revealed that the 'Adaptive NK' cluster was enriched in the ER to Golgi transport vesicle gene set compared to the rest of the cells

from the 24-year female sample (**Figure 5.10.D**). Moreover, the positive regulation of IFN-γ production gene set was also enriched in this cluster, pinpointing the functional attributes of adaptive NK cells (**Figure 5.10.D**).

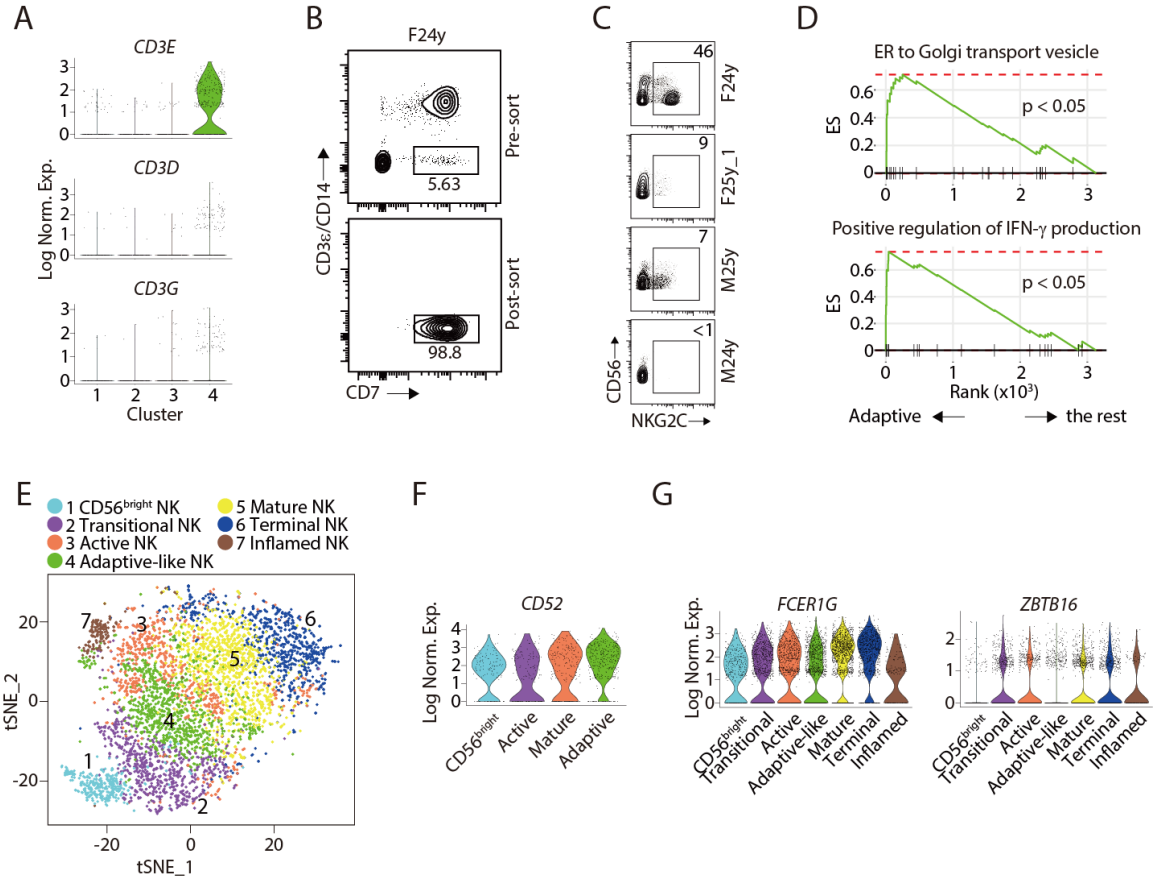


**Figure 5.10. Features associated with the 'Adaptive NK' cluster**

(**A**) Violin plots demonstrate the expression of *CD3E*, *CD3D*, *and CD3G* in four clusters from the 24-year old female donor sample. The y-axis represents log-normalized expression value. (**B**) The purity of the 24-year old female sample was verified after sorting. Percentage of $CD3\varepsilon^{-}CD14^{-}CD7^{+}$ population within $CD19^{-}$ lymphocytes were shown as the flow plots both pre and post sorting. (**C**) Expression of NKG2C on NK cells (gated on $PI^{-}Lin^{-}TCR\alpha/\beta^{-}TCR\gamma/\delta^{-}CD56^{+}$ cells) were assessed by flow cytometry using

cryopreserved samples from four donors. (**D**) Selected gene sets enriched in the 'Adaptive NK' cluster compared to the rest of cells were plotted. (**E**) t-SNE plot demonstrated the 7 clusters from the clustering analyses of the BM sample without the adaptive NK cells from the 24-year old female donor. (**F**) The expression of *CD52* in the four clusters from 24-year female donor sample was shown as a violin plot. The y-axis represents log-normalized expression value. (**G**) Violin plots demonstrated the expression of *FCER1G, ZBTB16* in the clusters of the BM sample without the adaptive NK cells from the 24-year old female donor. The y-axis represents log-normalized expression value.

Interestingly, although the other five donors did not have cells with high *KLRC2* expression (**Figure 5.9.A**), some of them still clustered together with the *KLRC2*$^{+}$ adaptive NK cells from the 24-year old female donor (**Figure 5.3.E**). To avoid biased clustering resulting from the adaptive NK cells from the 24-year old female sample, we removed the cells of 24-year old female donor from the 'Adaptive NK' cluster and conducted the analyses to test whether this cluster still existed. We were still able to recover all the seven clusters with the original 'Adaptive NK' cluster becoming a cluster that only has one up-regulated DEG, *CD52* (**Figure 5.10.E**). *CD52* was the most up-regulated DEG in the original 'Adaptive NK' cluster (**Figure 5.3.B**) and had the highest expression in the 'Adaptive NK' cluster of the 24-year old female donor compared to the rest of clusters (**Figure 5.10.F**). In the absence of NKG2C$^{+}$ cells, we still found that this new cluster had lower expression of FcεRγ (*FCER1G*) and PLZF (*ZBTB16*) compared to the rest of the clusters (**Figure 5.10.G**). Because of these features, we named this cluster as 'Adaptive-like NK' cluster as it was transcriptionally similar to the conventional NKG2C$^{+}$ adaptive NK cells. One possible explanation for the generation of this subset of cells was that they were adaptive NK cells derived from infections other than HCMV.

5.2.6 Terminally-mature NK cells exhibit unique transcriptional profile

In the current development model, the cell surface expression of CD57 marks the functionally-matured human NK cells with the highest cytolytic potential [95, 96]. Although CD57 (*B3GAT1*) is under-represented in our scRNA-seq dataset (**Figure 5.5.C**), we were able to identify this functionally-matured NK population comprising the 'Mature and Terminal NK' clusters. The 'Mature NK' cluster featured high expression of molecules important for cytotoxic function (**Figure 5.11.A**). We found the highest expression of cytolytic molecules in the 'Mature NK' cluster including perforin (*PRF1*) and granzymes (*GZMA*, *GZMB*, *GZMH*). Optimal cytotoxicity requires cytoskeletal remodeling [391]. Indeed, the expression of β-actin (*ACTB*), actin-related protein 2/3 complex subunit 2 (*ARPC2*, assist actin polymerization), and Coronin 1A (*CORO1A*, remodel F-actin to enable granule release at the synapse) and Cofilin 1 (*CFL1*, depolymerize and remodel F-actin) peaked in the 'Mature NK' cluster (**Figure 5.11.A**) [392-394]. We also found high expression of the negative regulators related to the cytotoxicity such as Cystatin F (*CST7*) and Profilin 1 (*PFN1*) [395, 396]. In addition, the cell adhesion and signaling molecules were also up-regulated in this cluster (**Figure 5.11.A**). Moreover, GSEA demonstrated enrichment of gene sets including the apical junction, regulation of actin cytoskeleton, NK cell-mediated cytotoxicity, and structural constituent of cytoskeleton in the 'Mature NK' cluster compared to the rest of the cells.

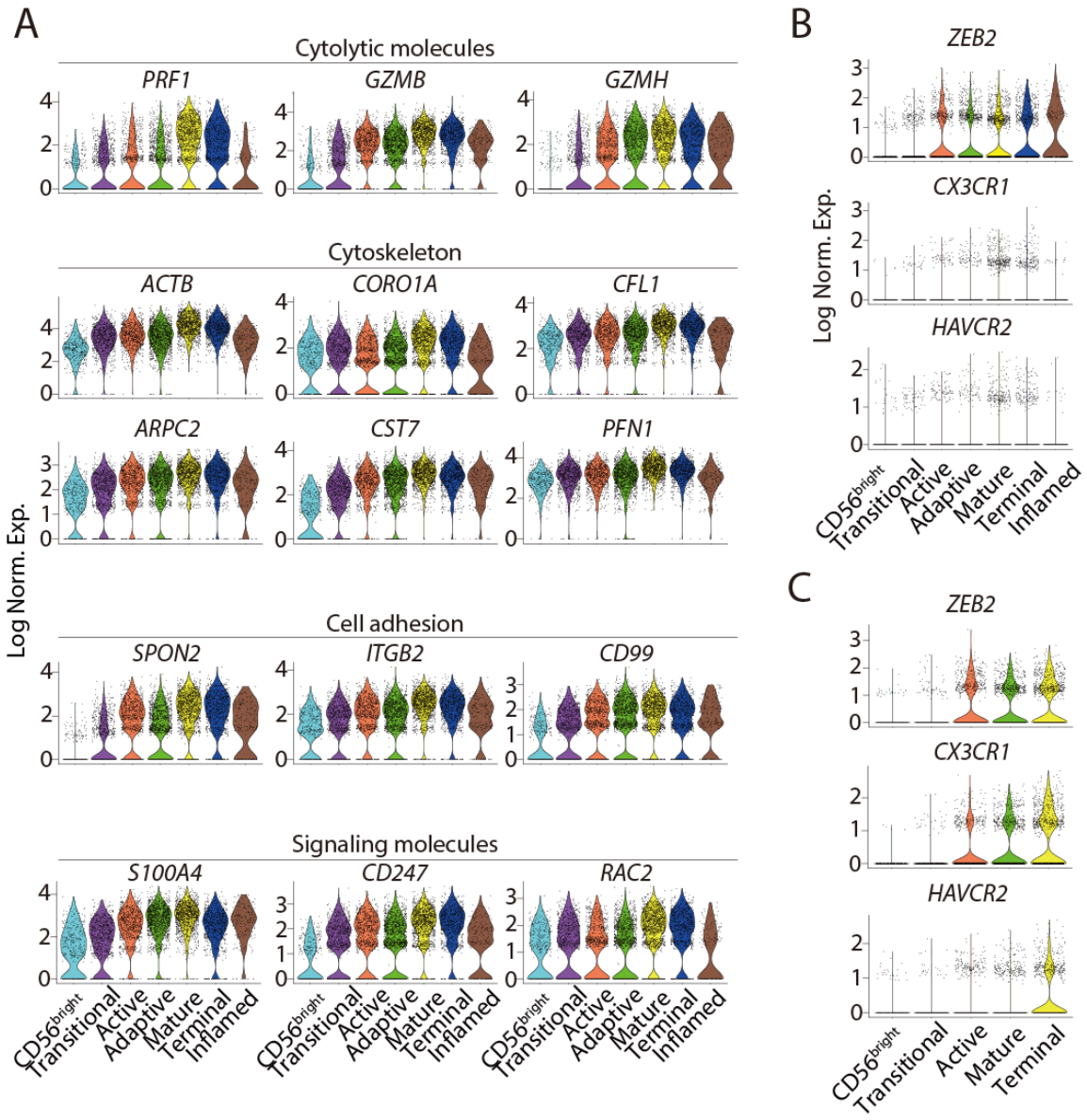


**Figure 5.11. Functional mature NK clusters**

(**A**) Representative genes associated with functionally-matured NK cells were grouped in four different categories and plotted via violin plots of the BM sample. The y-axis represents log-normalized expression value. (**B, C**) The expression of *ZEB2, CX3CR1, and HAVCR2* in each cluster of the BM (B) and blood (C) samples was shown as violin plots. The y-axis represents log-normalized expression value.

In both the BM and blood samples, we found another cluster, the ‘Terminal NK’ cluster, has similar expression level of the functional molecules as the ‘Mature NK’ cluster (**Figure 5.11.A**) and is transcriptionally similar to the ‘Mature NK’ cluster as indicated by the short Euclidean distance (**Figure 5.6.A and 5.6.B**). The high expression of transcription factor ZEB2 indicated terminal maturity of this cluster (**Figure 5.11.B and 5.11.C**). To further support the identification of the terminally matured cluster, we demonstrated increased expression of *CX3CR1* and *HAVCR2* (TIM-3), both of which mark the mature NK population with full responsiveness (**Figure 5.11.B and 5.11.C**) [397, 398]. There is also a higher percentage of this cluster in the blood compared to the BM (30% vs. 15%). Based on the percentage of the ‘Mature and Terminal NK’ clusters and elevated expression of the functional molecules, we believe these two clusters together form the $CD57^{+}$ NK cells. Although we found increased expression of *CX3CR1* and *HAVCR2* (TIM-3), the cell surface level of CX3CR1 or TIM-3 is not heterogeneous among the $CD56^{dim}$ NK population, rendering them insufficient in identifying this ‘Terminal NK’ cluster by flow cytometry [397, 398].

Next, we explored the DEGs between ‘Mature NK’ and ‘Terminal NK’ clusters. Strikingly, we found that the ‘Terminal NK’ cluster express distinct members of small nucleolar RNA, C/D box 3 (SNORD3) cluster and various histone subunits at very high level (**Figure 5.12.A and 5.12.B**). GSEA revealed that the ribosome gene set was depleted in the ‘Terminal NK’ cluster compared to ‘Mature NK’ cluster (**Figure 5.12.C and 5.12.D**). In contrast, the chromosome maintenance, histone methylation, and

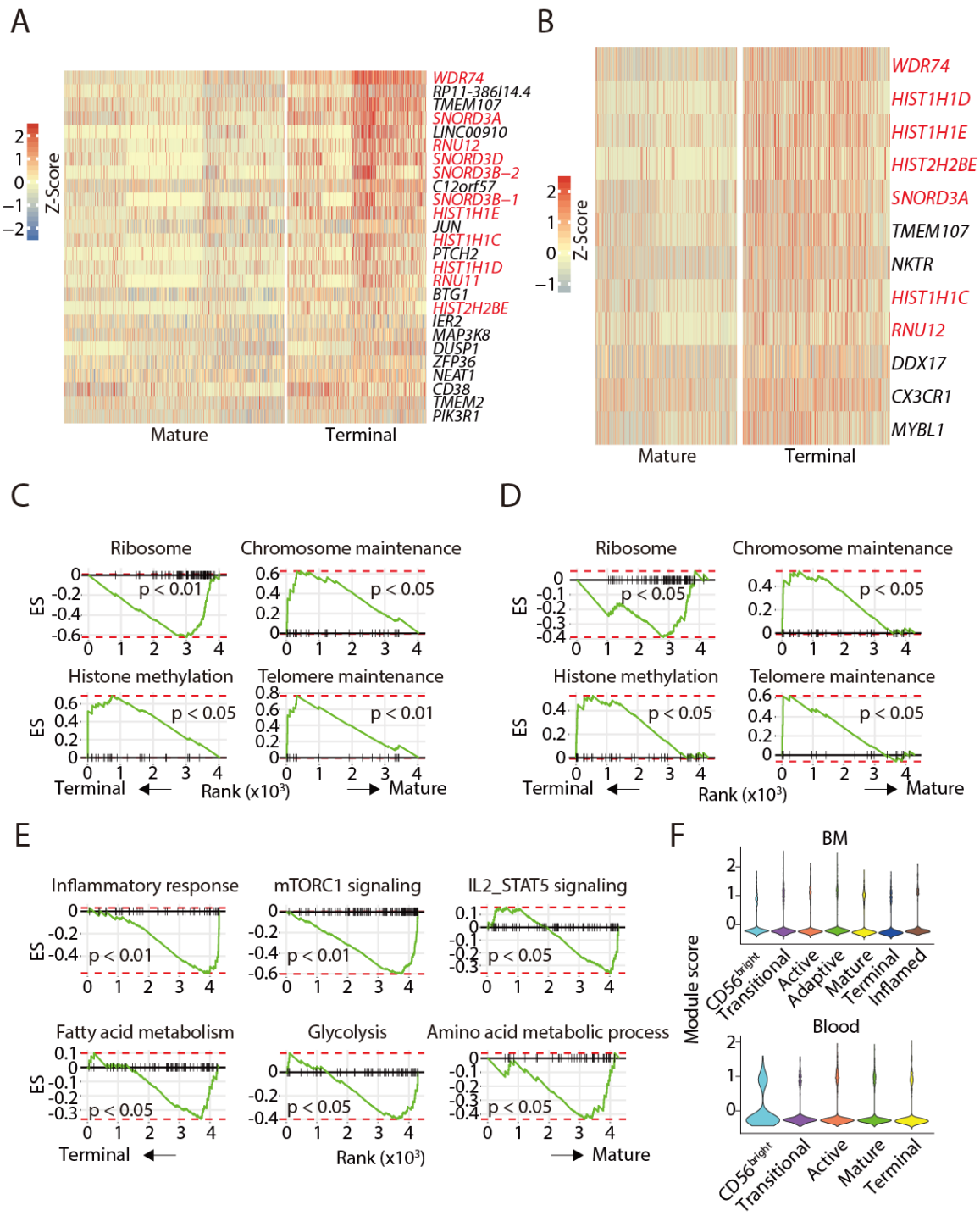


**Figure 5.12. Unique transcriptional profile associated with the 'Terminal NK' cell cluster**

(**A, B**) The expression of all the DEGs between 'Mature and Terminal NK' cluster of BM (A) and blood (B) sample were plotted via heatmap. Genes associated with histones or ribosomes were highlighted in red.

(**C, D**) Selected gene sets enriched in the 'Terminal NK' cluster compared to the 'Mature NK' cluster of

BM (C) and blood sample (D). (**E**) Signaling and metabolic gene sets were depleted in the 'Terminal NK' cluster of blood sample. (**F**) Module scores were calculated using previously defined NK cell quiescence gene set in BM (left) and blood (right) clusters and plotted via violin plots.

telomere maintenance gene set were all enriched in the 'Terminal NK' cluster (**Figure 5.12.C and 5.12.D**). We calculated the cell cycle score based on established gene sets [399]. We did not find substantially higher S.Score (module score of genes associated with S phase of cell cycle) or G2M.Score (module score of genes associated with G2M phase of cell cycle) of the 'Terminal NK' cluster indicating this unique transcriptional profile was not due to active cell cycling. Moreover, GSEA demonstrated decreased inflammatory response, down-regulated mTORC1/STAT5 signaling, and reduced metabolic activity of the 'Terminal NK' cluster compared to the 'Mature NK' cluster (**Figure 5.12.E**). Previously, murine NK cells have been shown to develop into a quiescent state as they become terminally mature. These dampened signaling and metabolic profiles indicated that the 'Terminal NK' cluster cells might be also in a quiescent state [161]. To further explore this, we utilized a previous established quiescence gene set using human NK cells and evaluated the expression level of quiescence-associated genes in our BM and blood clusters [400]. Module score indicated no significantly increased expression of these genes in the 'Terminal NK' cluster in either BM or blood samples (**Figure 5.12.F**). The physiological meaning of this unique transcriptional profile of 'Terminal NK' cluster remains elusive.

5.2.7 BM and blood contain similar developmental NK clusters

The presence of similar cluster composition in the BM and blood was consistent with previously reported cell surface markers-defined NK populations [91]. To compare the NK cell clusters between BM and blood, we combined the NK cell transcriptional data from the BM and blood of the same donor (F25y_2 and F26y) and performed a clustering analysis on the combined populations. Like the previous analyses conducted on the BM or blood separately, we have found 'CD56$^{bright}$ NK', 'Transitional NK', 'Active NK', 'Adaptive-like NK', 'Mature NK', and 'Terminal NK' clusters (**Figure 5.13.A and 5.13.B**). Generally, both BM and blood possessed similar heterogeneity of NK cells with difference in composition (**Figure 5.13.C and 5.13.D**). This is contrast to the organ-specific phenotype between human splenic and blood NK [401]. Consistent with independent analyses shown above, we had more cells in the 'Active NK' cluster in blood than BM (**Figure 5.13.C and 5.13.D**). Specific to 'Adaptive-like NK' cluster, it was mostly composed cells from BM (**Figure 5.13.C and 5.13.D**). This explains why there was no 'Adaptive-like NK' cluster in the analyses of blood samples alone. Due to the inadequate identification of this cluster with CD52 (data not shown), we are not sure whether cells from this cluster only existed in the BM. In terms of maturity, the blood possessed higher percentage of cells from the 'Mature NK' cluster than the BM consistent with more CD57$^{+}$ NK cells in the blood than the BM (**Figure 5.13.C and 5.13.D**).

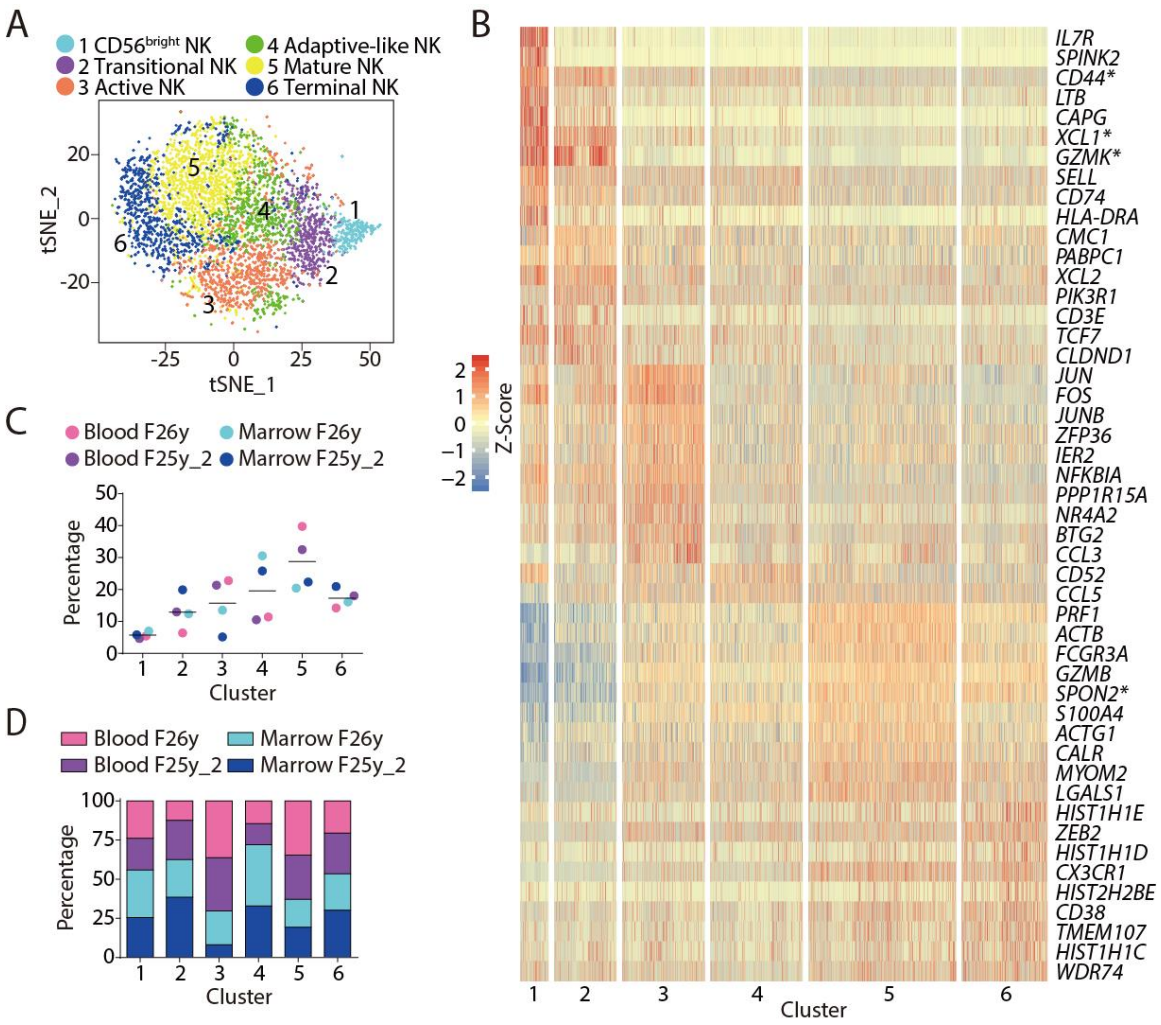


**Figure 5.13. Unbiased clustering of human NK cells from BM and blood of same donor**

(**A**) Clustering analyses of human NK cells from BM and blood of same donor were performed. Six distinct clusters were numbered, named and demonstrated with t-SNE plot. (**B**) Top 10 up-regulated DEGs (ranked by log fold change) of each cluster were plotted using heatmap. * indicates genes that are DEGs of more than one cluster. (**C**) Composition of the clusters within each donor. (**D**) Composition of the donors within each cluster. The input cell number from each donor is normalized to be equal.

5.2.8 Pseudotime reveals CD56$^{bright}$ is the precursor of CD56$^{dim}$ NK cells

One advantage of scRNA-seq analyses is the ability to simulate the ontology among a developmentally heterogeneous population based on the transcriptional changes during cell differentiation. We used Monocle2 pseudotime trajectory analysis to develop a developmental course of NK cells [402]. As shown in **Figure 5.14A and 5.14.B**, both BM and blood NK cells demonstrated a relative linear developmental progression with few branches. The 'CD56$^{bright}$ NK' cluster and 'Mature/Terminal NK' cluster dominate the two ends of the progression trajectory in both BM and blood. Based on the current human NK development model, we assigned the 'CD56$^{bright}$ NK' cluster as the least mature branch in the pseudotime. Importantly, in both the BM and blood samples, cells from the 'Transitional NK' cluster clearly develop from the 'CD56$^{bright}$ NK' cluster and extend in the direction of functionally 'Mature NK' cluster. This result not only demonstrates the existence of the transitional subset from CD56$^{brignt}$ to CD56$^{dim}$ NK cells as illustrated above (**Figure 5.6**), but also provides new evidence from transcriptional profiling supporting CD56$^{bright}$ NK cells as the precursors of CD56$^{dim}$ NK cells.

Next, we focused on the analyses of the branches along the developmental trajectory. In the BM sample, branch points A and B separated the cell trajectory into five states (**Figure 5.14.C**). We calculated and plotted the percentage contribution of each cluster within each state using the pie charts (**Figure 5.14.D**). It was evident that State-1 cells were mainly comprised of 'CD56$^{bright}$ and Transitional NK' clusters, while the State-4

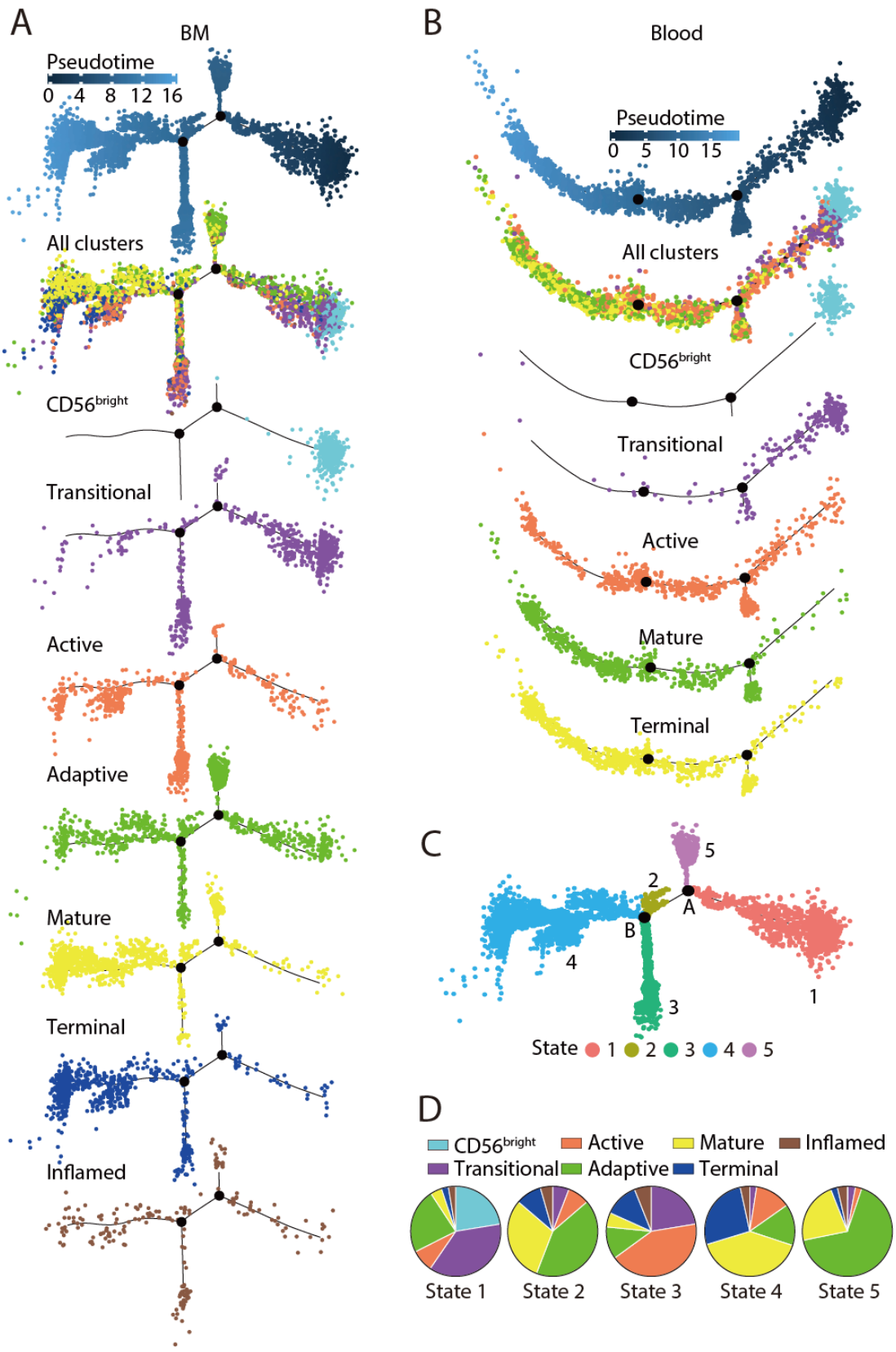
A
BM
Pseudotime
0 4 8 12 16
All clusters
CD56bright
Transitional
Active
Adaptive
Mature
Terminal
Inflamed
B
Blood
Pseudotime
0 5 10 15
All clusters
CD56bright
Transitional
Active
Mature
Terminal
C
5
2
A
B
4
3
1
State 1 2 3 4 5
D
CD56bright
Active
Mature
Inflamed
Transitional
Adaptive
Terminal
State 1
State 2
State 3
State 4
State 5

**Figure 5.14. Single cell trajectory analysis reveals a linear NK cell developmental pathway, maturing from CD56$^{bright}$ to CD56$^{dim}$ NK cells**

(**A**, **B**) Pseudotime trajectory of BM (**A**) or blood (**B**) NK cells with pseudotime, all clusters and individual cluster demonstrated in the trajectory. (**C**) The BM trajectory was separated into 5 cell states by branch points A and B. (**D**) Composition of the clusters within each cell state were demonstrated via pie charts.

cells were mainly comprised of 'Mature and Terminal NK' clusters. Importantly, we found that State-5 cells branching out from point A was dominated by the 'Adaptive NK' cluster (**Figure 5.14.D**). Analyzing the genes that were significantly branch A-dependent, we found high expression of *CD3E*, *VIM* and *CCL5* in State-5 cells (**Figure 5.15.A**), matching with the gene signatures associated with 'Adaptive NK' cluster (**Figure 5.3.B**). Another evident branch was the State-3 cells stemming out from point B. This branch was heavily comprised of 'Active NK' cluster (**Figure 5.14.D**). The branch point B-dependent genes also revealed high expression of 'Active NK' cluster genes in State-3 cells including *CXCR4*, *JUNB*, *IER2*, *ZFP36* and *JUN* (**Figure 5.15.B**). The formation of branches mainly by the 'Active and Adaptive NK' clusters demonstrated that the transcriptome footprint of these two clusters differed from the steady-state maturation. When we plotted the composition of each state within each cluster (**Figure 5.15.C**), evidently, the 'CD56$^{bright}$, Transitional, Mature and Terminal NK' clusters were dominated by one cell state. However, this was not seen in the 'Active, Adaptive, or Inflamed NK' clusters, further manifesting the transcriptome alteration induced by the secondary stimuli.

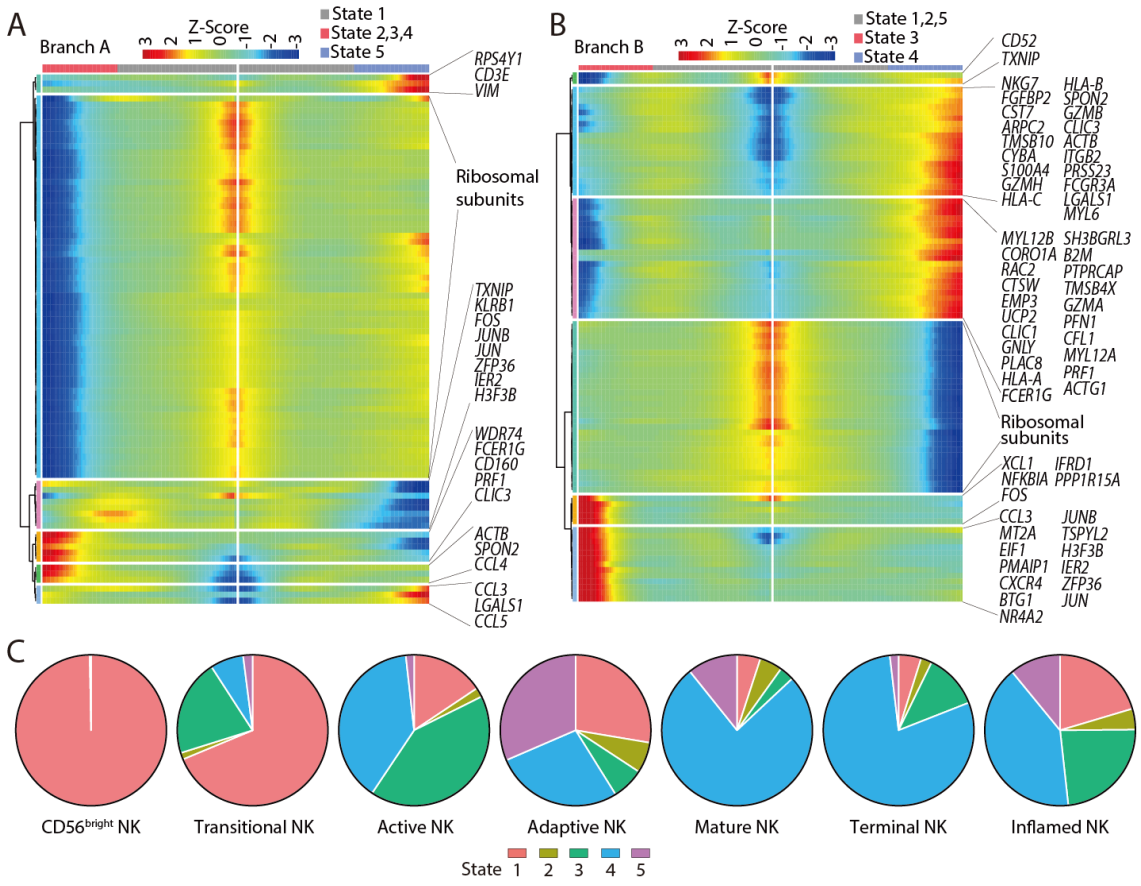


**Figure 5.15. Exploration of the branches in the single cell trajectory analysis**

(**A**, **B**) The expression of branch point A-dependent (**A**) or branch point B-dependent genes (**B**) were shown in heatmaps. (**C**) Composition of the cell states within each cluster were demonstrated via pie charts.

5.2.9 Altered NK cell transcriptome in GATA2$^{T354M}$ donor

Transcription factors are known to play critical roles in lineage specification and cellular differentiation [368]. Among the GATA transcription factor family, it is well-established that a haplo-insufficiency in *GATA2* locus results in human NK cell deficiency with specific loss of CD56$^{bright}$ subset [97]. This observation, to some extent, challenges the current developmental dogma that CD56$^{bright}$ NK cells give rise to CD56$^{dim}$ NK cells. However, the failure of flow-based detection of CD56$^{bright}$ NK cells in individuals with *GATA2* mutation does not rule out the possibility of insufficient expression of CD56 on the cell surface, which potentially masks the true CD56$^{bright}$ NK cell identity [321]. To further explore the human NK cell deficiency in individuals with *GATA2* mutation, we used scRNA-seq technology to profile the NK-lineage cells from the blood of a clinically asymptomatic female donor with GATA2$^{T354M}$ mutation. A missense mutation of C → T in a single allele at the 1061 codon of *GATA2* gene results in the conversion of threonine (ACG) to methionine (ATG). T354M transition is the most prevalent *GATA2* mutation identified so far, accounting for about 50% of all the *GATA2* mutation cases [305]. Clinical diagnoses of this donor revealed normal T cell number, moderately decreased absolute B cell number and absence of CD56$^{bright}$ NK cells. Considering the clinical diagnoses, we believe this donor is in the early stage of the disease caused by GATA$^{T354M}$ mutation. In our flow analyses, the CD56$^{bright}$ NK cells from this donor was not easily identifiable compared to the healthy control (**Figure 5.16.A**). With the help from the CD57 staining, we could only find 2% CD56$^{bright}$ NK cells within the NK population, which is substantially lower than the normal 5 - 10% range (**Figure 5.16.A**). This

provided us a unique opportunity to study the human NK cell defect at the early disease stage of *GATA2* mutation.

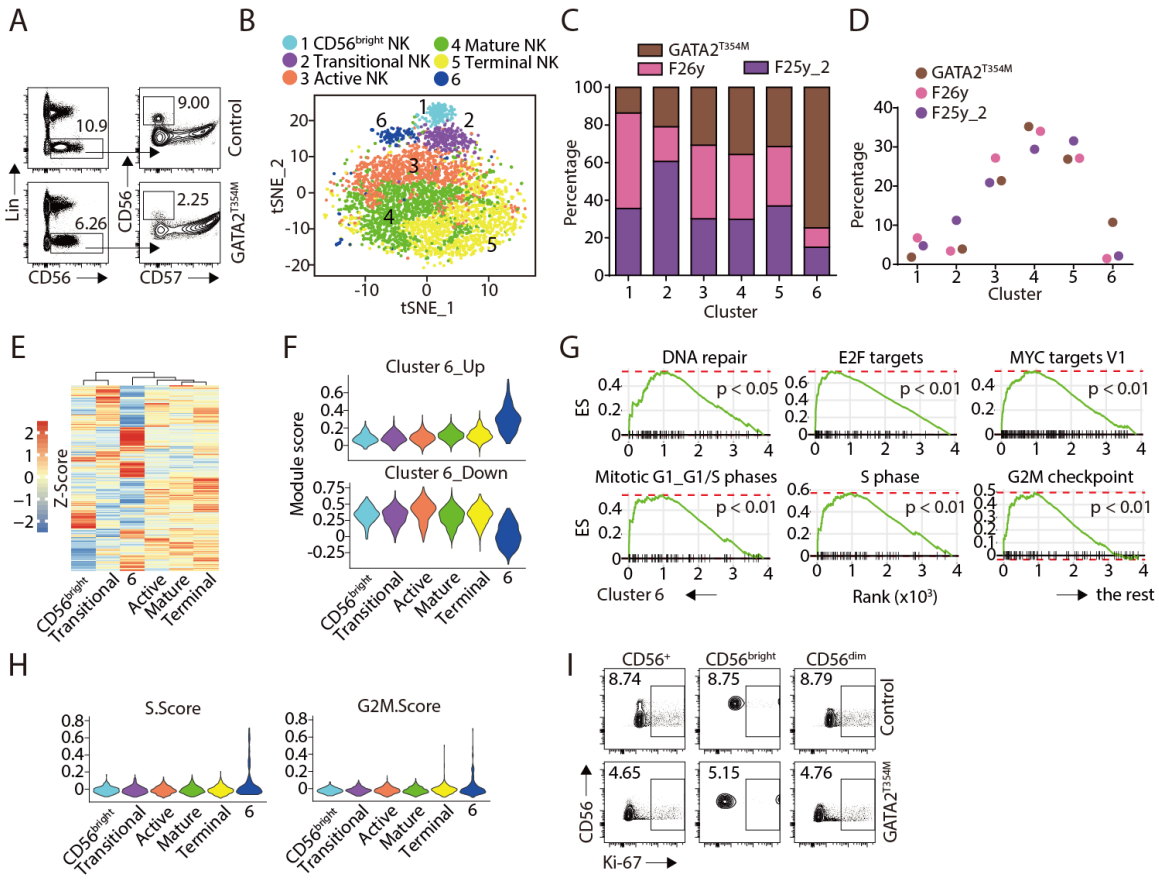


**Figure 5.16. *GATA2* mutation results in larger transcriptome alteration in CD56$^{bright}$ NK cells compared to CD56$^{dim}$ NK cells**

(**A**) The blood samples from the GATA2$^{T354M}$ donor and the healthy control were freshly collected and processed at the same time. Lin$^{-}$CD56$^{+}$ NK cells were evaluated via flow cytometry. The CD56$^{bright}$ NK cells were identified with the help of CD57. (**B**) The combined analyses of the blood samples from the GATA2$^{T354M}$ donor and the two healthy controls resulted in six clusters as shown in the t-SNE plot. (**C**) Composition of the donors within each cluster. The input cell number from each donor is normalized to be equal. (**D**) Composition of the clusters within each donor. (**E**) The transcriptome similarity among clusters was compared using the Euclidean distance and demonstrated via heatmap. (**F**) Module score was

calculated with up-regulated (top) or down-regulated DEGs (bottom) from the cluster #6 and demonstrated via violin plots. (**G**) Selected gene sets from the GSEA enriched in the Cluster #6 of the $GATA^{T354M}$ donor sample compared to the rest of cells. (**H**) The S phase score (top) and G2M phase score (bottom) were calculated and demonstrated via violin plots. (**I**) Proliferating NK cells from the $GATA2^{T354M}$ donor and the healthy control were evaluated via Ki-67 staining.

We performed the scRNA-seq experiment using the $Lin^{-}CD7^{+}$ cells from the blood of the donor with $GATA2^{T354M}$ mutation. After sequencing, we combined this dataset with the blood samples from two healthy female donors for a PCA analyses. As illustrated in the t-SNE plot, we were able to identify the original five NK clusters seen in the blood of the healthy donors with an additional new cluster, cluster #6 (**Figure 5.16.B**). This new cluster was mainly comprised of cells from the donor with $GATA2^{T354M}$ mutation (**Figure 5.16.C**). Consistent with the flow-based identification of $CD56^{bright}$ NK cells, scRNA-seq analyses also revealed only 2% of the total NK cells were in the '$CD56^{bright}$ NK' cluster of the $GATA2^{T354M}$ donor (**Figure 5.16.D**). The composition of the other four clusters were relatively similar among the $GATA2^{T354M}$ donor and the two healthy controls (**Figure 5.16.C and 5.16.D**). These results indicate that *GATA2* mutation indeed results in the loss of $CD56^{bright}$ NK cells instead of the loss of CD56 expression.

Next, we focused on the analyses of Cluster #6 due to its uniqueness to the *GATA2* mutation. The transcriptome signature of this cluster was substantially distinct to the previously identified five clusters as indicated by the Euclidean distance and module scores (**Figure 5.16.E and 5.16.F**). The GSEA results revealed significantly enrichment

of cell cycle gene sets in the Cluster #6 compared to the rest of the cells (**Figure 5.16.G**). We calculated the cell cycle score and did not find substantially higher S.Score or G2M.Score of the Cluster #6 (**Figure 5.16.H**). The GSEA also found highly significant enrichment of transcription factors E2F and MYC in the Cluster #6 compared to the rest of the cells, both involved in cell proliferation (**Figure 5.16.G**). From flow cytometry analyses, we did not find more cycling NK cells in the $GATA2^{T354M}$ donor compared to the control as indicated by Ki-67 staining (**Figure 5.16.I**). It is evident that the protein level of Ki-67 decreased one log-fold in the $GATA2^{T354M}$ donor compared to the control (**Figure 5.16.I**). However, as the negative population also shifted, this was likely due to a technical issue of the staining.

The majority of the $GATA2^{T354M}$ donor-derived NK cells clustered along with the healthy controls, indicating that the mutation so far has not caused a large transcriptome changes of the cells except for the cluster #6. This could potentially result from the early stage of the disease in this donor. To compare the similarity between the $GATA2^{T354M}$ donor and the healthy controls, we used a Spearman's correlational matrix to compare the average gene expression among each cluster from each donor (**Figure 5.17.A**). It was evident that the 'Active, Mature and Terminal NK' clusters from $GATA2^{T354M}$ donor sample correlated well with the corresponding clusters in the healthy controls. On the contrary, the '$CD56^{bright}$ and Transitional NK' clusters did not correlate well between $GATA2^{T354M}$ donor and healthy controls. This result demonstrates that GATA2 mutation renders larger transcriptome alteration of $CD56^{bright}$ NK cells compared to $CD56^{dim}$ NK cells, consistent

with more GATA2 protein in the CD56$^{bright}$ NK cells [97]. This could contribute to the specific loss of CD56$^{bright}$ NK cells.

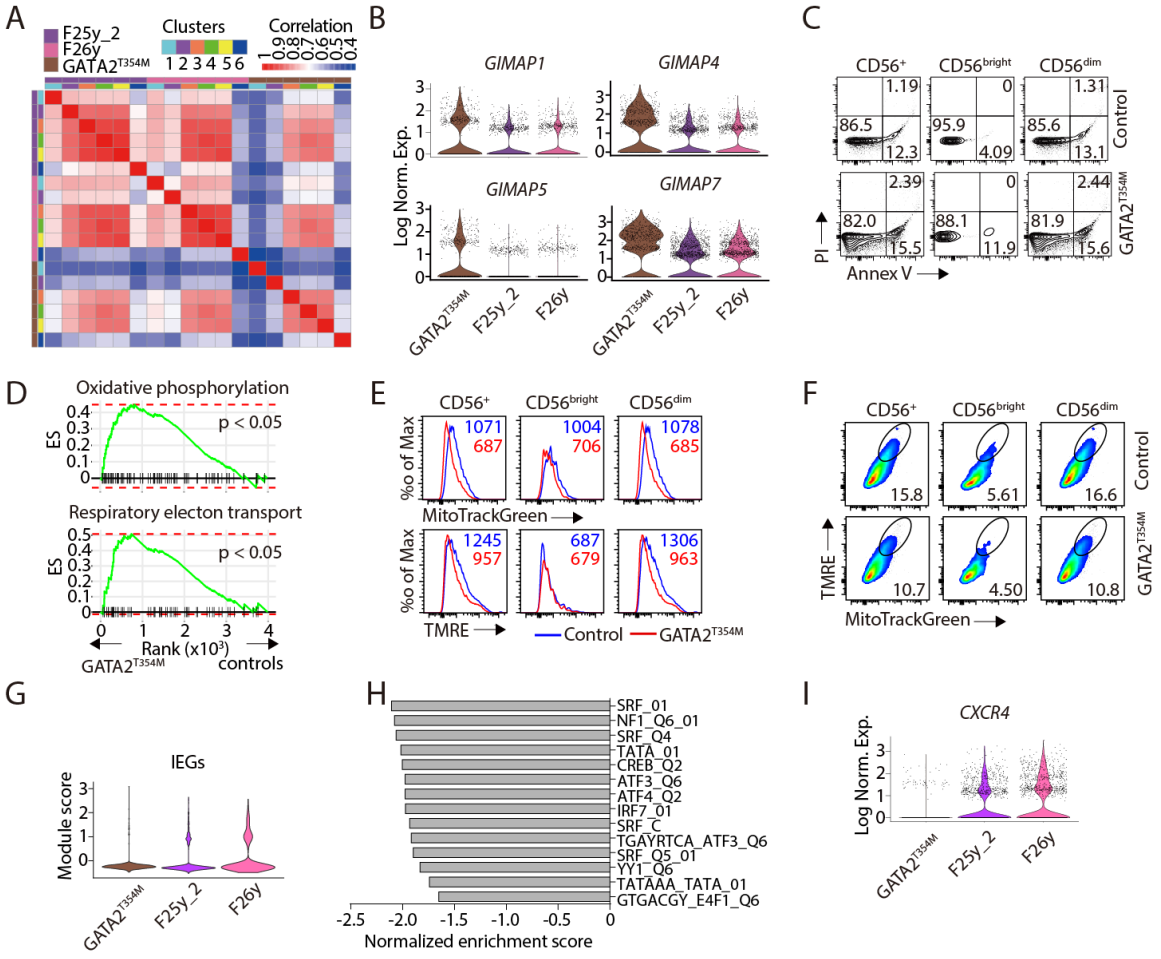


**Figure 5.17. Features associated with the GATA2$^{T354M}$ donor NK cells**

(**A**) Spearman's correlational matrix was used to compare the average gene expression among each cluster from each donor. (**B**) Four of the top 10 up-regulated DEGs of the GATA2$^{T354M}$ donor NK cells belong to GIMAP family and were shown in violin plots. The y-axis represents log-normalized expression value. (**C**) The viability of NK cells from the GATA2$^{T354M}$ donor and the healthy control were evaluated using Annexin V/PI staining. (**D**) GSEA reveals enrichment of oxidative phosphorylation and respiratory electron

transport gene sets in the GATA2$^{T354M}$ donor compared to the healthy controls. (**E**) Mitochondrial mass and membrane potential were assessed by MitoTrackGreen and TMRE staining, respectively. (**F**) The polarized mitochondria defined by high mitochondrial mass and membrane potential were gated. (**G**) Module score calculated based on IEGs (as in **Figure 5.7.G**) in GATA2$^{T354M}$ donor and the healthy controls. (**H**) All significantly enriched transcription factors and motifs in the GSEA C3 dataset when comparing the GATA2$^{T354M}$ donor with the healthy controls were shown in histogram. (**I**) The expression of *CXCR4* in the GATA2$^{T354M}$ donor and the healthy controls were shown as violin plots. The y-axis represents log-normalized expression value.

Direct comparison between the GATA2$^{T453M}$ donor and the healthy controls revealed significantly increased expression of genes among the GIMAP family in the GATA2$^{T354M}$ donor sample. Within the top 10 most up-regulated genes in the GATA2$^{T453M}$ donor-derived NK cells, four of them belong to GIMAP family (**Figure 5.17.B**). This family is known to play critical roles in the maintenance of the lymphocytes at steady-state [403, 404]. GIMAP4 has shown to be pro-apoptotic [405], whereas both GIMAP1 and GIMAP5 are anti-apoptotic[406-408]. This data implies an augmented pro-apoptotic propensity in the GATA2$^{T453M}$ donor NK cells. Indeed, flow analyses of freshly-collected samples revealed more apoptotic NK cells in the GATA2$^{T453M}$ donor than the healthy control (**Figure 5.17.C**). Although the CD56$^{bright}$ NK cells are more viable than the CD56$^{dim}$ NK cells, the difference of the percentage apoptotic cells is larger in the CD56$^{bright}$ compartment than the CD56$^{dim}$ when comparing the GATA2$^{T354M}$ donor with the healthy control (**Figure 5.17.C**). While this data needs further validation, it implies that the loss of CD56$^{bright}$ NK cells in patients with *GATA2* mutation could results from an increased apoptotic rate of CD56$^{bright}$ NK cells. Enrichment of gene sets related to

mitochondrial functions stood out in the GSEA when comparing the GATA2$^{T354M}$ donor to the healthy controls (**Figure 5.17.D**). However, with the staining of MitoTrackGreen and TMRE, we found cells from the GATA2$^{T354M}$ donor have lower mitochondrial mass and membrane potential compared to the healthy control (**Figure 5.17.E**). The percentage of cells with polarized mitochondria defined by high expression of both mass and membrane potential was also less in the GATA2$^{T354M}$ donor (**Figure 5.17.F**). Whether there is a metabolic alteration in *GATA2* mutant NK cells requires further exploration with larger sample size.

Among the gene that were expressed at significantly lower levels in the GATA2$^{T453M}$ donor compared to the healthy controls, we found that the 'Active NK' cluster-featured genes including IEGs are the genes that have greatest difference in expression level (**Figure 5.17.G**). This indicates a potential defect of the homeostatic activation of NK cells in the GATA2$^{T453M}$ donor. Along with this, the C3 gene set from GSEA revealed significant depletion of serum response factor (SRF) and ATF/CREB in the GATA2$^{T453M}$ donor sample compared to the healthy controls (**Figure 5.17.H**), key transcription factors involved in the expression of IEGs [384, 385, 409]. Maciejewski-Duval et al., reported that surface CXCR4 expression is diminished in NK cells of patients with *GATA2* mutation, but the total transcripts level is comparable to the healthy controls [323]. However, in our dataset, we found nearly diminished *CXCR4* expression at the transcripts level compared to the healthy controls (**Figure 5.17.I**). In summary, the reduced presence of the features associated with 'Active NK' cluster may further contribute to the developmental defects in patients with *GATA2* mutation.

## 5.3 Conclusions

We utilized scRNA-sequencing technology to explore the heterogeneity of human NK cells from both BM and blood of healthy donors and a donor with GATA2$^{T354M}$ mutation. We uncovered significant heterogeneity than cell surface markers-defined NK subsets. A unique cluster with high expression of IEGs implies cellular activation of NK cells at steady-state. The functionally-mature CD57$^{+}$ NK cells are not a homogeneous population. Nearly half of them marked with high expression of *CX3CR1*, *HAVCR2* (TIM-3), and *ZEB2* demonstrate unique transcriptional features and may comprise the terminal mature NK cells. Moreover, we provide evidence at the transcriptome level in supporting the developmental progression from CD56$^{bright}$ to CD56$^{dim}$ NK cells and identify a transitional population. Finally, in a donor at early disease stage caused by GATA2$^{T354M}$ mutation, we confirmed the loss of CD56$^{bright}$ NK cells via scRNA-seq. We found this mutation resulted in larger transcriptome alteration of the CD56$^{bright}$ NK cells compared to the CD56$^{dim}$ NK cells and the CD56$^{bright}$ NK cells were dying faster than the healthy control. The reduced expression of IEGs also implies that the homeostatic activation is altered in patients with *GATA2* mutation, which potentially contributes to the NK cell defects.

## 5.4 Discussion

The current human NK cell development model divides the $Lin^{-}CD56^{+}$ cells from the BM and blood into three distinct populations based on the surface expression level of CD56 and CD57 ($CD56^{bright} \rightarrow CD56^{dim}CD57^{-} \rightarrow CD56^{dim}CD57^{+}$) [86]. In our scRNA-seq analyses, we uncovered more discrete developmental stages than these three simple subsets. We found a bona fide '$CD56^{bright}$ NK' cluster in the scRNA-seq dataset, comprising 5 - 10% of total NK cells. We believe 'Mature and Terminal' NK clusters together form the functionally mature $CD57^{+}$ NK cells. Although both *CX3CR1* and *HAVCR2* (TIM-3) marks the 'Terminal NK' cluster at the RNA level, neither of them is sufficient to distinguish this population at cell surface level [397, 398]. GSEA indicated dampened signaling and metabolic activity in the 'Terminal NK' cluster compared to the 'Mature NK' cluster. Whether there are differences in function and longevity between the 'Mature' and 'Terminal' NK cells remain an open question. We found a transitional population between $CD56^{bright}$ and $CD56^{dim}$ NK cells, supporting the developmental progression from $CD56^{bright}$ to $CD56^{dim}$ NK cells at transcriptome level. Based on the expression of CD16 (*FCGR3A*), we reasoned that cells with intermediate cell surface expression of CD16 are potential cells in the 'Transitional NK' cluster, existing in a small portion of $CD56^{bright}$ NK cells and part of the $CD56^{dim}CD57^{-}$ NK cells. Based on flow cytometry analyses, there are more NK cells with intermediate CD16 expression in the BM than the blood, consistent with higher percentage of the 'Transitional NK' cluster in the BM than the blood of the scRNA-seq data. The scRNA-seq data also picked up the adaptive NK cells marked with high expression of NKG2C (*KLRC2*). Interestingly,

within the ‘Adaptive NK’ cluster, only one donor had significant expression of *KLRC2*. This implies adaptive NK cells arise from infections other than HCMV potentially share similar features with HCMV-induced NK memory.

One novel cluster that we found in both the BM and blood was the ‘Active NK’ cluster. This cluster had high expression of IEGs including *FOS*, *FOSB*, *JUN*, *JUNB*, etc. More than 50% of the up-regulated differentially expressed genes of this cluster were transcription factors. We hypothesize that this could reflect homeostatic activation of NK cells via certain stimuli. Interestingly, Crinier et al., have recently found a new NK population in the mouse spleen with similar active transcriptional signatures, though they did not find this cluster in their human dataset potentially due to low cell number and sequencing depth or even the age and health conditions of the donors [401]. This implies a conserved homeostatic activation of NK cells in both mice and humans, which is potentially critical to the survival, proliferation or even differentiation of NK cells.

*GATA2* mutation has been of interest to the human NK cell biology due to the specific loss of $CD56^{bright}$ NK population [97]. This observation has challenged the differentiation dogma from $CD56^{bright}$ to $CD56^{dim}$ NK to some extent. The nearly complete loss of $CD56^{bright}$ NK cells at the moment of *GATA2* mutation diagnose impedes any study of mechanism behind this phenomenon. The identification of a donor with $GATA2^{T453M}$ mutation at early disease stage with reduced number of $CD56^{bright}$ NK cells provided us a rare opportunity to address this phenomenon. Using scRNA-seq, we confirmed the loss of

the $CD56^{bright}$ NK cells from this patient. Although the heterogeneity of the NK cells in this donor was largely intact compared to healthy control, we found a larger transcriptome alteration in the 'CD56$^{bright}$ and Transitional NK' clusters than the rest of clusters. The $CD56^{bright}$ NK cells also have higher apoptotic rate than normal. Direct transcriptome comparison revealed significantly reduced expression of genes related to 'Active NK' cluster in the $GATA2^{T453M}$ donor, implying impaired steady-state activation. This may also contribute to the NK defects in patients with *GATA2* mutation.

Unlike the murine model, there are more NK progenitors and immature NK cells in the secondary lymphoidal organs. It is valuable to explore the heterogeneity of NK cells in these anatomic locations using this technology. Although Crinier et al. used scRNA-seq to profile the human NK cells from the spleen, little information was uncovered related to the early developmental stages presumably due to sorting of only the $CD56^{+}$ NK cells [401]. Moreover, with the limit RNA being captured at the single cell level, we do not have much success in determining the driving forces in promoting NK cell maturation, for example, the identification of unique transcription factors at distinct developmental stages. This problem will be solved with more advanced scRNA-seq technology in the future. Nevertheless, our study explored the heterogeneity of human NK cells at the transcriptome level and substantially expand our understanding of human NK cell. For future application, machine learning-based classifier algorithm could be built based on these datasets to characterize the developmental heterogeneity of human NK cells in patients with various genetic or pathological conditions.

# Chapter 6 – General Conclusions

Through generating *Ncr1*$^{iCre}$-mediated conditional knockout mice with Raptor- or Rictor-deficiency, we revealed the differential role of mTORC1 and mTORC2 in regulating the development of NK cells. Specific to mTORC2, we established the critical role of mTORC2-Akt$^{S473}$-FoxO1-T-bet in regulating the terminal maturation of NK cells. Using scRNA-seq technology, we defined five distinct murine NK subsets in the BM of WT mice based on transcriptome of individual cells. After establishing the relative maturity of the five WT NK clusters, we utilized machining learning algorithms-based classifiers to assign cellular identity of Raptor- or Rictor-deficient NK cells. Surprisingly, we found substantial immaturity of Rictor-deficient NK cells that was masked by the expression of cell surface markers. Further mechanistic investigation revealed even more pronounced immaturity of the T-bet-deficient NK cells, uncovering the previously unappreciated role of T-bet in suppressing immature NK transcriptional signature during the development of NK cells.

With successful usage of scRNA-seq technology in the murine NK cells, we subsequently profiled human NK cells from BM and blood of healthy donors. We identified distinct NK subsets and defined a novel NK population expressing higher levels of immediate early genes indicating a homeostatic activation. The CD57+ NK cells are a heterogeneous population containing both functionally and terminally mature NK subsets. Furthermore, the transcriptome and pseudotime analyses reveal the existence of a transitional population between CD56$^{bright}$ and CD56$^{dim}$ NK cells. Finally, we described a reduction of CD56$^{bright}$ NK cells at the single-cell transcriptome level in a donor with GATA2$^{T354M}$ mutation due to cell death that coincided with a larger transcriptomic

alteration in the $CD56^{bright}$ compared to $CD56^{dim}$ NK cell population. These data significantly expand our understanding of the heterogeneity and development of human NK cells.

# Chapter 7 – General Discussion

## 7.1 The linear development model of NK cells – true or not

After decades of research, a linear developmental model has been established in both murine and human NK cells. The adoptive transfer experiments have been used as the golden standard in establishing this model. Myriad work related to the developmental regulation of NK cells centers around this linear model which has become the fundamental knowledge we have regarding the development of NK cells.

Although this model is appealing and seems to be correct, it is important to consider the alternatives. Several basic questions related this model remain to be answered. Some of them are listed here: Whether each developmental stage is absolutely required for the terminal maturation? Does every single NK cell go through the same development stages and become terminal maturation? Whether the linear model is always one directory from immature to mature? Does plasticity exist? Whether intermediate developmental stages represent unique functional subsets?

Recent studies have begun to address some of these questions. Colonna's group have demonstrated the plasticity between conventional NK cells and ILC1 regulated through TGF-β signaling [410]. The CD27/CD11b DP stage NK in mice and the CD56bright NK cells in human are more potent cytokine producers compared to the terminal mature CD11b SP or CD56dim NK cells, respectively, arguing the functional importance of NK

cells at transitional stages [81, 321]. The linear model presents a valuable tool to study the development of NK cells. However, we should always think about the alternatives.

7.2 mTORC1 and the development of NK cells – questions remain to be answered

Through conditional deletion of *Rptor* in NK cells using *Ncr1*$^{iCre}$ system, we revealed the critical role of mTORC1 in regulate the early development of NK cells. However, the mechanisms behind this phenotype remain unknown. In terms of the developmental stages, the cell surface expression of CD27/CD11b revealed early developmental impairment of NK cells in *Rptor* cKO mice. Although the scRNA-seq analysis indicates that mTORC1-deficient NK cells are potentially more mature than CD27/CD11b-determined maturity, what the transcriptome-defined maturity does not take into account is the post-transcriptional regulation that is for sure altered in the Raptor-deficient NK cells. In fact, we found reduced expression of several Ly49 family members at per cell level with no difference in percentage expressing cells. More importantly, we found similar transcripts level of these Ly49 family members between the Raptor-deficient and WT NK cells. The large alteration of both transcriptome and proteome resulted from mTORC1 deficiency makes it hard to judge what is the precise developmental impairment of Raptor-deficient NK cell and extremely difficult to dissect the downstream targets that are responsible for the defects.

Eomes is a potential candidate downstream of mTORC1 that is partially responsible for the maturation defects. Currently, there is no Eomes over-expression transgenic mice that we could use to bred with *Rptor* cKO mice to rescue the developmental defects. We have tried the lentivirus-based over-expression of Eomes in Lin$^-$ BM cells with around 20% transfection efficiency indicated by the expression of eGFP. Future work is required to

further validate the over-expression of Eomes and conduct the BM reconstitution experiments in lethally-irradiated mice to evaluate the rescue *in vivo*. Another question remained to be answered is how mTORC1 regulates the expression of Eomes. The bulk RNA-seq indicated reduced transcripts level of Eomes. Whether the protein level of E4BP4 (also known as Nfil3), transcriptional activator of Eomes [105], is reduced in Raptor-deficient NK cells remain unknown. It requires the breeding of Rptor cKO mice with the *Nfil3*-reporter mice as currently there is no reliable antibody to detect E4BP4 with flow cytometry. Nevertheless, E4BP4 is probably not the reason for reduced Eomes expression as $Ncr1^{iCre}$-mediated deletion of *Nfil3* does not result in any developmental defects [110]. Considering the essential role of mTORC1 in regulating protein translation, especially mRNA containing 5′-terminal oligopyrimidine motif (5′-TOP mRNA) [208, 209], the translation of Eomes is potentially impaired in Raptor-deficient NK cells during development. In fact, the 5′-UTR of *Eomes* mRNA starts with a stretch of 4 pyrimidines, which is one pyrimidine less to the conserved definition of 5′-TOP mRNAs [208, 209]. Future work is required to test this possibility, presumably using an artificial expression system *in vitro* as the small number of NK cells in mice is technically challenging in addressing this question.

Although myriad targets have been identified downstream of mTORC1, 4E-BPs and S6K1 are the most well-established target proteins of mTORC1. mTORC1 phosphorylates and activates both. Currently, the phosphor-deficient (S999A) and phosphor-mimetic mutant (S999D) mice of S6K1 are available [411]. It will be instrumental in evaluating the development of NK cells in these transgenic mice. It will

be helpful in delineating the role of mTORC1 in the development of NK cells by breeding the phosphor-mimetic mutant (S999D) mice with *Rptor* cKO mice to evaluate the phenotypical changes or even rescues. Future investigation in this angel are warranted.

The role of mTORC1 in the commitment of NK lineage remains unknown as the $Ncr1^{iCre}$-mediated deletion happens after the commitment of NK cells. Previous work, using Vav1iCre-mediated deletion, has revealed the role of PDK1, upstream of mTORC1, in maintaining the NK lineage. It will be interesting to delineating the role of mTORC1 in the earliest developmental stage of NK lineage. We have tried to breed the $Rptor^{fl/fl}$ mice with the $Vav1^{iCre}$ mice to address this question. Unfortunately, the mice with homozygous deletion of *Rptor* suffer from severe anemia and succumb before birth [412]. We did not find any developmental alteration in the heterozygous mice. To further elucidate the role of mTORC1 in the early commitment of NK lineage, we need to breed the $Rptor^{fl/fl}$ mice with the $Il7r^{iCre}$ mice to overcome the erythropoiesis issue.

One important aspect of mTORC1 is its central regulation of cellular metabolism. The role of metabolism in regulating the development of NK cells are just beginning to be revealed. Several groups have reported the importance of autophagy in maintaining the development of NK cells [353, 413, 414]. As a master regulator in balancing the catabolic and anabolic metabolism, whether the altered metabolism resulted from Raptor-deficiency contributes to the developmental defects remains an open question. One

interesting observation from the bulk RNA-seq analysis is that the oxidative phosphorylation pathway is depleted in the Raptor-deficient NK cells, indicating defects in mitochondrial functions. This coincides with more than 10-fold induction of *Ppargc1a* in Raptor-deficient NK cells, which is known to be induced under mitochondrial stress conditions [415]. mTORC1 has been shown to regulate the mitochondria oxidative phosphorylation through the YY1-PGC1a axis [416]. Although work from our lab has shown that PGC1a is dispensable for the development of NK cells (currently under review), it would be interesting to delete *Ppargc1a* in Raptor-deficient NK cells to see whether the induction of PGC1a compensates the metabolic demands that is critical for the development of the Rictor-deficient NK cells.

## 7.3 More to be learned from FoxO1 and T-bet in the development of NK cells

In addition to the well-established role of T-bet in driving the terminal maturation of NK cells, single-cell RNA-seq analysis from our work revealed that T-bet is also critical in suppressing the immature transcriptional signature during the development of NK cells. As T-bet CHIP-seq dataset indicated that T-bet is unlikely to directly bind and suppress the large amounts of immature NK signature genes, other mechanisms are responsible for the induction of the immature NK transcriptional signature in T-bet-deficient NK cells. We hypothesized that transcription factor FoxO1 is potentially hyperactive in the T-bet-deficient NK cells and responsible for the induction of immature NK signature genes. To further prove this hypothesis, we should evaluate the protein level of FoxO1 in T-bet-deficient NK cells with an anticipation of increased expression. We need to conduct FoxO1 CHIP-seq experiment to evaluate whether FoxO1 is indeed binding to the regulatory elements associated with the immature NK signature genes. Furthermore, it would be critical to assess the transcriptome alteration of the NK cells either deficient of FoxO1 or expressing the constitutive active FoxO1 [354]. At last, to make a solid conclusion, we need to demonstrate that deletion of FoxO1 in T-bet-deficient NK cells will reverse the abnormal induction of immature NK signature genes, an observation we have seen in NK cells deficient of both Rictor and FoxO1. If the hypothesis turns out to be true, it further establishes an important transcriptional pathway with reciprocal regulation between FoxO1 and T-bet in governing the development of NK cells.

The complete rescue of the NK cellularity and maturation in *Rictor* cKO mice through deletion of *Foxo1* emphasizes that hyperactive FoxO1 is the causative factor responsible for the developmental defects of Rictor-deficient NK cells. Although we found rescued expression of T-bet in *Rictor*/*Foxo1* cDKO NK cells, it still does not definitely prove that the reduced expression of T-bet is the reason for terminal maturation defects of Rictor-deficient NK cells. To achieve that, we need to breed the *Rictor* cKO mice with T-bet over-expressing transgenic mice to rescue the maturation defects [349]. The reduced T-bet expression is unlikely to be responsible for the impaired homeostatic proliferation of the Rictor-deficient NK cells as T-bet-deficient NK cells have higher homeostatic proliferation rate than the WT control [121]. FoxO1 has been shown to promote cell cycle arrest through induction of cyclin-dependent kinase inhibitor $p27^{kip1}$ or down-regulation of cyclin D [417, 418]. Thus, it is possible that hyperactive FoxO1 directly inhibit the cycling of the Rictor-deficient NK cells. An alternative explanation would be the induction of *Socs2* in the Rictor-deficient NK cells due to the hyperactive of FoxO1. In the bulk RNA-seq dataset, we found three-fold induction of *Socs2* in the Rictor-deficient NK cells compared to the WT control. Socs2 negatively regulates the IL-15 signaling and homeostatic proliferation of NK cells [419]. It would be interesting to breed the *Rictor* cKO mice with the *Socs2* KO mice to reveal whether high expression of Socs2 in Rictor-deficient NK cells is responsible for the proliferation defects.

## 7.4 The ‘active NK’ cluster identified in both human and mice

The most novel finding from the exploration of the developmental heterogeneity of NK cells using scRNA-seq would be the identification of the ‘active NK’ cluster in both human and mice. The unique transcriptional profile with induction of immediate early genes defines this NK subset. There are certain concerns with the identity of these cells: whether they are truly a distinct group of NK cells or artifacts resulted from *in vitro* process of the sample. The expression of IEGs are known to be activated transiently and rapidly. The experimental manipulation of cells could potentially induce the expression of IEGs. However, as all the cells are going through the same experimental process, it is hard to explain why only a fraction of cells have high expression of IEGs if it is artifact. Rodda et al., has recently defined the heterogeneity of lymph node stromal cells using the 10X-based scRNA-seq technology and they also found a subset of stromal cells with high expression of IEGs [420]. Through using IEG *Nr4a1*-GFP reporter mice, they were able to identify heterogeneous expression of *Nr4a1* in different subsets of stromal cells. It would be of interest to identify these NK cells in the IEG reporter mice (*Nr4a1* or *Fos*). With the help from other maturation-defining markers, we can evaluate the expression pattern of IEGs among different developmental stages. This will allow us to determine whether this subset of NK cells is unique to a particular stage of NK cells or they are a heterogeneous population receiving similar stimuli. The physiological importance of this NK subset remains to be determined. The identification of the *in vivo* stimuli that induce the expression of IEGs in NK cells will be helpful in address this question.

## 7.5 Metadata-determined cellular identity

Cellular identity has been conventionally-defied by the expression of cell surface markers. The recent breakthrough of the single-cell RNA-sequencing technology enables quantification of thousands of transcripts in a given cell and provides a new way of defining cellular identity. It has been proven that this technology is powerful in determine cellular heterogeneity [421]. Through utilization of this technology, we re-defined the developmental heterogeneity of murine and human NK cells. With the identification of novel NK subsets, our datasets provide large amounts of molecular information associated with each NK subset. In addition, we took the methodology in determining the cellular identity of mutant cells resulted from genetic deletion or natural occurrence. In the study of Raptor- or Rictor-deficient NK cells, for the first time, we utilized the machine learning algorithms to assign cellular identity of each mutant cells based on the transcriptome information obtained from WT cells. Admittedly, the 70% accuracy of the machine learning classifiers are not ideal. However, this is mostly due to the limit WT cells in our sample. With increased training information from more WT cells, we are confident that the accuracy will increase substantially. With this methodology, we uncovered the previously unappreciated role of T-bet in suppressing the immature NK signature genes, a phenomenon that is masked by the expression of cell surface markers. Moreover, this study provides a new example of defining cellular identity with transcriptome.

Compared to the bulk RNA-seq, there is still limited coverage of the transcriptome by the scRNA-seq technology. This limitation profoundly restricts the identification of the low abundance transcripts which often encode proteins that are potential markers useful in identifying cellular population using antibodies. A major frustration in our study is the failure in identifying the novel population with cell surface markers. After all, the transcriptome is not the same as the proteome. Another limitation in our study resulted from the low transcriptome coverage is the lack of in-depth information associated with key transcription factors. As cell differentiation is fundamentally governed by the expression of tightly-regulated transcription factors, the unique transcription factors associated with each NK cluster are valuable in determining the cellular identity. Although we have performed the newly-developed SCENIC analysis based on transcriptional cis-regulation [422], we did not find novel cluster-defining transcription factors. With the advancement of the scRNA-seq technology of increased transcriptome coverage, these limitations should be addressed. Specific to the exploration of the heterogeneity of human NK cells, our study has only covered the BM and blood. It is well known that secondary lymphoid organs possess greater heterogeneity of NK cells in human. The tissue-resident NK cells located at distinct anatomic locations also possess unique origin and functions. In the future, it is valuable to use scRNA-seq technology to explore the heterogeneity of NK cells at these distinct locations.

Besides transcriptome-defined cellular identity, another metadata-based cellular classification has been recently developed based on the chromosome accessibility at single cell level, the single-cell ATAC-sequencing technology [423]. It will not be a

surprise that in the near future, the technological advance will allow us to profile the epigenome, the transcriptome, and even the proteome in one cell at the same time. The definition of a cell population will be further refined in the future.

# References


1. Oldham, R.K., *Natural killer cells: artifact to reality: an odyssey in biology.* Cancer Metastasis Rev, 1983. **2**(4): p. 323-36.
2. Rosenau, W. and H.D. Moon, *Lysis of homologous cells by sensitized lymphocytes in tissue culture.* J Natl Cancer Inst, 1961. **27**: p. 471-83.
3. Smith, H.J., *Antigenicity of carcinogen-induced and spontaneous tumours in inbred mice.* Br J Cancer, 1966. **20**(4): p. 831-7.
4. Kiessling, R., et al., *"Natural" killer cells in the mouse. II. Cytotoxic cells with specificity for mouse Moloney leukemia cells. Characteristics of the killer cell.* Eur J Immunol, 1975. **5**(2): p. 117-21.
5. Herberman, R.B., et al., *Natural cytotoxic reactivity of mouse lymphoid cells against syngeneic and allogeneic tumors. II. Characterization of effector cells.* Int J Cancer, 1975. **16**(2): p. 230-9.
6. Herberman, R.B., M.E. Nunn, and D.H. Lavrin, *Natural cytotoxic reactivity of mouse lymphoid cells against syngeneic acid allogeneic tumors. I. Distribution of reactivity and specificity.* Int J Cancer, 1975. **16**(2): p. 216-29.
7. Kiessling, R., E. Klein, and H. Wigzell, *"Natural" killer cells in the mouse. I. Cytotoxic cells with specificity for mouse Moloney leukemia cells. Specificity and distribution according to genotype.* Eur J Immunol, 1975. **5**(2): p. 112-7.
8. Oldham, R.K., et al., *Evaluation of a cell-mediated cytotoxicity assay utilizing 125 iododeoxyuridine-labeled tissue-culture target cells.* Natl Cancer Inst Monogr, 1973. **37**: p. 49-58.
9. Pross, H.F. and M. Jondal, *Cytotoxic lymphocytes from normal donors. A functional marker of human non-T lymphocytes.* Clin Exp Immunol, 1975. **21**(2): p. 226-35.
10. Carrega, P. and G. Ferlazzo, *Natural killer cell distribution and trafficking in human tissues.* Front Immunol, 2012. **3**: p. 347.
11. Orange, J.S., *Natural killer cell deficiency.* J Allergy Clin Immunol, 2013. **132**(3): p. 515-525.
12. Zamora, A.E., et al., *Models to Study NK Cell Biology and Possible Clinical Application.* Curr Protoc Immunol, 2015. **110**: p. 14 37 1-14.
13. Vivier, E., et al., *Functions of natural killer cells.* Nat Immunol, 2008. **9**(5): p. 503-10.
14. Abel, A.M., et al., *Natural Killer Cells: Development, Maturation, and Clinical Utilization.* Front Immunol, 2018. **9**: p. 1869.
15. Jewett, A., Y.G. Man, and H.C. Tseng, *Dual functions of natural killer cells in selection and differentiation of stem cells; role in regulation of inflammation and regeneration of tissues.* J Cancer, 2013. **4**(1): p. 12-24.
16. Popko, K. and E. Gorska, *The role of natural killer cells in pathogenesis of autoimmune diseases.* Cent Eur J Immunol, 2015. **40**(4): p. 470-6.
17. Kumar, P., et al., *IL-22 from conventional NK cells is epithelial regenerative and inflammation protective during influenza infection.* Mucosal Immunol, 2013. **6**(1): p. 69-82.
18. Schwartz, R.H., *Historical overview of immunological tolerance.* Cold Spring Harb Perspect Biol, 2012. **4**(4): p. a006908.
19. Antoniou, A.N. and S.J. Powis, *Pathogen evasion strategies for the major histocompatibility complex class I assembly pathway.* Immunology, 2008. **124**(1): p. 1-12.

20. Ljunggren, H.G. and K. Karre, *In search of the 'missing self': MHC molecules and NK cell recognition.* Immunol Today, 1990. **11**(7): p. 237-44.
21. Long, E.O. and S. Rajagopalan, *Stress signals activate natural killer cells.* J Exp Med, 2002. **196**(11): p. 1399-402.
22. Adams, E.J., et al., *Structural elucidation of the m157 mouse cytomegalovirus ligand for Ly49 natural killer cell receptors.* Proc Natl Acad Sci U S A, 2007. **104**(24): p. 10128-33.
23. Dorner, B.G., et al., *Coordinate expression of cytokines and chemokines by NK cells during murine cytomegalovirus infection.* J Immunol, 2004. **172**(5): p. 3119-31.
24. Cheng, T.P., et al., *Ly49h is necessary for genetic resistance to murine cytomegalovirus.* Immunogenetics, 2008. **60**(10): p. 565-73.
25. Fodil-Cornu, N., et al., *Ly49h-deficient C57BL/6 mice: a new mouse cytomegalovirus-susceptible model remains resistant to unrelated pathogens controlled by the NK gene complex.* J Immunol, 2008. **181**(9): p. 6394-405.
26. Guma, M., et al., *Imprint of human cytomegalovirus infection on the NK cell receptor repertoire.* Blood, 2004. **104**(12): p. 3664-71.
27. Muntasell, A., et al., *NKG2C zygosity influences CD94/NKG2C receptor function and the NK-cell compartment redistribution in response to human cytomegalovirus.* Eur J Immunol, 2013. **43**(12): p. 3268-78.
28. Hammer, Q., et al., *Peptide-specific recognition of human cytomegalovirus strains controls adaptive natural killer cells.* Nat Immunol, 2018. **19**(5): p. 453-463.
29. Rolle, A., et al., *Distinct HLA-E Peptide Complexes Modify Antibody-Driven Effector Functions of Adaptive NK Cells.* Cell Rep, 2018. **24**(8): p. 1967-1976 e4.
30. Gazit, R., et al., *Lethal influenza infection in the absence of the natural killer cell receptor gene Ncr1.* Nat Immunol, 2006. **7**(5): p. 517-23.
31. Jonjic, S., et al., *Immune evasion of natural killer cells by viruses.* Curr Opin Immunol, 2008. **20**(1): p. 30-8.
32. Scharton, T.M. and P. Scott, *Natural killer cells are a source of interferon gamma that drives differentiation of CD4+ T cell subsets and induces early resistance to Leishmania major in mice.* J Exp Med, 1993. **178**(2): p. 567-77.
33. Souza-Fonseca-Guimaraes, F., M. Adib-Conquy, and J.M. Cavaillon, *Natural killer (NK) cells in antibacterial innate immunity: angels or devils?* Mol Med, 2012. **18**: p. 270-85.
34. Horowitz, A., K.A. Stegmann, and E.M. Riley, *Activation of natural killer cells during microbial infections.* Front Immunol, 2011. **2**: p. 88.
35. Walch, M., et al., *Cytotoxic cells kill intracellular bacteria through granulysin-mediated delivery of granzymes.* Cell, 2014. **157**(6): p. 1309-23.
36. Jacquemin, G., et al., *Granzyme B-induced mitochondrial ROS are required for apoptosis.* Cell Death Differ, 2015. **22**(5): p. 862-74.
37. Dotiwala, F., et al., *Granzyme B Disrupts Central Metabolism and Protein Synthesis in Bacteria to Promote an Immune Cell Death Program.* Cell, 2017. **171**(5): p. 1125-1137 e11.
38. Teixeira, H.C. and S.H. Kaufmann, *Role of NK1.1+ cells in experimental listeriosis. NK1+ cells are early IFN-gamma producers but impair resistance to Listeria monocytogenes infection.* J Immunol, 1994. **152**(4): p. 1873-82.
39. Thale, C. and A.F. Kiderlen, *Sources of interferon-gamma (IFN-gamma) in early immune response to Listeria monocytogenes.* Immunobiology, 2005. **210**(9): p. 673-83.
40. Haller, D., et al., *Activation of human NK cells by staphylococci and lactobacilli requires cell contact-dependent costimulation by autologous monocytes.* Clin Diagn Lab Immunol, 2002. **9**(3): p. 649-57.

41. Feng, C.G., et al., *NK cell-derived IFN-gamma differentially regulates innate resistance and neutrophil response in T cell-deficient hosts infected with Mycobacterium tuberculosis.* J Immunol, 2006. **177**(10): p. 7086-93.
42. Esin, S., et al., *Functional characterization of human natural killer cells responding to Mycobacterium bovis bacille Calmette-Guerin.* Immunology, 2004. **112**(1): p. 143-52.
43. Schmidt, S., et al., *Natural killer cells and antifungal host response.* Clin Vaccine Immunol, 2013. **20**(4): p. 452-8.
44. Ma, L.L., et al., *NK cells use perforin rather than granulysin for anticryptococcal activity.* J Immunol, 2004. **173**(5): p. 3357-65.
45. Voigt, J., et al., *Human natural killer cells acting as phagocytes against Candida albicans and mounting an inflammatory response that modulates neutrophil antifungal activity.* J Infect Dis, 2014. **209**(4): p. 616-26.
46. Bar, E., et al., *IL-17 regulates systemic fungal immunity by controlling the functional competence of NK cells.* Immunity, 2014. **40**(1): p. 117-27.
47. Langers, I., et al., *Natural killer cells: role in local tumor growth and metastasis.* Biologics, 2012. **6**: p. 73-82.
48. Nicholson, S.E., N. Keating, and G.T. Belz, *Natural killer cells and anti-tumor immunity.* Mol Immunol, 2017.
49. Imai, K., et al., *Natural cytotoxic activity of peripheral-blood lymphocytes and cancer incidence: an 11-year follow-up study of a general population.* Lancet, 2000. **356**(9244): p. 1795-9.
50. Coca, S., et al., *The prognostic significance of intratumoral natural killer cells in patients with colorectal carcinoma.* Cancer, 1997. **79**(12): p. 2320-8.
51. Ishigami, S., et al., *Prognostic value of intratumoral natural killer cells in gastric carcinoma.* Cancer, 2000. **88**(3): p. 577-83.
52. Villegas, F.R., et al., *Prognostic significance of tumor infiltrating natural killer cells subset CD57 in patients with squamous cell lung cancer.* Lung Cancer, 2002. **35**(1): p. 23-8.
53. Van Elssen, C. and S.O. Ciurea, *NK cell therapy after hematopoietic stem cell transplantation: can we improve anti-tumor effect?* Int J Hematol, 2018. **107**(2): p. 151-156.
54. Ruggeri, L., et al., *Effectiveness of donor natural killer cell alloreactivity in mismatched hematopoietic transplants.* Science, 2002. **295**(5562): p. 2097-100.
55. Mehta, R.S., et al., *NK cell therapy for hematologic malignancies.* Int J Hematol, 2018. **107**(3): p. 262-270.
56. Lim, O., et al., *Present and Future of Allogeneic Natural Killer Cell Therapy.* Front Immunol, 2015. **6**: p. 286.
57. Fang, F., W. Xiao, and Z. Tian, *NK cell-based immunotherapy for cancer.* Semin Immunol, 2017. **31**: p. 37-54.
58. Bottino, C., et al., *Cellular ligands of activating NK receptors.* Trends Immunol, 2005. **26**(4): p. 221-6.
59. Ferrari de Andrade, L., et al., *Antibody-mediated inhibition of MICA and MICB shedding promotes NK cell-driven tumor immunity.* Science, 2018. **359**(6383): p. 1537-1542.
60. Rezvani, K., et al., *Engineering Natural Killer Cells for Cancer Immunotherapy.* Mol Ther, 2017. **25**(8): p. 1769-1781.
61. Tonn, T., et al., *Treatment of patients with advanced cancer with the natural killer cell line NK-92.* Cytotherapy, 2013. **15**(12): p. 1563-70.
62. Chen, K.H., et al., *Preclinical targeting of aggressive T-cell malignancies using anti-CD5 chimeric antigen receptor.* Leukemia, 2017. **31**(10): p. 2151-2160.

63. Andre, P., et al., *Anti-NKG2A mAb Is a Checkpoint Inhibitor that Promotes Anti-tumor Immunity by Unleashing Both T and NK Cells.* Cell, 2018. **175**(7): p. 1731-1743 e13.
64. van Montfoort, N., et al., *NKG2A Blockade Potentiates CD8 T Cell Immunity Induced by Cancer Vaccines.* Cell, 2018. **175**(7): p. 1744-1755 e15.
65. Seaman, W.E., et al., *Depletion of natural killer cells in mice by monoclonal antibody to NK-1.1. Reduction in host defense against malignancy without loss of cellular or humoral immunity.* J Immunol, 1987. **138**(12): p. 4539-44.
66. Sentman, C.L., et al., *Effector cell expression of NK1.1, a murine natural killer cell-specific molecule, and ability of mice to reject bone marrow allografts.* J Immunol, 1989. **142**(6): p. 1847-53.
67. Arase, H., et al., *Cutting edge: the mouse NK cell-associated antigen recognized by DX5 monoclonal antibody is CD49b (alpha 2 integrin, very late antigen-2).* J Immunol, 2001. **167**(3): p. 1141-4.
68. Walzer, T., et al., *Identification, activation, and selective in vivo ablation of mouse NK cells via NKp46.* Proc Natl Acad Sci U S A, 2007. **104**(9): p. 3384-9.
69. Jiao, Y., et al., *Type 1 Innate Lymphoid Cell Biology: Lessons Learnt from Natural Killer Cells.* Front Immunol, 2016. **7**: p. 426.
70. Abolins, S., et al., *The comparative immunology of wild and laboratory mice, Mus musculus domesticus.* Nat Commun, 2017. **8**: p. 14811.
71. Kondo, M., I.L. Weissman, and K. Akashi, *Identification of clonogenic common lymphoid progenitors in mouse bone marrow.* Cell, 1997. **91**(5): p. 661-72.
72. Rosmaraki, E.E., et al., *Identification of committed NK cell progenitors in adult murine bone marrow.* Eur J Immunol, 2001. **31**(6): p. 1900-9.
73. Vosshenrich, C.A. and J.P. Di Santo, *Developmental programming of natural killer and innate lymphoid cells.* Curr Opin Immunol, 2013. **25**(2): p. 130-8.
74. Yang, Q., et al., *TCF-1 upregulation identifies early innate lymphoid progenitors in the bone marrow.* Nat Immunol, 2015. **16**(10): p. 1044-50.
75. Carotta, S., et al., *Identification of the earliest NK-cell precursor in the mouse BM.* Blood, 2011. **117**(20): p. 5449-52.
76. Fathman, J.W., et al., *Identification of the earliest natural killer cell-committed progenitor in murine bone marrow.* Blood, 2011. **118**(20): p. 5439-47.
77. Di Santo, J.P., *Natural killer cell developmental pathways: a question of balance.* Annu Rev Immunol, 2006. **24**: p. 257-86.
78. Kim, S., et al., *In vivo developmental stages in murine natural killer cell maturation.* Nat Immunol, 2002. **3**(6): p. 523-8.
79. Williams, N.S., et al., *Clonal analysis of NK cell development from bone marrow progenitors in vitro: orderly acquisition of receptor gene expression.* Eur J Immunol, 2000. **30**(7): p. 2074-82.
80. Goh, W. and N.D. Huntington, *Regulation of Murine Natural Killer Cell Development.* Front Immunol, 2017. **8**: p. 130.
81. Hayakawa, Y. and M.J. Smyth, *CD27 dissects mature NK cells into two subsets with distinct responsiveness and migratory capacity.* J Immunol, 2006. **176**(3): p. 1517-24.
82. Chiossone, L., et al., *Maturation of mouse NK cells is a 4-stage developmental program.* Blood, 2009. **113**(22): p. 5488-96.
83. Huntington, N.D., et al., *NK cell maturation and peripheral homeostasis is associated with KLRG1 up-regulation.* J Immunol, 2007. **178**(8): p. 4764-70.
84. Walzer, T., et al., *Natural killer cell trafficking in vivo requires a dedicated sphingosine 1-phosphate receptor.* Nat Immunol, 2007. **8**(12): p. 1337-44.

85. Marcenaro, E., et al., *Editorial: NK Cell Subsets in Health and Disease: New Developments.* Front Immunol, 2017. **8**: p. 1363.
86. Freud, A.G., et al., *The Broad Spectrum of Human Natural Killer Cell Diversity.* Immunity, 2017. **47**(5): p. 820-833.
87. Freud, A.G., J. Yu, and M.A. Caligiuri, *Human natural killer cell development in secondary lymphoid tissues.* Semin Immunol, 2014. **26**(2): p. 132-7.
88. Roy, A., et al., *Perturbation of fetal liver hematopoietic stem and progenitor cell development by trisomy 21.* Proc Natl Acad Sci U S A, 2012. **109**(43): p. 17579-84.
89. Renoux, V.M., et al., *Identification of a Human Natural Killer Cell Lineage-Restricted Progenitor in Fetal and Adult Tissues.* Immunity, 2015. **43**(2): p. 394-407.
90. Scoville, S.D., A.G. Freud, and M.A. Caligiuri, *Modeling Human Natural Killer Cell Development in the Era of Innate Lymphoid Cells.* Front Immunol, 2017. **8**: p. 360.
91. Freud, A.G., et al., *NKp80 Defines a Critical Step during Human Natural Killer Cell Development.* Cell Rep, 2016. **16**(2): p. 379-391.
92. Poli, A., et al., *CD56bright natural killer (NK) cells: an important NK cell subset.* Immunology, 2009. **126**(4): p. 458-65.
93. Cooper, M.A., T.A. Fehniger, and M.A. Caligiuri, *The biology of human natural killer-cell subsets.* Trends Immunol, 2001. **22**(11): p. 633-40.
94. Luetke-Eversloh, M., M. Killig, and C. Romagnani, *Signatures of human NK cell development and terminal differentiation.* Front Immunol, 2013. **4**: p. 499.
95. Lopez-Verges, S., et al., *CD57 defines a functionally distinct population of mature NK cells in the human CD56dimCD16+ NK-cell subset.* Blood, 2010. **116**(19): p. 3865-74.
96. Bjorkstrom, N.K., et al., *Expression patterns of NKG2A, KIR, and CD57 define a process of CD56dim NK-cell differentiation uncoupled from NK-cell education.* Blood, 2010. **116**(19): p. 3853-64.
97. Mace, E.M., et al., *Mutations in GATA2 cause human NK cell deficiency with specific loss of the CD56(bright) subset.* Blood, 2013. **121**(14): p. 2669-77.
98. Wu, C., et al., *Clonal tracking of rhesus macaque hematopoiesis highlights a distinct lineage origin for natural killer cells.* Cell Stem Cell, 2014. **14**(4): p. 486-499.
99. Allan, D.S.J., et al., *Transcriptome analysis reveals similarities between human blood CD3(-) CD56(bright) cells and mouse CD127(+) innate lymphoid cells.* Sci Rep, 2017. **7**(1): p. 3501.
100. Horowitz, A., et al., *Genetic and environmental determinants of human NK cell diversity revealed by mass cytometry.* Sci Transl Med, 2013. **5**(208): p. 208ra145.
101. Barton, K., et al., *The Ets-1 transcription factor is required for the development of natural killer cells in mice.* Immunity, 1998. **9**(4): p. 555-63.
102. Colucci, F., et al., *Differential requirement for the transcription factor PU.1 in the generation of natural killer cells versus B and T cells.* Blood, 2001. **97**(9): p. 2625-32.
103. Gascoyne, D.M., et al., *The basic leucine zipper transcription factor E4BP4 is essential for natural killer cell development.* Nat Immunol, 2009. **10**(10): p. 1118-24.
104. Kamizono, S., et al., *Nfil3/E4bp4 is required for the development and maturation of NK cells in vivo.* J Exp Med, 2009. **206**(13): p. 2977-86.
105. Male, V., et al., *The transcription factor E4bp4/Nfil3 controls commitment to the NK lineage and directly regulates Eomes and Id2 expression.* J Exp Med, 2014. **211**(4): p. 635-42.
106. Yokota, Y., et al., *Development of peripheral lymphoid organs and natural killer cells depends on the helix-loop-helix inhibitor Id2.* Nature, 1999. **397**(6721): p. 702-6.

107. Boos, M.D., et al., *Mature natural killer cell and lymphoid tissue-inducing cell development requires Id2-mediated suppression of E protein activity.* J Exp Med, 2007. **204**(5): p. 1119-30.
108. Delconte, R.B., et al., *The Helix-Loop-Helix Protein ID2 Governs NK Cell Fate by Tuning Their Sensitivity to Interleukin-15.* Immunity, 2016. **44**(1): p. 103-115.
109. Gordon, S.M., et al., *The transcription factors T-bet and Eomes control key checkpoints of natural killer cell maturation.* Immunity, 2012. **36**(1): p. 55-67.
110. Firth, M.A., et al., *Nfil3-independent lineage maintenance and antiviral response of natural killer cells.* J Exp Med, 2013. **210**(13): p. 2981-90.
111. Ruzinova, M.B. and R. Benezra, *Id proteins in development, cell cycle and cancer.* Trends Cell Biol, 2003. **13**(8): p. 410-8.
112. Zook, E.C., et al., *Transcription factor ID2 prevents E proteins from enforcing a naive T lymphocyte gene program during NK cell development.* Sci Immunol, 2018. **3**(22).
113. Intlekofer, A.M., et al., *Effector and memory CD8+ T cell fate coupled by T-bet and eomesodermin.* Nat Immunol, 2005. **6**(12): p. 1236-44.
114. Lohoff, M., et al., *Deficiency in the transcription factor interferon regulatory factor (IRF)-2 leads to severely compromised development of natural killer and T helper type 1 cells.* J Exp Med, 2000. **192**(3): p. 325-36.
115. Taki, S., et al., *IFN regulatory factor-2 deficiency revealed a novel checkpoint critical for the generation of peripheral NK cells.* J Immunol, 2005. **174**(10): p. 6005-12.
116. Ohno, S., et al., *Runx proteins are involved in regulation of CD122, Ly49 family and IFN-gamma expression during NK cell differentiation.* Int Immunol, 2008. **20**(1): p. 71-9.
117. Levanon, D., et al., *Transcription factor Runx3 regulates interleukin-15-dependent natural killer cell activation.* Mol Cell Biol, 2014. **34**(6): p. 1158-69.
118. Aliahmad, P., B. de la Torre, and J. Kaye, *Shared dependence on the DNA-binding factor TOX for the development of lymphoid tissue-inducer cell and NK cell lineages.* Nat Immunol, 2010. **11**(10): p. 945-52.
119. Ali, A.K., et al., *NK Cell-Specific Gata3 Ablation Identifies the Maturation Program Required for Bone Marrow Exit and Control of Proliferation.* J Immunol, 2016. **196**(4): p. 1753-67.
120. Vosshenrich, C.A., et al., *A thymic pathway of mouse natural killer cell development characterized by expression of GATA-3 and CD127.* Nat Immunol, 2006. **7**(11): p. 1217-24.
121. Townsend, M.J., et al., *T-bet regulates the terminal maturation and homeostasis of NK and Valpha14i NKT cells.* Immunity, 2004. **20**(4): p. 477-94.
122. van Helden, M.J., et al., *Terminal NK cell maturation is controlled by concerted actions of T-bet and Zeb2 and is essential for melanoma rejection.* J Exp Med, 2015. **212**(12): p. 2015-25.
123. Kallies, A., et al., *A role for Blimp1 in the transcriptional network controlling natural killer cell maturation.* Blood, 2011. **117**(6): p. 1869-79.
124. Deng, Y., et al., *Transcription factor Foxo1 is a negative regulator of natural killer cell maturation and function.* Immunity, 2015. **42**(3): p. 457-70.
125. Knox, J.J., et al., *Characterization of T-bet and eomes in peripheral human immune cells.* Front Immunol, 2014. **5**: p. 217.
126. Yun, S., et al., *TOX regulates the differentiation of human natural killer cells from hematopoietic stem cells in vitro.* Immunol Lett, 2011. **136**(1): p. 29-36.
127. Vong, Q.P., et al., *TOX2 regulates human natural killer cell development by controlling T-BET expression.* Blood, 2014. **124**(26): p. 3905-13.

128. Schotte, R., et al., *Synergy between IL-15 and Id2 promotes the expansion of human NK progenitor cells, which can be counteracted by the E protein HEB required to drive T cell development.* J Immunol, 2010. **184**(12): p. 6670-9.
129. Heemskerk, M.H., et al., *Inhibition of T cell and promotion of natural killer cell development by the dominant negative helix loop helix factor Id3.* J Exp Med, 1997. **186**(9): p. 1597-602.
130. Noguchi, M., et al., *Interleukin-2 receptor gamma chain mutation results in X-linked severe combined immunodeficiency in humans.* Cell, 1993. **73**(1): p. 147-57.
131. DiSanto, J.P., et al., *Lymphoid development in mice with a targeted deletion of the interleukin 2 receptor gamma chain.* Proc Natl Acad Sci U S A, 1995. **92**(2): p. 377-81.
132. Boulanger, M.J. and K.C. Garcia, *Shared cytokine signaling receptors: structural insights from the gp130 system.* Adv Protein Chem, 2004. **68**: p. 107-46.
133. Grabstein, K.H., et al., *Cloning of a T cell growth factor that interacts with the beta chain of the interleukin-2 receptor.* Science, 1994. **264**(5161): p. 965-8.
134. Giri, J.G., et al., *Utilization of the beta and gamma chains of the IL-2 receptor by the novel cytokine IL-15.* EMBO J, 1994. **13**(12): p. 2822-30.
135. Bamford, R.N., et al., *The interleukin (IL) 2 receptor beta chain is shared by IL-2 and a cytokine, provisionally designated IL-T, that stimulates T-cell proliferation and the induction of lymphokine-activated killer cells.* Proc Natl Acad Sci U S A, 1994. **91**(11): p. 4940-4.
136. Stauber, D.J., et al., *Crystal structure of the IL-2 signaling complex: paradigm for a heterotrimeric cytokine receptor.* Proc Natl Acad Sci U S A, 2006. **103**(8): p. 2788-93.
137. Rickert, M., et al., *The structure of interleukin-2 complexed with its alpha receptor.* Science, 2005. **308**(5727): p. 1477-80.
138. Giri, J.G., et al., *Identification and cloning of a novel IL-15 binding protein that is structurally related to the alpha chain of the IL-2 receptor.* EMBO J, 1995. **14**(15): p. 3654-63.
139. Dubois, S., et al., *IL-15Ralpha recycles and presents IL-15 In trans to neighboring cells.* Immunity, 2002. **17**(5): p. 537-47.
140. Mortier, E., et al., *IL-15Ralpha chaperones IL-15 to stable dendritic cell membrane complexes that activate NK cells via trans presentation.* J Exp Med, 2008. **205**(5): p. 1213-25.
141. Kennedy, M.K., et al., *Reversible defects in natural killer and memory CD8 T cell lineages in interleukin 15-deficient mice.* J Exp Med, 2000. **191**(5): p. 771-80.
142. Lodolce, J.P., et al., *IL-15 receptor maintains lymphoid homeostasis by supporting lymphocyte homing and proliferation.* Immunity, 1998. **9**(5): p. 669-76.
143. Vosshenrich, C.A., et al., *Roles for common cytokine receptor gamma-chain-dependent cytokines in the generation, differentiation, and maturation of NK cell precursors and peripheral NK cells in vivo.* J Immunol, 2005. **174**(3): p. 1213-21.
144. Boyman, O. and J. Sprent, *The role of interleukin-2 during homeostasis and activation of the immune system.* Nat Rev Immunol, 2012. **12**(3): p. 180-90.
145. Boussiotis, V.A., et al., *Prevention of T cell anergy by signaling through the gamma c chain of the IL-2 receptor.* Science, 1994. **266**(5187): p. 1039-42.
146. Miyazaki, T., et al., *Functional activation of Jak1 and Jak3 by selective association with IL-2 receptor subunits.* Science, 1994. **266**(5187): p. 1045-7.
147. Russell, S.M., et al., *Interaction of IL-2R beta and gamma c chains with Jak1 and Jak3: implications for XSCID and XCID.* Science, 1994. **266**(5187): p. 1042-5.

148. Zhu, M.H., et al., *Delineation of the regions of interleukin-2 (IL-2) receptor beta chain important for association of Jak1 and Jak3. Jak1-independent functional recruitment of Jak3 to Il-2Rbeta.* J Biol Chem, 1998. **273**(17): p. 10719-25.
149. Truitt, K.E., et al., *SH2-dependent association of phosphatidylinositol 3'-kinase 85-kDa regulatory subunit with the interleukin-2 receptor beta chain.* J Biol Chem, 1994. **269**(8): p. 5937-43.
150. Fujii, H., et al., *Functional dissection of the cytoplasmic subregions of the IL-2 receptor betac chain in primary lymphocyte populations.* EMBO J, 1998. **17**(22): p. 6551-7.
151. Park, S.Y., et al., *Developmental defects of lymphoid cells in Jak3 kinase-deficient mice.* Immunity, 1995. **3**(6): p. 771-82.
152. Eckelhart, E., et al., *A novel Ncr1-Cre mouse reveals the essential role of STAT5 for NK-cell survival and development.* Blood, 2011. **117**(5): p. 1565-73.
153. Imada, K., et al., *Stat5b is essential for natural killer cell-mediated proliferation and cytolytic activity.* J Exp Med, 1998. **188**(11): p. 2067-74.
154. Villarino, A.V., et al., *Subset- and tissue-defined STAT5 thresholds control homeostasis and function of innate lymphoid cells.* J Exp Med, 2017. **214**(10): p. 2999-3014.
155. Viant, C., et al., *Cell cycle progression dictates the requirement for BCL2 in natural killer cell survival.* J Exp Med, 2017. **214**(2): p. 491-510.
156. Gotthardt, D., et al., *STAT5 Is a Key Regulator in NK Cells and Acts as a Molecular Switch from Tumor Surveillance to Tumor Promotion.* Cancer Discov, 2016. **6**(4): p. 414-29.
157. Okkenhaug, K., *Signaling by the phosphoinositide 3-kinase family in immune cells.* Annu Rev Immunol, 2013. **31**: p. 675-704.
158. Guo, H., et al., *The p110 delta of PI3K plays a critical role in NK cell terminal maturation and cytokine/chemokine generation.* J Exp Med, 2008. **205**(10): p. 2419-35.
159. Kim, N., et al., *The p110delta catalytic isoform of PI3K is a key player in NK-cell development and cytokine secretion.* Blood, 2007. **110**(9): p. 3202-8.
160. Tassi, I., et al., *p110gamma and p110delta phosphoinositide 3-kinase signaling pathways synergize to control development and functions of murine NK cells.* Immunity, 2007. **27**(2): p. 214-27.
161. Marcais, A., et al., *The metabolic checkpoint kinase mTOR is essential for IL-15 signaling during the development and activation of NK cells.* Nat Immunol, 2014. **15**(8): p. 749-57.
162. Mavropoulos, A., et al., *Stabilization of IFN-gamma mRNA by MAPK p38 in IL-12- and IL-18-stimulated human NK cells.* Blood, 2005. **105**(1): p. 282-8.
163. Chen, X., et al., *Many NK cell receptors activate ERK2 and JNK1 to trigger microtubule organizing center and granule polarization and cytotoxicity.* Proc Natl Acad Sci U S A, 2007. **104**(15): p. 6329-34.
164. Vezina, C., A. Kudelski, and S.N. Sehgal, *Rapamycin (AY-22,989), a new antifungal antibiotic. I. Taxonomy of the producing streptomycete and isolation of the active principle.* J Antibiot (Tokyo), 1975. **28**(10): p. 721-6.
165. Martel, R.R., J. Klicius, and S. Galet, *Inhibition of the immune response by rapamycin, a new antifungal antibiotic.* Can J Physiol Pharmacol, 1977. **55**(1): p. 48-51.
166. Eng, C.P., S.N. Sehgal, and C. Vezina, *Activity of rapamycin (AY-22,989) against transplanted tumors.* J Antibiot (Tokyo), 1984. **37**(10): p. 1231-7.
167. Kuo, C.J., et al., *Rapamycin selectively inhibits interleukin-2 activation of p70 S6 kinase.* Nature, 1992. **358**(6381): p. 70-3.
168. Chung, J., et al., *Rapamycin-FKBP specifically blocks growth-dependent activation of and signaling by the 70 kd S6 protein kinases.* Cell, 1992. **69**(7): p. 1227-36.

169. Sabatini, D.M., et al., *RAFT1: a mammalian protein that binds to FKBP12 in a rapamycin-dependent fashion and is homologous to yeast TORs.* Cell, 1994. **78**(1): p. 35-43.
170. Sabers, C.J., et al., *Isolation of a protein target of the FKBP12-rapamycin complex in mammalian cells.* J Biol Chem, 1995. **270**(2): p. 815-22.
171. Brown, E.J., et al., *A mammalian protein targeted by G1-arresting rapamycin-receptor complex.* Nature, 1994. **369**(6483): p. 756-8.
172. Sabatini, D.M., *Twenty-five years of mTOR: Uncovering the link from nutrients to growth.* Proc Natl Acad Sci U S A, 2017. **114**(45): p. 11818-11825.
173. Saxton, R.A. and D.M. Sabatini, *mTOR Signaling in Growth, Metabolism, and Disease.* Cell, 2017. **169**(2): p. 361-371.
174. Hara, K., et al., *Raptor, a binding partner of target of rapamycin (TOR), mediates TOR action.* Cell, 2002. **110**(2): p. 177-89.
175. Kim, D.H., et al., *mTOR interacts with raptor to form a nutrient-sensitive complex that signals to the cell growth machinery.* Cell, 2002. **110**(2): p. 163-75.
176. Jacinto, E., et al., *Mammalian TOR complex 2 controls the actin cytoskeleton and is rapamycin insensitive.* Nat Cell Biol, 2004. **6**(11): p. 1122-8.
177. Sarbassov, D.D., et al., *Rictor, a novel binding partner of mTOR, defines a rapamycin-insensitive and raptor-independent pathway that regulates the cytoskeleton.* Curr Biol, 2004. **14**(14): p. 1296-302.
178. Yang, Q., et al., *Identification of Sin1 as an essential TORC2 component required for complex formation and kinase activity.* Genes Dev, 2006. **20**(20): p. 2820-32.
179. Jacinto, E., et al., *SIN1/MIP1 maintains rictor-mTOR complex integrity and regulates Akt phosphorylation and substrate specificity.* Cell, 2006. **127**(1): p. 125-37.
180. Frias, M.A., et al., *mSin1 is necessary for Akt/PKB phosphorylation, and its isoforms define three distinct mTORC2s.* Curr Biol, 2006. **16**(18): p. 1865-70.
181. Yang, Q. and K.L. Guan, *Expanding mTOR signaling.* Cell Res, 2007. **17**(8): p. 666-81.
182. Yip, C.K., et al., *Structure of the human mTOR complex I and its implications for rapamycin inhibition.* Mol Cell, 2010. **38**(5): p. 768-74.
183. Aylett, C.H., et al., *Architecture of human mTOR complex 1.* Science, 2016. **351**(6268): p. 48-52.
184. Baretic, D., et al., *Tor forms a dimer through an N-terminal helical solenoid with a complex topology.* Nat Commun, 2016. **7**: p. 11016.
185. Zhou, P., et al., *Defining the Domain Arrangement of the Mammalian Target of Rapamycin Complex Component Rictor Protein.* J Comput Biol, 2015. **22**(9): p. 876-86.
186. Schroder, W., et al., *Alternative polyadenylation and splicing of mRNAs transcribed from the human Sin1 gene.* Gene, 2004. **339**: p. 17-23.
187. Schroder, W.A., et al., *Human Sin1 contains Ras-binding and pleckstrin homology domains and suppresses Ras signalling.* Cell Signal, 2007. **19**(6): p. 1279-89.
188. Liu, P., et al., *PtdIns(3,4,5)P3-Dependent Activation of the mTORC2 Kinase Complex.* Cancer Discov, 2015. **5**(11): p. 1194-209.
189. Sarbassov, D.D., et al., *Prolonged rapamycin treatment inhibits mTORC2 assembly and Akt/PKB.* Mol Cell, 2006. **22**(2): p. 159-68.
190. Dibble, C.C., et al., *TBC1D7 is a third subunit of the TSC1-TSC2 complex upstream of mTORC1.* Mol Cell, 2012. **47**(4): p. 535-46.
191. Inoki, K., T. Zhu, and K.L. Guan, *TSC2 mediates cellular energy response to control cell growth and survival.* Cell, 2003. **115**(5): p. 577-90.

192. Tee, A.R., et al., *Tuberous sclerosis complex gene products, Tuberin and Hamartin, control mTOR signaling by acting as a GTPase-activating protein complex toward Rheb.* Curr Biol, 2003. **13**(15): p. 1259-68.
193. Long, X., et al., *Rheb binds and regulates the mTOR kinase.* Curr Biol, 2005. **15**(8): p. 702-13.
194. Inoki, K., et al., *TSC2 is phosphorylated and inhibited by Akt and suppresses mTOR signalling.* Nat Cell Biol, 2002. **4**(9): p. 648-57.
195. Manning, B.D., et al., *Identification of the tuberous sclerosis complex-2 tumor suppressor gene product tuberin as a target of the phosphoinositide 3-kinase/akt pathway.* Mol Cell, 2002. **10**(1): p. 151-62.
196. Ma, L., et al., *Phosphorylation and functional inactivation of TSC2 by Erk implications for tuberous sclerosis and cancer pathogenesis.* Cell, 2005. **121**(2): p. 179-93.
197. Roux, P.P., et al., *Tumor-promoting phorbol esters and activated Ras inactivate the tuberous sclerosis tumor suppressor complex via p90 ribosomal S6 kinase.* Proc Natl Acad Sci U S A, 2004. **101**(37): p. 13489-94.
198. Kim, E., et al., *Regulation of TORC1 by Rag GTPases in nutrient response.* Nat Cell Biol, 2008. **10**(8): p. 935-45.
199. Sancak, Y., et al., *The Rag GTPases bind raptor and mediate amino acid signaling to mTORC1.* Science, 2008. **320**(5882): p. 1496-501.
200. Menon, S., et al., *Spatial control of the TSC complex integrates insulin and nutrient regulation of mTORC1 at the lysosome.* Cell, 2014. **156**(4): p. 771-85.
201. Gwinn, D.M., et al., *AMPK phosphorylation of raptor mediates a metabolic checkpoint.* Mol Cell, 2008. **30**(2): p. 214-26.
202. Shaw, R.J., et al., *The LKB1 tumor suppressor negatively regulates mTOR signaling.* Cancer Cell, 2004. **6**(1): p. 91-9.
203. Kalender, A., et al., *Metformin, independent of AMPK, inhibits mTORC1 in a rag GTPase-dependent manner.* Cell Metab, 2010. **11**(5): p. 390-401.
204. Merrick, W.C., *Cap-dependent and cap-independent translation in eukaryotic systems.* Gene, 2004. **332**: p. 1-11.
205. Richter, J.D. and N. Sonenberg, *Regulation of cap-dependent translation by eIF4E inhibitory proteins.* Nature, 2005. **433**(7025): p. 477-80.
206. Brunn, G.J., et al., *Phosphorylation of the translational repressor PHAS-I by the mammalian target of rapamycin.* Science, 1997. **277**(5322): p. 99-101.
207. Gingras, A.C., et al., *Regulation of 4E-BP1 phosphorylation: a novel two-step mechanism.* Genes Dev, 1999. **13**(11): p. 1422-37.
208. Thoreen, C.C., et al., *A unifying model for mTORC1-mediated regulation of mRNA translation.* Nature, 2012. **485**(7396): p. 109-13.
209. Meyuhas, O., *Synthesis of the translational apparatus is regulated at the translational level.* Eur J Biochem, 2000. **267**(21): p. 6321-30.
210. Pearson, R.B., et al., *The principal target of rapamycin-induced p70s6k inactivation is a novel phosphorylation site within a conserved hydrophobic domain.* EMBO J, 1995. **14**(21): p. 5279-87.
211. Pullen, N., et al., *Phosphorylation and activation of p70s6k by PDK1.* Science, 1998. **279**(5351): p. 707-10.
212. Alessi, D.R., et al., *3-Phosphoinositide-dependent protein kinase 1 (PDK1) phosphorylates and activates the p70 S6 kinase in vivo and in vitro.* Curr Biol, 1998. **8**(2): p. 69-81.

213. Holz, M.K., et al., *mTOR and S6K1 mediate assembly of the translation preinitiation complex through dynamic protein interchange and ordered phosphorylation events.* Cell, 2005. **123**(4): p. 569-80.
214. Dorrello, N.V., et al., *S6K1- and betaTRCP-mediated degradation of PDCD4 promotes protein translation and cell growth.* Science, 2006. **314**(5798): p. 467-71.
215. Duvel, K., et al., *Activation of a metabolic gene regulatory network downstream of mTOR complex 1.* Mol Cell, 2010. **39**(2): p. 171-83.
216. Peterson, T.R., et al., *mTOR complex 1 regulates lipin 1 localization to control the SREBP pathway.* Cell, 2011. **146**(3): p. 408-20.
217. Ben-Sahra, I., et al., *mTORC1 induces purine synthesis through control of the mitochondrial tetrahydrofolate cycle.* Science, 2016. **351**(6274): p. 728-733.
218. Ben-Sahra, I., et al., *Stimulation of de novo pyrimidine synthesis by growth signaling through mTOR and S6K1.* Science, 2013. **339**(6125): p. 1323-8.
219. Robitaille, A.M., et al., *Quantitative phosphoproteomics reveal mTORC1 activates de novo pyrimidine synthesis.* Science, 2013. **339**(6125): p. 1320-3.
220. Sarbassov, D.D., et al., *Phosphorylation and regulation of Akt/PKB by the rictor-mTOR complex.* Science, 2005. **307**(5712): p. 1098-101.
221. Yang, G., et al., *A Positive Feedback Loop between Akt and mTORC2 via SIN1 Phosphorylation.* Cell Rep, 2015. **12**(6): p. 937-43.
222. Zinzalla, V., et al., *Activation of mTORC2 by association with the ribosome.* Cell, 2011. **144**(5): p. 757-68.
223. Hsu, P.P., et al., *The mTOR-regulated phosphoproteome reveals a mechanism of mTORC1-mediated inhibition of growth factor signaling.* Science, 2011. **332**(6035): p. 1317-22.
224. Yu, Y., et al., *Phosphoproteomic analysis identifies Grb10 as an mTORC1 substrate that negatively regulates insulin signaling.* Science, 2011. **332**(6035): p. 1322-6.
225. Harrington, L.S., et al., *The TSC1-2 tumor suppressor controls insulin-PI3K signaling via regulation of IRS proteins.* J Cell Biol, 2004. **166**(2): p. 213-23.
226. Shah, O.J., Z. Wang, and T. Hunter, *Inappropriate activation of the TSC/Rheb/mTOR/S6K cassette induces IRS1/2 depletion, insulin resistance, and cell survival deficiencies.* Curr Biol, 2004. **14**(18): p. 1650-6.
227. Guertin, D.A., et al., *Ablation in mice of the mTORC components raptor, rictor, or mLST8 reveals that mTORC2 is required for signaling to Akt-FOXO and PKCalpha, but not S6K1.* Dev Cell, 2006. **11**(6): p. 859-71.
228. Hill, M.M., et al., *Insulin-stimulated protein kinase B phosphorylation on Ser-473 is independent of its activity and occurs through a staurosporine-insensitive kinase.* J Biol Chem, 2001. **276**(28): p. 25643-6.
229. Alessi, D.R., et al., *Characterization of a 3-phosphoinositide-dependent protein kinase which phosphorylates and activates protein kinase Balpha.* Curr Biol, 1997. **7**(4): p. 261-9.
230. Gan, X., et al., *PRR5L degradation promotes mTORC2-mediated PKC-delta phosphorylation and cell migration downstream of Galpha12.* Nat Cell Biol, 2012. **14**(7): p. 686-96.
231. Li, X. and T. Gao, *mTORC2 phosphorylates protein kinase Czeta to regulate its stability and activity.* EMBO Rep, 2014. **15**(2): p. 191-8.
232. Garcia-Martinez, J.M. and D.R. Alessi, *mTOR complex 2 (mTORC2) controls hydrophobic motif phosphorylation and activation of serum- and glucocorticoid-induced protein kinase 1 (SGK1).* Biochem J, 2008. **416**(3): p. 375-85.

233. Powell, J.D., et al., *Regulation of immune responses by mTOR.* Annu Rev Immunol, 2012. **30**: p. 39-68.
234. Delgoffe, G.M., et al., *The kinase mTOR regulates the differentiation of helper T cells through the selective activation of signaling by mTORC1 and mTORC2.* Nat Immunol, 2011. **12**(4): p. 295-303.
235. Delgoffe, G.M., et al., *The mTOR kinase differentially regulates effector and regulatory T cell lineage commitment.* Immunity, 2009. **30**(6): p. 832-44.
236. Lee, K., et al., *Mammalian target of rapamycin protein complex 2 regulates differentiation of Th1 and Th2 cell subsets via distinct signaling pathways.* Immunity, 2010. **32**(6): p. 743-53.
237. Zeng, H., et al., *mTORC1 couples immune signals and metabolic programming to establish T(reg)-cell function.* Nature, 2013. **499**(7459): p. 485-90.
238. Zeng, H., et al., *mTORC1 and mTORC2 Kinase Signaling and Glucose Metabolism Drive Follicular Helper T Cell Differentiation.* Immunity, 2016. **45**(3): p. 540-554.
239. Yang, J., et al., *Critical roles of mTOR Complex 1 and 2 for T follicular helper cell differentiation and germinal center responses.* Elife, 2016. **5**.
240. Araki, K., et al., *mTOR regulates memory CD8 T-cell differentiation.* Nature, 2009. **460**(7251): p. 108-12.
241. Pollizzi, K.N., et al., *mTORC1 and mTORC2 selectively regulate CD8(+) T cell differentiation.* J Clin Invest, 2015. **125**(5): p. 2090-108.
242. Zhang, L., et al., *Mammalian Target of Rapamycin Complex 2 Controls CD8 T Cell Memory Differentiation in a Foxo1-Dependent Manner.* Cell Rep, 2016. **14**(5): p. 1206-1217.
243. Linke, M., et al., *mTORC1 and mTORC2 as regulators of cell metabolism in immunity.* FEBS Lett, 2017. **591**(19): p. 3089-3103.
244. Finlay, D.K., et al., *PDK1 regulation of mTOR and hypoxia-inducible factor 1 integrate metabolism and migration of CD8+ T cells.* J Exp Med, 2012. **209**(13): p. 2441-53.
245. Frauwirth, K.A., et al., *The CD28 signaling pathway regulates glucose metabolism.* Immunity, 2002. **16**(6): p. 769-77.
246. Shi, L.Z., et al., *HIF1alpha-dependent glycolytic pathway orchestrates a metabolic checkpoint for the differentiation of TH17 and Treg cells.* J Exp Med, 2011. **208**(7): p. 1367-76.
247. Dang, E.V., et al., *Control of T(H)17/T(reg) balance by hypoxia-inducible factor 1.* Cell, 2011. **146**(5): p. 772-84.
248. Michalek, R.D., et al., *Cutting edge: distinct glycolytic and lipid oxidative metabolic programs are essential for effector and regulatory CD4+ T cell subsets.* J Immunol, 2011. **186**(6): p. 3299-303.
249. Pearce, E.L., et al., *Enhancing CD8 T-cell memory by modulating fatty acid metabolism.* Nature, 2009. **460**(7251): p. 103-7.
250. Iwata, T.N., et al., *Control of B lymphocyte development and functions by the mTOR signaling pathways.* Cytokine Growth Factor Rev, 2017. **35**: p. 47-62.
251. Iwata, T.N., et al., *Conditional Disruption of Raptor Reveals an Essential Role for mTORC1 in B Cell Development, Survival, and Metabolism.* J Immunol, 2016. **197**(6): p. 2250-60.
252. Zhang, S., et al., *Constitutive reductions in mTOR alter cell size, immune cell development, and antibody production.* Blood, 2011. **117**(4): p. 1228-38.
253. Zhang, Y., et al., *Rictor is required for early B cell development in bone marrow.* PLoS One, 2014. **9**(8): p. e103970.

254. Kalaitzidis, D., et al., *mTOR complex 1 plays critical roles in hematopoiesis and Pten-loss-evoked leukemogenesis.* Cell Stem Cell, 2012. **11**(3): p. 429-39.
255. Zhang, S., et al., *B cell-specific deficiencies in mTOR limit humoral immune responses.* J Immunol, 2013. **191**(4): p. 1692-703.
256. Keating, R., et al., *The kinase mTOR modulates the antibody response to provide cross-protective immunity to lethal infection with influenza virus.* Nat Immunol, 2013. **14**(12): p. 1266-76.
257. Jones, D.D., et al., *mTOR has distinct functions in generating versus sustaining humoral immunity.* J Clin Invest, 2016. **126**(11): p. 4250-4261.
258. Lee, K., et al., *Requirement for Rictor in homeostasis and function of mature B lymphoid cells.* Blood, 2013. **122**(14): p. 2369-79.
259. Limon, J.J., et al., *mTOR kinase inhibitors promote antibody class switching via mTORC2 inhibition.* Proc Natl Acad Sci U S A, 2014. **111**(47): p. E5076-85.
260. Weichhart, T. and M.D. Saemann, *The multiple facets of mTOR in immunity.* Trends Immunol, 2009. **30**(5): p. 218-26.
261. Ohtani, M., et al., *Mammalian target of rapamycin and glycogen synthase kinase 3 differentially regulate lipopolysaccharide-induced interleukin-12 production in dendritic cells.* Blood, 2008. **112**(3): p. 635-43.
262. Weichhart, T., et al., *The TSC-mTOR signaling pathway regulates the innate inflammatory response.* Immunity, 2008. **29**(4): p. 565-77.
263. Ohtani, M., et al., *Cutting edge: mTORC1 in intestinal CD11c+ CD11b+ dendritic cells regulates intestinal homeostasis by promoting IL-10 production.* J Immunol, 2012. **188**(10): p. 4736-40.
264. Brown, J., et al., *Mammalian target of rapamycin complex 2 (mTORC2) negatively regulates Toll-like receptor 4-mediated inflammatory response via FoxO1.* J Biol Chem, 2011. **286**(52): p. 44295-305.
265. Jorgensen, P.F., et al., *Sirolimus interferes with the innate response to bacterial products in human whole blood by attenuation of IL-10 production.* Scand J Immunol, 2001. **53**(2): p. 184-91.
266. Festuccia, W.T., et al., *Myeloid-specific Rictor deletion induces M1 macrophage polarization and potentiates in vivo pro-inflammatory response to lipopolysaccharide.* PLoS One, 2014. **9**(4): p. e95432.
267. Mercalli, A., et al., *Rapamycin unbalances the polarization of human macrophages to M1.* Immunology, 2013. **140**(2): p. 179-90.
268. Rocher, C. and D.K. Singla, *SMAD-PI3K-Akt-mTOR pathway mediates BMP-7 polarization of monocytes into M2 macrophages.* PLoS One, 2013. **8**(12): p. e84009.
269. Haidinger, M., et al., *A versatile role of mammalian target of rapamycin in human dendritic cell function and differentiation.* J Immunol, 2010. **185**(7): p. 3919-31.
270. Amiel, E., et al., *Inhibition of mechanistic target of rapamycin promotes dendritic cell activation and enhances therapeutic autologous vaccination in mice.* J Immunol, 2012. **189**(5): p. 2151-8.
271. Raich-Regue, D., et al., *mTORC2 Deficiency in Myeloid Dendritic Cells Enhances Their Allogeneic Th1 and Th17 Stimulatory Ability after TLR4 Ligation In Vitro and In Vivo.* J Immunol, 2015. **194**(10): p. 4767-76.
272. Pan, H., et al., *Critical role of the tumor suppressor tuberous sclerosis complex 1 in dendritic cell activation of CD4 T cells by promoting MHC class II expression via IRF4 and CIITA.* J Immunol, 2013. **191**(2): p. 699-707.

273. Nandagopal, N., et al., *The Critical Role of IL-15-PI3K-mTOR Pathway in Natural Killer Cell Effector Functions.* Front Immunol, 2014. **5**: p. 187.
274. Mah, A.Y., et al., *Glycolytic requirement for NK cell cytotoxicity and cytomegalovirus control.* JCI Insight, 2017. **2**(23).
275. Marcais, A., et al., *Regulation of mouse NK cell development and function by cytokines.* Front Immunol, 2013. **4**: p. 450.
276. Becknell, B. and M.A. Caligiuri, *Interleukin-2, interleukin-15, and their roles in human natural killer cells.* Adv Immunol, 2005. **86**: p. 209-39.
277. Donnelly, R.P., et al., *mTORC1-dependent metabolic reprogramming is a prerequisite for NK cell effector function.* J Immunol, 2014. **193**(9): p. 4477-84.
278. Viel, S., et al., *TGF-beta inhibits the activation and functions of NK cells by repressing the mTOR pathway.* Sci Signal, 2016. **9**(415): p. ra19.
279. Marcais, A., et al., *High mTOR activity is a hallmark of reactive natural killer cells and amplifies early signaling through activating receptors.* Elife, 2017. **6**.
280. Tremblay, M., O. Sanchez-Ferras, and M. Bouchard, *GATA transcription factors in development and disease.* Development, 2018. **145**(20).
281. Lentjes, M.H., et al., *The emerging role of GATA transcription factors in development and disease.* Expert Rev Mol Med, 2016. **18**: p. e3.
282. Martin, D.I. and S.H. Orkin, *Transcriptional activation and DNA binding by the erythroid factor GF-1/NF-E1/Eryf 1.* Genes Dev, 1990. **4**(11): p. 1886-98.
283. Morrisey, E.E., et al., *GATA-4 activates transcription via two novel domains that are conserved within the GATA-4/5/6 subfamily.* J Biol Chem, 1997. **272**(13): p. 8515-24.
284. Bossard, P. and K.S. Zaret, *GATA transcription factors as potentiators of gut endoderm differentiation.* Development, 1998. **125**(24): p. 4909-17.
285. Cirillo, L.A., et al., *Opening of compacted chromatin by early developmental transcription factors HNF3 (FoxA) and GATA-4.* Mol Cell, 2002. **9**(2): p. 279-89.
286. Eeckhoute, J., et al., *Positive cross-regulatory loop ties GATA-3 to estrogen receptor alpha expression in breast cancer.* Cancer Res, 2007. **67**(13): p. 6477-83.
287. Wang, Q., et al., *A hierarchical network of transcription factors governs androgen receptor-dependent prostate cancer growth.* Mol Cell, 2007. **27**(3): p. 380-92.
288. Bresnick, E.H., et al., *GATA switches as developmental drivers.* J Biol Chem, 2010. **285**(41): p. 31087-93.
289. Tsai, F.Y., et al., *An early haematopoietic defect in mice lacking the transcription factor GATA-2.* Nature, 1994. **371**(6494): p. 221-6.
290. Rodrigues, N.P., et al., *Haploinsufficiency of GATA-2 perturbs adult hematopoietic stem-cell homeostasis.* Blood, 2005. **106**(2): p. 477-84.
291. Tsai, F.Y. and S.H. Orkin, *Transcription factor GATA-2 is required for proliferation/survival of early hematopoietic cells and mast cell formation, but not for erythroid and myeloid terminal differentiation.* Blood, 1997. **89**(10): p. 3636-43.
292. Heyworth, C., et al., *A GATA-2/estrogen receptor chimera functions as a ligand-dependent negative regulator of self-renewal.* Genes Dev, 1999. **13**(14): p. 1847-60.
293. Persons, D.A., et al., *Enforced expression of the GATA-2 transcription factor blocks normal hematopoiesis.* Blood, 1999. **93**(2): p. 488-99.
294. Tipping, A.J., et al., *High GATA-2 expression inhibits human hematopoietic stem and progenitor cell function by effects on cell cycle.* Blood, 2009. **113**(12): p. 2661-72.
295. Ikonomi, P., et al., *Overexpression of GATA-2 inhibits erythroid and promotes megakaryocyte differentiation.* Exp Hematol, 2000. **28**(12): p. 1423-31.

296. Onodera, K., et al., *GATA2 regulates dendritic cell differentiation.* Blood, 2016. **128**(4): p. 508-18.
297. Zhou, Y., et al., *Rescue of the embryonic lethal hematopoietic defect reveals a critical role for GATA-2 in urogenital development.* EMBO J, 1998. **17**(22): p. 6689-700.
298. Lim, K.C., et al., *Conditional Gata2 inactivation results in HSC loss and lymphatic mispatterning.* J Clin Invest, 2012. **122**(10): p. 3705-17.
299. Kazenwadel, J., et al., *GATA2 is required for lymphatic vessel valve development and maintenance.* J Clin Invest, 2015. **125**(8): p. 2979-94.
300. Li, X., et al., *Gata2 Is a Rheostat for Mesenchymal Stem Cell Fate in Male Mice.* Endocrinology, 2016. **157**(3): p. 1021-8.
301. Kamata, M., et al., *GATA2 regulates differentiation of bone marrow-derived mesenchymal stem cells.* Haematologica, 2014. **99**(11): p. 1686-96.
302. Tsai, J., et al., *The transcription factor GATA2 regulates differentiation of brown adipocytes.* EMBO Rep, 2005. **6**(9): p. 879-84.
303. Kala, K., et al., *Gata2 is a tissue-specific post-mitotic selector gene for midbrain GABAergic neurons.* Development, 2009. **136**(2): p. 253-62.
304. Tsarovina, K., et al., *Essential role of Gata transcription factors in sympathetic neuron development.* Development, 2004. **131**(19): p. 4775-86.
305. Collin, M., R. Dickinson, and V. Bigley, *Haematopoietic and immune defects associated with GATA2 mutation.* Br J Haematol, 2015. **169**(2): p. 173-87.
306. Hirabayashi, S., et al., *Heterogeneity of GATA2-related myeloid neoplasms.* Int J Hematol, 2017. **106**(2): p. 175-182.
307. Callier, P., et al., *Detection of an interstitial 3q21.1-q21.3 deletion in a child with multiple congenital abnormalities, mental retardation, pancytopenia, and myelodysplasia.* Am J Med Genet A, 2009. **149A**(6): p. 1323-6.
308. Dickinson, R.E., et al., *The evolution of cellular deficiency in GATA2 mutation.* Blood, 2014. **123**(6): p. 863-74.
309. Spinner, M.A., et al., *GATA2 deficiency: a protean disorder of hematopoiesis, lymphatics, and immunity.* Blood, 2014. **123**(6): p. 809-21.
310. Hahn, C.N., et al., *Heritable GATA2 mutations associated with familial myelodysplastic syndrome and acute myeloid leukemia.* Nat Genet, 2011. **43**(10): p. 1012-7.
311. Dickinson, R.E., et al., *Exome sequencing identifies GATA-2 mutation as the cause of dendritic cell, monocyte, B and NK lymphoid deficiency.* Blood, 2011. **118**(10): p. 2656-8.
312. Ostergaard, P., et al., *Mutations in GATA2 cause primary lymphedema associated with a predisposition to acute myeloid leukemia (Emberger syndrome).* Nat Genet, 2011. **43**(10): p. 929-31.
313. Hsu, A.P., et al., *Mutations in GATA2 are associated with the autosomal dominant and sporadic monocytopenia and mycobacterial infection (MonoMAC) syndrome.* Blood, 2011. **118**(10): p. 2653-5.
314. Crispino, J.D. and M.S. Horwitz, *GATA factor mutations in hematologic disease.* Blood, 2017. **129**(15): p. 2103-2110.
315. Hsu, A.P., L.J. McReynolds, and S.M. Holland, *GATA2 deficiency.* Curr Opin Allergy Clin Immunol, 2015. **15**(1): p. 104-9.
316. Zhang, S.J., et al., *Gain-of-function mutation of GATA-2 in acute myeloid transformation of chronic myeloid leukemia.* Proc Natl Acad Sci U S A, 2008. **105**(6): p. 2076-81.
317. Carey, B. and B.C. Trapnell, *The molecular basis of pulmonary alveolar proteinosis.* Clin Immunol, 2010. **135**(2): p. 223-35.

318. Kazenwadel, J., et al., *Loss-of-function germline GATA2 mutations in patients with MDS/AML or MonoMAC syndrome and primary lymphedema reveal a key role for GATA2 in the lymphatic vasculature.* Blood, 2012. **119**(5): p. 1283-91.
319. Cuellar-Rodriguez, J., et al., *Successful allogeneic hematopoietic stem cell transplantation for GATA2 deficiency.* Blood, 2011. **118**(13): p. 3715-20.
320. Grossman, J., et al., *Nonmyeloablative allogeneic hematopoietic stem cell transplantation for GATA2 deficiency.* Biol Blood Marrow Transplant, 2014. **20**(12): p. 1940-8.
321. Michel, T., et al., *Human CD56bright NK Cells: An Update.* J Immunol, 2016. **196**(7): p. 2923-31.
322. Schlums, H., et al., *Adaptive NK cells can persist in patients with GATA2 mutation depleted of stem and progenitor cells.* Blood, 2017. **129**(14): p. 1927-1939.
323. Maciejewski-Duval, A., et al., *Altered chemotactic response to CXCL12 in patients carrying GATA2 mutations.* J Leukoc Biol, 2016. **99**(6): p. 1065-76.
324. Patro, R., et al., *Salmon provides fast and bias-aware quantification of transcript expression.* Nat Methods, 2017. **14**(4): p. 417-419.
325. Casper, J., et al., *The UCSC Genome Browser database: 2018 update.* Nucleic Acids Res, 2018. **46**(D1): p. D762-D769.
326. Haeussler, M., et al., *The UCSC Genome Browser database: 2019 update.* Nucleic Acids Res, 2018.
327. Soneson C, L.M.a.R.M., *Differential analyses for RNA-seq: transcript-level estimates improve gene-level inferences.* F1000Research, 2015. **4**(1521).
328. Love, M.I., W. Huber, and S. Anders, *Moderated estimation of fold change and dispersion for RNA-seq data with DESeq2.* Genome Biol, 2014. **15**(12): p. 550.
329. Butler, A., et al., *Integrating single-cell transcriptomic data across different conditions, technologies, and species.* Nat Biotechnol, 2018. **36**(5): p. 411-420.
330. Andrews, T.S. and M. Hemberg, *Identifying cell populations with scRNASeq.* Mol Aspects Med, 2018. **59**: p. 114-122.
331. Finak, G., et al., *MAST: a flexible statistical framework for assessing transcriptional changes and characterizing heterogeneity in single-cell RNA sequencing data.* Genome Biol, 2015. **16**: p. 278.
332. Subramanian, A., et al., *Gene set enrichment analysis: a knowledge-based approach for interpreting genome-wide expression profiles.* Proc Natl Acad Sci U S A, 2005. **102**(43): p. 15545-50.
333. Liberzon, A., et al., *Molecular signatures database (MSigDB) 3.0.* Bioinformatics, 2011. **27**(12): p. 1739-40.
334. Qiu, X., et al., *Reversed graph embedding resolves complex single-cell trajectories.* Nat Methods, 2017. **14**(10): p. 979-982.
335. Aiello, S., Eckstrand, E., Fu, A., Landry, M., and Aboyoun, P. , *Machine Learning with R and H2O*. 2018.
336. Schwarz, D.F., I.R. Konig, and A. Ziegler, *On safari to Random Jungle: a fast implementation of Random Forests for high-dimensional data.* Bioinformatics, 2010. **26**(14): p. 1752-8.
337. Shih, H.Y., et al., *Developmental Acquisition of Regulomes Underlies Innate Lymphoid Cell Functionality.* Cell, 2016. **165**(5): p. 1120-1133.
338. Langmead, B. and S.L. Salzberg, *Fast gapped-read alignment with Bowtie 2.* Nat Methods, 2012. **9**(4): p. 357-9.

339. Zhang, Y., et al., *Model-based analysis of ChIP-Seq (MACS).* Genome Biol, 2008. **9**(9): p. R137.
340. Heinz, S., et al., *Simple combinations of lineage-determining transcription factors prime cis-regulatory elements required for macrophage and B cell identities.* Mol Cell, 2010. **38**(4): p. 576-89.
341. Wullschleger, S., R. Loewith, and M.N. Hall, *TOR signaling in growth and metabolism.* Cell, 2006. **124**(3): p. 471-84.
342. Weichhart, T., M. Hengstschlager, and M. Linke, *Regulation of innate immune cell function by mTOR.* Nat Rev Immunol, 2015. **15**(10): p. 599-614.
343. Whitman, M., et al., *Type I phosphatidylinositol kinase makes a novel inositol phospholipid, phosphatidylinositol-3-phosphate.* Nature, 1988. **332**(6165): p. 644-6.
344. Suzuki, H., et al., *Abnormal development of intestinal intraepithelial lymphocytes and peripheral natural killer cells in mice lacking the IL-2 receptor beta chain.* J Exp Med, 1997. **185**(3): p. 499-505.
345. Zhu, X., et al., *Interleukin-2-induced tyrosine phosphorylation of Shc proteins correlates with factor-dependent T cell proliferation.* J Biol Chem, 1994. **269**(8): p. 5518-22.
346. Gu, H., et al., *New role for Shc in activation of the phosphatidylinositol 3-kinase/Akt pathway.* Mol Cell Biol, 2000. **20**(19): p. 7109-20.
347. Yang, M., et al., *PDK1 orchestrates early NK cell development through induction of E4BP4 expression and maintenance of IL-15 responsiveness.* J Exp Med, 2015. **212**(2): p. 253-65.
348. Leong, J.W., et al., *PTEN regulates natural killer cell trafficking in vivo.* Proc Natl Acad Sci U S A, 2015. **112**(7): p. E700-9.
349. Daussy, C., et al., *T-bet and Eomes instruct the development of two distinct natural killer cell lineages in the liver and in the bone marrow.* J Exp Med, 2014. **211**(3): p. 563-77.
350. Simonetta, F., A. Pradier, and E. Roosnek, *T-bet and Eomesodermin in NK Cell Development, Maturation, and Function.* Front Immunol, 2016. **7**: p. 241.
351. Brunet, A., et al., *Akt promotes cell survival by phosphorylating and inhibiting a Forkhead transcription factor.* Cell, 1999. **96**(6): p. 857-68.
352. Cahill, C.M., et al., *Phosphatidylinositol 3-kinase signaling inhibits DAF-16 DNA binding and function via 14-3-3-dependent and 14-3-3-independent pathways.* J Biol Chem, 2001. **276**(16): p. 13402-10.
353. Wang, S., et al., *FoxO1-mediated autophagy is required for NK cell development and innate immunity.* Nat Commun, 2016. **7**: p. 11023.
354. Ouyang, W., et al., *Novel Foxo1-dependent transcriptional programs control T(reg) cell function.* Nature, 2012. **491**(7425): p. 554-9.
355. Kerdiles, Y.M., et al., *Foxo1 links homing and survival of naive T cells by regulating L-selectin, CCR7 and interleukin 7 receptor.* Nat Immunol, 2009. **10**(2): p. 176-84.
356. Wang, F., et al., *Crosstalks between mTORC1 and mTORC2 variagate cytokine signaling to control NK maturation and effector function.* Nat Commun, 2018. **9**(1): p. 4874.
357. Grundy, M.A., T. Zhang, and C.L. Sentman, *NK cells rapidly remove B16F10 tumor cells in a perforin and interferon-gamma independent manner in vivo.* Cancer Immunol Immunother, 2007. **56**(8): p. 1153-61.
358. Lakshmikanth, T., et al., *NCRs and DNAM-1 mediate NK cell recognition and lysis of human and mouse melanoma cell lines in vitro and in vivo.* J Clin Invest, 2009. **119**(5): p. 1251-63.
359. Mayol, K., et al., *Sequential desensitization of CXCR4 and S1P5 controls natural killer cell trafficking.* Blood, 2011. **118**(18): p. 4863-71.

360. Yang, M., et al., *NK cell development requires Tsc1-dependent negative regulation of IL-15-triggered mTORC1 activation.* Nat Commun, 2016. **7**: p. 12730.
361. Crinier, A., et al., *High-Dimensional Single-Cell Analysis Identifies Organ-Specific Signatures and Conserved NK Cell Subsets in Humans and Mice.* Immunity, 2018. **49**(5): p. 971-986 e5.
362. Yang, C., et al., *mTORC1 and mTORC2 differentially promote natural killer cell development.* Elife, 2018. **7**.
363. Robinette, M.L., et al., *Transcriptional programs define molecular characteristics of innate lymphoid cell classes and subsets.* Nat Immunol, 2015. **16**(3): p. 306-17.
364. Conacci-Sorrell, M., L. McFerrin, and R.N. Eisenman, *An overview of MYC and its interactome.* Cold Spring Harb Perspect Med, 2014. **4**(1): p. a014357.
365. Chen, H.Z., S.Y. Tsai, and G. Leone, *Emerging roles of E2Fs in cancer: an exit from cell cycle control.* Nat Rev Cancer, 2009. **9**(11): p. 785-97.
366. Lanier, L.L., et al., *Expression of cytoplasmic CD3 epsilon proteins in activated human adult natural killer (NK) cells and CD3 gamma, delta, epsilon complexes in fetal NK cells. Implications for the relationship of NK and T lymphocytes.* J Immunol, 1992. **149**(6): p. 1876-80.
367. Klose, C.S.N., et al., *Differentiation of type 1 ILCs from a common progenitor to all helper-like innate lymphoid cell lineages.* Cell, 2014. **157**(2): p. 340-356.
368. Hesslein, D.G. and L.L. Lanier, *Transcriptional control of natural killer cell development and function.* Adv Immunol, 2011. **109**: p. 45-85.
369. Cella, M., et al., *A human natural killer cell subset provides an innate source of IL-22 for mucosal immunity.* Nature, 2009. **457**(7230): p. 722-5.
370. Cupedo, T., et al., *Human fetal lymphoid tissue-inducer cells are interleukin 17-producing precursors to RORC+ CD127+ natural killer-like cells.* Nat Immunol, 2009. **10**(1): p. 66-74.
371. Montaldo, E., et al., *Human RORgammat(+)CD34(+) cells are lineage-specified progenitors of group 3 RORgammat(+) innate lymphoid cells.* Immunity, 2014. **41**(6): p. 988-1000.
372. Scoville, S.D., et al., *A Progenitor Cell Expressing Transcription Factor RORgammat Generates All Human Innate Lymphoid Cell Subsets.* Immunity, 2016. **44**(5): p. 1140-50.
373. Lim, A.I., et al., *Systemic Human ILC Precursors Provide a Substrate for Tissue ILC Differentiation.* Cell, 2017. **168**(6): p. 1086-1100 e10.
374. Chen, L., et al., *CD56 Expression Marks Human Group 2 Innate Lymphoid Cell Divergence from a Shared NK Cell and Group 3 Innate Lymphoid Cell Developmental Pathway.* Immunity, 2018. **49**(3): p. 464-476 e4.
375. Milush, J.M., et al., *Functionally distinct subsets of human NK cells and monocyte/DC-like cells identified by coexpression of CD56, CD7, and CD4.* Blood, 2009. **114**(23): p. 4823-31.
376. Zheng, G.X., et al., *Massively parallel digital transcriptional profiling of single cells.* Nat Commun, 2017. **8**: p. 14049.
377. Hanna, J., et al., *Novel insights on human NK cells' immunological modalities revealed by gene expression profiling.* J Immunol, 2004. **173**(11): p. 6547-63.
378. Koopman, L.A., et al., *Human decidual natural killer cells are a unique NK cell subset with immunomodulatory potential.* J Exp Med, 2003. **198**(8): p. 1201-12.
379. Wendt, K., et al., *Gene and protein characteristics reflect functional diversity of CD56dim and CD56bright NK cells.* J Leukoc Biol, 2006. **80**(6): p. 1529-41.
380. Scheiter, M., et al., *Proteome analysis of distinct developmental stages of human natural killer (NK) cells.* Mol Cell Proteomics, 2013. **12**(5): p. 1099-114.

381. Le Bouteiller, P., et al., *CD160: a unique activating NK cell receptor.* Immunol Lett, 2011. **138**(2): p. 93-6.
382. Tirosh, I., et al., *Dissecting the multicellular ecosystem of metastatic melanoma by single-cell RNA-seq.* Science, 2016. **352**(6282): p. 189-96.
383. Tullai, J.W., et al., *Immediate-early and delayed primary response genes are distinct in function and genomic architecture.* J Biol Chem, 2007. **282**(33): p. 23981-95.
384. Bahrami, S. and F. Drablos, *Gene regulation in the immediate-early response process.* Adv Biol Regul, 2016. **62**: p. 37-49.
385. Mora-Garcia, P., et al., *Transcriptional regulators and myelopoiesis: the role of serum response factor and CREB as targets of cytokine signaling.* Stem Cells, 2003. **21**(2): p. 123-30.
386. Huntington, N.D., et al., *IL-15 trans-presentation promotes human NK cell development and differentiation in vivo.* J Exp Med, 2009. **206**(1): p. 25-34.
387. Lugthart, G., et al., *Human Lymphoid Tissues Harbor a Distinct CD69+CXCR6+ NK Cell Population.* J Immunol, 2016. **197**(1): p. 78-84.
388. Juelke, K., et al., *CD62L expression identifies a unique subset of polyfunctional CD56dim NK cells.* Blood, 2010. **116**(8): p. 1299-307.
389. Sun, J.C., et al., *NK cells and immune "memory".* J Immunol, 2011. **186**(4): p. 1891-7.
390. Schlums, H., et al., *Cytomegalovirus infection drives adaptive epigenetic diversification of NK cells with altered signaling and effector function.* Immunity, 2015. **42**(3): p. 443-56.
391. Mace, E.M., et al., *Cell biological steps and checkpoints in accessing NK cell cytotoxicity.* Immunol Cell Biol, 2014. **92**(3): p. 245-55.
392. Mace, E.M. and J.S. Orange, *Lytic immune synapse function requires filamentous actin deconstruction by Coronin 1A.* Proc Natl Acad Sci U S A, 2014. **111**(18): p. 6708-13.
393. Samstag, Y., I. John, and G.H. Wabnitz, *Cofilin: a redox sensitive mediator of actin dynamics during T-cell activation and migration.* Immunol Rev, 2013. **256**(1): p. 30-47.
394. Higgs, H.N. and T.D. Pollard, *Regulation of actin filament network formation through ARP2/3 complex: activation by a diverse array of proteins.* Annu Rev Biochem, 2001. **70**: p. 649-76.
395. Perisic Nanut, M., et al., *Cystatin F Affects Natural Killer Cell Cytotoxicity.* Front Immunol, 2017. **8**: p. 1459.
396. Schoppmeyer, R., et al., *Human profilin 1 is a negative regulator of CTL mediated cell-killing and migration.* Eur J Immunol, 2017. **47**(9): p. 1562-1572.
397. Ndhlovu, L.C., et al., *Tim-3 marks human natural killer cell maturation and suppresses cell-mediated cytotoxicity.* Blood, 2012. **119**(16): p. 3734-43.
398. Hamann, I., et al., *Analyses of phenotypic and functional characteristics of CX3CR1-expressing natural killer cells.* Immunology, 2011. **133**(1): p. 62-73.
399. Nestorowa, S., et al., *A single-cell resolution map of mouse hematopoietic stem and progenitor cell differentiation.* Blood, 2016. **128**(8): p. e20-31.
400. Dybkaer, K., et al., *Genome wide transcriptional analysis of resting and IL2 activated human natural killer cells: gene expression signatures indicative of novel molecular signaling pathways.* BMC Genomics, 2007. **8**: p. 230.
401. Crinier, A., et al., *High-Dimensional Single-Cell Analysis Identifies Organ-Specific Signatures and Conserved NK Cell Subsets in Humans and Mice.* Immunity, 2018.
402. Qiu, X., et al., *Single-cell mRNA quantification and differential analysis with Census.* Nat Methods, 2017. **14**(3): p. 309-315.
403. Ciucci, T. and R. Bosselut, *Gimap and T cells: a matter of life or death.* Eur J Immunol, 2014. **44**(2): p. 348-51.

404. Nitta, T. and Y. Takahama, *The lymphocyte guard-IANs: regulation of lymphocyte survival by IAN/GIMAP family proteins.* Trends Immunol, 2007. **28**(2): p. 58-65.
405. Schnell, S., et al., *Gimap4 accelerates T-cell death.* Blood, 2006. **108**(2): p. 591-9.
406. Webb, L.M., et al., *GIMAP1 Is Essential for the Survival of Naive and Activated B Cells In Vivo.* J Immunol, 2016. **196**(1): p. 207-16.
407. Datta, P., et al., *Survival of mature T cells in the periphery is intrinsically dependent on GIMAP1 in mice.* Eur J Immunol, 2017. **47**(1): p. 84-93.
408. Pandarpurkar, M., et al., *Ian4 is required for mitochondrial integrity and T cell survival.* Proc Natl Acad Sci U S A, 2003. **100**(18): p. 10382-7.
409. Miano, J.M., *Role of serum response factor in the pathogenesis of disease.* Lab Invest, 2010. **90**(9): p. 1274-84.
410. Cortez, V.S., et al., *SMAD4 impedes the conversion of NK cells into ILC1-like cells by curtailing non-canonical TGF-beta signaling.* Nat Immunol, 2017. **18**(9): p. 995-1003.
411. Arif, A., et al., *EPRS is a critical mTORC1-S6K1 effector that influences adiposity in mice.* Nature, 2017. **542**(7641): p. 357-361.
412. Knight, Z.A., et al., *A critical role for mTORC1 in erythropoiesis and anemia.* Elife, 2014. **3**: p. e01913.
413. Lopez-Soto, A., et al., *Involvement of autophagy in NK cell development and function.* Autophagy, 2017. **13**(3): p. 633-636.
414. O'Sullivan, T.E., et al., *Atg5 Is Essential for the Development and Survival of Innate Lymphocytes.* Cell Rep, 2016. **15**(9): p. 1910-9.
415. Finck, B.N. and D.P. Kelly, *PGC-1 coactivators: inducible regulators of energy metabolism in health and disease.* J Clin Invest, 2006. **116**(3): p. 615-22.
416. Cunningham, J.T., et al., *mTOR controls mitochondrial oxidative function through a YY1-PGC-1alpha transcriptional complex.* Nature, 2007. **450**(7170): p. 736-40.
417. Schmidt, M., et al., *Cell cycle inhibition by FoxO forkhead transcription factors involves downregulation of cyclin D.* Mol Cell Biol, 2002. **22**(22): p. 7842-52.
418. Medema, R.H., et al., *AFX-like Forkhead transcription factors mediate cell-cycle regulation by Ras and PKB through p27kip1.* Nature, 2000. **404**(6779): p. 782-7.
419. Kim, W.S., et al., *Suppressor of Cytokine Signaling 2 Negatively Regulates NK Cell Differentiation by Inhibiting JAK2 Activity.* Sci Rep, 2017. **7**: p. 46153.
420. Rodda, L.B., et al., *Single-Cell RNA Sequencing of Lymph Node Stromal Cells Reveals Niche-Associated Heterogeneity.* Immunity, 2018. **48**(5): p. 1014-1028 e6.
421. Papalexi, E. and R. Satija, *Single-cell RNA sequencing to explore immune cell heterogeneity.* Nat Rev Immunol, 2018. **18**(1): p. 35-45.
422. Aibar, S., et al., *SCENIC: single-cell regulatory network inference and clustering.* Nat Methods, 2017. **14**(11): p. 1083-1086.
423. Schwartzman, O. and A. Tanay, *Single-cell epigenomics: techniques and emerging applications.* Nat Rev Genet, 2015. **16**(12): p. 716-26.